Multiparameter index for the estimation of Depth of Anaesthesia based on Signal Processing and Soft computing Techniques

A Thesis Submitted for the Degree of

Doctor of Philosophy

in the Faculty of Engineering,

University of Calicut

by

Benzy V.K

Under the Guidance of

Dr. Jasmin E.A

Department of Electrical Engineering

Govt. Engineering College Thrissur, Thrissur

University of Calicut

September 2018

Certificate

This is to certify that the thesis entitled **Multiparameter index for the estimation of Depth of Anaesthesia based on Signal processing and Soft computing techniques** is the record of bonafide research work done by **Benzy V.K** under my supervision and guidance at Department of Electrical Engineering, Govt. Engineering College, Thrissur in partial fulfilment of the requirement for the Degree of Doctor of Philosophy under Faculty of Engineering, University of Calicut.

September 2018

Dr. Jasmin E.A
Associate Professor
Dept. of Electrical Engineering
Govt. Engineering College, Thrissur

Declaration

I **Benzy V.K** hereby declare that the thesis entitled **Multiparameter index for the estimation of Depth of Anaesthesia based on Signal processing and Soft computing techniques** is based on the original work done by me under the guidance of **Dr. Jasmin E.A**, Associate Professor, Department of Electrical Engineering, Govt. Engineering College, Thrissur for the award of PhD programme under University of Calicut. I further declare that this work has not been included in any other thesis submitted previously for the award of any Degree, Diploma, Associateship or Fellowship or any other title for recognition.

September 2018 Benzy V.K

Acknowledgement

First and above all, I bow my head before the ***Almighty*** *Lord whose grace has been with me always throughout the research work. I have been enormously benefited from the advice, support, co-operation and encouragement given by a number of individuals during the course of this research work. I would, therefore, like to offer my sincere thanks to all of them.*

Creative guidance makes a scientific research, qualitative and this has been imparted to me by ***Dr. Jasmin E. A****, Associate Professor, Department of Electrical Engineering, Govt. Engineering College, Thrissur, as a helpful guide. I want to express my sincere thanks to her for the trust, the insightful discussion, offering valuable advice and for the support during the whole period of the research which made this work possible. I also acknowledge her patience and guidance during the writing process.*

I extend my wholehearted thanks to ***Dr. Vijayakumar****, the former Joint Director of Kerala Technical University(Principal of GEC, Thrissur, during the period 2008-2014) for his healthy co-operation and encouragement. I am also thankful to* ***Dr. Indiradevi K.P****, Joint Director of Kerala Technical University(Principal of GEC, Thrissur, during the period 2015-2017),* ***Dr. Jayanand B****, Principal, GEC, Thrissur, and* ***Dr. M Nandakumar****, Head of the Electrical engineering Department, Government Engineering College, Thrissur, for providing the facilities to successfully carry out this research work.*

I express my sincere gratitude to ***Dr. B Jayanand*** *and* ***Dr. Amardutt A****, Former Head, Department of Electrical Engineering, Faculty and supporting staff members of Electrical Engineering for giving an opportunity to carry out my research work in the Department of Electrical Engineering, Govt. Engineering College, Thrissur. I sincerely thank the doctoral Committee members for providing valuable comments and suggestions at the time of interim presentations of research work.*

I gratefully acknowledge the efforts put by ***Dr. Rachel Cherian Koshy****, Professor, HOD, Dept. of Anaesthesiology, Regional Cancer Centre, Trivandrum*

and her team of doctors and technicians for providing timely guidance and assistance during data collection and literature survey at Regional Cancer Centre, Trivandrum. I also deeply thankful to all the patients and their relatives for co-operating throughout my data collection.

I would like to place on record my gratitude to ***Centre for Engineering Research and Development(CERD)****, Govt. Engineering College, Trivandrum for selecting me for the research scholarship. I have no words to express my deep sense of gratitude to my friends at Electrical department for making the research period a memorable one.*

I am highly indebted to my ***mother*** *and* ***mother-in-law*** *for the consistent support and sharing of my responsibilities at home when I was busy with my work. I thank my husband* ***Dr. Frank Amal*** *for the consistent encouragement and absolute support to accomplish the objective. I also thank my daughters* ***Christina Frank*** *and* ***Rebecca Frank*** *for patiently co-operating with me to complete the work successfully.I also thank my brother* ***Alex Bernard*** *for giving valuable suggestion and ideas during the course of my study.*

Thrissur
September 2018

Benzy V.K

Abstract

Name of the student: **Benzy VK**
Degree for which submitted: **PhD.**
Department: **Electrical Engineering**
Thesis title: **Multiparameter index for the estimation of Depth of Anaesthesia based on Signal Processing and Soft computing Techniques**
Thesis supervisor: **Dr. Jasmin E A**
Month and year of thesis submission: **January 2018**

Anaesthesia is provided to assist the progress of surgery by minimising pain, patient recall and discomfort during the surgical procedure. When anaesthesia is adequate the patient feels no pain during the surgical procedure and often does not recall the proceedings. One of the current challenges in Anaesthesia is the estimation of patient's Depth of Anaesthesia for adequate dosing of anaesthetic drugs. The most formidable complications of anaesthesia are the awareness of the patient during surgery due to the inadequate doses of anaesthetic drugs and overdose of anaesthetic drugs which can cause prolonged recovery from anaesthesia. Therefore, continuous estimation of patient's anaesthetic depth prevents awareness due to the inadequate administration of anaesthetic drugs and also avoid the overdose of drugs by optimizing the quantity of drug delivered to a patient during surgery. Usually, depth of anaesthesia is estimated using clinical parameters such as Blood Pressure (BP), Heart Rate (HR), sweating, tearing etc. However, these parameters are incompetent to provide the exact plane of anaesthesia because these parameters vary depending on the patient, drug effect and surgical procedure. Hence, the scientific estimation of patient's Depth of Anaesthesia during surgery is a challenging task.

The understanding of the effect of anaesthetic drugs and their response is very important for anaesthesia decision making and for patient's dose calculation. Actually, the anaesthetic drugs cause effects on neurophysiological signals

and clinical parameters such as Heart Rate and Blood pressure. In the current research, multiple inputs derived from clinical and neurophysiological signals are used to quantify the Depth of Anaesthesia. The data used for the study is obtained from 25 female patients who have undergone breast cancer surgery at Regional Cancer Centre (RCC), Trivandrum, Kerala, India. The collected dataset includes waveform data such as electroencephalogram (EEG) signal and numerical data such as Heart Rate, Systolic Blood Pressure and Diastolic Blood Pressure. The EEG signals represent the neurophysiological signal and are collected using BIS sensor whereas Heart Rate, Systolic and Diastolic Blood Pressure are extracted from the standard monitoring devices. These signals are collected from the patient throughout the surgical procedure.

The objectives of the research are:

- Prepare the collected EEG signals and the standard monitoring parameters for analysis by applying pre-processing techniques.
- Extract the time domain, frequency domain, time-frequency domain and non-linear features from EEG signals.
- Extract features from vital parameters such as HR and BP collected from standard monitoring devices.
- Analyze the extracted features during different anaesthetic phases awake, Induction, Maintenance and Recovery.
- Compare the extracted features with the commercially available Depth of Anaesthesia monitoring Index(BIS)
- Select the combination of features which enhance the accuracy of classification according to the Depth of Anaesthesia as deep anaesthesia, moderate anaesthesia, light anaesthesia and awake.
- To develop an integrated index to estimate Depth of Anaesthesia by combining the selected combination of EEG features and standard monitoring parameters.

The first stage of the research is concerned with data preprocessing. After the data collection, the signals are preprocessed using filters to remove the noises

from the data. Initially, the signals are segmented for the effective filtering and analysis. Both the uniform segmentation and non-uniform segmentation are applied to the signals. In the uniform segmentation, signals are divided into fixed time intervals of 5 sec whereas the non-uniform segmentation is implemented by applying modified Varri's algorithm on the collected EEG signals. After segmentation, the noises from the signals are removed by applying filtering methods. In the case of EEG signals, a two-level filtering method is applied. In the first level, a 50 Hz notch filter is designed to remove the power line interferences. In the second level, wavelet-based thresholding algorithm is applied to the EEG signals to remove the artifacts. The performance of the filter is evaluated by calculating 3 measures Mean Square Error, Signal to Noise Ratio and Correlation Coefficient.

The second stage of the research is concentrated in different feature extraction methods. At the beginning of this stage, EEG signals are represented in various domains to extract features that depict the amplitude and frequency variations. A non-linear analysis is also done on EEG signals to study the complexity/regularity of the EEG signals. The extracted time domain features include Standard Deviation, Entropy, Energy, Mean Absolute Deviation, Zero Crossing Rate and Inter-Quartile Range. Among these features Standard Deviation, Energy, Mean Absolute Deviation and Inter-Quartile Range shows a direct relationship with Depth of Anaesthesia whereas Entropy and Zero Crossing Rate shows an inverse relation with Depth of Anaesthesia. The frequency domain features extracted from EEG signals are Spectral Edge Frequency and Spectral Entropy. Both these features show an inverse relation with DoA. The extracted time-frequency domain features are Wavelet Entropy (WEn) and Relative Wave Energy(RWE) of each EEG frequency band. All these features vary in accordance with DoA. Finally, nonlinear features such as Approximate Entropy(ApEn) and Permutation Entropy(PEn) are extracted from the collected EEG signals to study the complexity and nonlinear behaviour of EEG signals during different phases of anaesthesia. In order to study the hemodynamic variability due to the anaesthetic drugs, features such as ΔHeart Rate, ΔMean Blood Pressure and Pulse Pressure are extracted from the HR and BP data. Abnormalities of these extracted features during the four phases of anaesthesia such as awake, induction, maintenance and recovery are analyzed to quantify the variations. The capability of the extracted features in estimating Depth of Anaesthesia is analysed

by comparing the features with a commercially available DoA index(BIS index).

In the third stage, optimum features are selected by applying different feature ranking methods like 'T-Test', 'Entropy', 'Bhattacharyya', 'ROC' and 'Wilcoxon'. The kNN, SVM, Multilayer Perceptron and Naive Base Classifier outputs are compared based on their accuracy to select the best-ranked features of EEG signals from the time, frequency, time-frequency and nonlinear analysis. In the case of hemodynamic parameters Kruskal Wallis test is used to select the best features from the extracted hemodynamic parameters.

In the last stage of the research, an Adaptive Neuro-Fuzzy Inference System (ANFIS) model is implemented to estimate the multiparameter DoA index. In the implementation process of ANFIS model, two algorithms called Subtractive clustering and Fuzzy C Means clustering are used to generate fuzzy functions and rules. A hybrid learning algorithm consisting of Least Square Estimator(LSE) method and the backpropagation gradient descent method is used to learn and adjust the ANFIS parameters. Root Mean Square Error(RMSE) is calculated to compare the performance of the two ANFIS models. ANFIS model based on subtractive clustering algorithm produced lowest RMSE for the training, testing and combined data set. Finally, a multiparameter Depth of Anaesthesia index is generated by integrating EEG features and hemodynamic features using subtracting clustering based ANFIS model.

Contents

List of Figures

List of Tables

Abbreviations

GA	**G**eneral **A**naesthesia
DoA	**D**epth **o**f **A**naesthesia
EEG	**E**lectroencephalogram
HR	**H**eart **R**ate
BP	**B**lood **P**ressure
NIBP	**N**on **I**nvasive **B**lood **P**ressure
SBP	**S**ystolic **B**lood **P**ressure
DBP	**D**iastolic **B**lood **P**ressure
MBP	**M**ean **B**lood **P**ressure
BIS Index	**B**ispectral Index
AEP	**A**uditory **E**voked **P**otential
MAD	**M**ean **A**bsolute **D**eviation
ZCR	**Z**ero **C**rossing **R**ate
IQR	**I**nter **Q**uartile **R**ange
SEn	**S**pectral **En**tropy
SEF	**S**pectral **E**dge **F**requency
WT	**W**avelet **T**ransform
DWT	**D**iscrete **W**avelet **T**ransform
WEn	**W**avelet **En**tropy
RWE	**R**elative **W**ave **E**nergy
ApEn	**Ap**proximate **En**tropy
PEn	**P**ermutation **En**tropy

kNN	**k-** **N**earest **N**eighbors
SVM	**S**upport **V**ector **M**achine
MLPNN	**M**ulti **L**ayer **P**erceptron **N**eural **N**etwork
ANN	**A**rtificial **N**eural **N**etwork
NBC	**N**aive **B**ase **C**lassifier
ANFIS	**A**daptive **N**euro- **F**uzzy **I**nference **S**ystem
LSE	**S**quare **E**stimator
FCM	**F**uzzy **C** **M**eans

Dedicated to my Father...

Chapter 1

Introduction

Anaesthesia is a medically induced clinical state that inhibits patients from sensing pain during surgery. The word anaesthesia is originated from two Greek words "an" meaning "without" and "aesthesis" meaning "sensation". When anaesthesia works the patient feels no pain during the procedure and often does not remember the surgical proceedings. There are two types of anaesthesia namely General Anaesthesia (GA) and Regional Anaesthesia (RA). General anaesthesia is a drug-induced, reversible state that leads to loss of consciousness, loss of pain perception and loss of thought processing of the surgical procedures. Regional anaesthesia is accomplished using drugs that temporarily block the sensation of pain in a certain area of the body while the patient remains awake.

The advancement in medical research has transformed anaesthesiology into an active area of research. Many of the surgical procedures would not be possible without anaesthesia. In order to improve the quality and understanding of anaesthesia, implementation of uniform process and standardization in the field of anaesthesia is required. This emerges new technologies and research areas that promote multidisciplinary research.

Estimation of patient's Depth of Anaesthesia (DoA) during GA is one of the current challenges in anaesthesia research because too little anaesthetic drugs can make a patient aware during surgery. On the other hand, too much anaesthetic drugs can result in anaesthetic overdosing that leads to prolonged recovery from

anaesthesia. Therefore, continuous monitoring and estimation of anaesthesia prevent patient awareness due to the inadequate dose of anaesthetic drugs and avoid the overdose of anaesthetic drugs by optimizing the quantity of drug delivered to a patient during surgery. Many of the anaesthesiologist control and monitor the DoA by observing the parameters such as Blood Pressure(BP), Heart Rate(HR), Body movement and Airway Pressure etc. These parameters are incompetent to provide the exact plane of anaesthesia due to their insufficiency in giving exact dynamic characteristics of anaesthetic drug effect. Use of other drugs like muscle relaxants and vasodilators makes the analysis of those parameters difficult and unreliable [Shalbaf *et al.* , 2013].

1.1 Depth of Anaesthesia (DoA)

Depth of Anaesthesia is defined as the drug-induced probability of non-response to stimulation calibrated against the strength of the stimulus and difficulty of suppressing the responses. DoA depends on three main factors: (1) The equilibration of drug's concentration in plasma with concentration of drug at its site of action and with measured drug effect (2) The relationship between drug concentration and drug effect (3) The influence of noxious stimuli [Kaul *et al.* , 2002]. The process of

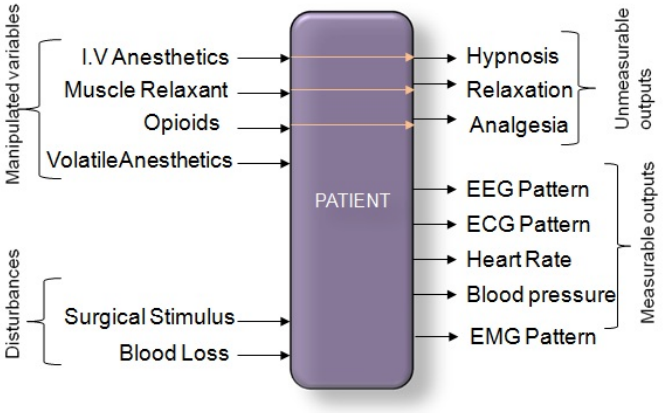

Figure 1.1: Process of General Anaesthesia

GA is presented in Figure 1.1. The three main components that an anaesthesiologist has to suppress through anaesthetic drugs are consciousness, sensitivity to pain and patient movement. Anaesthesiologist uses Intravenous (IV) anaesthetic drugs for suppressing consciousness and would induce a state of unconsciousness called Amnesia (Hypnosis). Opioid drugs were used by the anaesthesiologist to suppress the pain and would lead to a state of insensitivity to pain called Analgesia. The muscle relaxant drugs were provided to prevent patient's movement and would result in a state of muscle relaxation called Akinesia. The combination of hypnotic, analgesic and muscle relaxation drugs is referred as 'triad of anaesthesia'.

The standard dose of these drugs is calculated based on the patient's body weight and age. Dose ratio can be modified according to the relative importance of each component depending on the surgical and patient factors like previous history, the physical condition of the patient, complexity of the surgery [Miller *et al.* , 2014]. The effects of anaesthetic drugs are (1) transition from a state of wakefulness to a state of unconsciousness (2) transition from a state of pain sensitivity to state insensitivity to pain and (3) transition from muscle movement to muscle relaxation. The volatile anaesthetic agents called inhaled anaesthetics like nitrous oxide, desflurane, isoflurane were provided for maintaining the anaesthesia till the end of the surgery. Anaesthetic drugs were administered to the patients intravenously (by needle into a vein) whereas administration of volatile anaesthetic agents was done with the help of an endotracheal tube. The endotracheal tube also helps in ventilation of the patient during the surgery. The introduction of an endotracheal tube into the trachea is called intubation which is done with the help of laryngoscope. Laryngoscopy is done to visualize larynx after the administration of IV drugs.

The amnesia state defines that it is a state of drug-induced unconsciousness in which patient neither perceives nor recalls surgical proceedings. Unconsciousness can be induced by deep sleep or by anaesthetic drugs. What distinguishes the unconsciousness of anaesthetic state from the non-responsiveness of normal sleep is the stimulus intensity required to break the state of unconsciousness and arouse the brain to conscious perception. The various stimuli that arouse the brain to conscious perception include loud music, hard and cold operating table and painful stimuli. But the hypnotic drugs are capable of producing profound depression on the neurons of Central Nervous System (CNS) that even most painful surgical stimulus cannot

awaken the patient from a state of unconsciousness. Hence, the consciousness can be defined as the balance between excitation and depression of the neurons in the CNS. Cortical neuron depression promotes unconsciousness. The neuron on the CNS can be depressed pharmacologically by hypnotic drugs and other drugs such as N_2O. But this state of unconsciousness is difficult to measure directly because of the variability in unconsciousness due to the varying depression of neuron in the CNS. The variability in unconsciousness can only be measured by the analysis of information on EEG. This EEG based quantification measures the conscious and unconscious state by measuring the predictive probability of response that balance the electrophysiological measures.

The various responses that the patient can have during the surgical stimulation are the perception of pain and movement of the stimulated part. The patient can also have hemodynamic responses like increase in HR and BP due to the stress response of surgery. The analgesic drugs called Opioids are given to suppress these responses. The magnitude of the painful stimulus is determined by the magnitude of the painful outcomes of the surgery and also by the potency of the opioid. More opioids are required to blunt the powerful surgical stimuli. Opioid primarily acts on peripheral nervous system and have a little action on midbrain and thalamus. Opioid receptors are widely distributed in those regions of CNS which mediate various hemodynamic responses. After the interaction of opioid at the peripheral nervous system, the resultant painful stimulus is then projected to the CNS. The pain output from the peripheral nervous system is balanced by the analgesic drug concentration attained by the administration of opioid. As the pain intensity increases the potency of the opioid decreases. Then the painful stimuli projected from the peripheral nervous system and surrounding environment stimulate the CNS. The CNS activates the sympathetic neural and autonomic humoral pathways and which cause changes in hemodynamic responses like HR and BP. Thus the response to the painful stimuli is measured by the probability of responsiveness to hemodynamic parameters and different doses of analgesic drug administration. Muscle relaxants are used for laryngoscopy and to improve the surgical access. They are neither a component of anaesthesia nor an alternative to adequate anaesthesia. Hence, the effect of muscle relaxant is not necessary for the measurement of DoA.

1.2 Phases of General Anaesthesia

GA has four phases

1. Awake phase: This phase is 5-10 minutes before administration of IV anaesthetic agent. At this phase patient is premedicated and all the essential monitors are attached to the patient.

2. Induction phase: The time of administration of IV anaesthetic agents to the absence of response to the verbal stimuli checked by the anaesthesiologist is the Induction phase. Usually, it is 1-5 minutes after the administration of IV anaesthetic agents. During this phase laryngoscopy and intubation are done.

3. Maintenance phase: The period after the insertion of endotracheal tube and administration of inhalation agent till the end of the surgery.

4. Recovery phase: The period after the cutoff of inhalation agent and administration of reversal agent (Neostigmine and Glycopyrrolate) to till the Return of Consciousness (RoC)[Miller *et al.* , 2014].

1.3 Effect of General Anaesthesia on EEG signals

EEG signals are the cortical electrical activity derived from summated excitatory and inhibitory postsynaptic activity as a result of sub cortical events passing through the thalamic nuclei. EEG signals are primarily analyzed by their frequency content and amplitude. The amplitude range of EEG signal varies from 20μV to 200μV. The primary range frequencies of interest for EEG signals is from one to 60 Hz. Five main frequency ranges are normally included in all EEG studies: Delta (0.5-4 Hz), Alpha (4-8 Hz), Beta (8-12 Hz), Theta (12-30 Hz), and Gamma (30-60 Hz). These frequency ranges and their features are illustrated in the Table 1.1 [Al-Kadi *et al.* , 2013].

The direct and indirect inhibitory effects of anaesthetic agents on EEG signals are (1) transition from low amplitude, high-frequency signals to high amplitude,

TABLE 1.1: EEG Rhythms

Frequency Range	Amplitude Range	Features
32-60 Hz (γ)	3 μ V - 5 μ V	Involved in learning, memory, information processing, anxiety, high arousal and stress
16-32 Hz (β)	2 μ V - 20 μ V	Associated with conscious thought, logical thinking and active concentration
8-16 Hz (α)	20 μ V - 60 μ V	Associated with relaxed, alert state of consciousness
4-8 Hz (θ)	20 μ V - 100 μ V	Associated with drowsiness, daydreaming and sleep
0-4 Hz (δ)	20 μ V - 200 μ V	Associated with the deepest levels of relaxation and in deep stage of sleep

low-frequency signals and vice versa (2) the presence of spindles and K-complexes in the case of very deep anaesthetic states [VOSS & SLEIGH, 2007]. But very deep anaesthetic states are not analyzed in the present research as it would cause hemodynamic instability of the patient during surgery and hence spindles and K-complexes are beyond the scope of the present study.

1.4 Effect of General Anaesthesia on Hemodynamic Parameters

As the anaesthetic drugs affect CNS as well as autonomic nervous system, the autonomic nervous system activity should be evaluated to improve the accuracy of estimation of DoA. The most common way of determining the activity of the autonomic nervous system is that the quantification of the changes in Heart Rate (HR) which is measured from the electrocardiogram (ECG) signal and Mean Arterial Pressure (MAP) which measured from the Noninvasive Blood Pressure (NBP) signal. The administration of hypnotic drugs such as propofol causes decrease in

BP and minimal change in HR whereas laryngoscopy and intubation cause an immediate increase in HR and BP which last for 5 minutes. Hence, opioid and local anaesthetic drugs are given to bring down the BP and HR which in turn suppress the stress response of Laryngoscopy and Intubation. During the surgical procedure various surgical stimuli such as skin incision, sternotomy, skin closure, opening of peritoneal cavity etc. may lead to increase in HR and BP. The hypnotic drugs have poor analgesic effect whereas opioids have good analgesic property. Inhalation agents and opioid play an important role in the maintenance period of anaesthesia. Inadequate analgesia in the maintenance phase of anaesthesia is reflected by increase in HR more than 90bpm and 15 percent increase in systolic blood pressure from the initial blood pressure of the patient (Baseline BP).

1.5 Motivation of the Research

Estimation and monitoring of patient's DoA have been changing with the evolution of technology. For decades, depth of anaesthesia was estimated based on clinical parameters like Blood Pressure (BP), Heart Rate (HR) and the patient reactions like sweating, tearing, and many more. However, the characteristics of these parameters are patient dependent and hence accurate estimation of patient's Depth of Anaesthesia during surgery is a challenging task. One of the most formidable complications of anaesthesia is the awareness of the patient during surgery due to the inadequate doses of anaesthetic drugs. On the other hand overdose of anaesthetic drugs can cause prolonged recovery from anaesthesia. Accurate estimation of the anaesthetic depth will prevent these complications. The developments in mathematical modelling of biological systems fascinate researchers to study EEG extracted parameters for the estimation of Depth of Anaesthesia. The efforts made, for the estimation of DoA from EEG was still a biased approach of analysis since it is unable to reproduce the same depth value every time we execute the EEG extracted parameters for different patients with same anaesthetic drug combination. This challenge opens new possibilities for the current research. In order to reduce the variability, some other information is to be acquired, like heart rate, blood pressure other than EEG signals. By including this information the estimation of the DoA was less subjective and more accurate. The purpose of this research is to bridge this gap between the

subjective perception of DoA monitoring and objective measurement of concomitant physiological changes.

Modern anaesthesia is moving towards the monitoring, modelling, and classification of multiple inputs from clinical and physiological signals for the drug control of anaesthesia. There are no direct measurements available to estimate the outcomes of anaesthetic drug effects such as Hypnosis (Amnesia), Analgesia and Akinesia. Therefore intelligent modelling techniques using multiple inputs derived from clinical and physiological signals are used to quantify these outcomes. During surgery, the anaesthesiologist needs to know whether the depth of anaesthesia composed of hypnotic component or analgesic component. As long as the EEG derived parameters gives only the measure of consciousness or hypnosis, we cannot discriminate the other outcome using EEG parameters alone [Duarte & Saraiva, 2009]. The effect of anaesthetic drugs, the degree of surgical stimuli and pain varies from patient to patient. Also, the use of concomitant analgesic drugs produces different results. The indirect indicators HR and BP reveals the adequacy of analgesic drugs which are the classical parameters used by the anaesthesiologists. Intelligent modelling of these multiple parameters derived from clinical and physiological measures accelerate the accurate estimation of DoA.

1.6 Objective of the Research

The limitation of EEG based DoA monitors is that they may not reflect the clinical status of a patient due to the effect of anaesthetic drugs on the autonomic nervous system[Shalbaf *et al.* , 2015; Schneider *et al.* , 2014]. These monitors work only on the hypnotic components of the anaesthetic drugs. Anaesthetic drugs cause effects on neurophysiologic and hemodynamic parameters. The current research estimates DoA by integrating central nervous system monitoring parameters which are extracted from the EEG signals and autonomous nervous system monitoring parameters derived from the standard monitoring devices. This intelligent model analyzes whether the integration provides reliable information about the depth of anaesthesia. The objectives of the research are:

- Prepare the EEG signals and the standard monitoring parameters for analysis by applying pre-processing techniques.
- Extract the time domain, frequency domain, time-frequency domain and non-linear features from EEG signals.
- Extract the vital parameters such as HR and BP from standard monitoring devices.
- Analyze the extracted features during different anaesthetic phases awake, Induction, Maintenance and Recovery.
- Compare the extracted features with the commercially available DoA monitor Index (BIS)
- Select the combination of features which enhance the accuracy of classification according to the depth of anaesthesia as awake, light anaesthesia, moderate anaesthesia, and deep anaesthesia.
- To develop an integrated index to estimate Depth of Anaesthesia by combining the selected combination of EEG features and standard anaesthetic monitoring parameters.

1.7 Outline of the thesis

Present research handles the EEG signals, Systolic Blood pressure, Diastolic Blood pressure, Mean Arterial Pressure (MAP) and Heart Rate collected during anaesthesia for the estimation of DoA. Discrete Wavelet Transforms (DWT) based filtering method is applied to pre-process the EEG signals. Preprocessing of other numerical data is done by removing the power line interference from the data. The time domain, frequency domain, time-frequency domain and non-linear features are extracted from the EEG signals. The conceptual framework of the research is presented in Figure 1.2. The time domain features Standard Deviation, Energy, Entropy and Zero Crossover are extracted to study the variations in amplitude over time of the EEG signal. The frequency domain features like Spectral Entropy and Spectral Edge Frequency are extracted to analyze the response of EEG signal at different

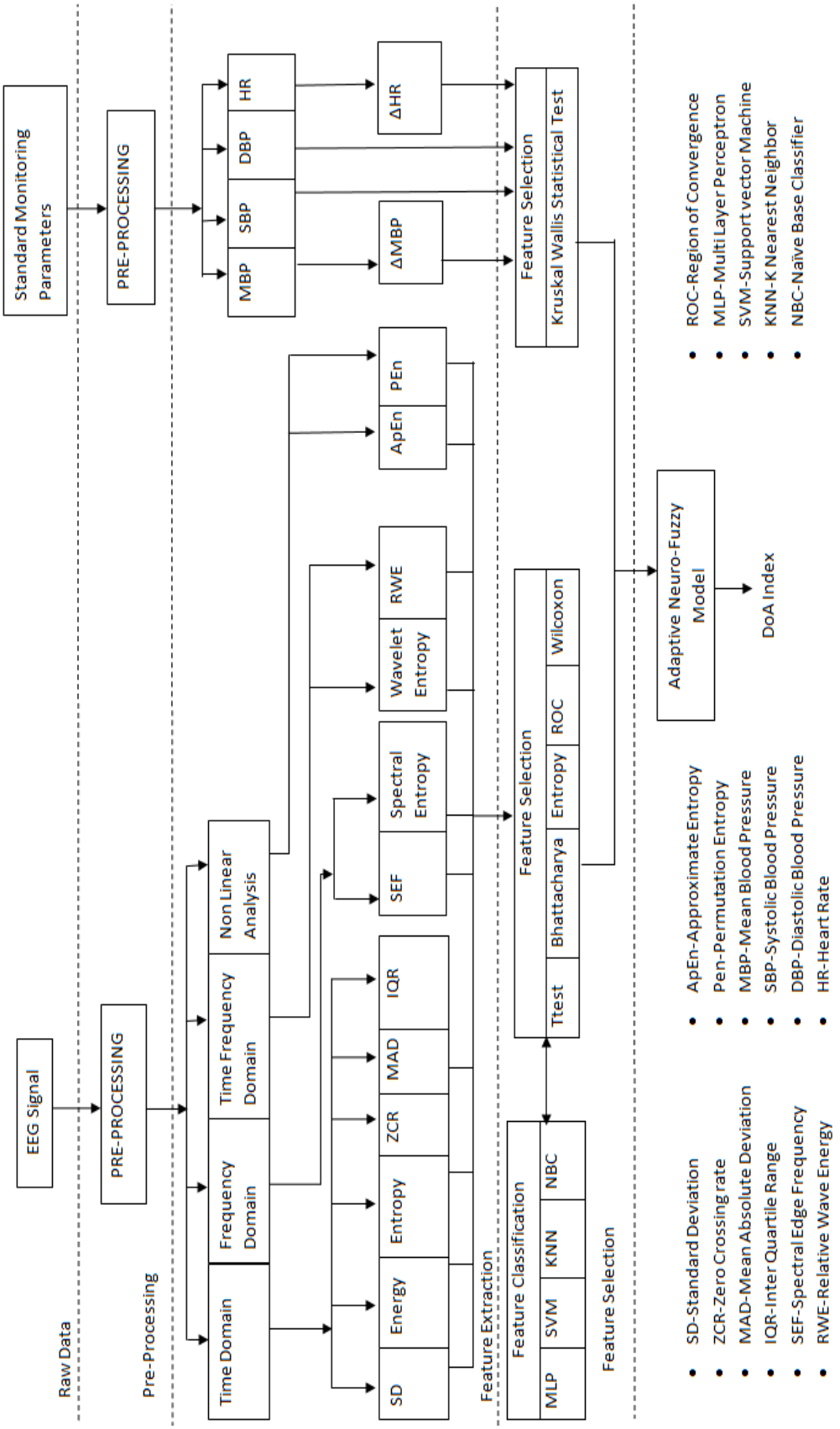

FIGURE 1.2: Conceptual Framework of the Research

frequencies. The time-frequency domain features wavelet entropy and relative wave energies are extracted to get the characteristics of EEG signals in both time and frequency domains. Nonlinear features like Approximate Entropy and Permutation Entropy are extracted to study the nonlinear behaviour of the EEG signals. The performance of the extracted EEG features are evaluated by comparing with commercially available BIS monitoring index of each patient. The dimensionality of the feature vectors are reduced by applying Feature selection by feature ranking methods. The algorithms used for feature ranking are T-Test, Bhattacharyya, Wilcoxon, ROC and Entropy. The combination of features which gives highest classification accuracy in the anaesthetic EEG classification as awake, light anaesthesia, moderate anaesthesia and deep anaesthesia is selected for the final DoA estimation model. The features extracted from the standard monitoring devices to study the analgesic effects of the patient are ΔHR and ΔMAP. Finally, the selected EEG features and the extracted standard monitoring device parameters are fed to a Neuro-fuzzy system to estimate the DoA Index. The efficiency of the model is checked using the response given by the anaesthesiologist.

1.8 Thesis organization

The thesis consists of eight chapters and each chapter contributes relevant information to establish the focus of our research.

Chapter 2-Literature Review : provides an overview of DoA monitoring techniques and its background knowledge. At first, this chapter briefly introduces the history of DoA monitoring and overviews various algorithms, the core features extracted from the signals and the methodology of analysis. This chapter also provides details of various commercially available DoA monitors.

Chapter 3-Data Acquisition : gives an idea of data acquisition techniques and the details of materials and equipment used for data acquisition. This chapter also explains how the collected data is converted into a readable form for the easiness of analysis. Finally, the demographic details of each data and their representation are also given.

Chapter 4-Pre-processing of Data to attenuate the effects of noises : explains how the data is prepared for further analysis. This chapter describes the signal processing and thresholding techniques used to remove the noises affected by the collected signals. It is organized into two parts describing the segmentation and filtering methods.

Chapter 5-Feature Extraction : has two parts. First part describes the feature extraction from the EEG signals which aims to reduce the dimensionality of the EEG signals and also helps to project the inherent properties of the EEG signal. The second part gives the extraction of features from the standard monitoring parameters.

Chapter 6-Feature Selection : has two sections. Feature ranking techniques rank the features based on their discrimination ability. This chapter covers various feature ranking techniques and how these techniques help to rank the features. Feature classification helps to select the best combination of features from the available feature set based on their classification accuracy.

Chapter 7- Adaptive Neuro-Fuzzy Inference System based Estimation of Depth of Anaesthesia : contributes the formulation of a neuro-fuzzy model using the multiple parameters. This chapter focuses on adaptive neuro-fuzzy model to generate an integrated index for depth of anaesthesia estimation

Chapter 8- Conclusion : provides a summary of the results and contributions of the research. This chapter also provides the information on the future scope of the work.

Chapter 2

Literature Survey

One of the most important achievements in modern anaesthesia research is the ability to measure DoA. During the last century researchers have gained new insights in the area of biological signal analysis to measure DoA. EEG, EMG, ECG and BP are the electrical representation of biological signals that reflect changes in the activity of the human brain, muscles, heart and blood vessels by the administration of anaesthetic drugs. Estimation of DoA is an important subject area since it helps to avoid patient awareness due to the inadequate dose of anaesthetic drugs and also overloading of anaesthetic drugs during the surgery.

This chapter provides the history of DoA monitoring and overviews the different techniques and methodologies available for the estimation of DoA. The clinical techniques used by anaesthesiologist for monitoring DoA are response to verbal commands, loss of eyelash reflex, sweating and lacrimation. Commonly accepted DoA monitoring technique is Evan's Scoring system. Isolated forearm technique and Surgical Stress monitor are some of the other techniques used for monitoring DoA. Numerous concepts and techniques have been developed, which are directed to quantify the changes in EEG signals during anaesthesia. These techniques were built on statistical or spectral analysis. Most of the EEG based DoA monitoring techniques extract different measures from time domain, frequency domain and time-frequency domain representations for the quantification of DoA. In addition to techniques and methodologies, this chapter presents some of the commercially

available DoA monitors like Bispectral Index, Narcotrend, Entropy, Patient State Index, Auditory Evoked Potential and Cerebral State Index.

2.1 History of DoA

Anaesthesia is an essential element of surgery. The discovery of anaesthetic effect of ether by William Morton in 1846 was a turning point in the history of anaesthesia. The two major concerns during ether anaesthesia were frequent awareness during the closing moments of anaesthesia and partial insensibility due to the brief periods of ether administration. The excitement produced by ether anaesthesia was prolonged and caused inevitable consequences. This is because the anaesthetic gas ether controls all the components of general anaesthesia. In 1847, John Snow made careful observations of the patient's responses to ether and described five levels of anaesthesia.

1. Consciousness and voluntary movement on command
2. Confused and disorderly voluntary movement on command
3. Unconsciousness and involuntary movement with respiration
4. Absence of involuntary movement with respiratory effort
5. Respiratory failure and eventual death

He recommended that patients should be operated in the fourth level of anaesthesia[Snow, 1953]. Table 2.1-2.3 presents the advancement in DoA in chronological order.

The concept of anaesthetic depth was the same over the next 90 years. In 1934 John Lundy analyzed intravenous anaesthetic agent thiopental sodium and introduced the concept of balanced anaesthesia with reduced use of multiple agents. Hence, GA became safe and the dose of each agent became reduced which resulted in fewer side effects. In 1937 Arthur Guedel designed a wall chart based on ocular signs, muscle tone and respiratory parameters. This chart gained wide acceptance

Year	Author	Method	Agents	Parameters	Insufficiency
1847	John Snow	5 level anaesthesia chart	Ether	Voluntary movement on command and respiratory efforts	Ether is explosive and has side effects
1937	Arthur Guedel	Guedel's Chart	Ether	Muscle tone, ocular sign and respiratory parameters	Pulse rate and Blood Pressure not considered
1950	Cecil Gray	Liverpool Technique	N2O, Oxygen and Curare	-	Inadequate anaesthesia and pain during surgery
1963	Merkel and Eger	Inhalational Anaesthesia	Fluorinated anaesthetics	MAC	Movement during surgery and inadequate anaesthesia and analgesia
1977	Tunstall	Isolated Forearm	Balanced anaesthesia	Movement of hand to indicate the awake or not	Difficulty in interpreting the results during anaesthesia
1991	Van de Velde and Cluitmans	Power spectral analysis on EEG signal	Balanced anaesthesia	Spectral Edge Frequency (SEF)	Unreliable autonomic responsesGhouri *et al.* [1993] and EEG based model
1998	Rampil et al.	EEG Analysis	Balanced anaesthesia	Absolute and relative power of EEG frequency bands, total power of EEG, median and spectral edge frequency	Depicts only the hypnotic component

Table 2.1: Developments of DoA in Chronological order

Year	Author	Method	Agents	Parameters	Insufficiency
2001	Zang et al.	Lempelziv Complexity analysis of EEG signal	Balanced anaesthesia	Complexity of EEG dynamics	Fails to capture the modulations of EEG signals when rapid rhythms of EEG signals present
2005	Gifani et al.	Detrend Fluctuation Analysis	Balanced anaesthesia	Correlation parameters	Difficulty in the discrimination of moderate to deep anaesthesia states
2006	Ferenets et al.	Nonlinear analysis	Balanced anaesthesia	Spectral entropy, Approximate entropy, Higuchi fractal dimension, Lempel-Ziv complexity	highly sensitive behaviour
2008	Esmaeili et al.	Integration of fuzzy logic concept and EEG features	Balanced anaesthesia	Spectral features and Burst suppression ratio	Unreliable autonomic responses and represents only the hypnotic components of anaesthesia
2013	Shalbaf et al.	Integration of EEG features and Artificial Neural Network	Balanced anaesthesia	Permutation Entropy	Fails to work in deep anaestheic states

TABLE 2.2: Developments of DoA in Chronological order

Year	Author	Method	Agents	Parameters	Insufficiency
2014	Schneider et al	Combination of EEG and hemodynamic features	Balanced anaesthesia	EEG parameters (Approximate Entropy and permutation entropy) and hemodynamic parameters (ΔMBP and HR)	Differentiate only the conscious and unconscious states [[Schneider *et al.* , 2014]]
2015	Sadrawi et al.	Integration of EEG features and Artificial Neural Network	Balanced anaesthesia	Sample entropy, HR, SBP and DBP	Variability in hemodynamic parameter values
2016	Mirsadeghi et al.	Locally Linear Embedding technique and quadratic discriminant analysis	Balanced anaesthesia	Linear and non-linear EEG parameters	Differentiate consciousness and unconsciousness only
2017	Kab-Mun Cha et al.	Quantification of Dominant Information Flow	Balanced anaesthesia	Mutual information and Transfer Entropy	Differentiate consciousness and unconsciousness only

Table 2.3: Developments of DoA in Chronological order

among the anaesthesiologists and became a useful tool to measure DoA[Atkinson & GB Lee, 1984]. As ether was explosive and had several side effects newer fluorinated anaesthetics like halothane, isoflurane, sevoflurane, desflurane were developed as inhalation agent. During the same period, intravenous anaesthetic drug paraldehyde along with intravenous opioid such as morphine was used in obstetric anaesthesia. This was popularly known as 'Twilight sleep' which was subsequently abandoned due to unpredictable side effects.

Claude Bernard in his study demonstrated that the muscle relaxant called curare acts between the skeletal muscle and the nerve[Paton, 1976]. Lewis H Wright convinced Herald R Griffith to use the drug curare during general anaesthesia for abdominal surgery. In 1950 Cecil Gray and his colleagues developed the popular 'Liverpool Technique' using Nitrous Oxide (N_2O), Oxygen (O_2) and curare that lead to light anaesthesia with profound muscle relaxation. This technique raised the issue of inadequate anaesthesia and waking of patient with excruciating pain during surgery. In 1954 D P Todd concluded that the use of curare leads to 6 fold increase in postoperative complication and death. Hence, curare was replaced with latest steroid based synthetic neuromuscular blocking agents such as Pancuronium and Vecuronium [Miller *et al.* , 2014].

The use of muscle relaxant and intravenous anaesthetic agents changed the concept of anaesthesia into balanced anaesthesia. Thus Guedel's chart became irrelevant and anaesthesiologist started relying on clinical parameters such as pulse rate, blood pressure and sweating. But these clinical parameters were inadequate to assess the DoA. In 1963 Merkel and Eger introduced the concept of the Minimum Alveolar Concentration (MAC) of inhalation agent at which 50% patient move in response to a painful stimulus. This concept significantly enhanced the understanding of volatile anaesthetic requirement and safe use of these drugs. MAC value helped the anaesthesiologist to calculate the amount of anaesthetic agent delivered to paralyzed patient. Eger drew attention to previous work by Seymore.S.Kety and Severinghaus that the end-tidal partial pressure of anaesthetic gases at the steady state was the same as the brain cerebral partial pressure of those gases. Hence, MAC has widely used as a measure of end-tidal vapour concentration [Miller *et al.* , 2014].

In 1977, Tunstall attempted to measure awareness using isolated forearm

technique in which a tourniquet was inflated immediately prior to the administration of muscle relaxant and the patient were informed to indicate whether he or she was awake by movement of hand. The drawback of the test was in interpreting the result as no patient would respond to commands during anaesthesia and none recalled the events. It neither prevented awareness and nor was an effective monitor [Tunstall, 1977]. But the discovery of electroencephalogram (EEG) by a German psychiatrist Hans Berger changed the concept of DoA and he suggested EEG for anaesthesia monitoring.

2.1.1 History of EEG based DoA Monitoring

In 1937 Gibbs et al. reported the transition of EEG activity from low voltage fast waves to high voltage slow waves after the administration of anaesthetic drugs. In 1952 Faulconer demonstrated that different arterial concentration of ether had different EEG patterns. He also demonstrated that presence of N_2O reduced the requirement of ether to produce the same effect on EEG pattern.

Analysis of EEG signals for exploring anaesthetic states lead to the evolution of different anaesthesia monitors. But the complexity of the EEG signals, as well as its high sensitivity to various types of artifacts, prevented the development in the area of anaesthetic monitoring for a long time. In 1991, Van de Velde and Cluitmans gauged DoA by assessing EEG spectra from cats and concluded that 'Spectral Edge Frequency' is a favourable EEG feature for the assessment of DoA [Van de Velde & Cluitmans, 1991; Gurman *et al.* , 1993]. In 1994, Watt et al. classified DoA as light, moderate and deep anaesthesia by considering EEG as a non-linear dynamic system. They found that adequate doses of anaesthetic agents make changes in EEG frequency with increasing anaesthetic depth. These changes in EEG frequency is favourable in the classification of EEG activity due to the anaesthetic drugs [Watt *et al.* , 1994].

Power spectral analysis is the classic methodology used for the quantification of EEG activity. It reflects the amount of EEG activity in different frequency bands. In power spectral analysis, EEG signal is digitized first and then Fast Fourier Transform (FFT) is applied to transform the time domain EEG signal to frequency

domain. In 1998 Rampil et al. suggested several EEG based variables like total power, absolute and relative power, median edge frequency and spectral edge frequency [Rampil, 1998].

In 2001 Zang et al. analyzed the complexity of EEG signals quantitatively using Lempelziv complexity (LZC) algorithm [Zhang *et al.* , 2001]. In LZC analysis the EEG signals are transformed into different sequences whose components are some symbols. A counter is used to count the number of distinct patterns present in the sequence. This counter is increased by one when a subsequence of consecutive characters is encountered in the scanning process. The complexity of EEG dynamics is high when the patient is awake because the brain is active during awake state. In the anaesthetized state, the brain activity is less and therefore the complexity measure shows low values. In between states indicate intermediate values with gradual scaling. In the same year, Gugino et al. studied the changes in EEG by the administration of anaesthetic drugs remifentanil, propofol and sevoflurane and found that light anaesthesia is accompanied by decreasing posterior alpha waves and increasing the intensity of frontal/central beta waves [Gugino *et al.* , 2001]. The insufficiency of LZC measures is that it fails to capture the modulations of EEG signals when the EEG contains rapid rhythms [Ibáñez-Molina *et al.* , 2015]. Also in real-world applications, they are easily affected by artifacts due to its sensitivity to the amplitude distribution [Bai *et al.* , 2015].

In 2005 Gifani et al. handled Detrended Fluctuation Analysis (DFA) on EEG signals to differentiate awake and anaesthetized states [Gifani *et al.* , 2005]). DFA on EEG signals provides a quantitative parameter based on the correlation properties of the signal. The dominance of DFA is that it allows detection of long-range correlations present in a non-stationary EEG signal. The DFA algorithm works on the fractal and self-similarity properties of EEG signals which are originated from the fractal structure and dynamic system of the brain. It detects the trend from the integrated EEG signals. The results of DFA on EEG signals can clearly discriminate awake to moderate anaesthesia levels but the moderate to deep anaesthesia states cannot be discriminated. This was further proved by Jospin et al. and Kaplan et al. in 2007 [Kaplan, 2006; Jospin *et al.* , 2007]. In order to overcome the difficulties of DFA in discriminating deep anaesthesia level, Nguyen et al. developed an improved detrended moving-average method in 2010[Nguyen-Ky *et al.* , 2010].

From 2006-2011 Fan et al. and Frenets et al. adopted nonlinear methods like approximate entropy, Lempel-Ziv complexity (LZC), spectral entropy and Higuchi fractal dimension (HFD) to measure EEG variations during anaesthesia [Fan *et al.* , 2011; Ferenets *et al.* , 2006]. Their results indicate that these measures are sensitive to the dose of anaesthetic agents and frequency of EEG signals [Ferenets *et al.* , 2007]. In 2014 Palendeng et al. used the phase and amplitude of EEG signals as measures of DoA [Palendeng *et al.* , 2014].

To improve the accuracy and performance of DoA monitors the extracted features were broadened to include techniques commonly associated with intelligent systems. Most of the medical research applications uses intelligent techniques for the estimation and classification of different physiological signals [Yuvaraj *et al.* , 2014], [Nguyen *et al.* , 2015], [Übeyli, 2009b]. The intelligent modelling in DoA monitoring incorporates the EEG measures as input to the Artificial Neural Network, Fuzzy Inference systems and Hybrid systems. In 2008 Esmaeili et al. developed a fuzzy rule-based system that integrates EEG features for the estimation of DoA. Here the designed fuzzy classifier trains the system to learn the awake and anaesthetized states from spectral EEG measures [Baig *et al.* , 2011; Esmaeili *et al.* , 2008]. In 2013 the classification of DoA using ANN and EEG extracted permutation entropy was done by Shalbaf et al. [Shalbaf *et al.* , 2013]. But the computation of Permutation Entropy (PEn) is efficient in EEG analysis but it fails to work in deep anaesthetic states [Shalbaf *et al.* , 2014].

There are several EEG based DoA monitors commercially available and among these monitors, BIS monitor developed by Aspect Medical Systems in 1996 is found to be a reliable comparison standard for DoA monitoring due to its usefulness and effectiveness. BIS monitor provides a dimensionless index ranging from 0 to 100. 0 indicate no brain activity state (brain dead state) and 100 indicate fully awake state. The range 0 - 100 can be subdivided into five states. The range 0-20 is the burst suppression state considered to be very deep anaesthetic state, 20-40 is deep anaesthetic state, 40-60 moderate anaesthetic state, 60-80 light anaesthetic state and 80-100 is awake state. Moderate anaesthesia state is considered to be an appropriate level for surgery under general anaesthesia [Zoughi *et al.* , 2012].

The limitations of BIS and EEG based DoA monitors is that these monitors

cannot reliably detect all the levels of anaesthesia because of the changes in clinical applications. EEG patterns are influenced by the age of the patient as the neurons are lost irreversibly during normal ageing and EEG amplitude decreases as age advances [Shalbaf *et al.* , 2013; Nguyen-Ky *et al.* , 2013]. Several case reports have been reported that these monitors are unable to distinguish between the awake and anaesthetized state [Messner *et al.* , 2003; Pilge *et al.* , 2006; Zanner *et al.* , 2009; Schneider *et al.* , 2004].

Other limitations BIS and other existing monitors are that they showed a long time delay in the transition from awake to anaesthetised state and vice-versa. The estimated time delay of BIS index is 61 sec, Narcotrend monitor is 90 sec, Entropy module showed high time delay but no specific data is available and Cerebral State Index module showed 106 sec time delay [Musizza & Ribaric, 2010]. Although the BIS index is a popular one, it received some criticisms, such as non-responsive to some anaesthetic agents [Johansen *et al.* , 2000] and not robust across patients [Hall & Lockwood, 1998]. Therefore it is not reliable to measure DoA with the features extracted from EEG alone, but rather preferred the use of multiple features that characterize different levels of anaesthesia from awake to deep anaesthesia [Kortelainen *et al.* , 2011].

Anaesthetic drugs act on the CNS and autonomic nervous system. EEG based monitors process the activity of the CNS only. The activities of autonomic nervous system are reflected by the changes in hemodynamic parameters. The hemodynamic parameters that reflect the changes in DoA are Heart Rate (HR) which is derived from the Electrocardiogram (ECG) and Mean Arterial Pressure (MAP) which is derived from non-invasive blood pressure signals Systolic Blood Pressure (SBP) and Diastolic Blood Pressure (DBP). These hemodynamic parameters vary with different levels of anaesthesia [Baharav *et al.* , 1995; Shieh *et al.* , 2005]. This challenge opens new possibilities for the researchers to integrate the EEG features and hemodynamic features. As a result, Schneider et al. in 2014, Shalbaf et al. and Sadrawi et al. in 2015 tried to monitor DoA by combining hemodynamic parameters and EEG parameters [Schneider *et al.* , 2014; Sadrawi *et al.* , 2015; Shalbaf *et al.* , 2015]. In 2016 Mirsadeghi et al. differentiated consciousness and unconsciousness using Locally Linear Embedding technique and quadratic discriminant analysis. The Locally Linear Embedding technique is used for the dimensionality

reduction of the EEG features [Mirsadeghi *et al.* , 2016]. The latest development in DoA estimation was done by Kab-Mun Cha et al. in 2017 and the study quantifies the dominant information flow in multichannel EEG signals [Cha *et al.* , 2017].

2.2 Basic Methods and Techniques for monitoring DoA

There are many conventional methods to estimate DoA. They are mainly based on the clinical signs and brain electrical activity. The clinical signs are used to assess the intraoperative consciousness through surrogate indicators. The brain electrical activity monitoring estimate consciousness based on the response on EEG, EMG and Evoked potential due to the anaesthetic drugs.

2.2.1 Clinical techniques and conventional monitoring

The clinical techniques used for monitoring DoA are movement of the patient, response of the patient to verbal commands, loss of eyelash reflex, pupillary response, sweating and lacrimation. These techniques are simple, easy to perform and do not require any computational analysis. One of the commonly used conventional monitoring technique is Patient Response to Surgical Stimulus (PRST) also called Evan's scoring system where P, R, S, T stands for SBP, HR, Sweating and Tears respectively. The score ranges from 0-8. But it is a poor indicator of awareness as the hemodynamic response alone does not reflect the awareness or recall. This scoring system provides an useful information regarding the adequacy of analgesia. Details of Evan's scoring system is given in Table 2.4 [Sinha *et al.* , 2007].

The drawback of the scoring system was that the various drugs such as Beta blockers and opioid blunt the hemodynamic responses to pain. The local anaesthesia techniques also dampen the sympathetic response to pain. The anticholinergic drugs increase HR without the response to pain. This cause drying of secretion and prevent lacrimation [Ghoneim & Block, 1997; Moerman *et al.* , 1993]. Intraoperative consciousness can also be assessed by reflex and purposeful movement of patient.

TABLE 2.4: PRST Scoring System [KAUL *et al.* , 2002; EVANS & DAVIES, 1984]

Index	Condition	score
SBP	<Base Value+15 mmHg	0
	<Base Value+30 mmHg	1
	>Base Value+30 mmHg	2
HR	<Base Value+15 bpm	0
	<Base Value+30 bpm	1
	>Base Value+30 bpm	2
Sweating	Nil	0
	Skin moist	1
	Visible beads of sweat	2
Tears	No excess tears in open eyes	0
	Excess tears in open eyes	1
	Tears over flowing	2

But neuromuscular blocking agents prevent reflex and purposeful movement even in the presence of pain. The studies of Sandin et al. and Sebel et al. have also proved that the use of muscle relaxants does not inhibit the response of awareness [SEBEL *et al.* , 2004; SANDIN *et al.* , 2000].

2.2.2 Isolated forearm technique

Isolated forearm technique is an experimental method for assessing awareness under GA and was also used in various clinical trials for assessing awareness. In this method, a tourniquet placed on patient's forearm was inflated above the SBP just before giving the muscle relaxant. After the administration of muscle relaxant, the patient has to move his/her hand according to verbal command. It is late indicative of intraoperative awareness and not all the patients recall the event. This technique does not prevent awareness and can only be used for limited time as it would limit the blood flow to the forearm [RUSSELL, 1993; TUNSTALL, 1977].

2.2.3 Surgical Stress Monitoring

Surgical Stress Index (SSI) was developed by Huiku et al. and it was later known as Surgical Pleth Index. SSI helps to quantify the surgical stress level of anaesthetized

patients. SSI measures the balance between intensity of surgical stimulation and the level of antinociception (opioid analgesia). SSI uses two parameters collected from photoplethysmographic (PPG) waveforms [Huiku *et al.* , 2007]. The parameters are the PPG waveform Amplitude (PPGA) and the Heart Beat-to-beat Interval (HBI). The index range from 0 to 100 and values near 100 correspond to high-stress level and values near zero represent low-stress level. SSI is calculated using the equation

$$SSI = 100 - (0.7PPGA + 0.3HBI). \tag{2.1}$$

But the disadvantage of SSI is that it is minimally influenced by changes in the hypnotic drug concentration whereas SSI is strongly dependent on the analgesic concentration. Therefore SSI is used as a better measure of analgesia [Struys *et al.* , 2007].

2.2.4 EEG based methods and techniques

During the last two decades, several methods based on EEG signals such as time domain measures, frequency domain measures, time-frequency measures, entropy measures and nonlinear dynamic measures have been proposed to evaluate the level of consciousness during anaesthesia. The basic technologies behind all these measures are depicted below.

2.2.4.1 Time Domain measures

The time domain measures of EEG signals are characterized by the amplitude distribution and its moment of action.

Statistical Measures : The basic statistical features that describe the EEG characteristics during anaesthesia are listed in Table 2.5

Hjorth parameters : The Hjorth parameters are the measures of signal complexity. These measures are used in the analysis of EEG during sleep [Koht *et al.* ,

TABLE 2.5: Statistical measures of EEG analysis

Fature	Description
Mean	$\bar{x} = \frac{1}{n}\sum_{i=1}^{n} x_i$
Standard Deviation	$\sigma_x = \sqrt{\frac{1}{n}\sum_{i=1}^{n}(x_i - \bar{x})^2}$
Maximum Value	Maximum positive amplitude
Minimum Value	Maximum negative amplitude
Skewness	Measure of asymmetry of the distribution, $S = \frac{\frac{1}{n}\sum_{i=1}^{n}(x_i-\bar{x})^3}{\sigma_x^3}$ [BEDEEUZZAMAN *et al.* , 2014]
Kurtosis	Measure of flatness of the distribution, $K = \frac{\frac{1}{n}\sum_{i=1}^{n}(x_i-\bar{x})^4}{\sigma_x^4}$ [BEDEEUZZAMAN *et al.* , 2014]
Median	The middle value of set of ordered data

2012]and they are clinically useful tools for the quantitative description of an EEG [HJORTH, 1970]. The Hjorth parameters are mobility and complexity. Mobility is defined by equation 2.2

$$Mobility = \delta_x = \frac{\sigma'_x}{\sigma_x} \tag{2.2}$$

where σ_x the variance of the time function and its value returns a large value if high frequency components of the signal exists and vice versa, σ'_x is the first derivative of variance. The mobility parameter has a proportion of standard deviation of power spectrum.

Complexity is the 2^{nd} Hjorth parameter and is given by

$$Complexity = \lambda_x = \frac{\sigma''_x/\sigma'_x}{\sigma'_x/\sigma_x} \tag{2.3}$$

where σ''_x is the second derivative of variance. Complexity parameter indicates how the shape of a signal is similar to a pure sine wave. The value of complexity converges to 1 as the shape of the signal gets more similar to a pure sine wave.

Burst Suppression Detection Burst suppression is an EEG pattern which has periods of high-voltage electrical activity alternating with periods of no activity in the brain. This pattern is commonly found in patients with inactivated brain states due to general anaesthesia, coma and hypothermia. In order to quantify the burst suppression patterns, the EEG signals were subjected to thresholding and segmentation functions. This process separates burst and suppression patterns based on the threshold voltage level. When the voltage of a particular EEG segment is below the threshold level, it is classified as suppression and when it exceeds the threshold, it is considered a burst. Burst Suppression Ratio (BSR) is the most common burst suppression derivative in anaesthesia practice and is proposed by Rampil et al. [Rampil, 1998]. It assigns binary values of 0 to bursts and 1 to suppression patterns. If the BSR is 1 then it is indicated as a state with no electrical activity in the brain, while the ratio shows 0 indicate that the brain is active. BSR is calculated using the equation 2.4 [Liang *et al.* , 2014].

$$BSR\% = \frac{total\ time\ of\ suppression}{epoch\ length} * 100\% \tag{2.4}$$

2.2.4.2 Frequency Domain measures

The basic technology behind frequency based EEG signal processing is the Fourier Transform (FT) in which signals from the time domain is transformed to the frequency domain. Since the EEG signals were recorded digitally, the Discrete Fourier Transform (DFT) is commonly used to calculate the frequency components of the signals. The DFT decomposes a sequence of values into components of different frequencies. The discrete-time Fourier transform of a sequence $x(n)$ is defined as

$$X(e^{j\omega}) = \sum_{n=-\infty}^{\infty} x(n)e^{-j\omega n} \tag{2.5}$$

where the time index n is discrete, and ω is the normalized frequency. If there is a finite duration signal with N samples then Discrete Fourier transform (DFT) is defined as

$$X(k) = \sum_{n=0}^{N-1} x(n)W_N^{nk} \leftrightarrow x(n) = \frac{1}{N}\sum_{k=0}^{N-1} X(k)W_N^{-nk} \tag{2.6}$$

where $W = e^{\frac{-j2\pi}{N}}$.

An efficient algorithm to compute the DFT is Fast Fourier Transform (FFT). The DFT or FFT of a real signal is a complex number, having a real and an imaginary part. The power in each frequency component represented by the DFT or FFT is obtained by squaring the magnitude of that frequency component. Thus, the power in the k^{th} frequency component i.e. the k^{th} element of the DFT or FFT is calculated using the equation 2.7 [Stoica & Moses, 1997; Marple & Marple, 1987].

$$P_k = \left|X[k]\right|^2 \tag{2.7}$$

where $\left|X[k]\right|$ is the magnitude of the frequency component.

Power Spectral Density (PSD) PSD defines the distribution of the power of a signal in frequency domain. PSD is generally evaluated by taking square of the Fourier Transform of a signal or by evaluating the Fourier transform of the autocorrelation function of a signal [Stoica & Moses, 1997; Marple & Marple, 1987]. They are the most commonly used feature in the development of DoA monitors and served as one of the efficient ways to identify a large number of neurophysiological signals. The power spectrum returns an array that contains the two-sided power spectrum of a time-domain signal and that shows the power in each of the frequency components.

2.2.4.3 Time-Frequency domain measures

Wavelet Analysis is a time-frequency analysis method which is capable of representing the characteristics of a signal in both time and frequency domains. At low frequencies, it gives lower time resolution and high frequency resolution. At high frequencies it gives high time resolution and lower frequency resolution. Basic wavelet function is given by the equation

$$\Psi_{a,b}(t) = \frac{1}{\sqrt{a}}\Psi(\frac{t-b}{a}) \tag{2.8}$$

where a is the scale parameter and the b is the translation parameter. The Wavelet Transform of a signal is given by the equation

$$W(a,b) = \int x(t) \frac{1}{\sqrt{(a)}} \Psi(\frac{t-b}{a}) dt \tag{2.9}$$

where $W(a,b)$ is the Wavelet coefficients of the signal $x(t)$

Discrete Wavelet Transform (DWT) is commonly used for EEG signal analysis and can capture various signal features like breakpoints, discontinuities, general trends and self-similarities. DWT splits the EEG signals into different frequency components which decide the five EEG rhythms: δ-band, θ-band, α-band, β-band and γ-band. DWT with Mallat's fast algorithm is commonly used for EEG signal analysis [Mallat, 2008]. DWT can be interpreted as multi-stage filter banks with High-Pass (HP) and Low -Pass (LP) filters performing a series of dilation. Coefficients obtained after the HP filters are called detail coefficients while those after the LP filter are called the approximation coefficients. Figure 2.1 shows the discrete wavelet decomposition of a signal x(n).

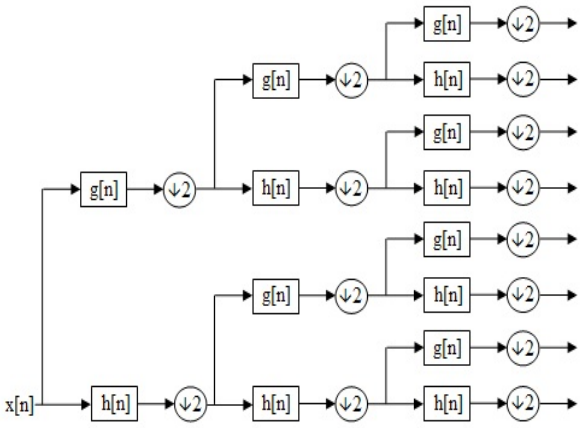

Figure 2.1: DWT decomposition

At each level, the approximation/detail coefficients represent a filtered signal spanning i.e. only half of the frequency band. This improves the frequency resolution as the frequency uncertainty is reduced by half. Following the Nyquist's theorem, the output of each LP and HP filter is decimated by a factor of two. Various features that can be extracted from EEG signals after wavelet domain representation are statistical features, zero crossing rate and wavelet energy. In EEG

signal analysis $x[n]$ represents the EEG signal and was passed through a high pass filter $g[n]$ and a low pass filter $h[n]$. Half of the samples were considered for further analysis according to Nyquist rule. Decomposition of EEG signals into Detail and Approximation coefficients are done with the equations 2.10 and 2.11 [Chun-Lin, 2010; Kessler *et al.* , 2003]

$$cA_j(n) = \Sigma g(l - 2n)cA_{j-1}(l) \tag{2.10}$$

$$cD_j(n) = \Sigma h(l - 2n)cD_{j-1}(l) \tag{2.11}$$

where $cD_j(n)$ and $cA_j(n)$ represents the Detail and Approximation coefficients of the EEG signal, h and g represents low pass and high pass filters to filter the EEG signals. The actual signal is obtained by combining all the coefficients starting from last level of decomposition. This type of decomposition provides good time resolution at high frequencies and good frequency resolution at low frequencies [Polikar, 1996].

2.3 Commercially available DoA Monitors

DoA monitors were developed during the last century. Most of these monitors were EEG based DoA monitors. In addition to EEG based DoA monitors MAC based DoA monitors are also available which measure the concentration of inhalational agents. Some of the commercially available DoA monitors are shown in Table 2.6.

2.3.1 BIS Monitor

The BIS monitor was introduced by Aspect Medical Systems in 1992. Bispectral analysis is the main component of the BIS monitor. It measures the phase relation of the single channel EEG signals collected from patient's forehead. The BIS monitor generates a dimensionless index 0-100 depending on the DoA. Rampil et al. disclosed some parts of the algorithm in 1998 [Rampil, 1998]. The basic block diagram of the BIS algorithm is depicted in Figure 2.2. The single channel EEG signal collected

TABLE 2.6: Commercially available DoA Monitors[AL-KADI *et al.* , 2013]

Monitor	Company	Index range	Works with Agents	Not Work with Agents
BIS	Aspect Medical Systems; Now Covidien, USA, 1992	0-100	Propofol, midazolam and isoflurane	Nitrous Oxide and ketamine
Narcotrend	Monitor Technik, Germany, 2000	0-100	Sevoflurane, propofol/remifentanil	Neuromuscular blocking agents
Entropy	Datex-Ohmeda Company in 2003	0-100, 1–91	Desflurane, sevoflurane, propofol and thiopental	Ketamine
Patient State Index	Physiomatrix, USA,2001 ,Now SED Line Systems	0-100	Propofol, alfentanil, nitrous oxide	-
AEP	Danmeter, Denmark, 2001	0-100 or 0-60	Propofol, midazolam and isoflurane	Nitrous oxide and ketamine
Cerebral State Index	Danmeter A/S,Denmark, 2004	0-100	Propofol	nitrous oxide

from the patient is sampled and preprocessed. Preprocessing stage performs the artifact detection and removal algorithms. BIS algorithm detects two suppression parameters. They are Burst Suppression Ratio (BSR) and Quazi Suppression Rate (QSR). BSR is calculated from the intervals over 0.5 seconds in which EEG voltage is below $\pm$ 5.0μ V. EEG signals having amplitude within the $\pm$ 5.0μ V limit are called isoelectric EEG signals. QSR was calculated to detect burst suppression of erratic EEG signals due to the power line interference and baseline drift. The frequency analysis of BIS algorithm extracts the parameter relative β power and is calculated using the equation 2.12 [MUSIZZA & RIBARIC, 2010]. Relative β power is defined as the logarithm of ratio of sums of spectral energies of frequencies bands between

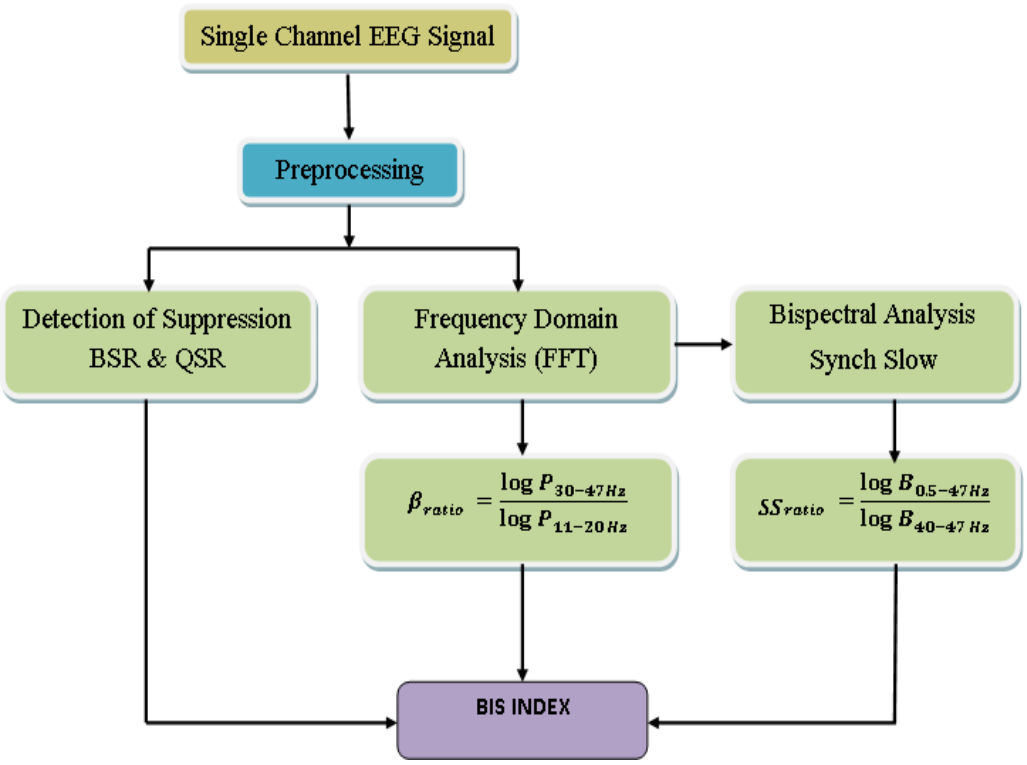

FIGURE 2.2: Block diagram of BIS algorithm

30-47Hz and 11-20Hz.

$$\beta_{ratio} = \log \frac{P_{30-47Hz}}{P_{11-20Hz}} \tag{2.12}$$

The bispectral analysis measures the phase correlation of waves obtained by Fourier analysis among different frequencies. This analysis helps to suppress Gaussian noise, to increase *signal/noise* ratio, to identify non-linear situations. Another parameter extracted from bispectral is the SyncFastSlow and is calculated using the equation 2.13

$$SS_{ratio} = \log \frac{B_{0.5-47Hz}}{B_{40-47Hz}} \tag{2.13}$$

It is defined as the logarithm of ratio of sum of all spectral peaks between 0.5–47 Hz and 40–47 Hz. Finally, all parameters are fed to a weighting algorithm, which produces the BIS index [BRUHN *et al.* , 2000b, 2006; VAKKURI, 2006; NUNES *et al.* , 2012].

2.3.2 Narcotrend Monitor

The Narcotrend monitor was introduced by MonitorTechnik in the year 2000. The algorithm of Narcotrend monitor is presented in Figure 2.3. Here the time domain and frequency domain features were extracted from the EEG signal for analysis. The extracted spectral parameters include relative δ, θ, α, β, Spectral Edge frequency (SEF), Median Frequency (MEF), spectral entropy and time domain features such as Autoregressive (AR) parameters [Bauerle *et al.* , 2004; Kreuer & Wilhelm, 2006].

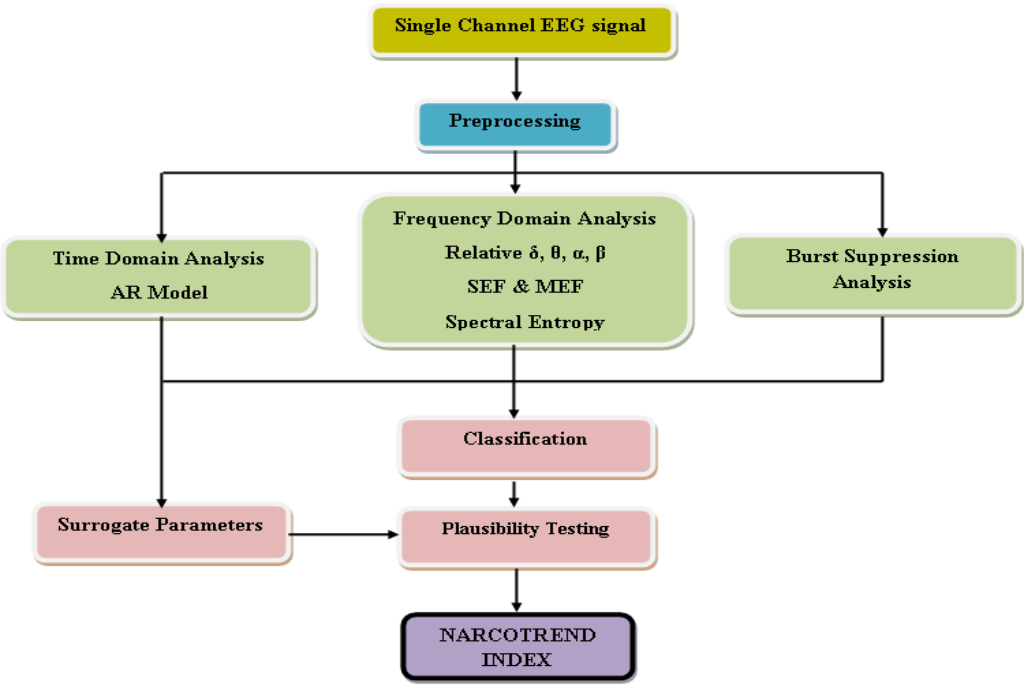

Figure 2.3: Block diagram of Narcotrend algorithm

Burst Suppression (BS) analysis was done similar to BIS index. The extracted features were passed through a classification function which classifies the state of anaesthesia into five stages according to the work of Loomis et al. as A-alpha, B-low voltage, C-spindle, D-spindle, E-random [Loomis *et al.* , 1937]. The monitor calculates the surrogate parameters and was used in plausibility testing of the generated index. Latest versions of the monitor generate the index range (0–100) similar to BIS [Kreuer *et al.* , 2003].

2.3.3 Entropy Monitor

Entropy Monitor was introduced by the Datex-Ohmeda in 2003. The idea behind the Entropy Monitor is that increasing depth of anaesthesia increases the regularity of the EEG signals and was inferred by the measure entropy. The block diagram of the Entropy Monitoring algorithm is presented in Figure 2.4.

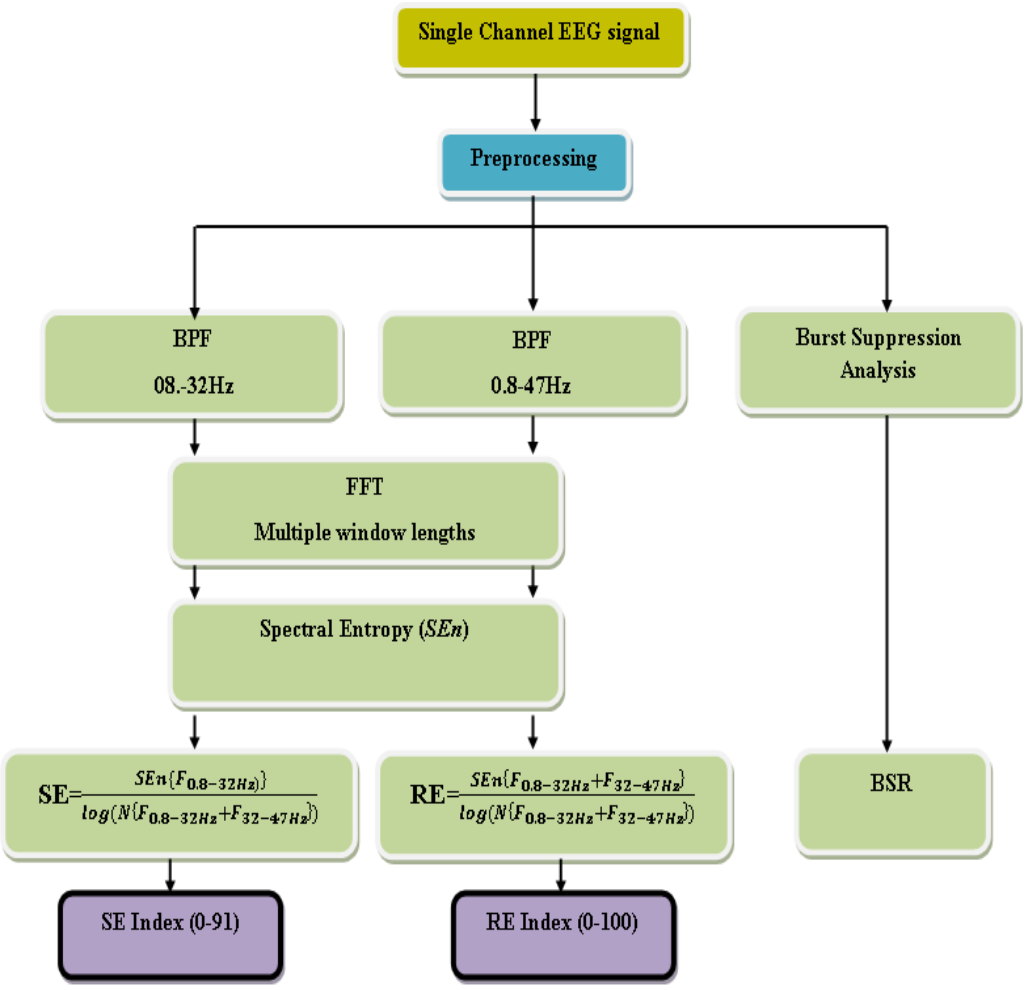

FIGURE 2.4: Block diagram of Entropy index algorithm

After digitization and preprocessing, the signal is divided into two frequency bands 0.8–32 Hz and 0.8–47 Hz. Then FFT of both the bands was calculated with various window lengths. This technique is similar to wavelet analysis, where different window lengths ensure optimal resolution for each frequency band. The spectral entropy is then calculated from the power spectrum of the particular epoch of the signal within a particular frequency band. The features extracted are

State Entropy (SE) and Response Entropy (RE) using the equations 2.14 and 2.15 [Musizza & Ribaric, 2010].

$$SE = \frac{SEn[F_{0.8-32Hz}]}{\log(N[F_{0.8-32Hz} + F_{32-47Hz}])} \tag{2.14}$$

$$RE = \frac{SEn[F_{0.8-32Hz} + F_{32-47Hz}]}{\log(N[F_{0.8-32Hz} + F_{32-47Hz}])} \tag{2.15}$$

where SEn is the spectral entropy, N is the total number of frequency components, $F_{0.8-32Hz}$ is the frequency range from 0.8 Hz to 32 Hz, $F_{32-47Hz}$ is the frequency range from 32 Hz to 47 Hz and $F_{0.8-32Hz} + F_{32-47Hz}$ is the frequency range from 0.8 Hz to 47 Hz. The state entropy generates an index from 0 to 91 and RE generates an index from 0 to 100. Burst suppression analysis was done to extract the BSR. The discrepancy of entropy monitor is that it generates two indices. The index generated by SE incorporates the information from EEG frequency bands only whereas RE contains information from EMG frequency bands. Entropy module doesn't generate a single index like BIS or Narcotrend monitor. The two indices are interpreted as if the difference between the two are more than 10 then increased EMG activity otherwise only the EEG activity [Viertiö-Oja *et al.* , 2004].

2.3.4 Patient State Index (PSI) Monitor

The PSI monitor was developed by the Physiometrix in 2001. PSI uses 4 channel EEG signals for the analysis. Figure 2.5 shows the block diagram of PSI. At first frequency domain analysis was applied to get the specific EEG frequency bands $(\delta, \theta, \alpha, \beta, \ and\ \gamma)$ and of total EEG frequency band(0–50 Hz). Then six features were extracted from the EEG power spectrum. They are 1) Absolute power gradient between front-polar and vertex regions in γ, 2) Absolute power changes between midline frontal and central regions in β and between midline frontal and parietal region in α, 3) Total spectral power in the front-polar region, 4) Mean frequency of the total spectrum in midline frontal region, 5) Absolute power in the δ band at the vertex and 6) Posterior relative power in slow δ[Musizza & Ribaric, 2010]. All

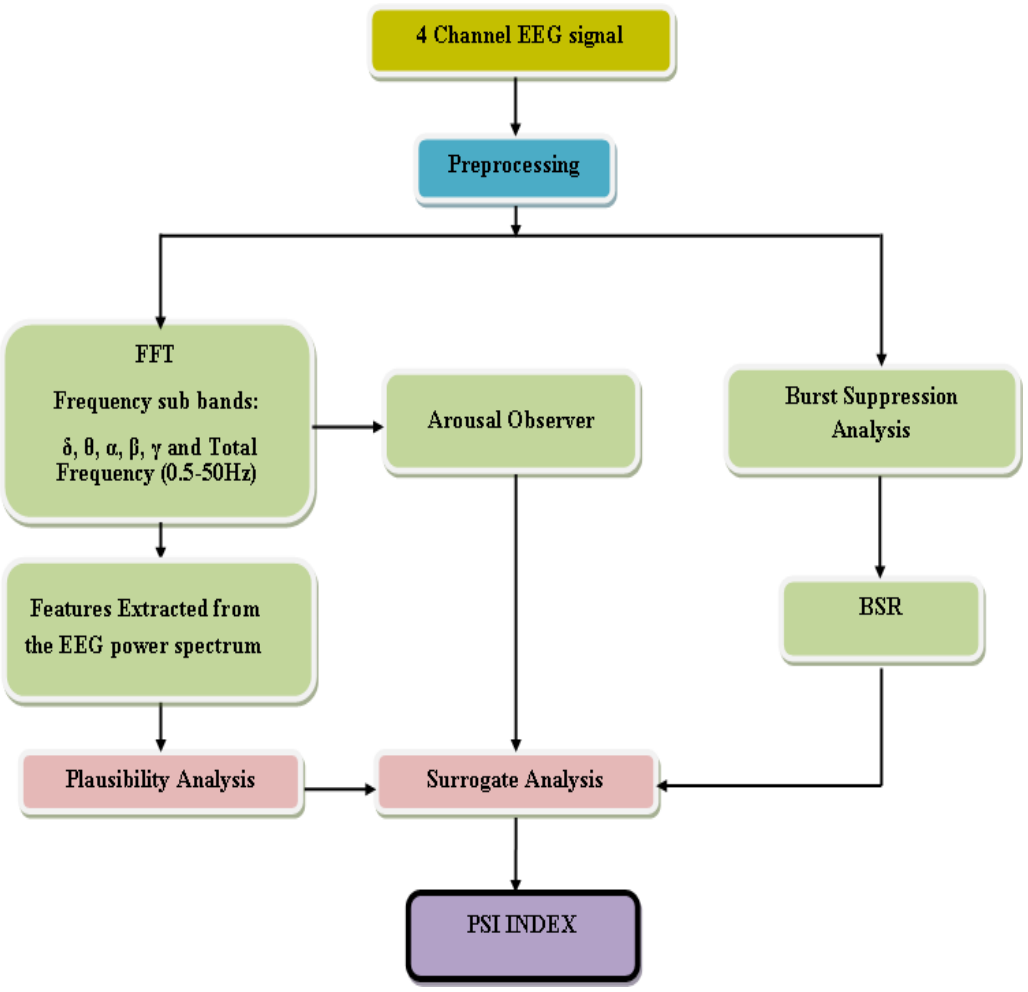

FIGURE 2.5: Block diagram of Patient State Index algorithm

the extracted features met with a plausibility analysis and a surrogate analysis. The surrogate analysis includes BSR and arousal score. Arousal scores were assigned retrospectively to each stage using the Observer's Assessment of Alertness/Sedation Scale (OAA/S). OAA/S rated 0 to 5 based on patient's response to verbal commands and painful stimuli. Finally, the Patient State Index (PSI) was calculated using an averaging algorithm and which generate a dimensionless index from 0 to 100 similar to BIS [MUSIZZA & RIBARIC, 2010; PRICHEP *et al.* , 2004; DROVER & ORTEGA, 2006].

2.3.5 Auditory Evoked Potential (AEP) Monitor

The AEP monitor was introduced by Danmeter in 2001. The new version of the AEP monitor is called AEP-ARX-Index (also called A-line autoregressive index (AAI)), which is not only based on AEP, but it also includes EEG spectral parameters. The monitor uses autoregressive models with exogenous input (ARX) to detect the AEP. The ARX was used because the method enables fast responses of the monitor. AAI can be scaled as 0 to 60 or 0 to 100. The second scale is recommended and the optimal anaesthesia is achieved if the index values are between 15 and 25. The algorithm of the AEP index is shown in Figure 2.6.

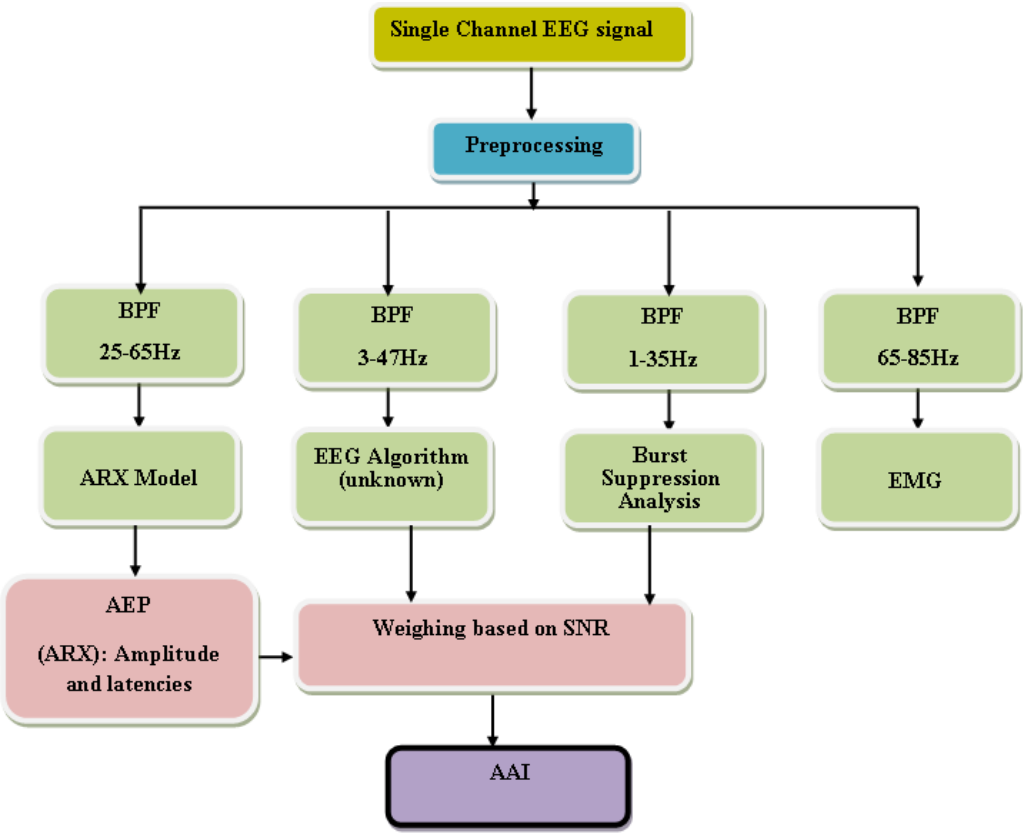

FIGURE 2.6: Block diagram of Auditory Evoked Potential algorithm

After digitization and preprocessing the signal is passed through several band-pass filters (BPF) to detect various features in different frequency bands. The AEP index is calculated from the frequency range 25–65 Hz and which uses the ARX model. The reconstructed amplitudes and latencies are evaluated after the ARX analysis. At the same time the frequency band 3–47Hz is analyzed by an

undisclosed algorithm which evaluates the propagation of EMG in the frequency band. The AAI is generated using the equation 2.16 [Musizza & Ribaric, 2010].

$$AAI = k_0 AEP + k_1 \log \frac{P_{30-47Hz}}{P_{10-20Hz}} + k_2 BS \tag{2.16}$$

Where Where P_{m-n} is the sum of the spectral power in the frequency band m to n. Burst Suppression (BS) is the percentage of burst suppression patterns detected during the last 30 s and is given by the equation 2.17.

$$BS\% = \frac{t_{BS}}{30\ Seconds} \tag{2.17}$$

where t_{BS} is the Burst Suppression time and $k0$, $k1$, and $k2$ are functions of the Signal to Noise Ratio (SNR) and were determined during the averaging process of the raw signal. It evaluates the detection quality of the signal under investigation [Vereecke *et al.* , 2005; Horn *et al.* , 2009; Plourde, 2006].

2.3.6 Cerebral State Index (CSI) Monitor

The Cerebral State Index (CSI) monitor was introduced by the Danmeter in 2004. This monitor algorithm is based on the EEG-algorithm of AEP and both use same electrodes to collect the EEG signals. The advantage of CSI monitor is that it is portable and the wireless device present in the monitor uses fuzzy logic to calculate the CSI. The algorithm is depicted in Figure 2.7. At first one channel EEG signals were preprocessed and passed through an artifact removal algorithm. The features extracted from frequency domain analysis are β_{ratio}, α_{ratio} and D_{ratio} and were calculated using the equations 2.18-2.20 [Musizza & Ribaric, 2010].

$$\beta_{ratio} = log \frac{P_{30-42.5Hz}}{P_{11-21Hz}} \tag{2.18}$$

$$\alpha_{ratio} = log \frac{P_{30-42.5Hz}}{P_{6-12Hz}} \tag{2.19}$$

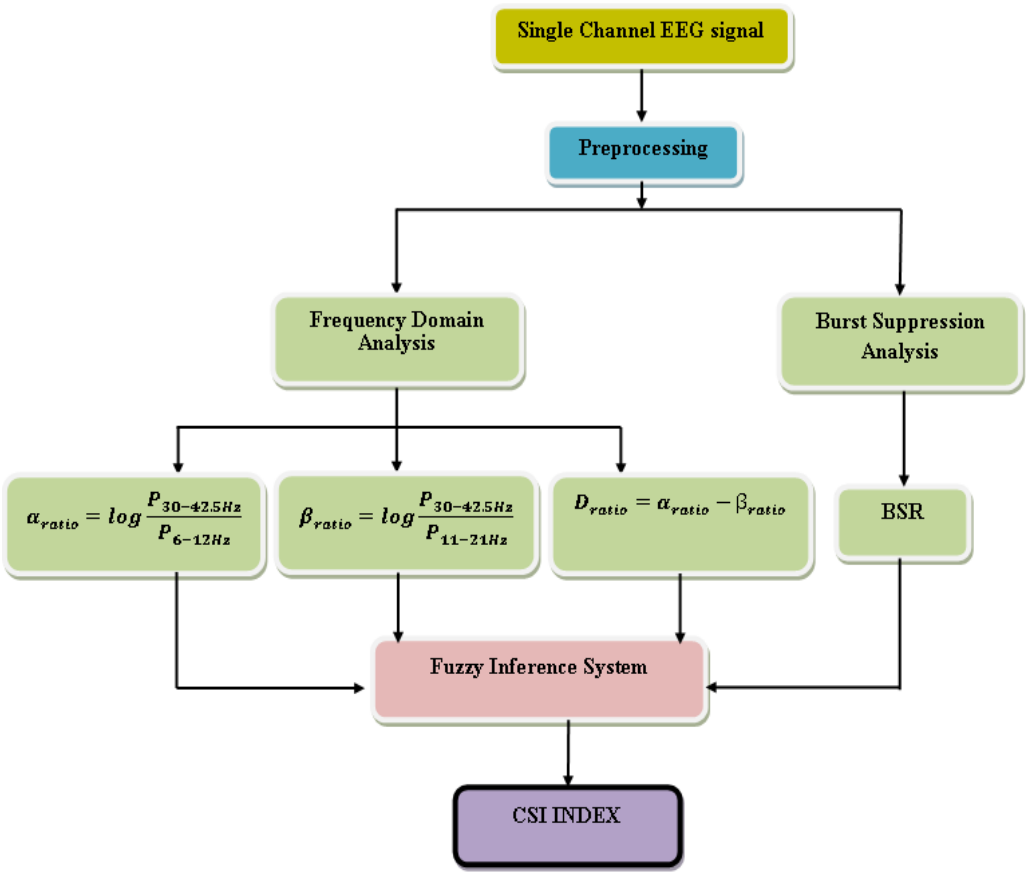

FIGURE 2.7: Block diagram of Cerebral State Index algorithm

$$D_{ratio} = \alpha_{ratio} - \beta_{ratio} \tag{2.20}$$

where P_{m-n} is the sum of the spectral power in the frequency band m to n.

Burst suppression analysis was performed to extract the feature BSR. The Burst Suppression (BS)% is calculated using the same equation as in 2.17. Finally, all the extracted features were fed to a Fuzzy Inference System as input to calculate the Cerebral State Index (CSI). The CSI monitor displays the CSI Index, EMG and BSR value [JENSEN, 2005].

2.3.7 Index of Consciousness (IoC) Monitor

The Index of Consciousness (IoC) monitor was developed by the Morpheus Medical in 2007. The algorithm of IoC is presented in Figure 2.8. The features extracted from

EEG signals are frequency domain parameter β_{ratio} and a nonlinear parameter. In the nonlinear analysis, EEG signals are divided into subunits and assign a symbol to each unit. The symbolic dynamics detects the complex non-linear properties of the EEG and the outcome is inferred to DoA. Additionally, burst suppression analysis was done to extract the feature BSR. Finally, all the extracted features were combined through fuzzy logic system to generate an index from 0-100 [Jensen *et al.* , 2008; Revuelta *et al.* , 2008].

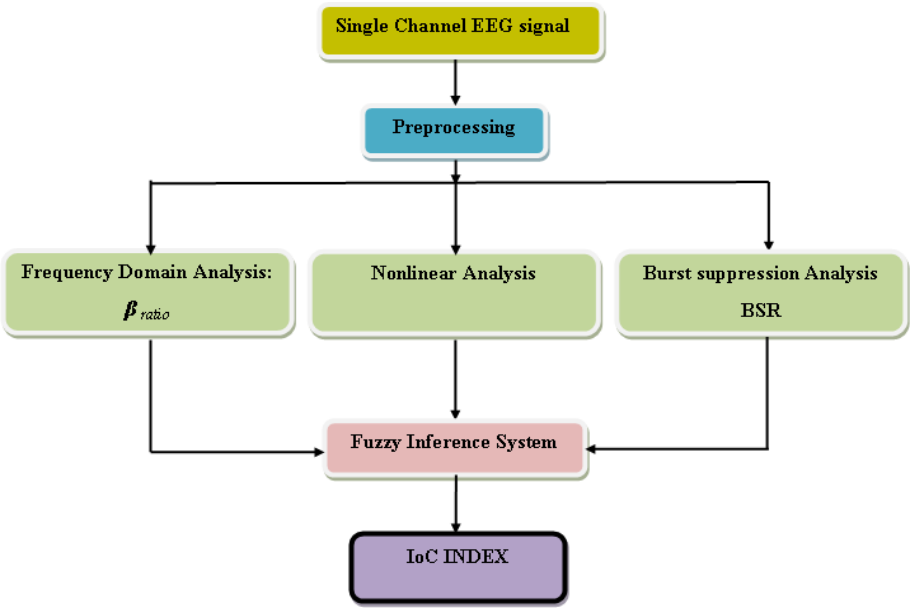

Figure 2.8: Block diagram of Index of Consciousness monitor algorithm

2.4 Summary

This chapter provides a comprehensive review of the existing DoA monitors. The chapter also covers the necessary background knowledge and the technology related to Clinical signs of DoA and EEG based DoA. From the literature review of DoA, it can be concluded that there are some limitations such as time delay and inflexibility in describing all the phases of anaesthesia are associated with the existing methods. Hence, developing a reliable index by integrating both the EEG extracted features and hemodynamic features are necessary in the field of anaesthesia.

Chapter 3

Data Acquisition

Data Acquisition is a very important and time-consuming phase of any research. This has to be done patiently and meticulously to obtain the desired result. This chapter incorporates the detailed explanation of data acquisition procedure and all equipment used for data acquisition. All the data used in this study was collected from Regional Cancer Centre (RCC), Trivandrum, Kerala, India. Regional Cancer Centre is an internationally acclaimed centre for cancer treatment and research. By conducting a wide range of cancer research RCC provides state-of-the-art facilities for cancer diagnosis, treatment, palliation and rehabilitation.

Before collecting real data from patients present research conducted a feasibility study using the data selected from the University of Queensland Vital Signs Data set [Liu *et al.* , 2012]. Four patients data who had undergone general anaesthesia were analysed. The downloaded data included EEG signal and the corresponding BIS index. The study classified EEG signals according to DoA as awake, light anaesthesia, moderate anaesthesia and deep anaesthesia. Finally, the classification accuracy obtained was 96.6%. The features extracted from the EEG signals were Relative Wave Energy (RWE), Energy, Maximum value, Minimum value, Mean value and Standard Deviation [Benzy & Jasmin, 2015]. The study was further extended by collecting and analysing more patient's data from RCC.

The RCC's institutional procedures for clinical studies approval includes details of the main researcher, the definition of the research problem, identification

of responsible researcher in the hospital, obtaining approvals from the concerned department involved in the study and obtaining approvals from the RCC research department, Clinical protocol design, preparation of informed consent and finally approval of Institutional Review Board (IRB) and Ethical Committee. Ethical Committee approval and informed consent are the key elements of the research on human participants. The current study has got approval of institutional review board (Appendix A) and ethical committee (Appendix B) of RCC, Trivandrum. Following the approval, data collection was initiated at the Anaesthesiology department of RCC.

Present chapter has three sections: 1. Clinical Protocol Design 2. Materials and Equipment 3. Data overview. At first, a clinical protocol and informed consent were submitted to Regional Cancer Centre for approval, both by the Institutional Review Board and Ethical Committee. After the approval of institutional review board and ethical committee all the patients who were willing to participate in the study were selected by signing a consent form. The purpose and procedure of data acquisition were clearly explained to the patient before signing the consent form. Data for the current study were obtained from 25 female patients in the age group 30-78 years who had undergone breast cancer surgery under General Anaesthesia (GA). EEG signal, Heart Rate (HR), Systolic Blood Pressure (SBP) and Diastolic Blood Pressure (DBP) are the signals collected from patients throughout the surgical procedure. Finally, all the data obtained were transferred to a computer and represented with respect to time to visualize the changes over time.

3.1 Clinical Protocol Design

Clinical Protocol Design is an important step in the process of data acquisition and for the management of real-time clinical data with its regulatory standards. The clinical protocol provides formal design or plan of the data collection procedure by considering scientific, ethical, regulatory, and safety requirements. This was done to ensure patient's safety, data integrity and uniformity in data collection. The clinical protocol designed for the current study includes selection criteria, premedication procedure, medication procedure and finally the data collection procedure.

3.1.1 Selection Criteria

The patients who gave consent to participate in the study by signing the informed consent (presented in Appendix C) were included and scheduled for breast cancer surgery under general anaesthesia. The informed consent was obtained by one of the anaesthesiologists who participated in the study during the pre-anaesthetic visit. The sample size of the study was determined using the Equation 3.1. This was the equation used to calculate the sample size from an infinite population [Daniel & Cross, 1995; Pourhoseingholi *et al.* , 2013; Charan & Biswas, 2013].

$$N = \frac{Z^2 p(1-p)}{e^2} \tag{3.1}$$

where N is the required sample size, Z is Z statistics for a level of confidence. ie. The value from standard normal distribution corresponding to desired confidence level, p is prevalence rate, which is estimated from previous studies published in the same study domain and e is absolute error or precision.

Steps adopted for sample size calculation in the study is as follows

- Assume 95% confidence interval and the corresponding Z statistic value (Z) is 1.96
- Estimation of prevalence percentage p which provides the proportion (prevalence) of the study in the proportion of one. Prevalence percentage was selected based on previous studies and it is 1.5% in the current study, therefore $p = 0.015$ [Miller *et al.* , 2014].
- The absolute error selected in the study is 5% and therefore $e = 0.05$.
- Finally, Sample size was calculated using the Equation 3.1 and its value is $22.703 \sim 25$

Each patient was identified with a generated code for preserving privacy and confidentiality and the collected data were registered during the procedures. Exclusion criteria includes patient body weight 30% above or lower the average recommended weight ($Height\ in\ cm - 105$) in kg, serious cardiovascular or respiratory

disease, neurological defect or contra-indication to the anaesthetic technique such as difficult airway.

3.1.2 Pre-medication and Medication procedure

- Pre-medicate the patient with Alprazolam (0.25 to 0.5mg), Pantoprazole (40mg), Domperidone (10mg) at 10 PM the day before surgery and 6 AM on the day of surgery.
- Start an Intravenous line at 6 AM on the day of surgery and administer intravenous fluid 0.9% normal saline.
- Give the injections Glycopyrrolate ($4\mu g/kg$), Midazolam ($20\mu g/kg$), Fentanyl ($1\mu g/kg$) just before the start of surgery.
- In addition, provide analgesic drugs like Paracetamol (1gram), Diclofenac sodium (75mg), anaesthetic drug propofol (2mg/kg), muscle relaxant drug Vecuronium Bromide (0.1mg/kg) intravenously.
- Ventilate the patient with Oxygen (O_2)- Sevoflurane and Nitrous Oxide (N_2O) for maintaining the anaesthesia until the end of the surgery.
- Provide an additional dose of Fentanyl up to 2 $\mu g/kg$ if Blood Pressure(BP) or Heart Rate(HR) increased more than 20% of the baseline value. If BP or HR is not controlled with Fentanyl then provide Nitro Glycerine (NTG) to control BP and Metoprolol to control HR.
- At the end of the surgery give the injections Glycopyrrolate ($8\mu g/kg$) and Neostigmine ($0.05mg/kg$) for the recovery of the patient.

3.1.3 Data collection Procedure

The study was focused on the hemodynamic and EEG signal variations of patient during the anaesthetic procedure. Therefore, EEG signals, Heart Rate, Non-invasive systolic BP and diastolic BP and BIS value were simultaneously collected from each

patient during the 4 phases of anaesthesia (Awake, Induction, Maintenance and Recovery) for comparison and analysis.

Data collection procedure of the study is as follows.

1. Set the BIS monitor and standard monitoring devices are in continuous mode for monitoring
2. Register the baseline values of Heart Rate (HR), Systolic Blood Pressure (SBP), Diastolic Blood Pressure (DBP) before the administration of anaesthetic drugs.
3. Record the awake dataset which are collected 5-10 minutes before administrating the anaesthetic agents. The dataset consists of EEG waveform data and numeric data including BIS value (usually in the range 80-100), HR, SBP and DBP. The pre-medication drugs were administered during this period.
4. Induce the patient with the anaesthetic drug, analgesic drug and muscle relaxation drug and record EEG signals from the time of administration to 1-5 minutes after administration of induction agents. Correspondingly record HR, SBP, DBP and BIS value (usually in the range 20-40) continuously.
5. Start the inhalation agent O_2 - Sevoflurane (sevo) and N_2O
6. Start the surgical procedure and record EEG signals, HR, SBP and DBP. The corresponding BIS value variation was in the range between 40-60.
7. At the end of the surgery, stop the inhalation agent (sevo) and start inducing reversal drugs for the recovery of the patient. Record recovery EEG signals, HR, SBP and DBP after the end of surgery to the return of conscious state of the patient. Correspondingly record BIS value variations (Usually in the range 60-80).
8. The attending anaesthesiologist's response to the outcome DoA was also recorded throughout the surgery as awake, light anaesthesia, moderate anaesthesia and deep anaesthesia.

9. The data corresponding to BIS value variation of 0-20 is not considered as it would cause hemodynamic instability of the patient during surgery and hence it is beyond the scope of the study.

3.2 Materials and Equipment

The physiological signals which are required for the current study were monitored and acquired according to the protocol mentioned above. These signals were continuously recorded throughout the surgical procedure using synchronization and data acquisition software RugloopII© Waves developed by Demed, Temse, Belgium. After data collection, the files recorded were extracted to spreadsheets using Labgrab 2.20© software developed by Demed, Temse, Belgium.

The materials and Equipment used in data collection are listed below:

- BIS Sensor
- BISx^{TM} System
- Phillips BIS Module
- Phillips Intellivue MP 80 Monitor
- Non-Invasive Blood Pressure (NIBP) Measurement Device
- Heart Rate Measurement Device (ECG electrodes)
- RugloopII© Waves software (2000)

A brief description of the materials and equipment are given below:

3.2.1 BIS Sensor

BIS sensor is a non-invasive sensor introduced by Aspect Medical Systems and it is used to record the electrical activity of the brain as EEG signals. It is a single-use

sensor and it should be replaced after each use. There are four types of BIS sensors used for EEG recording namely Quatro electrode sensor, extended sensor, pediatric sensor and bilateral sensor as shown in Figure-3.1.

FIGURE 3.1: Types of BIS Sensors

1. BIS Quatro Electrode: This sensor is used for adult patients undergoing GA.
2. BIS Extended Sensor: Used for adult patients in ICU to record EEG data for long period of time.
3. BIS Pediatric Sensor: Used for pediatric patients.
4. BIS Bilateral Sensor: To capture EEG signals from both hemispheres simultaneously in order to detect the differences in the brain signals. It is one of the advanced modes of monitoring.

In the current study, BIS Quatro pre-gelled Electrode was used because of its enhanced performance in deep anaesthetic states and resistant to interference from noise sources like high-frequency electromyography (EMG) conditions in operating room/intensive care unit. BIS sensor was placed on the forehead and temporal region of the brain according to the manufacturer's instructions. This sensor is an electrode strip consisting of four electrodes in which three of the electrodes collect the EEG activity between the forehead and temporal regions of the brain. The fourth electrode is used to measure the electromyographic resistance which reflects muscle stimulation. This EMG value will rise with an increase in muscle tone or movement [VISTA, 2008].

The sensor can be assembled unilaterally at the left or right forehead according to the international 10–20 electrode system. The basic electrode is placed on the frontotemporal position FT9 on the left or FT10 position on the right and the frontopolar position FPz as shown in Figure-3.2 indicates the reference electrode. The electrode in the position FT7 on the left or FT8 on the right detects the EMG activity. The electrode placed on the position FP1 or FP2 (on the right) is the virtual ground which increases rejection of common mode [Nunes *et al.* , 2012; Johansen, 2006].

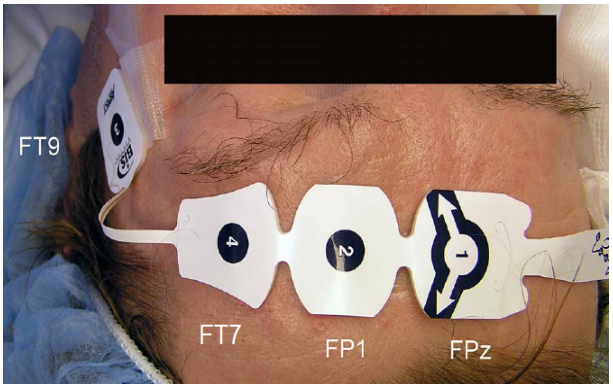

Figure 3.2: BIS Sensor

3.2.2 BISx^{TM} System

The BISx^{TM} System developed by Aspects Medical Systems is used to receive, filter and process the patient's EEG signals. Figure-3.3 shows BISx^{TM} System and is placed near to patient's head because to avoid the interference of other devices. It has two cables called Monitor Interface Cable and Patient Interface Cable (PIC). The Monitor Interface Cable connects the system to the monitor and the PIC connects to the BIS sensor [VISTA, 2008].

3.2.3 Phillips BIS Module

Phillips BIS Module shown in Figure 3.4 which works as an interface between Aspects BISx system and Phillips Intellivue MP-80 monitor. The Philips BIS module gives high-resolution numeric and graphic trends to the monitor for displaying BIS related

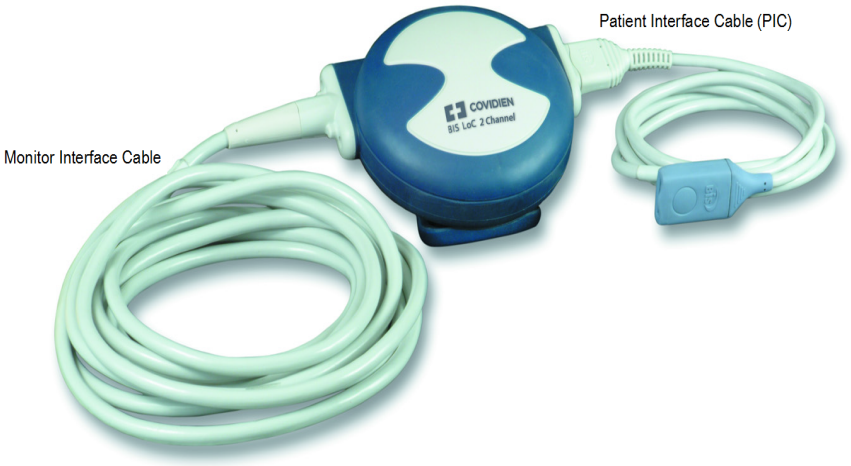

FIGURE 3.3: BISx^{TM} System

data like EEG waveform, BIS index, Signal quality index, Suppression ratio and EMG frequency band [INTELLIVUE, 2006].

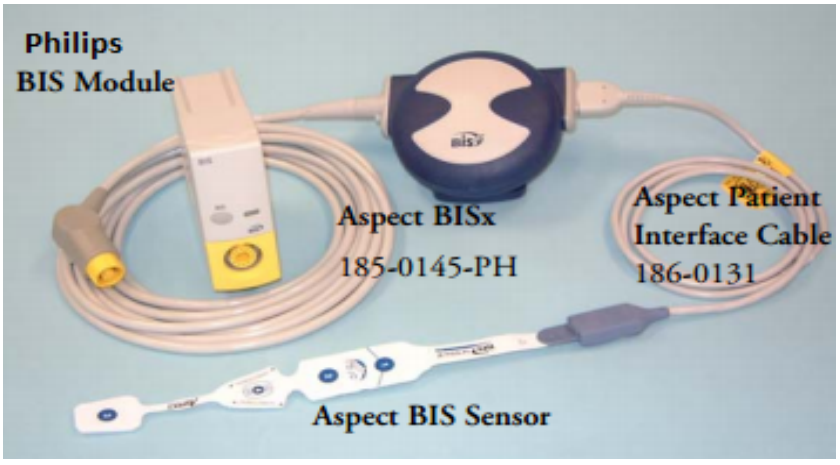

FIGURE 3.4: BIS module

3.2.4 Phillip's IntelliVue MP80 Monitor

The Philips Intellivue MP80 patient monitor offers monitoring solution for various medical applications. Multiple measurements can be monitored by connecting other modules to the monitor. This monitor can store the trends in data and it can perform required calculations from the database. The display and processing units of the monitor are separate components and it can display eight

waves at a time. Other modules like Invasive blood pressure (M1006B), Temperature (M1029A), Cardiac output (M1012A), Continuous cardiac output with M1012A Option, Transcutaneous gas (M1018A), Mixed venous oxygen saturation - SvO2 (M1021A), Recorder (M1116B), EEG (M1027A), Bispectral Index - BIS (M1034A) and Spirometry (M1014A) can be plugged in to its Multi-Measurement Server (MMS) and Flexible Module Server (FMS) slots. MMS and FMS were used in the present study to connect 5-lead ECG (including arrhythmia) electrode and BIS module respectively. The ECG electrode connected through MMS helps to monitor ECG signal and HR. On the other hand, FMS module helps to provide the EEG signal and BIS related parameters by connecting BIS module to the FMS slots [Monitor, 2008; IntelliVue, 2006]. Figure-3.5 shows Phillip's Intellivue MP80 Monitor with Multi-Measurement Server and Flexible Module Server.

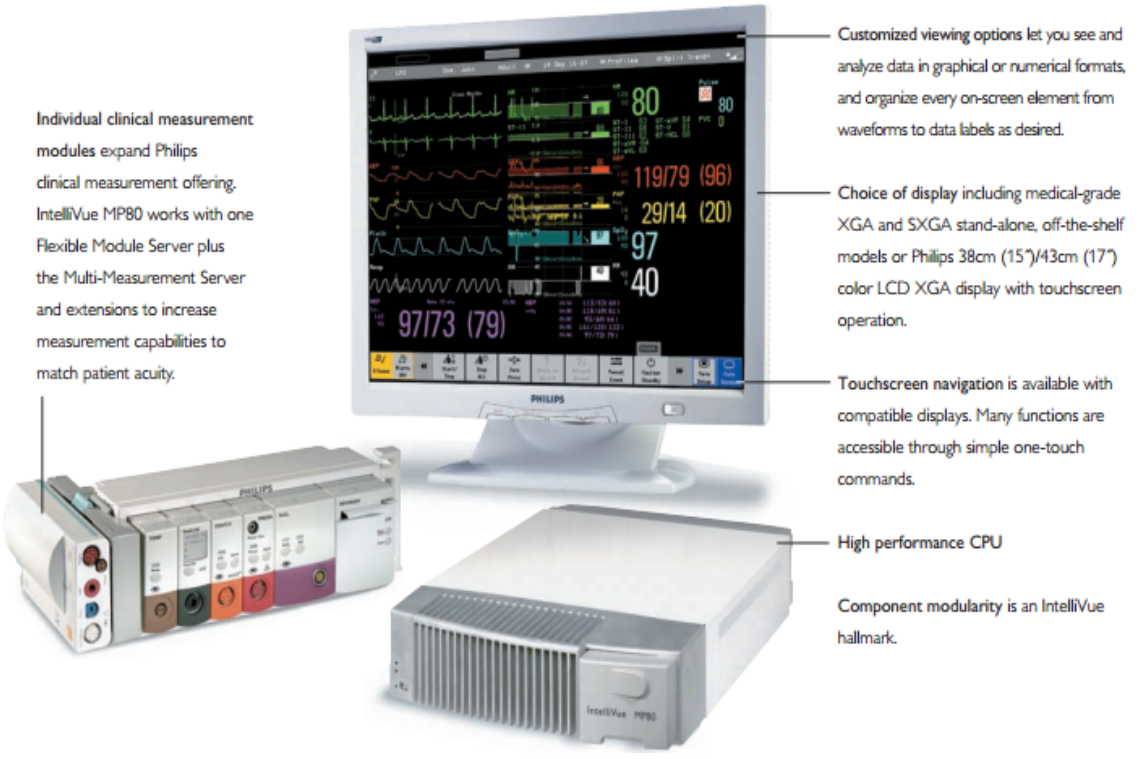

Figure 3.5: Phillips IntelliVue MP80 Monitor

3.2.5 Blood Pressure (BP) Measurement Device

Arterial blood pressure is one of the most important vital sign of the human body and many of the diagnostic and remedial decisions are taken based on this measure. This can be measured invasively or non-invasively. Invasive BP measurement method measures of arterial pressure directly by inserting a cannula needle in the artery. But in Non-Invasive Blood Pressure (NIBP) measurement method, an oscillometric device consisting of pneumatic cuff which acts as the pressure sensor and measures the amplitude of pressure changes in the pneumatic cuff. The pneumatic cuff is inflated and released by an electrically operated pump and valve. Blood pressure is measured by occluding a major artery (typically the brachial artery in the arm) with the pneumatic cuff. The device records and evaluates the oscillations of arteries and calculates blood pressure. Blood pressure is measured using two numbers: Systolic Blood Pressure (SBP) and Diastolic Blood Pressure (DBP). SBP measures the pressure in the blood vessels when the heart beats whereas DBP measures the pressure in the blood vessels when the heart rests between beats [Weiss *et al.* , 1995; Rantala, 2006].

Present study adopted NIBP method to acquire the BP signals and it calculates the SBP and DBP based on the oscillations of the arteries with the help of an algorithm. The calculated values are visualized on the display of Phillips's Intellivue MP80 monitor thorough the NIBP connector of the monitor.

3.2.6 Electrocardiogram (ECG) Electrodes

The electrocardiogram (ECG) provides the measure of electrical activity of the heart over a period of time and it is measured using electrodes placed on the skin. The ECG electrodes detect electrical changes in the skin due to the depolarizing and repolarizing electrophysiologic patterns of heart muscles during each heartbeat. In the current study, ECG electrodes were used to extract the parameter Heart Rate (HR) in beats per minute (bpm) [MSP430, 2005]. The hemodynamic parameter HR is included in the study to examine the abnormality on HR due to the anaesthetic drug effect. Normal HR is in the range 60–100 bpm whereas HR above 100 bpm

is defined as Tachycardia and HR below 60 bpm is defined as Bradycardia. If the heart is not beating in a regular pattern then it is called arrhythmia.

In the study, ECG electrodes were placed on the patient according to the 5 lead placement system as shown in Figure 3.6. The five electrodes were placed on the patient's limbs and on the surface of the chest. The overall magnitude of heart's electrical potential is measured from different angles ("leads") and is recorded as ECG waveform over a period of time.

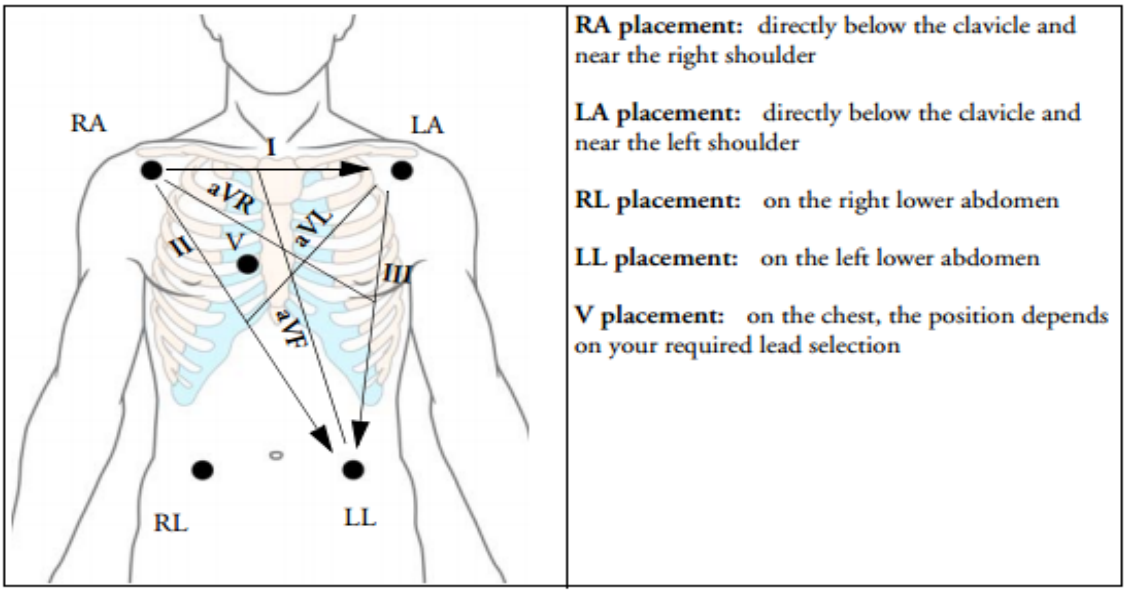

FIGURE 3.6: 5 Lead ECG electrode placement system

In order to display the ECG waveform on the Phillip's Intellivue MP80 Monitor the electrode cable is connected to the ECG connector of the Phillip's IntelliVue MP80 Monitor. The arrhythmia option of the monitor performs an algorithm called arrhythmia detection analysis on the patient's ECG waveform and calculates patients HR in beats per minute (bpm).

3.2.7 RugloopII © Waves(2000)

RugloopII © Waves is a Windows-based synchronization and data acquisition software developed by Tom DeSmet (Demed Engineering, Gent, Belgium). It can record and capture waveform data and numerical data electronically from Aspect Medical

Systems A2000 or Datex-Ohmeda AS3/S5 monitor or Phillips Intellivue monitor [Ribeiro *et al.* , 2009; DeSmet, 2000].

In the present research patient's physiological signals were continuously collected and recorded in the Personal Computer (PC) through RugloopII © Waves software installed in the PC. It captures all data from Phillips Intellivue monitor and synchronizes them in the time reference. The software connects PC to the Philips Intellivue Monitor through serial line or Ethernet connector. The Phillips Intellivue monitor collects data from various devices at a different sampling rate. It collects the real-time data and other processed variables like HR, SBP and DBP in every 5sec and BIS value in every 1sec. The waveform data (EEG signal) is sampled at a sampling rate of 128 samples/sec. The waveform data (EEG Signal) is extracted to ASCII files using software called Labgrab developed by Demed, Temse, Belgium. Figure-3.7 shows the screenshot of RugloopII © Waves software. Here the black

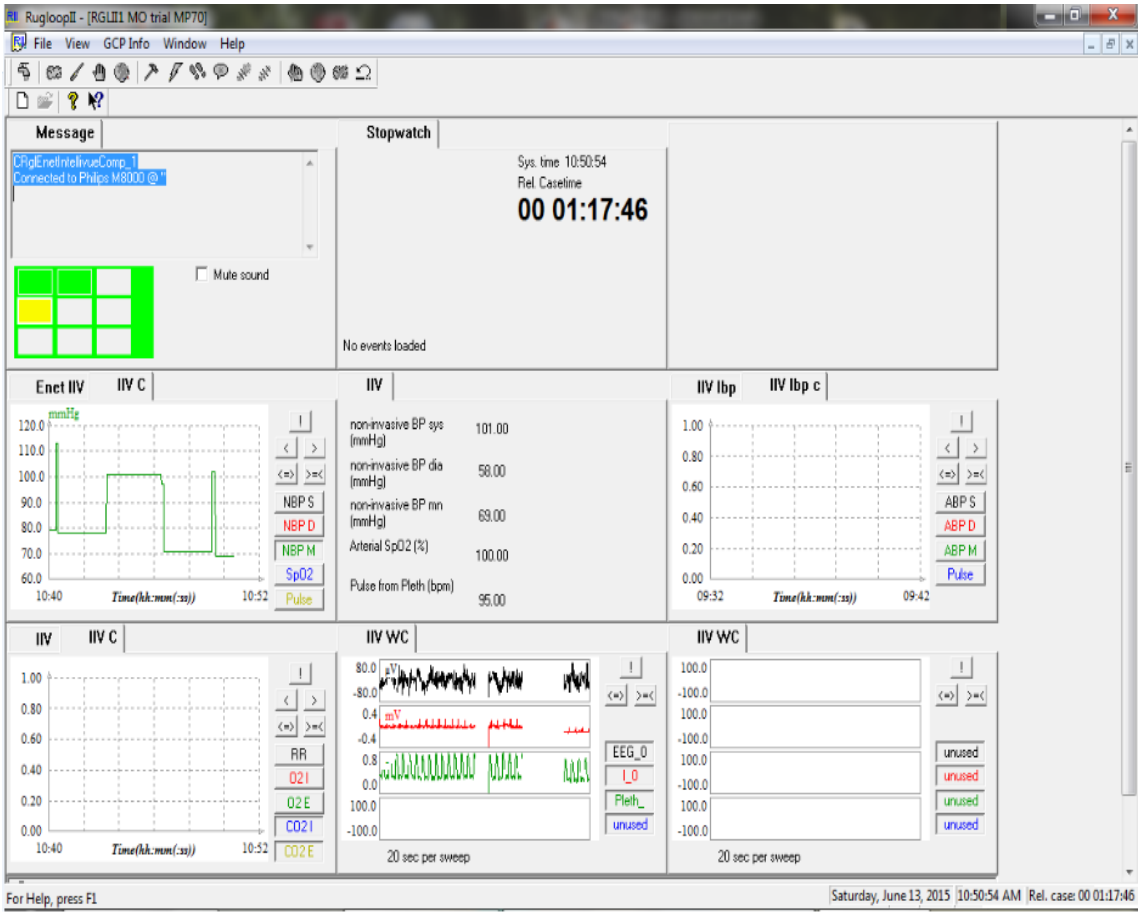

Figure 3.7: RugloopII © Waves software

color signal is the single channel EEG signal collected from the patient as waveform data. The numerical data presented in the figure are the Noninvasive Systolic Blood Pressure, Noninvasive Diastolic Blood Pressure, Noninvasive Mean Blood Pressure and HR (represented as Pulse from Pleth) at a particular instant of a patient's data. The other parameters and wave data shown in the figure were not considered for the current study.

3.3 Data Overview

A pictorial representation of flow of data in the study is presented in Figure 3.8. The BIS sensor senses the electrical activity of the brain and sends the raw EEG information through the cable and converter to the BIS module. BIS module processes the EEG data according to an algorithm and provides BIS index and EEG data to the monitor. The BP apparatus calculates the systolic blood pressure and diastolic

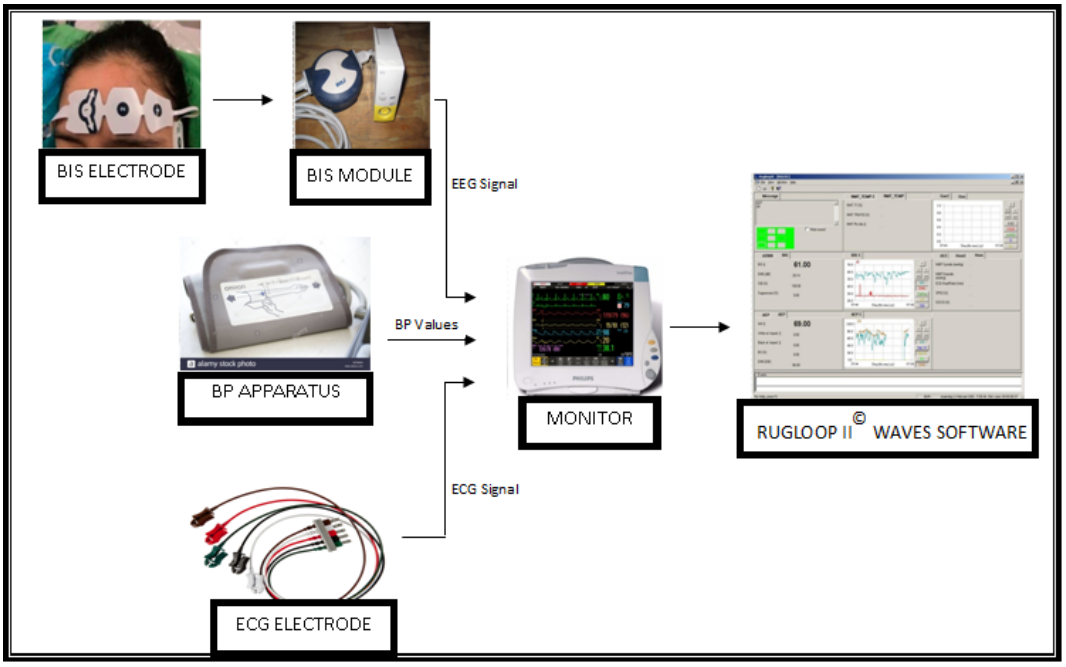

FIGURE 3.8: Data Flow

blood pressure based on an algorithm and passes to the monitor. Similarly, ECG leads collects the ECG signals and the arrhythmia algorithm calculates Heart rate from the ECG signals and monitored in the monitor. RugloopII © Waves software

loaded in the PC captures all the data monitored in the monitor through RJ 45 Ethernet LAN cable connector and store it on the PC.

Collected data from patients include EEG waveform data and numerical data like BIS value, HR, SBP and DBP. The demographic details of the data collected from all patients are given in Table 3.1. Data is presented as mean ± Standard Deviation (SD). The summary of acquired data is depicted in Table 3.2.

TABLE 3.1: Patient demographic Details

Details	Mean ± SD
Age (yrs)	53 ± 13
Weight (Kg)	57 ± 10
Height (cm)	155 ± 5

TABLE 3.2: Details of the collected data

Sensor	Numeric/Waveform data	Sampling frequency
ECG Electrodes	Heart Rate(bpm)	0.2 Hz
Oscillometric pressure sensor	SBP (mmHg))	0.2 Hz
Oscillometric pressure sensor	DBP (mmHg)	0.2 Hz
BIS Sensor	BIS Value	1 Hz
BIS Sensor	EEG waveform (μ V)	128 Hz

3.3.1 Data Representation

Time domain representation of the data/signals provides the information of signal amplitude and time information. A raw signal represented in time domain needs to be processed to find out more information in that signal. The collected signals are categorized into four groups namely awake signal, induction signal, maintenance signal and recovery signal.

- Awake signal: The signals collected 5-10 minutes before administrating the anaesthetic agents. The corresponding BIS value variation is noted to be in the range 80-100.

- Induction signal: The signals acquired at the time of administration of induction agents to 1-5 minutes after administration of induction agents. The corresponding BIS value variation was in the range 20-40 which is the deep anaesthetic signal.
- Maintenance signal: The signals obtained during the surgery. BIS value variation was in the range 40-60 and it is the moderate anaesthetic signal.
- Recovery signal: The signals collected after the end of the surgery to the return of conscious state of the patient. BIS variation is in the range 60-80(Light anaesthetic signal).
- The signals corresponding to BIS value variation of 0 - 20(very deep anaesthetic signal) could not be obtained from the patients as it would cause hemodynamic instability of the patient during surgery and hence it is beyond the scope of the study.

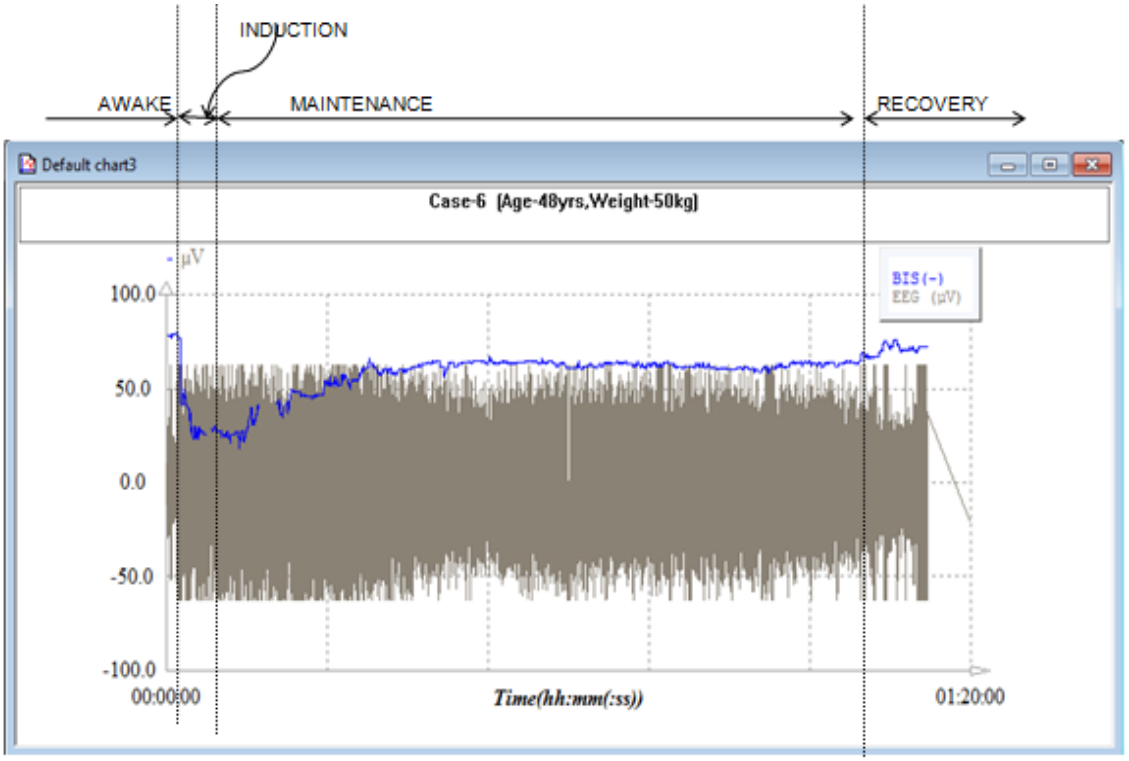

FIGURE 3.9: EEG Signal Representation

Figure 3.9 shows the representation of a patient's EEG signal in time domain and the corresponding BIS index values as the depth of anaesthesia. Similarly, the changes

in noninvasive blood pressure and heart rate of a patient in accordance with depth of anaesthesia are shown in Figures 3.10 and 3.11 respectively

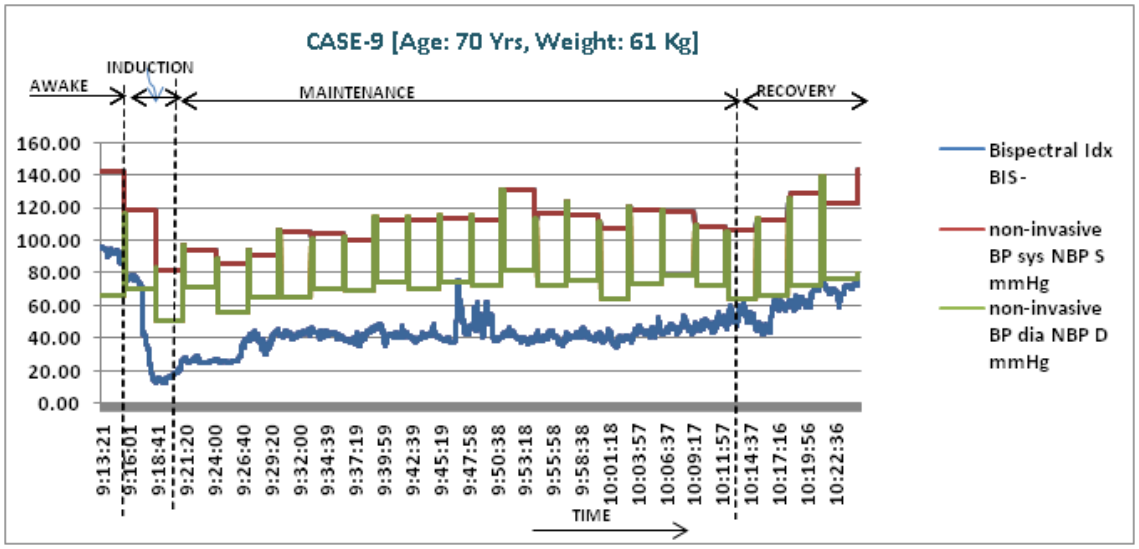

FIGURE 3.10: Blood Pressure Data Representation

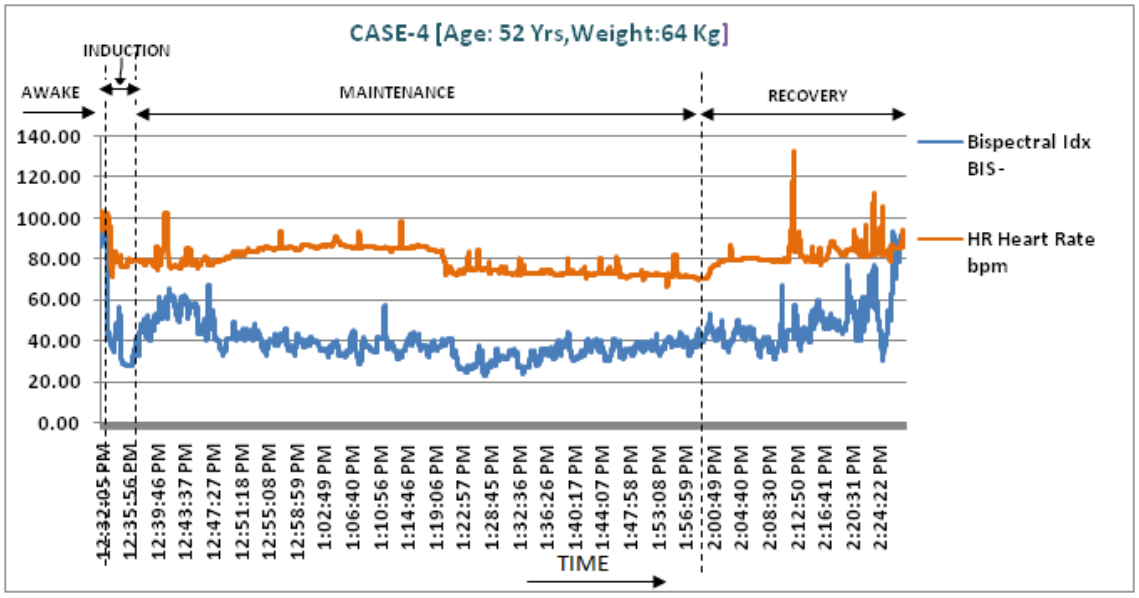

FIGURE 3.11: Heart Rate Data Representation

3.3.2 Time and Frequency spectrum of EEG signal

Initially, the amplitude and frequency distribution of the awake, induction, maintenance and recovery EEG signals were analyzed using histograms and frequency

distribution plots. These plots help to study the variations in EEG signals during the different phases of anaesthesia. Figures 3.12 and 3.13 represent the histogram and frequency spectrum corresponding to an EEG recording of a patient in each anaesthetic phase.

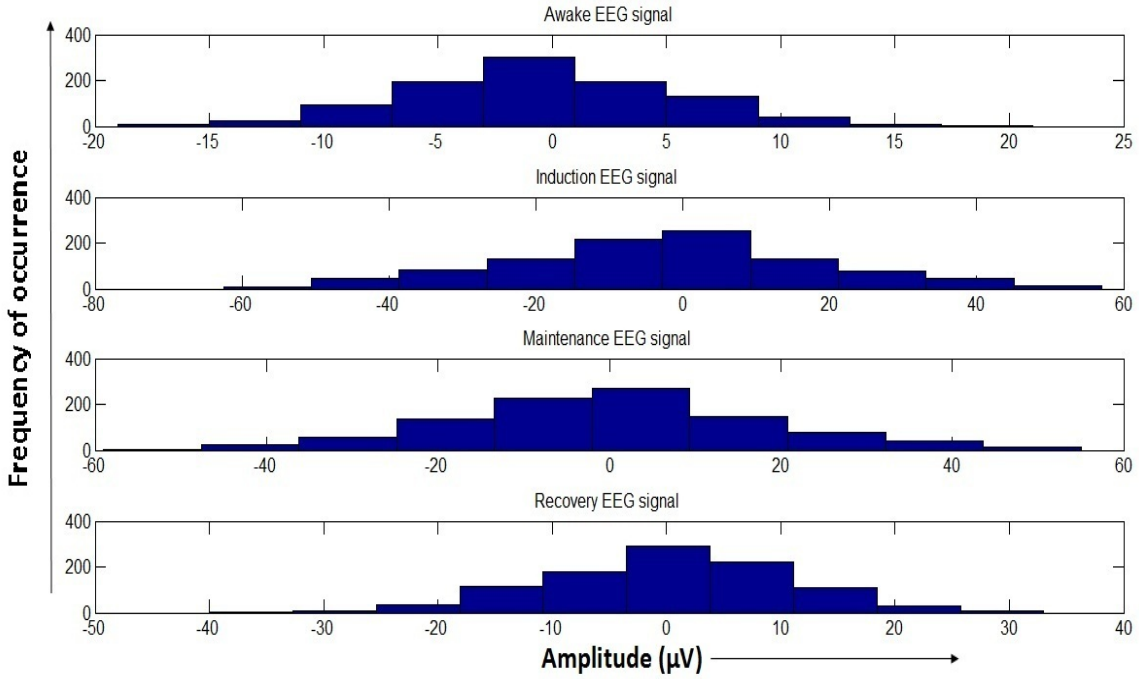

FIGURE 3.12: Histogram of EEG signals

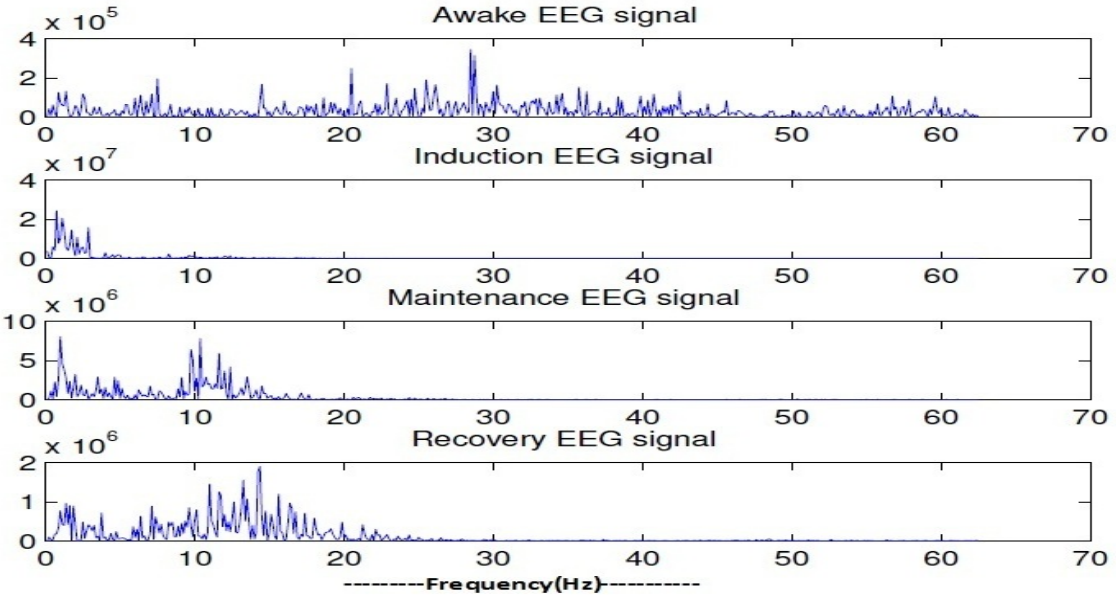

FIGURE 3.13: Frequency Spectrum of EEG signals

According to Kelley et al average amplitude of the EEG signal increases and the average frequency decreases when DoA increases[Kelley, 2003]. The horizontal axis in the histogram representation is the amplitude of the signal and the vertical axis is the frequency of occurrence. The amplitude variations of different anaesthetic EEG signals are more visible in the histogram. Here the amplitude of the EEG signal increases as the depth of anaesthesia increases. For awake EEG signals, the amplitude range is -15 to +15 μV, induction signals are deep anaesthetic signals and their amplitude range is -50 to +50μV, maintenance signals are moderate anaesthetic signals and amplitude range is -40 to +40μV. Finally, recovery signals are light anaesthetic signals and their amplitude range is from -25 to +25μV. The frequency spectrum shown in Figure 3.13 reveals that the frequency of EEG signals reduces when the depth of anaesthesia increases. Here, EEG signals of deep anaesthetic state (induction phase) contain lower frequency components whereas the awake EEG signals contain higher frequency components.

3.4 Summary

The first section of the chapter explains clinical protocol designed for data collection including selection criteria, medication and pre-medication procedure and data collection procedure. Next section provides the details of materials and equipment used for data collection which includes BIS sensor, BISx^{TM} system, Phillips BIS module, Phillips Intellivue MP 80 monitor, NIBP measurement device, ECG electrodes for heart rate measurement and the synchronization and data acquisition software-RugloopII© Waves. The last session explains the summary of collected data and its representation. EEG signal, HR, SBP and DBP are the collected data from each patient during the whole surgery. Finally, these data were represented in the time domain to observe the variations during different phases of anaesthesia. .

Chapter 4

Preprocessing of Data to attenuate the effects of noises

Data preprocessing aims to remove noises from the collected raw data and prepares for further analysis. The dataset includes numerical data of vital signs like HR, SBP, DBP and waveform data of EEG signals collected during anaesthesia. HR, SBP and DBP are called hemodynamic variables which keep on changing in accordance with the flow of blood in the blood vessels and with each contraction of the heart. The noises affecting these variables are power line interferences and electromagnetic interferences. Since the amplitude of EEG signal is very small (in μV) they are easily contaminated by noises due to electrode movement, disturbance in the power supply, strong electromagnetic effect caused by other equipment and interference of other signals like Electrocardiogram (ECG), Electromyogram (EMG), Electrooculogram (EOG) etc. The presence of these noises inversely affects the accuracy of estimation of DoA. Therefore it is necessary to attenuate these effects to get an optimized DoA index.

The current chapter has two sections: Data Segmentation and Data Filtering. Data segmentation splits the datasets into shorter segments which are appropriate for the effective analysis of data. The data filtering method is necessary to remove the contaminated noises which will degrade effects of signal analysis. These two sections describe different segmentation and filtering methods which are applied

to the collected dataset depending on the kind of data analyzed and the type of noise present.

4.1 Segmentation

EEG signals and the hemodynamic variables are non-stationary because the statistical characteristics of both vary with time. Therefore, for the subsequent analysis, it is necessary to segment the datasets into sub-sections in hemodynamic variables and epochs in EEG signals. Segmentation is done in the time domain such that each segment is considered as approximately stationary. Segmentation can be performed uniformly or non-uniformly.

4.1.1 Uniform segmentation

Uniform segmentation divides the signals or the datasets into fixed intervals with time duration of 30 sec, 20 sec or even 1 sec. This method is widely used in data segmentation application related to biomedical signal processing and other applications. The selection of suitable segment length affects the efficiency of analysis. But the choice of segment length is usually influenced by the algorithm used for the data analysis. Some algorithms require more data for analysis and thus longer segment length is needed to obtain a reliable result. On the other hand use of longer segment length increases the overall computational burden of the algorithm. Selection of smaller segment length may exhibit a significant degree of non-stationarity, which may cause the processing algorithm to lose its sensitivity and may end up with misleading results. This conflict forces to adopt segment length which exceeds the number of data points over which the signal is regarded as stationary [Motamedi-Fakhr *et al.* , 2014; Azami *et al.* , 2012a,b].

4.1.2 Non Uniform segmentation

Non-uniform segmentation is also called adaptive segmentation and is commonly used in waveform data analysis. Here the signals are automatically segmented into variable subsections based on statistical characteristics. That means it divides the signal into segments of variable length. If the statistical characteristics of a signal exhibit a considerable change, then the signal is segmented at the boundary of change. Since statistical characteristics are the main concern in signal segmentation, Standard Deviation (SD) and Fractal Dimension (FD) are some of the suitable tools used for monitoring statistical characteristics variations along the signal. Here two successive windows which slide along the signal and for each window SD or FD is computed. If any changes on the signal characteristics are reflected on the extracted SD or FD of the signal then the boundary of change would be the boundary of each segment.

Present research tried to experiment both the segmentation methods. Non-uniform segmentation is implemented by applying modified Varri's algorithm on collected EEG signals. In this algorithm, a feature called kurtosis is extracted from EEG signals to find out the boundary of characteristic changes of the signal. The feature kurtosis has opted because normal brain signals are having low kurtosis value whereas the seizure EEG or spikes EEG are having high kurtosis value [Sanei, 2013; Krajča *et al.* , 1991; Agarwal *et al.* , 1998; Azami *et al.* , 2015]. The algorithm followed for adaptive segmentation is as follows

- Step 1: Select two connected windows W_1 and W_2, allow it to slide over the EEG signal. The length of both windows together is defined by a parameter Window Length (W) and each window has $Length = \frac{1}{2} * W$.
- Step 2: Calculate the feature kurtosis for each window to indicate changes in the signal characteristics and it is represented as Ku_i and Ku_{i+1}.
- Step 3: Use the function F to detect segment boundaries. The function F is the degree of difference between the two consecutive kurtosis values, Ku_i and Ku_{i+1} extracted from both windows and is given by

$$F = [F_1, F_2, \ldots, F_{N-1}], \text{where } F_i = Ku_{i+1} - Ku_i, i = 1, \ldots, N-1 \quad (4.1)$$

where N is the total number of windows analyzed.

- Step 4: In order to localize the segment boundaries, apply two threshold functions T_1 and T_2 to the F function. The local maxima above the threshold value T_1 is considered as the positions of the segment boundary in the transition of the signal from high-frequency low amplitude to low-frequency high amplitude. On the other hand, local minima below the threshold value T_2 is the segment boundary in the transition of signal from low-frequency high amplitude to high-frequency low amplitude.

4.2 Filtering

In signal processing, filtering means complete or partial suppression of unwanted components called noises from a signal. Mostly the biomedical signals like HR and BP are affected by the noises from the external environment called environmental noise. These are due to the disturbances in AC power line and electromagnetic field created by other equipment in the operation theatre. But the EEG signals are affected by the noises caused by external sources and physiological sources called physiological noise. The physiological noises are the artifacts due to the interference of ECG, Electromyography (EMG) and Electrooculography (EOG) signals. Usually, EEG signals collected through noninvasive methods have low Signal to Noise Ratio (SNR) due to the artifacts caused by muscle and eye movements. Therefore, contamination of EEG signals by the above-mentioned noises would affect the accuracy of DoA estimation. Hence, the estimation of DoA without removing the noise may result in an incorrect assessment. The conventional filtering methods are not able to eliminate artifacts well enough because they work based on the frequency component of data whereas the EEG signals contain different scales and amplitudes. Therefore, current research adopted wavelet-based filtering method to remove the noises from the collected EEG signals. This allows shrinking of the amplitude of the wavelet coefficient to remove artifacts.

4.2.1 Technique used to remove environmental noises

The environmental noises or power line interferences are due to the difference in the electrode impedance and stray currents in the cable connected to the patient. Cables carrying signals from the patient to the monitoring equipment are prone to electromagnetic interference (EMI) of frequency 50 Hz or 60 Hz by ubiquitous supply lines [Mateo *et al.* , 2015]. The frequency of the power line interference lies within the frequency range of the EEG signal. Therefore the first step in the EEG signal prepossessing is to remove the power line interference produced by the electric supply used in various devices such as ventilator, electric cutter, ECG recorder and lots of specific lights in the operating room. Here a 50 Hz notch filter is used to remove the power line interference from the EEG signals [Zoughi *et al.* , 2012].

4.2.2 Removing the physiological noise

As reported by Rampil et al. [Rampil, 1998] EEG signals are often contaminated by EMG artifacts and eye blinking artifacts. Estimation of DoA without removing these artifacts may lead to erroneous results. Artifacts due to eyeball movement and blinking are known as Electrooculogram (EOG) artifacts and artifacts due to muscle movements are called EMG artifacts [Sanei & Chambers, 2013]. EOG artifacts are high amplitude and low-frequency signals and usually affect the lower bands of EEG signals [Kavitha *et al.* , 2007]. Therefore, the characteristics of EOG artifacts would affect the accuracy of DoA estimation. Similarly, the presence of EMG artifacts in the EEG signals may result in unreliable estimation. Bowdle et al. and Bruhn et al. reveal that BIS index provides an inaccurate output when more EMG activity present in the EEG signal [Bowdle, 2006; Bruhn *et al.* , 2000a]. The frequency spectrum of the EMG artifacts is greatly overlapped with EEG signals and also the intensity of the EMG signals is larger than EEG signals.

Researchers have proved various techniques to remove these artifacts from EEG signal like adaptive filtering method, empirical mode decomposition method, independent component analysis (ICA), FIR-median Hybrid Filter, regression analysis in the frequency domain and wavelet transform analysis [Kavitha *et al.* , 2007; Zeng *et al.* , 2013; Astolfi *et al.* , 2006; Woestenburg *et al.* , 1983; Croft &

Barry, 2000]. However, a most popular technique to filter the artifacts from EEG signals is wavelet-based threshold filtering [Yu, 2009].

4.2.2.1 Wavelet based threshold filter

In biomedical applications especially in EEG signals wavelet coefficients which are small in value are considered as artifacts. Wavelet-based thresholding filter shrinks the effect of those small coefficients or removes them without affecting the quality of the signal in the wavelet domain. Finally, an inverse wavelet transform will retrieve the desired signal from the wavelet domain.

In the present study wavelet-based thresholding algorithm is used to remove the spikes and low-frequency noises from raw EEG signals. The mother wavelet adopted for the wavelet analysis is db4 and the level of decomposition is 4. The db4 wavelet is selected as mother wavelet because its characteristics are more similar to EEG signal characteristics. The six steps used for the computation of wavelet-based thresholding algorithm is summarized below.

- Step 1: Select a basic wavelet function that matches the characteristics of collected EEG signals.
- Step 2: Decompose the EEG signals into detail and approximation coefficients to obtain the desired frequency resolution.
- Step 3: Calculate the standard deviation of the wavelet coefficients at each level using Equation 4.2

$$\sigma_j = \text{MAD}(|cW_j|)/0.6745. \tag{4.2}$$

where MAD is the Mean Absolute Deviation, cW_j is the wavelet coefficient at level j

This method of estimating the standard deviation is typically used in wavelet de-noising because it is less sensitive to outliers than the traditional calculation of standard deviation [Donoho, 1995].

- Step 4: Calculate the Universal threshold value using the Equation 4.3

$$T = \sigma\sqrt{2log(n)} \tag{4.3}$$

where n is the length of the signal and T is the threshold value.

- Step 5: Apply Hard or soft thresholding based on the Equations 4.4 and 4.5

The hard threshold function is

$$cW_j^* = \begin{cases} cW_j, & \text{if } |cW_j| > T. \\ 0, & \text{if } |cW_j| \leq T. \end{cases} \tag{4.4}$$

where $cW_j$is the coefficients of the sub-band.

The soft-threshold function is

$$cW_j^* = \begin{cases} sgn(cW_j)(|cW_j| - T), & \text{if } |cW_j| > T. \\ 0, & \text{if } |cW_j| \leq T. \end{cases} \tag{4.5}$$

- Step 6: The original signal is reconstructed from the retained coefficients using inverse wavelet transform.

The major problem with wavelet-based thresholding is that it is very difficult to find out the optimal value of threshold T. If the value of T is small then it will surpass the entire noisy coefficients and the result is still a noisy signal. On the other hand, a large value of T makes a large number of coefficients as zero and will shrink a maximum number of coefficients to smoothen the signal. This will result in blurring of the signal. Therefore, it is necessary to find an optimum value for T depending on the decomposition level and sub-band characteristics.

There are many threshold selection methods available in which SURE Shrink is the one that used commonly in wavelet-based applications [Geetha & Geethalakshmi, 2011; Tibdewal *et al.* , 2016; Mukhopadhyay & Mandal, 2013]. The SURE Shrink threshold is developed by Donoho and Johnstone and it is a sub-band adaptive thresholding scheme where a different threshold is estimated for each sub-band based on Stein's Unbiased Risk Estimator (SURE). The SURE

Shrink method can generate thresholds under a risk rule which minimizes SURE with the shrinkage function and with the level of multiresolution [Mukhopadhyay & Mandal, 2013; Xiao & Zhang, 2011; Antoniadis *et al.* , 2001; Donoho & Johnstone, 1994].

The SURE Shrink threshold T_{SURE} is defined as

$$T_{SURE} = \underset{T \geq 0}{\operatorname{argmin}} SURE(T, cW_j) \tag{4.6}$$

where $SURE(T, cW_j)$ is given by

$$SURE(T, cW_j) = N - 2.\#\{j : |cW_j| \leq T\} + \sum_{j=1}^{N} min(|cW_j|^2, T^2) \tag{4.7}$$

where N is the number of coefficients in the sub-band, $\#\{\}$ represents the cardinality of the set.

This method is useful in the optimization of threshold because it orders the wavelet coefficients in terms of magnitude and then selects the threshold as the wavelet coefficient that minimizes the risk. The advantages of SURE Shrink is that it uses the wavelet coefficients (cW_j) at each level to choose the threshold value T_{SURE}.

4.3 Experimental results

4.3.1 Segmentation

Current research tried to experiment both uniform segmentation and non-uniform segmentation. In uniform segmentation, the collected EEG signals are divided into a non-overlapping rectangular window of 5 sec length (640 data samples). Figure 4.1 shows one segment EEG signal of a patient corresponding to different phases of anaesthesia. The sampling frequency of the collected EEG signals is 128 samples/second. It can be observed from the figure that the amplitude of the EEG signals increases with increase in DoA and frequency decreases with increase in

DoA. Here induction phase is the deep anaesthetic phase, maintenance phase is a moderate anaesthetic phase and recovery phase is the light anaesthesia phase.

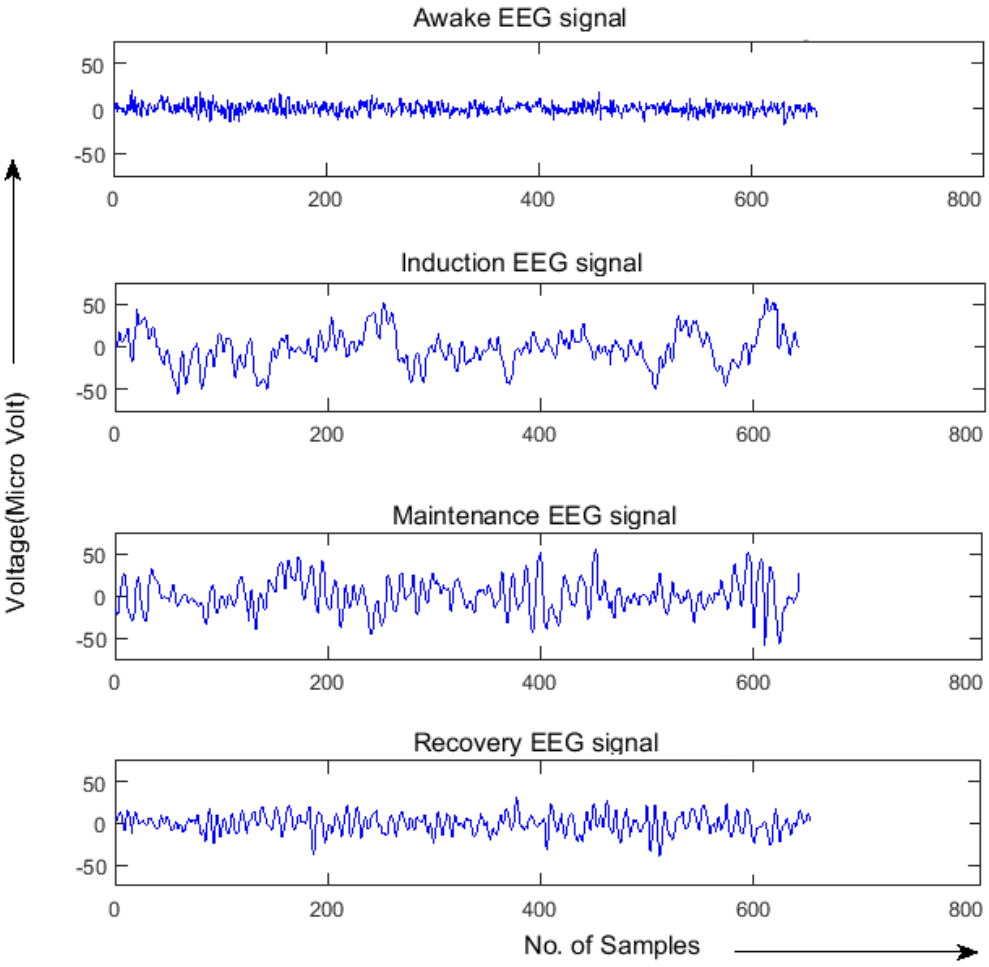

FIGURE 4.1: Uniformily segmented EEG signal.

In non-uniform segmentation method, the window length selected is 5 sec (640 data samples). Here the adaptive segmentation is driven by the amplitude and frequency changes on the EEG signal. These changes are encountered by analyzing the feature kurtosis. Figure 4.2 shows the adaptive segmentation of EEG signal collected from a patient. EEG signal with high-frequency low amplitude region is the awake phase signal region, the low-frequency high amplitude region is induction phase region and medium frequency and medium amplitude region is maintenance phase region. The F function is calculated using the equation 4.1 and is normalized to standardize the values. The two threshold values T_1 and T_2 are selected on an empirical basis and its value in the current study is ± 0.35. From the figure, it is clear

that the local maxima above the threshold T_1 are the transition points of the signal from the high-frequency low amplitude signal to low-frequency high amplitude signal whereas the local minima below the threshold T_2 are the transition of the signal from the low-frequency high amplitude signal to high-frequency low amplitude signal. These transition points are considered as the boundary of segmentation.

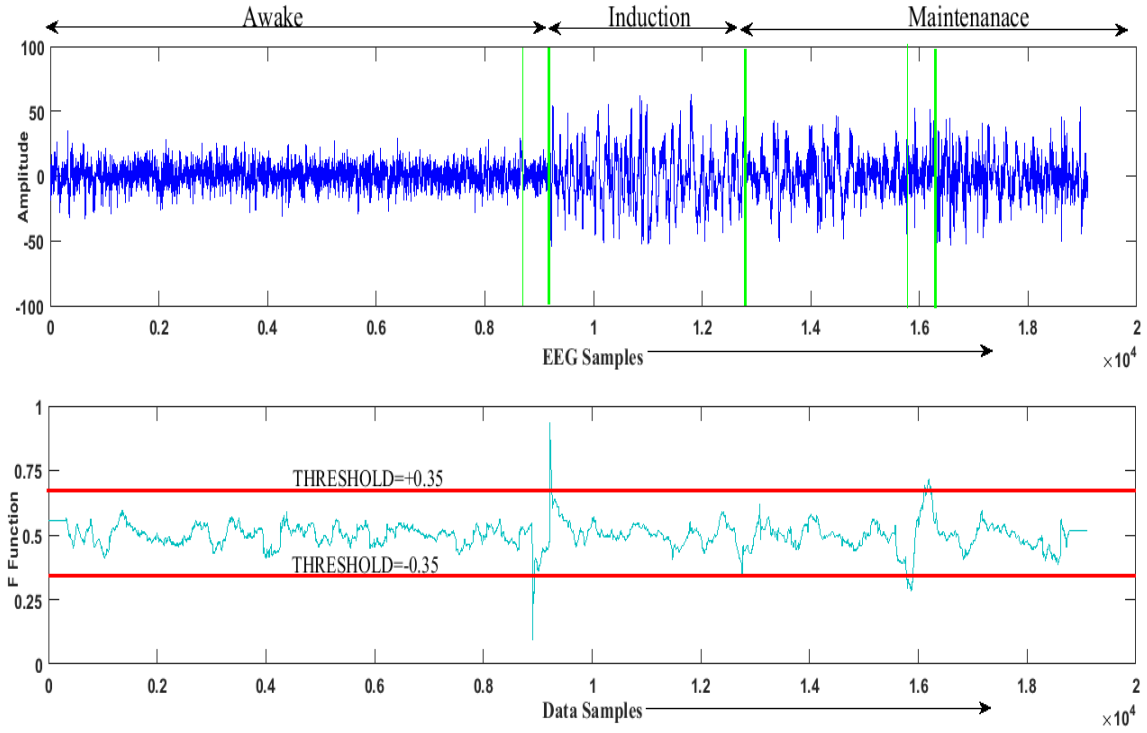

FIGURE 4.2: Non Uniformily Segmented EEG signals.

Further analysis of EEG signals is done with uniform segmentation in order to synchronize the EEG signals and hemodynamic parameters with respect to time. The collected hemodynamic parameters are numerical values and their sampling frequency is 0.2 Hz.

4.3.2 Filtering the physiological noises from EEG signal

Wavelet-based threshold filtering is applied on the EEG signals to improve the accuracy of DoA estimation by suppressing the unwanted artifacts. The current research adopted Discrete Wavelet Transform (DWT) with Daubechies-4 (db4) as mother

wavelet for analysis based on the characteristics of the collected EEG signals. Selection of levels of wavelet decomposition is usually done based on the dominant frequency components of the signals. Here the levels are chosen in such a way that the range of resulting frequency correlates with the five EEG rhythms: δ -band, θ -band, α -band, β -band, and γ -band. The decomposition of the EEG signals into its constituent frequency bands is obtained by successive convolution with high-pass and low-pass filtering. The low-frequency components are obtained from the approximation coefficients and high-frequency components are obtained from the detail coefficients. Table 4.1 and Figure 4.3 shows the 4 level the decomposition of EEG signal with sampling frequency 128 Hz. CA1, CA2, CA3 and CA4 are the approximation coefficients and CD1, CD2, CD3 and CD4 are the detail coefficients obtained after successive decomposition.

TABLE 4.1: Decomposition of EEG signal using DWT

Frequency Range	Frequency Bands	Wavelet Coefficients	Frequency Bandwidth
32-64Hz	Gamma (γ)	CD1	32
16-32Hz	Beta(β)	CD2	16
8-16Hz	Alpha (α)	CD3	8
4-8Hz	Theta (θ)	CD4	4
0-4Hz	Delta (δ)	CA4	4

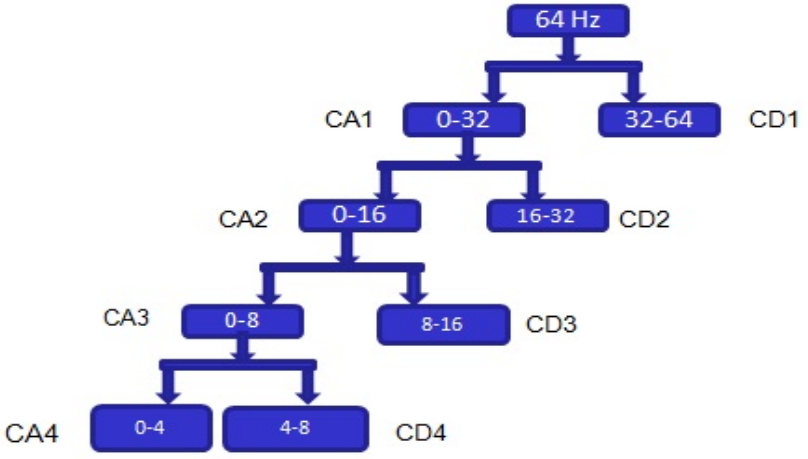

FIGURE 4.3: Decomposition of EEG signals using DWT (4 level decomposition)

In Table 4.1, the component CA_4 represents the δ -band and CD_4, CD_3, CD_2 and CD_1 represent the θ -band, α-band, β -band and γ-band respectively. The sub-band frequencies obtained from the DWT coefficients of awake EEG signal of a patient (including details coefficients CD1 - CD4 and one approximate coefficient (CA4)) representing the EEG frequency bands are shown in Figure 4.4.

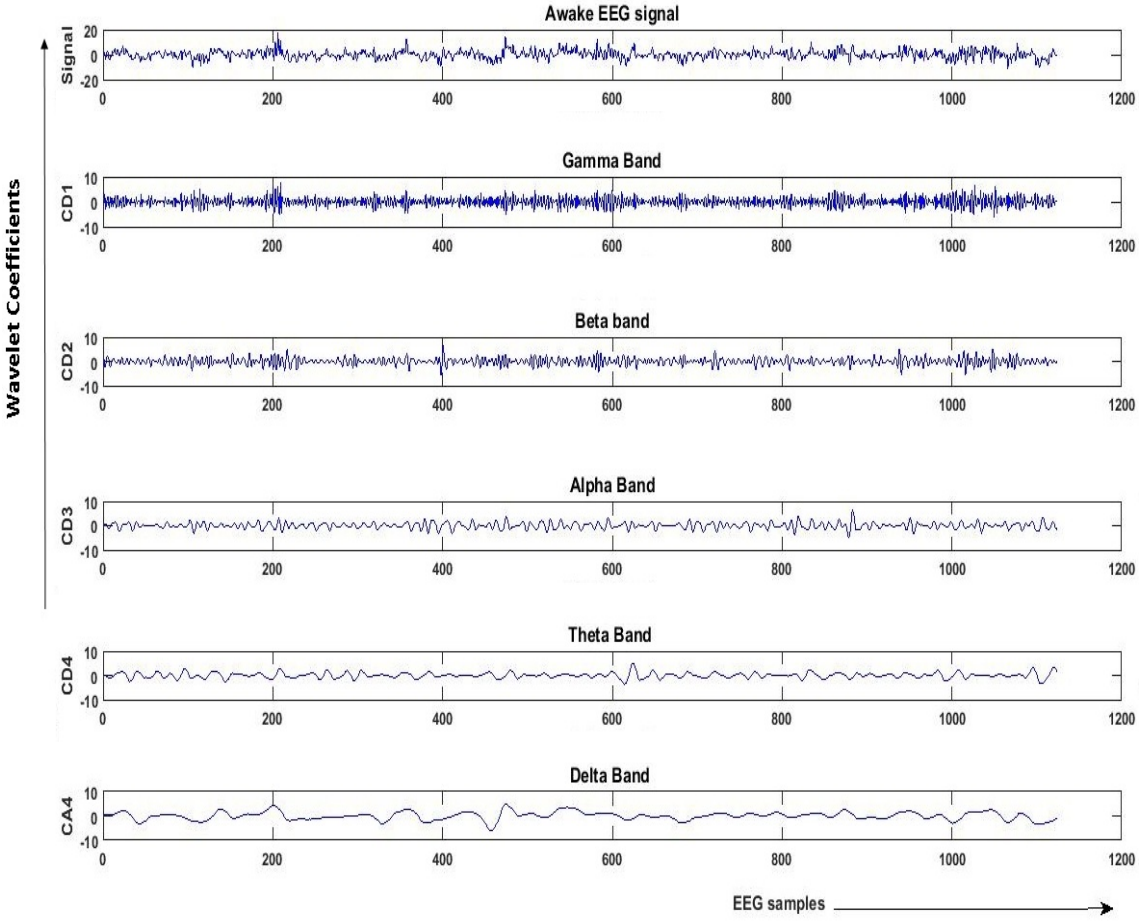

FIGURE 4.4: DWT coefficients of 8 sec duration awake EEG signals

The wavelet-based threshold filtering method filters each coefficient from the sub-bands with a threshold function. In the current research SURE shrink thresholding is incorporated to get the different threshold values at different levels. To obtain the hard threshold, wavelet coefficient cW_j with an absolute value below the threshold T is replaced with 0. A wavelet coefficient with an absolute value above the threshold is kept as it is. To obtain soft threshold, a coefficient with a magnitude

above the threshold value is 'shrink' and otherwise it is replaced with 0. The present study calculated both soft threshold and hard threshold separately to compare the efficiency of the filtering method. The application of this threshold value to CA4 and all detail coefficients removed the unwanted noises from the coefficients. Finally, an inverse wavelet transform is applied to the new coefficients to reconstruct the signals.

Figure 4.5 represents the output of wavelet-based threshold filtering when applied to a 3 minute (23040 data samples) duration EEG signal collected from a patient. The effectiveness of the filtered EEG signal is checked by calculating the cross-correlation between raw EEG signal and filtered EEG signal. Figure 4.6 represents the cross-correlation outcome of the above mentioned 3 sec duration EEG signal. The balance in the data graph indicates that there is a strong correlation between the original EEG signal and the denoised signal. This shows that the frequency information in original EEG signal and the denoised signal are still the same.

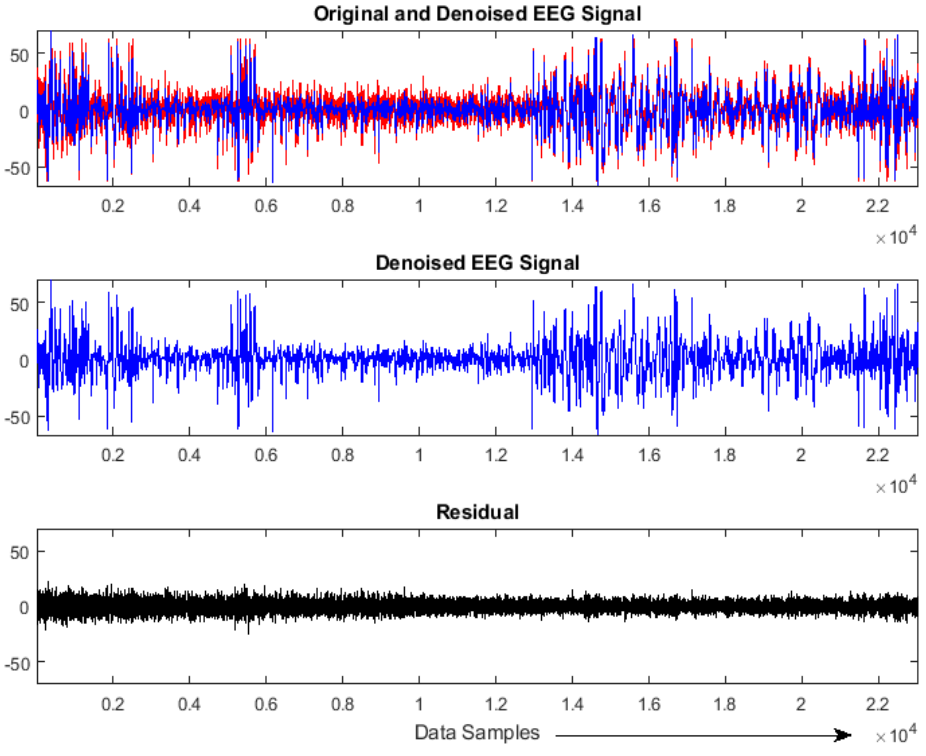

FIGURE 4.5: Result of signal denoising using wavelet based thresholding method

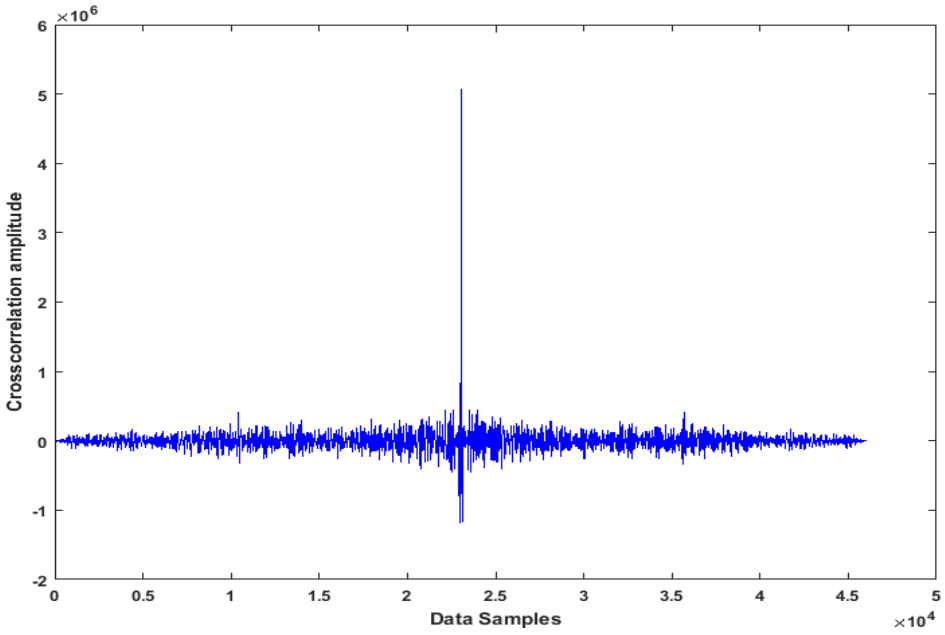

FIGURE 4.6: Cross correlation output

4.3.3 Performance Evaluation of the filter

Performance analysis is usually done to measure the efficiency of denoised signals. In the present study performance of the filtered signals are evaluated by calculating 3 measures Signal to Noise Ratio (SNR), Mean Square Error (MSE) and correlation coefficient.

SNR : is defined as the ratio of signal power to the noise power. It is used to measure dominance of signal over the noises [JIANHUI *et al.* , 2009]. SNR ratio is expressed in dB. The value of the SNR is linear with the performance of the filter. The higher value of SNR means that the performance of the filtering method adopted is acceptable [HE *et al.* , 2015].
Let $X(i) = [x_0, x_1, ..., x_n]$ is the collected EEG signal, $\hat{X}(i) = [\hat{x}_0, \hat{x}_1 ... \hat{x}_n]$ represents the denoised EEG signal and then the noise signal is expressed as equation 4.8

$$N = X(i) - \hat{X(i)} \tag{4.8}$$

SNR is given by

$$SNR = 10log_{10}\frac{\sum_{i=1}^{n} X^2(i)}{\sum_{i=1}^{n} |X(i) - \hat{X}(i)|^2} \tag{4.9}$$

MSE : measures the average of squares of errors or difference between the original signal and the denoised signal which is given by the equation 4.10

$$\text{MSE} = \frac{1}{n}\sum_{i=1}^{n}[\hat{X(i)} - X(i)]^2 \tag{4.10}$$

Correlation Coefficient (γ): is a statistical concept to measure how well a denoised signal follows the original signal

The correlation coefficient is given by

$$\gamma = \frac{\sum_{i=1}^{n}(x_i - \bar{x})(\hat{x_i} - \bar{\hat{x}})}{\sqrt{\sum_{i=1}^{n}(x_i - \bar{x})^2 \sum_{i=1}^{n}(\hat{x_i} - \bar{\hat{x}})^2}} \tag{4.11}$$

Tables 4.2-4.5 indicate the performance evaluation result of wavelet-based threshold filtering with different thresholding techniques applied to the entire 25 patient's EEG data collected during the whole surgery. Here the performance is compared by calculating the measures SNR, MSE and correlation coefficient. Table 4.2 and 4.3 represents the performance of wavelet-based SURE Shrink thresholding technique applied with hard and soft thresholding respectively whereas Table 4.4 and 4.5 provides the performance of wavelet-based Universal thresholding techniques applied with hard and soft thresholding. From the mean and standard deviation presented in the tables, it is evident that the wavelet-based SURE Shrink thresholding applied with soft thresholding has better filtering performance than other thresholding techniques because its SNR is high for all the 25 patient's EEG data and also the values of MSE is very small compared to all other thresholding techniques. Therefore, current research adopted wavelet-based SURE Shrink thresholding applied with soft thresholding for denoising the collected EEG signals.

TABLE 4.2: Performance Evaluation of Wavelet denoising using SURE shrink Threshold and Hard Thresholding

Patient	**Correlation**	**SNR**	**MSE**
Patient 1	0.99994	38.03529458	0.022313494
Patient 2	0.99999	45.02328399	0.011673452
Patient 3	0.99998	42.38776316	0.018039378
Patient 4	0.99994	38.77505173	0.032461232
Patient 5	0.99995	38.95318857	0.017411208
Patient 6	0.99997	41.54181985	0.020176804
Patient 7	0.99999	45.19018456	0.01434957
Patient 8	0.99993	37.29763934	0.022213141
Patient 9	0.99997	41.03018241	0.01742742
Patient 10	0.99999	45.65539309	0.00761527
Patient 11	0.99995	39.33312044	0.024981269
Patient 12	0.99993	37.81588101	0.025151882
Patient 13	0.99998	41.78224008	0.012926934
Patient 14	0.99994	37.99121646	0.025570017
Patient 15	0.99998	42.58179226	0.01182634
Patient 16	0.99993	37.60320551	0.029589321
Patient 17	0.99997	41.85286537	0.019844594
Patient 18	0.99999	44.99702131	0.008696276
Patient 19	0.99965	30.91379258	0.069672835
Patient 20	0.99996	40.60693247	0.024462815
Patient 21	0.99996	40.49899834	0.018645194
Patient 22	0.99993	38.08433182	0.036534701
Patient 23	0.99997	42.12119842	0.018055264
Patient 24	0.99946	29.17142133	0.079651451
Patient 25	0.99994	38.70802136	0.024167648
Mean ± STD	0.99993±0.00011	39.9181±3.9285	0.0245±0.0167

TABLE 4.3: Performance Evaluation of Wavelet denoising using SURE shrink Threshold and Soft Thresholding

Patient	**Correlation**	**SNR**	**MSE**
Patient 1	0.999997735	53.43902256	0.000642976
Patient 2	0.999999794	63.85570656	0.000152741
Patient 3	0.999999277	58.40007821	0.000451846
Patient 4	0.999998198	54.43131108	0.000882549
Patient 5	0.999999114	57.51500932	0.000242464
Patient 6	0.999999025	57.09759056	0.000561404
Patient 7	0.999999223	58.08720807	0.000736439
Patient 8	0.99999826	54.58281055	0.000415043
Patient 9	0.999998953	56.78948793	0.000462703
Patient 10	0.999999548	60.43932641	0.0002531
Patient 11	0.999997527	53.05771396	0.001059632
Patient 12	0.999995527	50.48399432	0.00136069
Patient 13	0.999999052	57.22365343	0.000369279
Patient 14	0.999995065	50.05667212	0.001589225
Patient 15	0.999998853	56.39403401	0.000491616
Patient 16	0.999997637	53.2543095	0.000805424
Patient 17	0.999999481	59.83804265	0.000315591
Patient 18	0.999999736	62.77248551	0.00014514
Patient 19	0.999883028	36.30908688	0.020115649
Patient 20	0.999999017	57.06215461	0.00055333
Patient 21	0.999998888	56.52961439	0.000465056
Patient 22	0.99999784	53.64483596	0.001015442
Patient 23	0.99999961	61.08060609	0.000229437
Patient 24	0.999966467	41.73460304	0.004414439
Patient 25	0.999998527	55.30872083	0.000528645
Mean ± STD	0.999993±0.000024	55.1755±5.9804	0.00153±0.00396

TABLE 4.4: Performance Evaluation of Wavelet denoising using Universal Threshold and Hard Thresholding

Patient	**Correlation**	**SNR**	**MSE**
Patient 1	0.98469619	13.17669185	6.830112332
Patient 2	0.993020226	16.64899822	8.028379288
Patient 3	0.992112709	16.24426019	7.422870065
Patient 4	0.990832987	15.71659841	6.564631167
Patient 5	0.985283577	12.87268972	7.061204653
Patient 6	0.991049571	15.84937853	7.48335767
Patient 7	0.994460303	17.92399394	7.646416397
Patient 8	0.983008131	12.4445063	6.790836667
Patient 9	0.98873159	14.71095487	7.467166732
Patient 10	0.992177634	15.25749603	8.345935174
Patient 11	0.990118601	15.08002868	6.651562349
Patient 12	0.985517644	13.33295707	7.060945815
Patient 13	0.987342614	13.94788038	7.851117841
Patient 14	0.987540354	13.84012945	6.650276779
Patient 15	0.990274225	14.41267546	7.758219011
Patient 16	0.98721962	14.30491887	6.323589336
Patient 17	0.992443921	16.68832962	6.517721249
Patient 18	0.991902497	15.30259457	8.105429087
Patient 19	0.978335806	11.59959344	5.949540141
Patient 20	0.991758043	16.35782167	6.507549851
Patient 21	0.989816924	14.88444756	6.792380207
Patient 22	0.990555677	15.7731976	6.220409561
Patient 23	0.99179511	16.34769993	6.822659427
Patient 24	0.971957699	11.30798947	4.870088788
Patient 25	0.987575858	14.41299797	6.497356998
Mean ± STD	0.9883811±0.00500	14.73755±1.6543	6.96879±0.7755

TABLE 4.5: Performance Evaluation of Wavelet denoising using Universal Threshold and soft Thresholding

Patient	**Correlation**	**SNR**	**MSE**
Patient 1	0.996145245	21.10840048	1.099656342
Patient 2	0.998793068	26.16361082	0.89777317
Patient 3	0.998449542	25.07589147	0.971423781
Patient 4	0.998088944	24.16588869	0.938169483
Patient 5	0.996042838	20.99363347	1.088389702
Patient 6	0.998416905	24.98340363	0.913469376
Patient 7	0.99891804	26.64173178	1.027268947
Patient 8	0.995748638	20.67486805	1.020674136
Patient 9	0.997693591	23.34464644	1.022790514
Patient 10	0.998366039	24.84502461	0.917745258
Patient 11	0.997305578	22.67535445	1.157153809
Patient 12	0.996661602	21.73469588	1.02020864
Patient 13	0.997376043	22.78136965	1.027028674
Patient 14	0.996739411	21.84049156	1.053909962
Patient 15	0.997692663	23.34305584	0.992485104
Patient 16	0.997003743	22.20735132	1.024991852
Patient 17	0.998123513	24.24816044	1.143174955
Patient 18	0.998196129	24.4161908	0.994068671
Patient 19	0.994465654	19.52792185	0.958628989
Patient 20	0.997994521	23.95941227	1.130468443
Patient 21	0.997425897	22.87030573	1.080030875
Patient 22	0.997952175	23.86570568	0.965090794
Patient 23	0.998037569	24.05300261	1.157239968
Patient 24	0.991722015	17.78333585	1.096483854
Patient 25	0.997024828	22.23922857	1.071799795
Mean ± STD	0.99721±0.00154	23.02170±2.03557	1.03080±0.07652

4.4 Summary

This chapter explains two major areas of data preprocessing: segmentation and filtering. The segmentation of signals was done for the effective analysis of the data. Uniform segmentation of the collected EEG signals was done by splitting the signals into equal time interval of 5 sec duration. Non-uniform segmentation of EEG signals was done by calculating the feature kurtosis and splitting the signal at boundary of change occurs. As a result, the EEG signals were segmented when a change from low-frequency high amplitude to high-frequency low amplitude and vice versa occurs. To denoise, the EEG signals current research adopted wavelet-based threshold filtering method. Two thresholding techniques such as SURE Shrink thresholding and Universal thresholding were experimented to improve the accuracy of DoA estimation. Finally, the performances of the filter with different thresholding techniques were compared by calculating the measures SNR, MSE and correlation coefficient. The results revealed that wavelet denoising based on SURE Shrink Threshold with soft thresholding technique was able to remove noises from the EEG signals effectively.

Chapter 5

Feature Extraction

A feature is a functional component extracted from a signal or from a set of data that represent the characteristics of data/signal without losing significant information embedded in the data. The features are obtained by applying the different feature extraction methods on the signals. Feature extraction part is included in the current research to minimize the complexity of implementation and to reduce the time consumption of information processing. In this chapter, the inherent properties of EEG signals and hemodynamic variables are extracted as features. This chapter has two parts:

1. Feature extraction from EEG signals
2. Feature extraction from hemodynamic variables

The variations on EEG signals due to the effects of anaesthetic drugs are reflected as amplitude and frequency variations [Voss & Sleigh, 2007]. Feature extracted from EEG signals depicts these amplitude and frequency variations and thus the hypnotic state of the patient whereas features extracted from hemodynamic variables can quantify the hemodynamic variability due to the anaesthetic drugs. Therefore, features extracted from both EEG and hemodynamic variables are necessary for the accurate estimation of DoA.

5.1 Feature Extraction from EEG Signals

EEG signals are non-stationary signals arising from cortical, subcortical and brain-stem structures in the brain. Analysis on these signals is a time-consuming process because of the size of EEG data. In order to reduce the dimensionality of EEG signals, some features are extracted that represent the characteristics of original EEG signal. If a surgery is of 3-hour duration then one patient's collected EEG signal consists of more than 13 lakh of data points (10800 seconds duration data). Analyzing all these data points is a time-consuming process. Therefore, the dimensionality of the EEG signals is reduced by extracting core features from the signals. A variety of methods have been used to extract features from the time domain, frequency domain and time-frequency domain representation of EEG signals. Apart from this non-linear analysis provides some features that represent the distinguishing property of EEG signal.

5.1.1 Time Domain Parameters

Time domain behaviour of a signal is one of the most important property that decides the shape of the collected signals and carries information like amplitude, phase and rate of change. Time domain analysis of EEG signals provides information about the changes in the signal with respect to time based on the morphological features of the signal. This analysis is purely statistical where mean, standard deviation and variance are considered. The time domain parameters extracted from collected EEG signals for the estimation of DoA are given below.

5.1.1.1 Variance and Standard Deviation

Variance and standard deviation of a signal measures how the signal is spread out and indicates how much variation or dispersion from the mean exists. A low standard deviation indicate that the data points of the signals are tend to be very close to the mean and high standard deviation indicate that the data points are spread out over a large range of values.

The variance of a signal is the square of its standard deviation and it is represented as.

$$var(x) = \sigma^2 \tag{5.1}$$

where σ is the Standard Deviation(SD) which is the Root-Mean-Square(RMS) deviation of data points from the mean $\overline{x}$ and is given by the equation

$$\sigma = \sqrt{\frac{\sum(x_i - \overline{x})^2}{N-1}} \tag{5.2}$$

$$\sigma = \sqrt{\frac{1}{N-1}\sum_{i=1}^{N}(x_i - \overline{x})^2} \tag{5.3}$$

where N is the total number of data samples in the signal and x_i is a data instance.

5.1.1.2 Energy

Energy of a signal is defined as the area under the squared signal and is used to measure the signal strength. It is given by the equation

$$E_s = \sum_{n=0}^{N-1} |x(n)|^2 \tag{5.4}$$

where x(n) represent discrete samples of a signal at regular interval of N points stretching from 0 to N-1.

5.1.1.3 Entropy

Entropy is defined as a measure of uncertainty in a given random variable or it can be defined as the measure of the order in a signal. Signal order is the degree of randomness of the signal.
Let X be a signal of length N represented as $X = x_1, x_2, ..., x_N$, then Entropy is calculated using the equation

$$H(X) = -\sum_{i=1}^{N} p(x_i) log_{10} p(x_i) \tag{5.5}$$

where $p(x_i)$ is a probability of a random value x_i of the signal.

5.1.1.4 Mean Absolute Deviation (MAD)

Mean Absolute Deviation (MAD) is defined as the mean of absolute deviations from the mean of a signal. It calculates the average distance from the mean of a signal. Let X be a signal of length N represented as $X = x_1, x_2, ..., x_N$, then MAD is given by the equation.

$$MAD(X) = \frac{\sum_{i=1}^{N} \left| x_i - \mu \right|}{N} \tag{5.6}$$

where x_i is a data point and μ is the mean of the signal.

5.1.1.5 Zero Crossing Rate (ZCR)

Zero Crossing Rate is the rate at which the waveform crosses zero. It can also be defined as the rate of sign changes along the signal. ZCR gives information about the number of zero-crossings present in a given signal. If the number of zero crossings is more in a given signal, then the signal is changing rapidly and accordingly the signal may contain high-frequency information. On the other hand, if the number of zero crossing is less, then the signal is changing slowly and accordingly the signal may contain low-frequency information. Thus ZCR gives indirect information about the frequency content of the signal [Bachu *et al.* , 2008].
The zero-crossing rate of N samples of a signal starting at sample m is given by [Iser *et al.* , 2008]

$$ZCR = \frac{1}{2(N-1)} \sum_{n=m+1}^{m+N-1} \left| sgn\left\{s(n)\right\} - sgn\left\{s(n-1)\right\} \right|, \tag{5.7}$$

where

$$sgn\left\{s(n)\right\} = \begin{cases} +1, & \text{s(n)}\geq 0. \\ -1, & \text{s(n)}< 0. \end{cases} \tag{5.8}$$

where $s(n)$ and $s(n-1)$ are the current value and the previous value respectively.

5.1.1.6 Inter Quartile Range (IQR)

The interquartile range (IQR) is the measure of variability of a signal and divide the signal into quartiles. Quartiles divide the rank-ordered signal data into four equal parts. The values that separate the parts are called first, second, and third quartiles and they are denoted by Q1, Q2, and Q3, respectively. IQR is also called the midspread or middle 50%[Deller Jr *et al.* , 1993]. It is a measure of statistical dispersion, being equal to the difference between 75^{th} and 25^{th} percentiles or between upper and lower quartiles and is given by the equation.

$$IQR = Q3 - Q1 \tag{5.9}$$

In other words, the IQR is the 1^{st} quartile subtracted from the 3^{rd} quartile[Deller Jr *et al.* , 1993].

5.1.2 Frequency Domain features

Frequency domain analysis examines the EEG signal based on the frequency spectrum. Fast Fourier Transform (FFT) and Wavelet Transform (WT) are the most popular methods which transform a data/signal in time domain to frequency domain. Frequency domain analysis is an important approach to signal processing and analysis, where the signal is examined with respect to frequency. Fourier analysis provides amplitude and a phase spectrum, which is analogous to the histogram of amplitudes and phase angles of signal components. It also plays an important role in the implementation of filters and spectral analysis. When applied to EEG signals it is mostly used to extract different spectral features, which are important for the EEG applications. For the estimation DoA, current research extracted the frequency domain features spectral entropy and spectral edge frequency.

5.1.2.1 Spectral Entropy (SEn) :

Spectral entropy is Shannon's entropy computed over normalized power spectral density function. Power spectral density is the distribution of power as a function

of frequency. Spectral Entropy uses the amplitudes of the power spectrum of a signal as probabilities in entropy calculation [Subha *et al.* , 2010; Fell *et al.* , 1996]. Spectral Entropy calculation in the current research uses the following steps [Sharma *et al.* , 2015]

1. Calculation of the Fast Fourier Transform (FFT) of EEG signal using the equation

$$X(k) = \sum_{n=0}^{N-1} x(n).W_N^{nk} \tag{5.10}$$

where $W_N = e^{-j(\frac{2\Pi}{N})}$, $k = 0, 1, ...N-1$ and $X(k)$ is the Fourier transformed form of the signal.

2. Calculation of Power Spectral Density (PSD) using the equation

$$PSD(K) = |X(k)|^2 \tag{5.11}$$

which is the squared magnitude of the FFT

3. Normalize the Power Spectral Density between [0-1] by computing the total power spectral density and dividing the power level corresponding to each frequency by the total power and is given by

$$PSD_N(K) = \frac{PSD(K)}{\sum PSD(K)} \tag{5.12}$$

4. Finally, spectral Entropy is calculated using the equation

$$H(s) = -\sum PSD_N(k) log(PSD_N(k)) \tag{5.13}$$

The use of spectral entropy in the current study is that it permits separation of frequency contributed from different frequency ranges of the signal. That means it can separate high-frequency contribution of a signal from its low-frequency contributions.

5.1.2.2 Spectral Edge Frequency (SEF)

Spectral Edge Frequency is the frequency below which total power of the signal is located. It is expressed as "SEF x" which stands for the frequency below which x percent of the total power of a given signal is located (usually x is in the range 75 to 95). 95 % spectral edge frequency has been widely used to assess Depth of Anaesthesia [Doi *et al.* , 1997; De Deyne *et al.* , 1998]. Steps followed in the current research for the Spectral Edge Frequency calculation is given below [Long *et al.* , 1989]

1. Calculation of Fast Fourier transform of the EEG signal using the equation

$$X(f) = \sum_{n=0}^{N-1} x(n).W_N^{nf} \tag{5.14}$$

   where $W_N = e^{-j(\frac{2\Pi}{N})}$, $f = 0, 1, ...N-1$ and $X(f)$ is the Fourier transformed form of signal.

2. Calculation of Power spectrum $P(f)$ by multiplying themselves with Fourier's transformed amplitudes of each element $X(f)$.

$$P(f) = X(f) * X'(f); \tag{5.15}$$

   where $X'(f)$ is the Fourier's complex conjugated $X(f)$

3. Finally, Spectral Edge Frequency 95^{th} percentile (SEF_{95}) is calculated using the equation

$$\int_0^{SEF_{95}} P(f)df = 0.95 \int_0^{\frac{fs}{2}} P(f)df \tag{5.16}$$

   where fs is the sampling frequency

SEF performs the analysis of a signal in the energy plane (potency) as a function of frequency. i.e. SEF_{95} is the frequency below which 95 % of the whole potency (or energy) of the original signal is located.

5.1.3 Time-Frequency Domain Features

In order to localize the EEG signals in both time and frequency domains simultaneously researchers use Time-Frequency domain representation. Time-frequency representation of a signal can be done effectively using Wavelet Transform (WT). WT is capable of providing the time and frequency information simultaneously, hence it is called time-frequency representation of the signal. At low frequencies, it provides lower time resolution and high-frequency resolution. At high frequencies, it gives high time resolution and lower frequency resolution. That means higher frequencies are better resolved in time and lower frequencies are better resolved in frequency [POLIKAR, n.d.]. Most of the biomedical signals are non-stationary signals and therefore WT is well suited for locating its transient events. Present study takes the advantages of wavelet's feature extraction and multiresolution analysis to analyze various transient events in awake and anaesthetized states of EEG signals. Multiresolution analysis decomposes EEG signals into a number of frequency bands. These decomposed signals are capable of capturing transient features and localized in both time and frequency context. For EEG signal analysis Discrete Wavelet Transform (DWT) with Mallat's fast algorithm is commonly used [Mallat, 2008].
Basic wavelet function is given by the equation

$$\Psi_{a,b}(t) = \frac{1}{\sqrt{a}}\Psi(\frac{t-b}{a}) \tag{5.17}$$

where 'a' is the scale parameter and 'b' is the translation parameter. The wavelet Transform of a signal is given by the equation

$$W(a,b) = \int x(t)\frac{1}{\sqrt{(a)}}\Psi(\frac{t-b}{a})dt \tag{5.18}$$

where '$W(a,b)$' is the wavelet coefficients of the signal $x(t)$

For the estimation of DoA, current research extracted the features Relative Wave Energy and Wavelet Entropy from collected EEG signals through DWT analysis.

5.1.3.1 Relative Wavelet Energy (RWE) and Wavelet Entropy (WEn) :

Two main features extracted from the wavelet domain representation are Relative Wavelet Energy (RWE) and Wavelet Entropy (WEn). The feature RWE is extracted to find out the degree of importance of different EEG frequency bands associated with different anaesthetic phases such as awake, induction, maintenance and recovery. WEn provides information about the degree of order/disorder associated with multi-frequency EEG signals. WEn integrates frequency decomposition and entropy principles to estimate the degree of order/disorder of collected EEG signals with a high time-frequency resolution. The algorithm adopted for the extraction of WEn and RWE features is as follows [Rosso *et al.* , 2001]

1. Decomposition of the EEG signals to its detail and approximation coefficients using the DWT equations.

$$cA_j(n) = \sum g(l-2n)cA_{j-1}(l) \tag{5.19}$$

$$cD_j(n) = \sum h(l-2n)cD_{j-1}(l) \tag{5.20}$$

   where $cA_j(n)$ and $cD_j(n)$ represents the detail and approximation coefficients of the EEG signal, g and h represents low pass and high pass filter to filter the EEG signals.

2. Calculation of total energy of the wavelet coefficients using the equation

$$E_{m,total} = \sum_{j=1}^{4}\sum_{k=1}^{m}|cD_j(k)|^2 = \sum_j E_{m,j} \tag{5.21}$$

   where m is the window length of EEG segment, j is the levels of decomposition(If 4 level decomposition is preferred then its value ranges from 0-4, $E_{m,j}$ is the energy of the EEG segment at level j and which is given by

$$E_{m,j} = \sum_{j=1}^{4}|cD_j(k)|^2 \tag{5.22}$$

3. Calculation of Relative Wavelet Energy($\rho_{m,j}$) using the equation

$$\rho_{m,j} = \frac{E_{m,j}}{E_{m,total}} \tag{5.23}$$

4. Wavelet Entropy is given by

$$WEn_m(\rho) = -\sum \rho_{m,j} log \rho_{m,j} \tag{5.24}$$

WEn provides the information about the degree of order associated with awake and anaesthetic EEG signals whereas RWE reveals the prominent frequency band associated with DoA estimation. The advantage of Wavelet-based analysis is that it can be localized in both time and frequency whereas the standard Fourier transform is localized only in frequency.

5.1.4 Non linear Features

EEG signals are complex signals having nonlinear properties. Therefore, other than the amplitude and frequency variations the complexity and nonlinear behaviour of EEG signals are to be considered. Practically various measures are available to characterize the complexity and behaviour of time series signals like Lempel-Ziv (LZ) Complexity analysis, Approximate Entropy and Chaos-based estimates of complexity. These analysis were based on regular, chaotic and stochastic behaviour of time series signals [Lempel & Ziv, 1976; Pincus, 1991; Efstathiou *et al.* , 2001]. According to Rain Ferenets et al., nonlinear properties of EEG signals are very important to consider during general anaesthesia [Ferenets, 2007]. Current research extracted the features Approximate Entropy (ApEn) and Permutation Entropy (PEn) to study the regularity/complexity property of collected EEG signals.

5.1.4.1 Approximate Entropy (ApEn)

Approximate entropy is an uncertainty measure originally proposed in the context of dynamic systems and time series. The ApEn was introduced by Pincus et al. to quantify the information available in the time series data. A low value of ApEn

indicate that the time series data is deterministic while a high value indicate randomness [Pincus & Keefe, 1992]. In the current research, approximate entropy measures the regularity and the degree of randomness of the EEG signals during different phases of anaesthesia, where each EEG signal is considered as a time series data. The algorithm adopted for the calculation of approximate entropy is detailed below [Guo *et al.* , 2010; Pincus & Keefe, 1992].

Consider an EEG signal X of length N which is indicated by $X = \{x(1), x(2), x(3)$ $.....x(N)\}$.

Let $X(1), X(2), X(3).....X(N-m+1)$ are the sub segments of the EEG signal X formed according to

$$X(i) = \{x(i), x(i+1), x(i+2).....x(i+m-1)\}; for\ i = 1, 2, ...N-m+1 \quad (5.25)$$

where m is the length of sub segment or number of subsequent samples

1. Calculate the distance between two sub segments $X(i)$ and $X(j)$ is given by the equation

$$d[X(i), X(j)] = max|x(i+k) - x(j+k)| \quad (5.26)$$

where $k = 0, 1, 2 \ldots m-1$

2. Calculate the measure C_i^m which describes the similarity between sub segment $X(i)$ and other sub segment $X(j)$ using the equation

$$C_i^m(r) = \frac{M^m(i)}{N-m+1} \quad (5.27)$$

where M^m is the count for $j(j = 1, 2....N-m+1, j \neq i)$ under the condition $d[X(i), X(j)] \leq r$; for $i = N-m+1$, r is a predetermined tolerance value defined as $r = k * std(signal)$; k is a constant (typically $k = 0.2$) and $std(signal)$ represents the standard deviation of the time series signal.

3. Compute ϕ_i^m which is the average of natural logarithm of each $C_i^m(r)$

$$\phi^m(r) = \frac{1}{N-m+1} \sum_{i=1}^{N-m+1} \ln C_i^m(r) \quad (5.28)$$

4. Approximate entropy is calculated using the equation

$$ApEn = \phi^m(r) - \phi^{m+1}(r) \tag{5.29}$$

ApEn is insensitive to low level noises and hence, it is very suitable for EEG signal analysis. Higher regularity of EEG signals produces smaller ApEn values and low regularity produces higher ApEn values [Acharya *et al.* , 2012].

5.1.4.2 Permutation Entropy (PEn)

Permutation Entropy (PEn) was developed to overcome the difficulties of classical entropy measures like Shannon entropy and Approximate Entropy. Most of the classical entropy measures ignore the temporal order of the time series and therefore it requires more computation time. In PEn the complexity of time series signal is quantified using symbolic dynamics. This method was proposed by Bandt et al. in 2002[Bandt & Pompe, 2002]. It combines the concepts of entropy and symbolic dynamics to create Permutation Entropy. The computational considerations of PEn in the current research is detailed below[Shi *et al.* , 2016]

Consider a time series signal $x(n)$ represented as $x(n) = \{x_1, x_2, ..., x_N\}$

1. Represent the signal symbolically to generate $N - (m-1)$ vectors as $\{X_1, X_2, \ldots X_{N-(m-1)}\}$ which is defined by $X_t = [x_t, x_{t+\tau}, ..., x_{t+(m-1)\tau}]$ where the embedding dimension m determines how much information is contained in each vector and τ is the delay component and its value in the current study is 1

2. Calculate the ranks of the values in each sequence $X_t = [x_t, x_{t+\tau}, ..., x_{t+(m-1)\tau}]$ which leads to the rank sequence $r_t = r_1, r_2 \ldots r_m$. The ranks are the indices of the values in ascending sorted order of each sequence X_t as $[x_t \leq x_{t+\tau} \leq ...x_{t+(m-1)\tau}]$.

3. Create a permutation pattern $\pi_i = [r_1, r_2 \ldots r_m]$ with the offset of the permuted values. For m different numbers, there will be $m!$ possible order patterns. In

general, to each time series, it is possible to associate a probability distribution Π, whose elements π_i are the frequencies associated with the i possible permutation patterns.

4. Compare the rank sequence of step 2 with all permutations pattern and count the occurrences of the order pattern π_i, which is denoted as $C(\pi_i)$ where $i = 1, 2, 3...m!$.

5. Calculate the relative frequency using the Equation

$$p(\pi) = C(\pi)/(N - (m-1)\tau) \tag{5.30}$$

6. Finally, Permutation Entropy is calculated using the Equation

$$PEn = -\sum_{m=1}^{m!} p(\pi) \ln p(\pi) \tag{5.31}$$

The largest value of PEn is $log(m!)$, which indicate that the time series is completely random; the smallest value of PEn is zero, indicating the time series is very regular. In short, the permutation entropy refers to the local order structure of the time series which can give a quantitative complexity measure for a dynamic time series. Permutation entropy calculation depends only on the selection of m. When m is too small (less than 3), the scheme will not work well since there are only a few distinct states for EEG signal. For long duration EEG signals high value of m is better [Li *et al.* , 2014]. Current study opted the value of m as 3 to detect the dynamic changes of EEG signals.

5.2 Feature Extraction from Hemodynamic Parameters

The introduction of hemodynamic variables in the estimation of DoA helps to provide information about changes in clinical parameters which are necessary for anaesthesia decision-making. EEG extracted features provide the hypnotic response of

anaesthetic drugs whereas hemodynamic variability due to the drugs are measured by extracting features from hemodynamic variables such as Heart Rate and Blood Pressure. An increase in HR or BP is an indicator of increased sympathetic activity and parasympathetic activity. The sympathetic activity of the body is the intense physical activity and is usually called fight-or-flight response. The parasympathetic activity is the opposite effect i.e. it relaxes the body and inhibits or slows many high energy functions. Therefore, feature extraction from these hemodynamic variables is more appropriate to study the analgesic state of the patient.

Collected hemodynamic variables in the current research are HR, SBP and DBP. The features extracted from these variables are Change in Heart Rate (Δ HR), Change in Mean Blood Pressure (ΔMBP) and Pulse Pressure (PP). These extracted features are good indicators of hemodynamic variability and are used in several studies related to hemodynamic variables. Balick et al. used PP to measure the hemodynamic instability during anaesthesia[Balick Weber *et al.* , 2011; Nora *et al.* , 2007; Hosseinzadeh *et al.* , 2013].
The feature extracted from HR is ΔHR and is calculated using the equation

$$\Delta HR = \frac{\text{HR at the moment} - \text{baseline HR}}{\text{baseline HR}} \times 100 \tag{5.32}$$

The features extracted from BP signals are Δ Mean Blood Pressure (ΔMBP) and Pulse Pressure(PP) which are calculated using the equations

$$MBP = \frac{SBP + 2 \times DBP}{3} \tag{5.33}$$

$$\Delta MBP = \frac{\text{MBP at the moment} - \text{baseline MBP}}{\text{baseline MBP}} \times 100 \tag{5.34}$$

$$PP = SBP - DBP \tag{5.35}$$

Where baseline HR and baseline MBP are the average of HR and MBP collected

from each patient before inducing the anaesthetic drugs.

The extracted features Δ HR and ΔMBP are used instead of HR and MBP because their values are patient dependent. That means their values vary from patient to patient. Finally, the features Δ HR and ΔMBP are normalized using the Equation 5.36 to standardize their variations.

$$X_{i_{norm}} = \frac{X_i - X_{min}}{X_{max} - X_{min}} \tag{5.36}$$

where X_i is the i^{th} data point of feature X, X_{min} and X_{max} represents the minimum and maximum values of feature X.

5.3 Experimental Results of EEG feature Extraction

5.3.1 Time Domain Features

The time domain features Standard deviation, Energy, Entropy, Mean Absolute Deviation, Zero Crossover Rate and Inter-Quartile Range are extracted from the collected EEG signals. Table 5.1 shows the extracted time domain features of six continuous EEG epochs (30 seconds EEG data) from each anaesthetic phase of a patient.

The feature values of Standard Deviation, Energy, Mean Absolute Deviation and Inter-Quartile Range are high in induction phase (deep anaesthetic phase) EEG signals and low in awake EEG signals whereas maintenance and recovery phase EEG signals exhibits some intermediate values. But the feature values of recovery phase EEG signals (light anaesthesia) are higher than the awake phase EEG signals and lesser than maintenance phase EEG signals. This indicates that values of these features increase with the increase in DoA. On the other hand, ZCR and Entropy feature values decrease with increase in DoA.

Table 5.1: Time Domain Features

Features	EEG segment	Anaesthetic Phases			
		Awake	Induction	Maintenance	Recovery
STDEV	1	7.98	23.51	10.60	8.29
	2	6.34	19.77	12.76	10.51
	3	7.56	23.39	10.08	7.97
	4	7.26	20.84	14.82	9.47
	5	5.76	21.18	10.86	8.71
	6	6.40	23.01	18.25	8.46
Energy	1	40941	334682	101234	68294
	2	46038	224543	129391	58877
	3	36573	364272	111278	54963
	4	27809	307862	104408	48659
	5	33742	431843	88398	54804
	6	43742	237966	98687	41539
Entropy	1	1.73	1.13	1.27	1.43
	2	1.69	1.13	1.4	1.47
	3	1.68	1.13	1.38	1.47
	4	1.55	1.19	1.33	1.47
	5	1.65	1.2	1.3	1.48
	6	1.76	1.18	1.31	1.45
MAD	1	4.57	17.8	11.63	10.53
	2	4.83	19.8	13.01	8.63
	3	4.3	16.97	12.79	9.45
	4	4.13	21.34	13.46	9.7
	5	5.07	16.06	12.8	8.64
	6	4.17	19.1	12.36	9.04
ZCR	1	0.4	0.08	0.15	0.22
	2	0.49	0.09	0.15	0.27
	3	0.33	0.1	0.16	0.28
	4	0.35	0.1	0.19	0.23
	5	0.31	0.09	0.14	0.22
	6	0.37	0.11	0.15	0.27
IQR	1	6.01	24.02	17.98	12
	2	5.01	22.51	21	16
	3	4	21.98	19.99	10.99
	4	5.01	23.5	18.48	9.98
	5	6.09	21.51	16.03	10.68
	6	5.9	22.06	19.96	13.56

To compare the generalized performance of time domain features during the awake, induction, maintenance and recovery phases mean and the standard deviation are calculated from all the 25 patients and are shown in Table 5.2.

TABLE 5.2: Mean ± standard deviation of extracted Time domain Features

	Awake	Induction	Maintenanace	Recovery
STDEV	7.59 ± 2.29	21.62 ± 2.38	11.40 ± 3.34	8.74 ± 2.93
Energy	37713 ± 12587	300118 ± 38153	96114 ± 34601	60279 ± 20005
Entropy	1.62 ± 0.05	1.18 ± 0.07	1.37 ± 0.11	1.52 ± 0.10
MAD	5.06 ± 0.95	17.00 ± 1.08	10.82 ± 2.07	8.87 ± 1.56
ZCR	0.39 ± 0.07	0.08 ± 0.01	0.13 ± 0.03	0.23 ± 0.03
IQR	6.62 ± 1.32	24.00 ± 2.46	17.58 ± 4.08	9.18 ± 2.30

Anaesthetic timeline of patient-24 is given in table 5.3 for reference. Figure 5.1-5.6 represents the extracted time domain features of patient-24 and its comparison with BIS index. The transition from all the phases is well defined in all the extracted features compared to BIS index. The 3 main transitions are

1. Awake to induction
2. Induction to maintenance
3. Maintenance to recovery.

From the figures it is evident that in the awake phase, values are low for the features Standard deviation, Energy, Mean Absolute Deviation and Inter-Quartile Range and high for ZCR and entropy. This indicates the conscious state of the patient. In induction phase Standard deviation, Energy, Mean Absolute Deviation and Inter-Quartile Range feature values are high and ZCR and entropy features show low values to indicate the deep anaesthetic which is the unconscious state of the patient. In the Maintenance phase, values of the features such as Standard deviation, Energy, Mean Absolute Deviation and Inter-Quartile Range are below induction phase values whereas the values are above induction phase for the features ZCR and entropy. Usually, surgery is carried out during the Maintenance phase. Finally, in the recovery phase, feature values decreases from the point of transition of maintenance to recovery in the case of Standard deviation, Energy, Mean Absolute Deviation and Inter-Quartile Range and increases in ZCR and entropy features.

Table 5.3: Anaesthetic time line of a patient

Time	Drug	Events	Drug dose
12:39:08 PM		Recording Started	
12:39:43 PM	Midazolam	Drugs Induced with	1mg
	Glycopyrolate		0.2mg
	Propofol(Anaesthetic drug)		100mg
	Vecronium Bromide (Muscle relaxant)		15mg
	Fentanyl(analgesic drug)		100 μ g
12:41:36 PM	Sevoflurane and N_2O	Inhalation agent started	
12:45:00 PM	Sevoflurane	Inhalation agent increased	
12:46:23 PM	Sevoflurane	Inhalation agent reduced slightly	
12:51:43 PM	Sevoflurane	Inhalation agent increased	
12:57:00 PM	Fentanyl (analgesic drug)	Analgesic drug to reduce BP and HR	100μ g
1:06:45 PM	Sevoflurane	Inhalation agent reduced	
1:14:07 PM	Sevoflurane	Inhalation agent closed	
1:20:26 PM	Neostigmate	Reversal drugs given	2.5 mg
	Glycopyrolate		0.4 mg
1:22:18 PM		stopped recording	

This indicates that in the recovery phase patient is coming out from the effects of anaesthetic drugs.

The adjustments in the administration of inhalation agent sevoflurane also affect the DoA estimation. If we increase the administration of the sevoflurane then it would increase the DoA and vice versa. In the case of patient-24, adjustments in the administration of inhalation agent sevoflurane was done at time points 12:41:36, 12:45:00, 12:51:43, 1:06:45 ,1:14:07 and 1:20:26 hours(refer Table 5.3). These adjustments of sevoflurane administration do not make any appreciable change in the extracted time domain features (refer Figures 5.1-5.6). The influence of time domain features in the current research is that the transitions from awake to induction

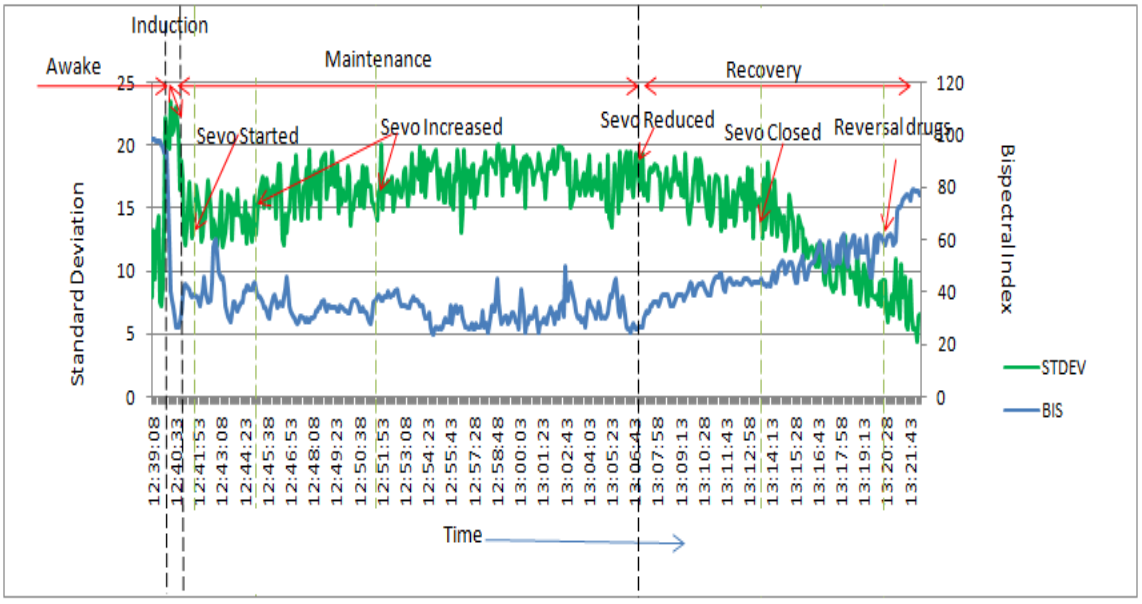

FIGURE 5.1: Comparison of BIS and extracted Standard deviation during the four phases of anaesthesia

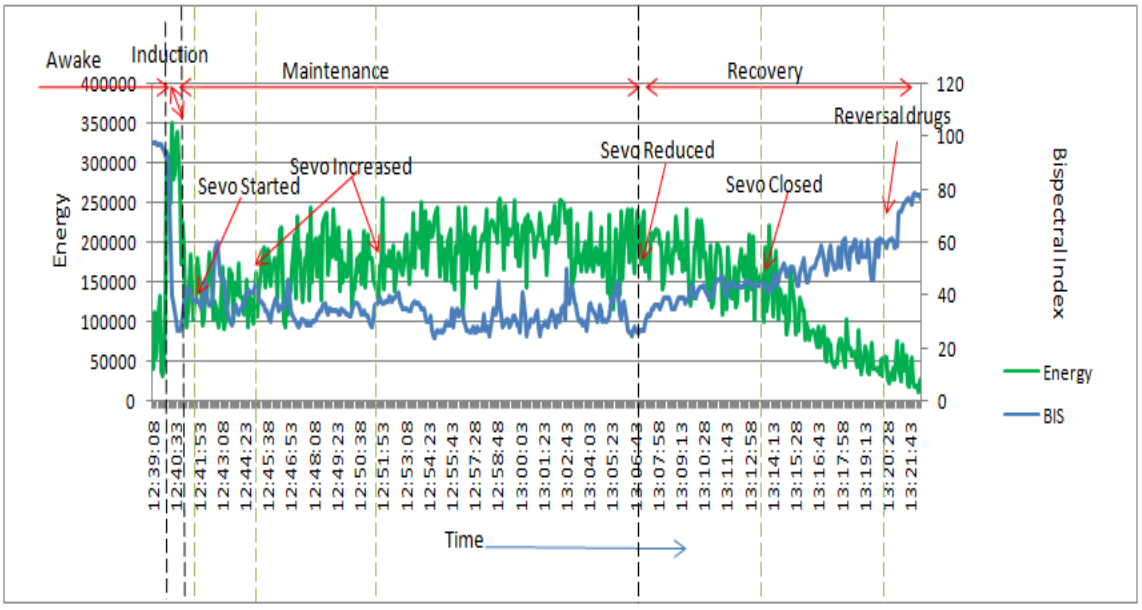

FIGURE 5.2: Comparison of BIS and Energy during the four phases of anaesthesia

and induction to maintenance are distinct in the entire time domain feature, but these transitions are not recognizable in BIS. Comparison of BIS with extracted time domain features is done by calculating Pearson correlation coefficient. Correlation coefficient value near to zero indicates weak correlation whereas near to one indicates

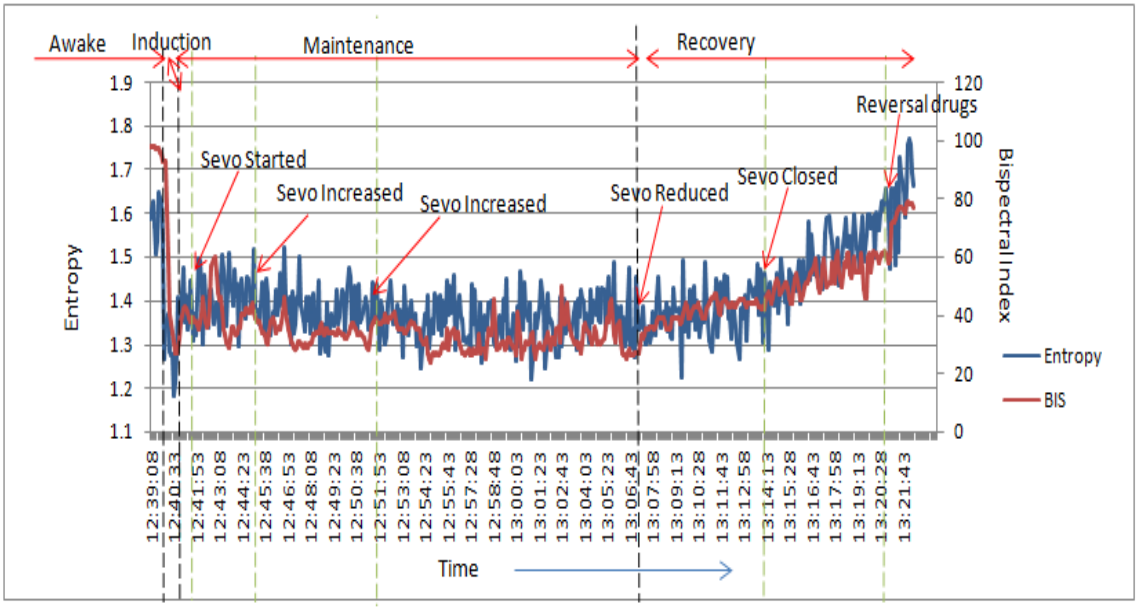

FIGURE 5.3: Comparison of BIS and Entropy during the four phases of anaesthesia

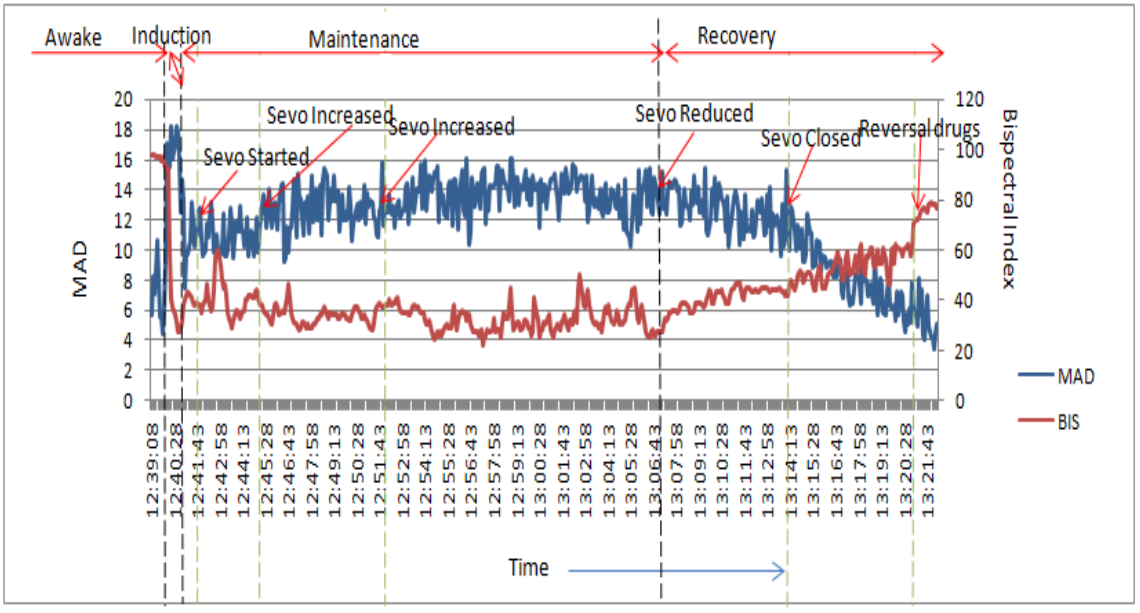

FIGURE 5.4: Comparison of BIS and MAD during the four phases of anaesthesia

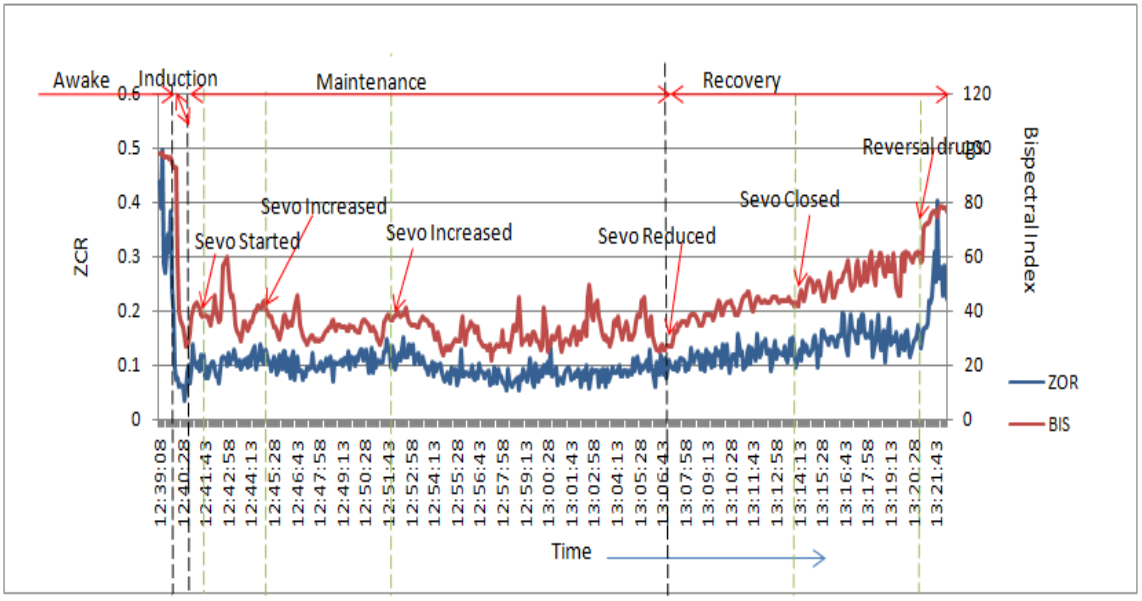

FIGURE 5.5: Comparison of BIS and ZCR during the four phases of anaesthesia

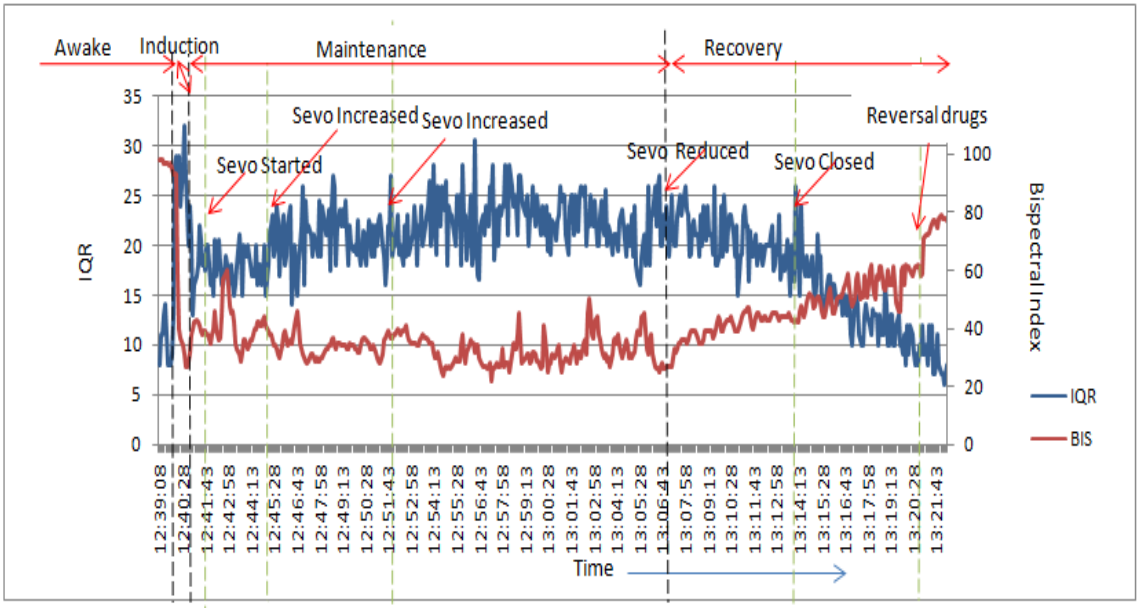

FIGURE 5.6: Comparison of BIS and IQR during the four phases of anaesthesia

strong correlation of the BIS and the extracted EEG features. The Pearson correlation coefficient values of patient-24 are shown Table 5.4 which are calculated using the Equation 4.11(in Chapter 4). Similarly, the time domain features and Pearson correlation coefficient values are calculated from the entire 25 patient's EEG data. In all the cases, the feature ZCR showed more correlation with BIS.

Table 5.4: Correlation of time domain features with BIS

	STDEV	Energy	Entropy	MAD	ZCR	IQR
Correlation coefficients	-0.70	-0.66	0.70	-0.72	0.80	-0.71

5.3.1.1 Time delay between BIS and Extracted time domain features

Figure 5.7 shows the comparison of BIS and extracted time domain features of patient-24 during the transition from awake phase to induction phase. The surgery started at 12:39:08 PM. The drug Midazolam-1 mg and Propofol-100 mg was administered at 12:39:43 PM as sedative and anaesthetic drug. The values of the extracted features Standard deviation, Energy, Mean Absolute Deviation and Inter-Quartile Range are increased rapidly just after the administration of above-mentioned drugs whereas entropy and ZCR values are decreased. It can be observed from the Figure 5.7 that BIS value shows a delay of 10-20 seconds from the extracted time domain features in the transition from awake to induction phase. The standard deviation increased steeply from the time point at 12:39:48 PM and reached its first peak at 12:39:58. The midpoint of these two time points i.e. 12:39:54 PM is used to calculate the time delay between BIS and standard deviation. Similarly, time delay is calculated for all the time domain features. The average time delay of BIS in all patients is 15 seconds from Standard deviation and Energy, 10 seconds from Entropy, MAD and IQR, whereas the average delay is 20 seconds from ZCR. Figure 5.7 also depicts the induction phase and it starts from the point of administration of the drugs to 1 minute after drug administration.

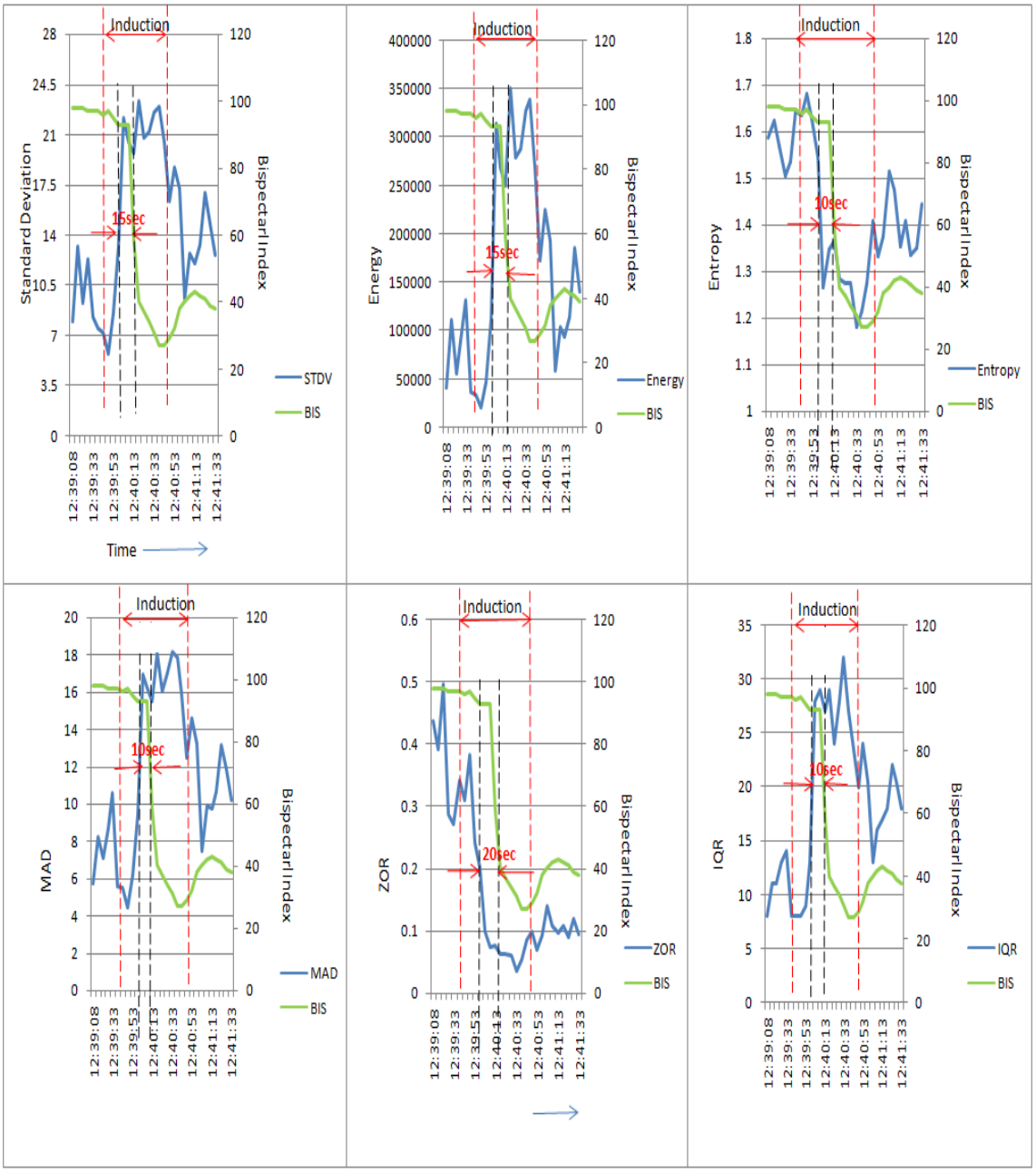

FIGURE 5.7: Time delay between BIS and the extracted Time domain features of patient-24

5.3.2 Frequency Domain Features

The frequency variations of collected EEG signals are examined by extracting the features Spectral Entropy and SEF. Values of these features extracted from 6 continuous epochs (30 seconds data) of four anaesthetic EEG signals of a patient is

shown in Figure 5.8. Values of the features spectral entropy and SEF decreases with increase in depth of anaesthesia. Awake and recovery signals showed higher values in both the features, whereas induction phase showed low values and maintenance phase showed some intermediate values. A high value of SEn corresponds to increase in irregularity or unpredictability of the signal frequencies while a low value represents a high level of regularity. In this study $SEF_{95\%}$ is used and which provide frequency below which 95% of the signal power is concentrated. In awake EEG signal, 95% of the signal power is concentrated in the frequency range 50-60Hz and SEF of recovery EEG signal is in the range 25-35Hz. Similarly 10-20 Hz in maintenance EEG signals and 5-10Hz in induction EEG signals. The results indicate that both the frequency domain feature values of EEG signals decrease with increase in DoA, which suggests that Spectral Entropy and SEF of EEG signal can differentiate different phases of anaesthesia.

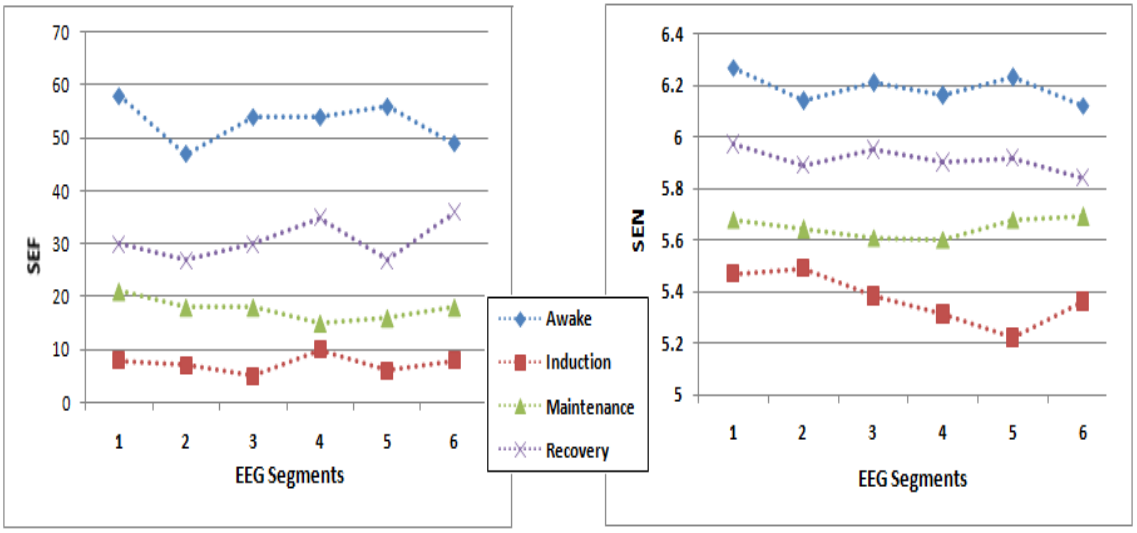

FIGURE 5.8: Comparison of frequency domain features during the 4 anaesthetic phases

Figure 5.9 and 5.10 represents the extracted frequency domain features of the same patient-24 during the whole surgery and its comparison with BIS index. Similar to time domain features all the anaesthetic phases and their transitions are well defined. Here values of both the frequency domain features in the awake phase are high and when DoA increases their values gets reduced. Therefore, the deep anaesthetic state (induction phase) is having the lowest values. One of the major advantages of SEn is that the effect of inhalation agent, sevoflurane is more visible.

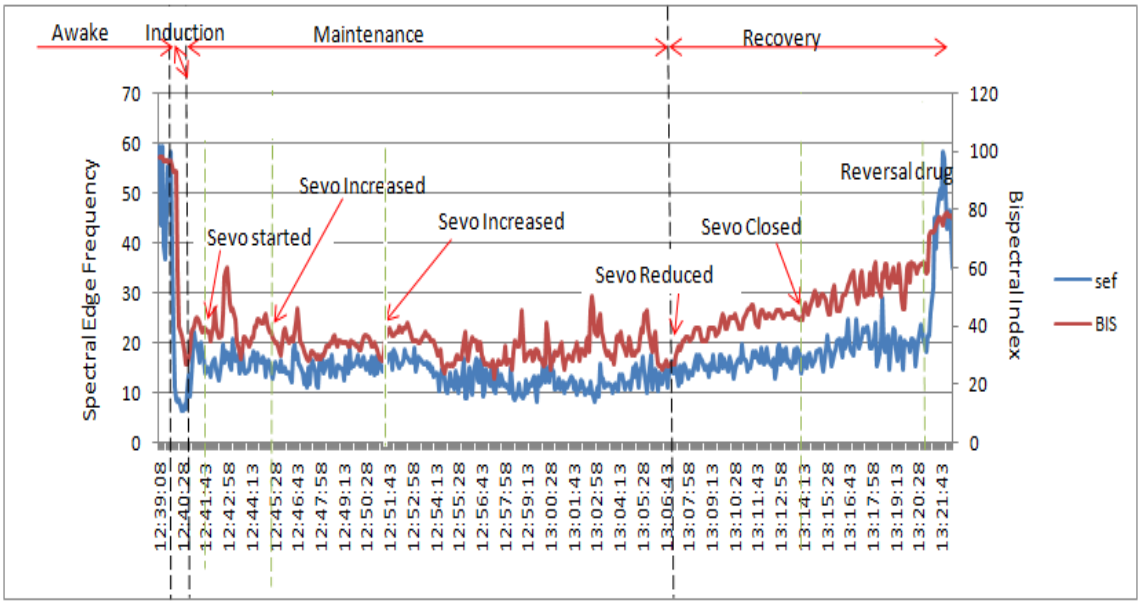

FIGURE 5.9: BIS and the spectral Edge Frequency

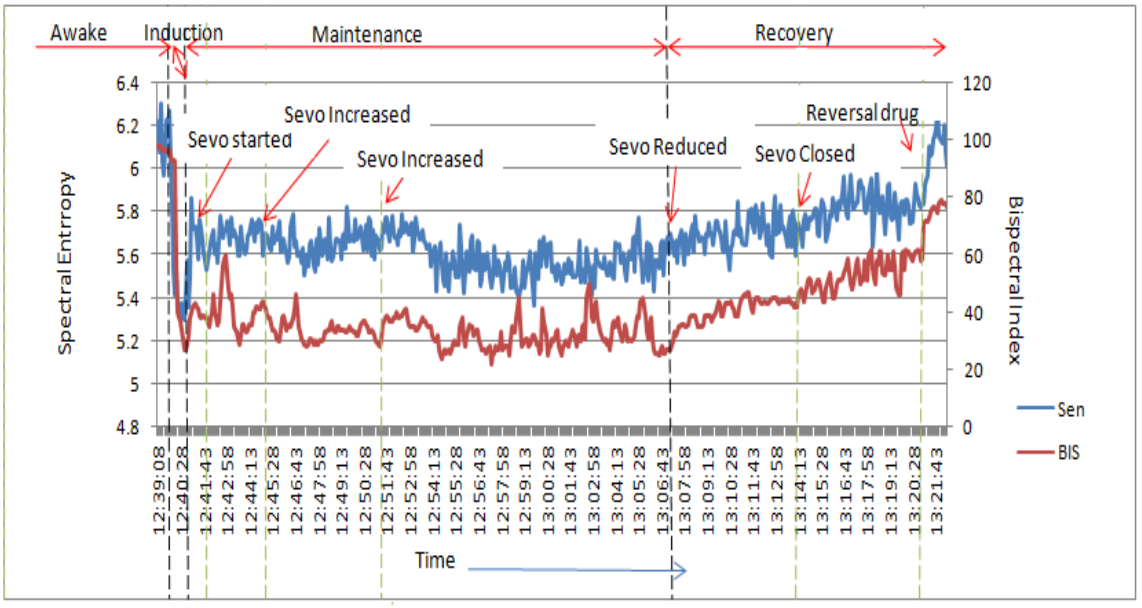

FIGURE 5.10: BIS and the Spectral Entropy

It is clear from the Figure 5.10 that at 12:51:43 administration of sevoflurane was increased which in turn increases the DoA which is reflected in the feature SEn as decrease in its values. This event is slightly reflected in feature SEF. When the administration of sevoflurane is reduced its action is well reflected in both time domain and frequency domain features. SEF and SEn showed high correlation with BIS and their Pearson correlation coefficient values are 0.78 and 0.75 respectively.

The time delay between BIS and the frequency domain features of patient-24 are shown Figure 5.11. The BIS index shows a delay of 15 sec with SEF and 10 sec with SEn.

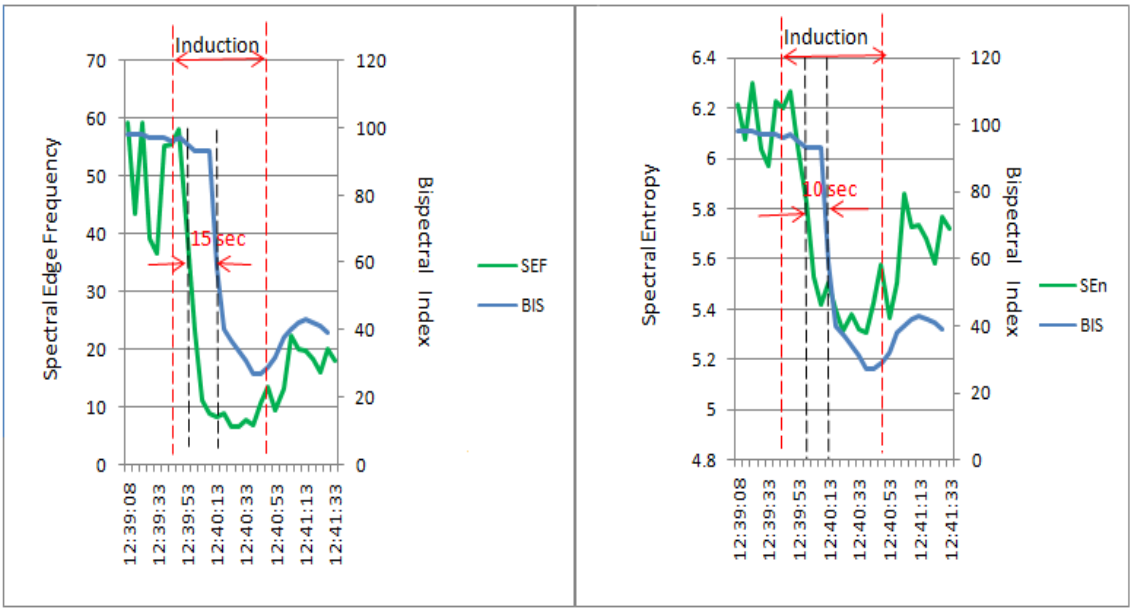

FIGURE 5.11: Time delay between BIS and Frequency Domain Features

5.3.3 Time-Frequency (Wavelet) Domain features

The advantage of wavelet-based analysis in the current research is that the decomposition of the EEG signals into its constituent frequency bands using multiresolution analysis of wavelet transform. Here awake and anaesthetized EEG signals are decomposed into its frequency ranges delta, theta, alpha, beta and gamma using the multiresolution analysis. Wavelet Entropy (WEn) and Relative Wave Energy (RWE) features are extracted from the frequency bands delta, theta, alpha and beta of EEG signals from each patient. These decomposed frequency bands and their details and approximations are given in Table 4.1 and Figure 4.3 of chapter 4.

As mentioned in chapter 4 Daubechies-4 mother wavelet with 4 level of decomposition is used. Table 4.1 and Figure 4.3 shows the 4 level the decomposition of EEG signal with sampling frequency 128Hz. cA1,cA2,cA3 and cA4 are the approximation coefficients and cD1,cD2,cD3 and cD4 are the detail coefficients obtained after successive decomposition. The RWE and WEn are calculated from

frequency bands δ, θ, α, β and γ using the equation given in equations 5.23 and 5.24. Therefore, the detail coefficient cD1, cD2, cD3, cD4 and approximation coefficient cA4 are used for the RWE and WEn calculation.

The variations of Wavelet Entropy extracted from 30 seconds (6 epochs) EEG signals of a patient is shown in Figure-5.12. Similar to all other features wavelet entropy also decreases with increase in depth of anaesthesia. The results indicate that WEn of EEG signal vary with change in DoA, which implies that WEn can also be employed as a feature of EEG signal to differentiate phases of anaesthesia.

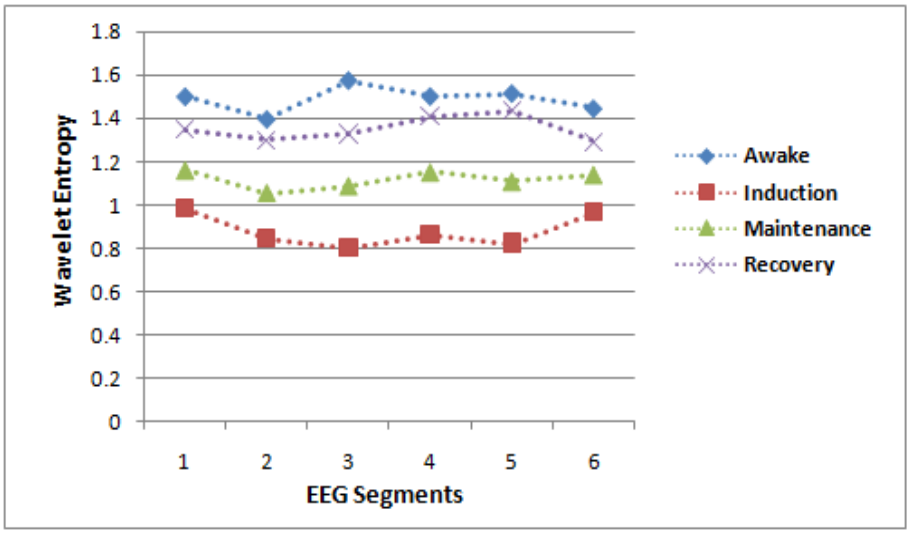

FIGURE 5.12: Comparison of Wavelet Entropy during the 4 phases

Figure 5.13 represent the extracted WEn feature of the patient-24 during the whole surgery and its comparison with BIS index. It is evident from the figure that the administration of sevoflurane was increased at two-time points 12:45:00 and 12:51:43 to increase the depth of anaesthesia which is reflected in the feature values of WEn as decrease in values. When the administration of sevoflurane is reduced its action is also well reflected as an increase in the values of WEn. WEn is the only feature which clearly depicts the effect of sevoflurane and N_2O. The Pearson correlation coefficient value of WEn and BIS is 0.52 and which indicate that WEn is less correlated to BIS. But the advantage of WEn is that the effect of the inhalation agent sevoflurane can be observed as increase or decrease in values depending on the administration of sevoflurane. The time delay between the BIS and WEn of patient-24 is shown Figure 5.14. The BIS index shows a delay of 20 sec with WEn.

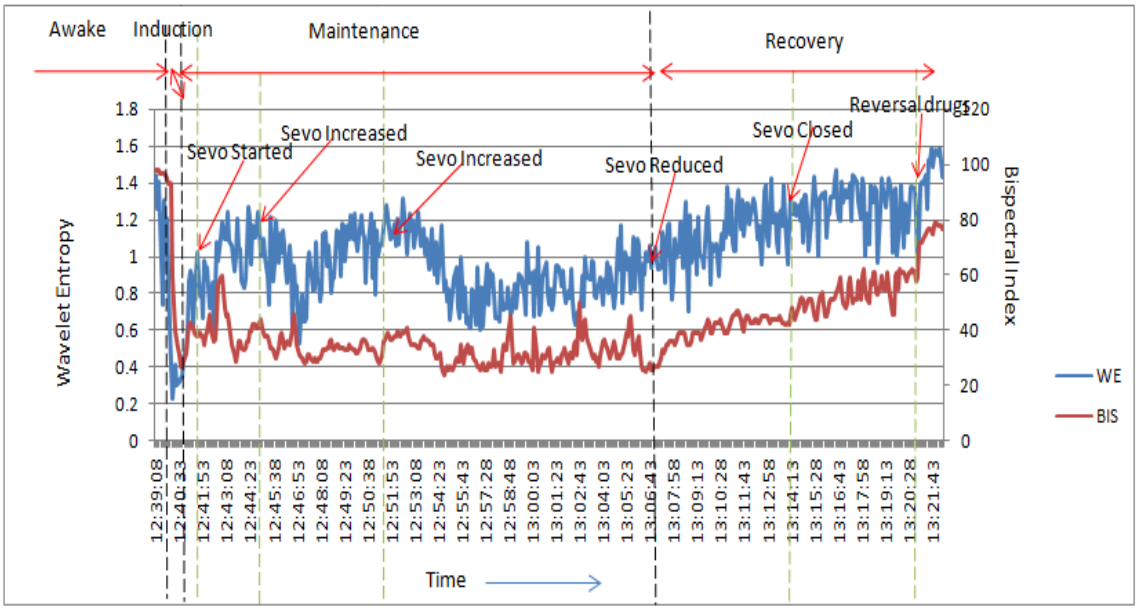

FIGURE 5.13: Comparison of BIS and Wavelet Entropy during the 4 phases of anaesthesia

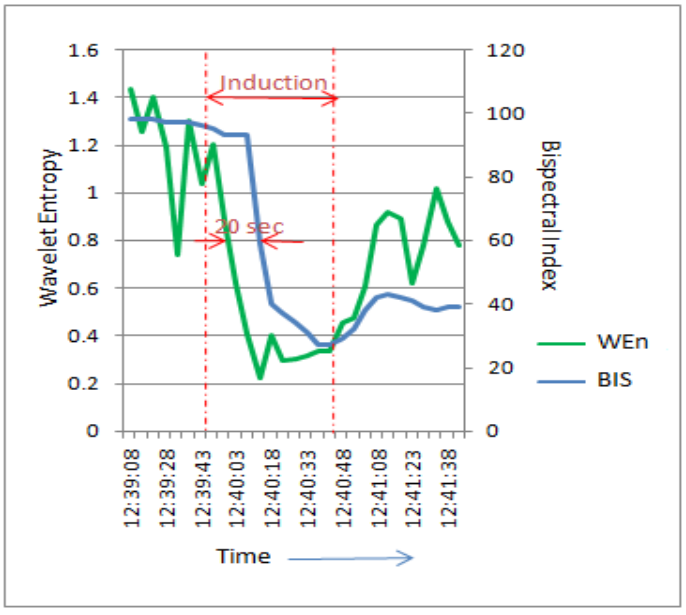

FIGURE 5.14: Time delay between BIS and Wavelet Entropy

RWE variations of one epoch EEG signal from all the four anaesthetic phases of a particular patient is shown in Table 5.5. RWE values of gamma band are high in the awake phase because when a patient is awake high-frequency components will be more active. But when anaesthetized the RWE values of low-frequency components will be active. Therefore during deep anaesthetic state (Induction phase)

TABLE 5.5: Comparison of RWE of Different frequency bands

Frequency Range	RWE	Awake	Induction	Maintenance	Recovery
32-64	RWE_{γ}	0.4408	0.0127	0.015	0.1775
16-32	RWE_{β}	0.1926	0.0492	0.0706	0.182
8-16	RWE_{α}	0.1385	0.107	0.2028	0.4262
4-8	RWE_{θ}	0.0868	0.0826	0.3289	0.144
0-4	RWE_{δ}	0.1413	0.7485	0.382	0.0694

RWE value of delta band is high. In the maintenance phase RWE values of theta and delta shows almost similar values and in recovery phase, RWE values of alpha band is active compared to other bands

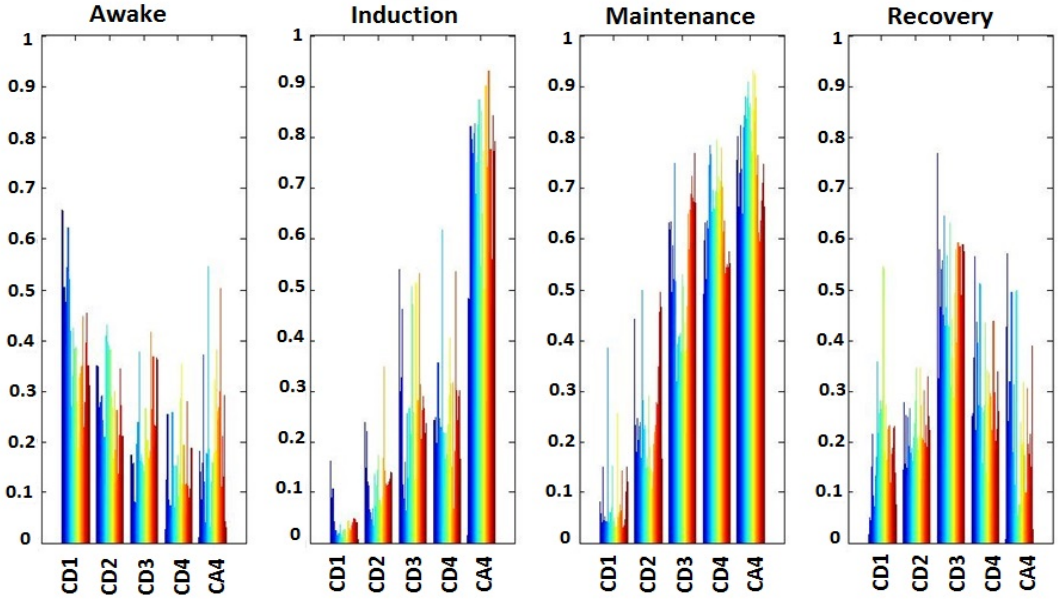

FIGURE 5.15: Comparison of Relative Wavelet Energy during the 4 phases

The RWE distribution of a patient's EEG signal during the four anaesthetic phases is shown in Figure 5.15. It can be observed from the figure that the Relative Wave Energy of the awake phase is high for high-frequency bands. When anaesthetized, Relative Wave Energy of the low-frequency bands becomes high. During the induction phase, RWE of the delta band (0-4) is more predominant. Maintenance phase shows high RWE values for low-frequency bands delta, theta and

alpha. In the recovery phase, RWE of high-frequency bands is high compared to low-frequency bands.

5.3.4 Nonlinear features

The nonlinear features extracted from collected EEG signals are ApEn and PEn. To compare the generalized performance of nonlinear features during the 4 anaesthetic phases, mean and standard deviation (SD) are calculated and presented in Table 5.6. Low values of features ApEn and PEn indicates the anaesthetized state, whereas high values indicate that the patient is awake. ApEn and PEn values are high for awake signals because of the increased randomness in the EEG signal. Induction phase EEG signals are more regular compared to all other EEG signals. Therefore, the value of ApEn and PEn in the Induction phase shows low values. The results reveal that ApEn and PEn values of EEG signal vary greatly with the changes in DoA, which suggest that the ApEn and PEn can be selected as two relevant features of EEG signal that can differentiate different phases of anaesthesia.

Table 5.6: Mean ± standard deviation of extracted Nonlinear Features

Extracted EEG Features	Awake	Induction	Maintenance	Recovery
ApEn	1.39 ± 0.10	0.76 ±0.09	1.11 ± 0.11	1.24 ± 0.72
PEn	2.52± 0.09	2.33±0.04	2.39± 0.12	2.46 ± 0.07

Figure 5.16 and 5.17 represents the extracted nonlinear features of patient-24 and its comparison with BIS index. All the anaesthetic phases and their transitions from one phase to another are well defined in the extracted features. Values of both the features are high in awake EEG signals and when DoA increases their values gets reduced. Therefore, the deep anaesthetic state (induction phase) is having the lowest values. The administration of inhalation agent-sevoflurane has less effect on non-linear features.

The time delay of the BIS with ApEn and PEn of patient-24 is shown Figure 5.18 which are 15 sec and 10 sec respectively. The correlation of features

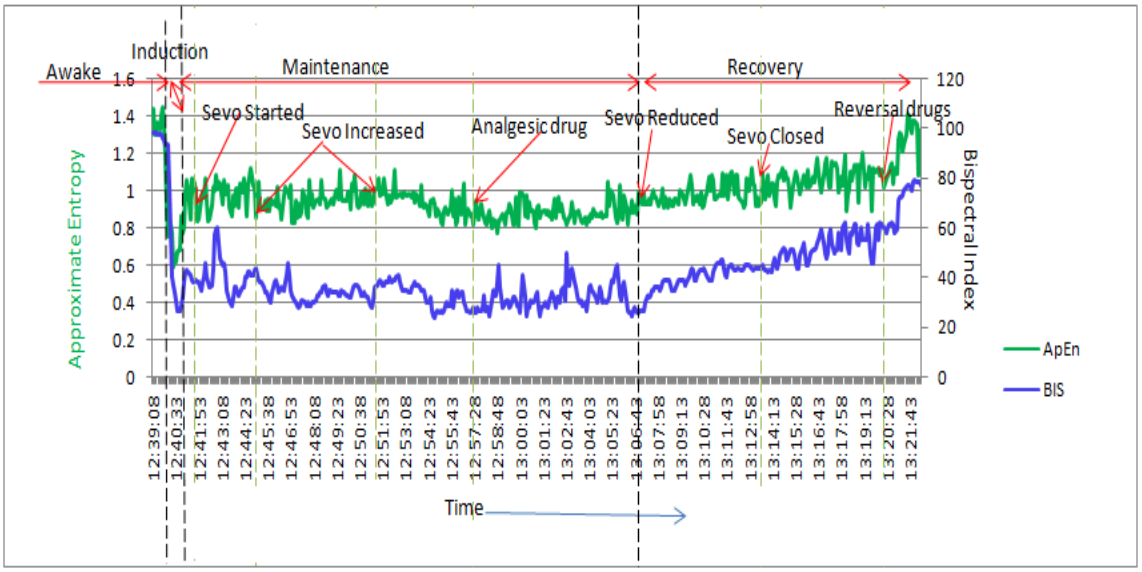

FIGURE 5.16: Comparison of BIS and Approximate Entropy during the 4 phases of anaesthesia

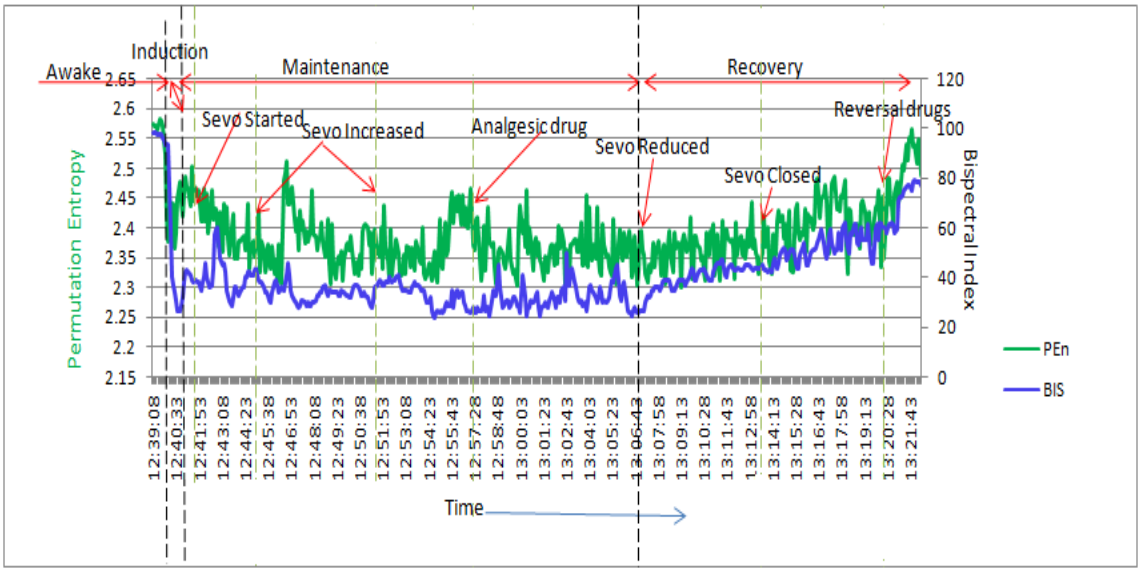

FIGURE 5.17: Comparison of BIS and Permutation Entropy during the 4 phases of anaesthesia

ApEn and PEn with BIS is calculated and Pearson correlation coefficient values are 0.75 and 0.61 respectively.

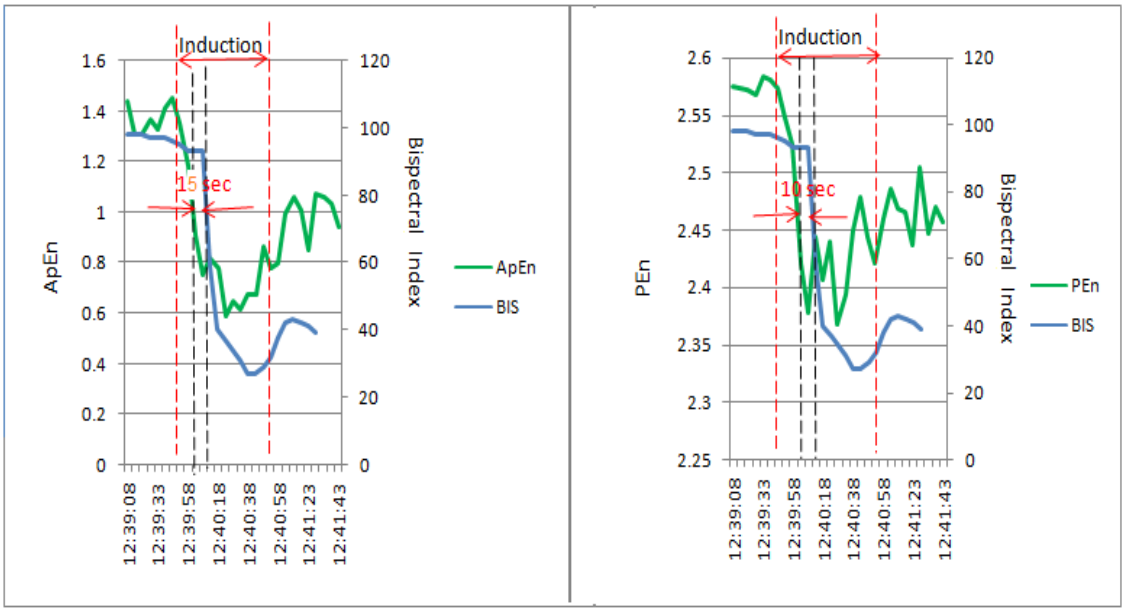

FIGURE 5.18: Delay between BIS and nonlinear features

5.3.5 Hemodynamic features

The hemodynamic features extracted from the patients are ΔHR, ΔMBP and PP. Normally values of these features decrease with increase in DoA. Figure 5.19 shows the ΔHR, ΔMBP and PP variations of the patient-24 which is a special case of hemodynamic instability.

After the administration of anaesthetic drugs the values of the features $\Delta HR, \Delta MBP$ and PP decreases similar to all other EEG extracted features. It can be observed that in the maintenance phase all the three the features increase drastically from the time point 12:49:23 PM causing a hemodynamic instability. But this variation is not visible in BIS and EEG extracted features. Here anaesthesiologist first tried to stabilize these features by increasing the inhalation agent sevoflurane and showed no effect on the hemodynamic variables. Then he administered the analgesic drug Fentanyl-100μg to the patient and which resulted in the reduction of the extracted hemodynamic parameters. These indications reveal that underdosing of drugs causes hemodynamic instability, but monitoring with EEG extracted parameters does not show this effect, which can lead to inadvertent anaesthetic overdosing or underdosing.

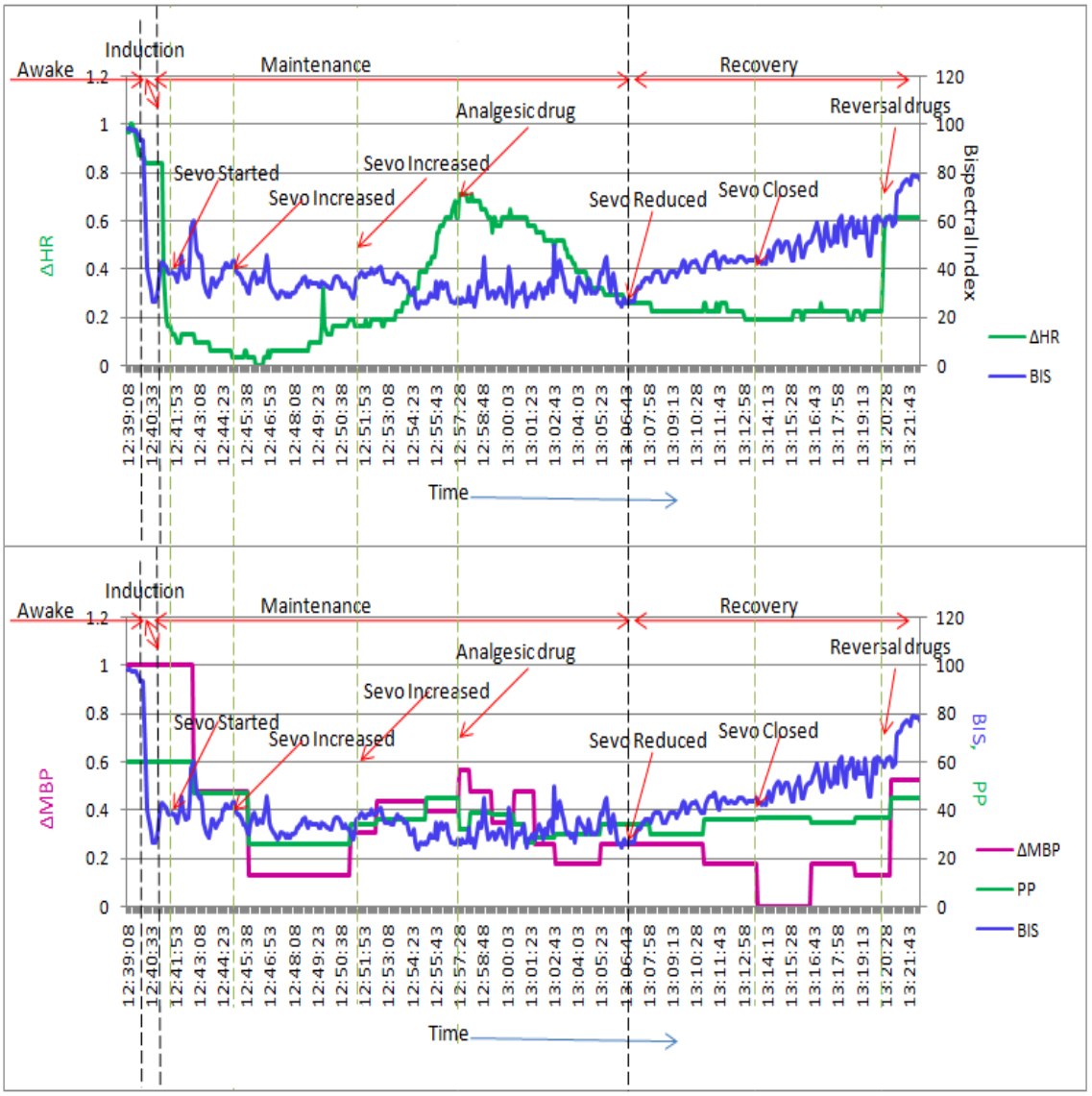

FIGURE 5.19: BIS and extracted hemodynamic features

5.4 Summary

This chapter provides the details of core features that vary in accordance with DoA. The chapter has two main sections explaining EEG extracted features and hemodynamic features. In the first section, features extracted from time domain, frequency domain, time-frequency domain and nonlinear analysis were used to study the amplitude, frequency and complexity/regularity of EEG signals. The extracted time domain features include Standard Deviation, Entropy, Energy, Mean Absolute Deviation, Zero Crossing Rate and Inter-Quartile Range. Among these features Standard

Deviation, Energy, Mean Absolute Deviation, and Inter-Quartile Range showed a direct relationship with DoA whereas Entropy and ZCR showed an inverse relation with DoA. The frequency domain features SEF and SEn also showed an inverse relation with DoA. The extracted wavelet domain features include Wavelet Entropy (WEn) and Relative Wave Energy (RWE) of each EEG frequency band. All these features vary in accordance with DoA. Finally, nonlinear features such as ApEn and PEn were extracted from collected EEG signals to study the complexity and nonlinear behaviour of EEG signals during different phases of anaesthesia

In the next section, the hemodynamic variability due to the anaesthetic drugs is analyzed by extracting the features such as ΔHR, ΔMBP and Pulse Pressure from the HR and BP data. This chapter also compares the variations of these extracted features during the four phases of anaesthesia such as awake, induction, maintenance and recovery. When comparing the extracted features with BIS, BIS showed a delay of 10-20 sec and also all the transitions were well defined in the extracted features.

Chapter 6

Feature Selection

The performance of the extracted features is evaluated by applying a range of classifiers such as k-Nearest Neighbor (kNN), Support Vector Machine (SVM), Multilayer Perceptron (MLP) and Naive Base Classifier (NBC) which classifies different anaesthetic states as awake, light anaesthesia, moderate anaesthesia and deep anaesthesia. The purpose of these classifiers is to verify the transitions of different anaesthetic states of extracted features in the feature vector. In the present research extracted feature vector accommodates 19 features consisting of 6 time-domain features, 2 frequency domain features, 6 time-frequency domain features, 2 nonlinear features and finally 3 hemodynamic features. But the main dilemma in considering a large number of features is that it is very difficult to determine which feature or combination of features provides better classification accuracy[Cheng *et al.* , 2006]. Therefore, it is exceptionally important to select an optimal subset of feature vector from the high dimensional feature vector.

The first part of this chapter explains different feature selection methods adopted for the classification of EEG extracted features as different anaesthetic states. The advantages of feature selection are that it reduces the system complexity and processing time which in turn improves the overall performance of the system. Finally, Kruskal-Wallis (KW) statistical test is applied to the selected features to check the discriminating capability of the features as awake, light anaesthesia, moderate anaesthesia and deep anaesthesia. Thus KW test would check the efficiency of selected features depending on the class separability of the features [Ho & Basu,

2002]. The second part of this chapter describes different classification methods used in the current study and their outcomes. The performance of these classifiers is compared with different combination of features.

Feature selection method selects a minimally sized subset of feature vector from the extracted feature vector, without affecting the classification accuracy significantly and maintaining the original class distribution of the features. Sometimes features in the feature vector may be unnecessary, uninformative or diverted from the application. On the other hand, some features may not have any relevance if they stand alone, but together with other features, they may provide synergic performance to the application [Guyon & Elisseeff, 2003].

Generally, feature selection methods are categorized into two as Filter method and Wrapper method. Filter method evaluates the applicability of features in the feature vector by looking at the intrinsic properties of the data. A suitable ranking criterion is used to score the features and a threshold value is used to remove the features below the threshold. Afterwards, this subset of feature vector is used as input to the classification algorithm. Filter method checks the applicability of each feature in the feature vector using the measures like distance, area, correlation and consistency. Advantages of filter methods are that they are fast, scalar and independent of the learning algorithm. Some of the filter feature selection methods are Person correlation, Linear Discriminant Analysis (LDA), Analysis of Variance (ANOVA) and Chi-square test. Pearson's Correlation is usually used as a measure for quantifying linear dependence between two continuous variables. LDA is used to find a linear combination of features that characterizes or separates two or more classes of a categorical variable. ANOVA is similar to LDA except for the fact that it is operated using one or more categorical independent features and one continuous dependent feature. It provides a statistical test of whether the means of several groups are equal or not. Chi-Square is a statistical test applied to the groups of categorical features to evaluate the likelihood of correlation or association between them using their frequency distribution [Kaushik, 2016].

In wrapper method, different combinations of feature subset are prepared and then a predictive model evaluates the combination of feature subset and finally assigns a score based on model accuracy. The computational cost of wrapper method

is high when compared with filter method and therefore filter model is considered as computationally efficient. However, in the performance concern wrapper model is better than filter model [Yu & Liu, 2004]. Some of the wrapper methods are forward selection, backward elimination, and recursive feature elimination method. Forward selection is an iterative method in which it starts with no feature in the model. In each iteration, keeps on adding the features which are making improvements to the model. This is continued till an addition of a new variable does not improve the performance of the model. In backward elimination, start with all the features and removes the least significant feature at each iteration which improves the performance of the model. This process is repeated until no improvement is observed on removal of features. Recursive Feature elimination is a greedy optimization algorithm which aims to find the best performing feature subset. It repeatedly creates models and keeps aside the best or the worst performing feature at each iteration. It constructs the next model with the left features until all the features are exhausted. It then ranks the features based on the order of their elimination [Kaushik, 2016]. In the present research, feature selection is carried out by ranking the features in the order of class separability which is a combined feature selection method.

6.1 Feature Ranking

Feature ranking methods rank the features based on their predictive scores. Features with highest predictive scores are selected to form a feature subset. Different feature ranking measures are 'T-Test', 'Entropy', 'Bhattacharyya', 'ROC'and 'Wilcoxon'. Each of these measures assigns a rank to the features in the feature vector and generates a feature ranking list. Top-ranked features from the ranking list of each measure are selected analytically to the feature subset[Osei-Bryson & Barclay, 2015]. Finally, the ability of selected features in terms of class separability is tested using Kruskal-Wallis (KW) statistical test.

6.1.1 T-Test

The Student's T-Test is a statistical method which evaluates the class discriminating nature of each feature in the feature vector. This method analyses the features and checks whether the means of two independent classes (samples) coming from the population (normal distributions) are statistically different from each other. According to Student's T-Test if the hypothesis is true (null hypothesis is rejected) then the feature is able to differentiate two subclasses of the feature.

The outcome of T-Test is expressed in terms of probability and is called p-value. The computation procedure of p-value calculates t-statistics of each feature corresponding to each class. The equation of t-statistic value calculation is given by

$$t_i = \frac{\bar{x_1} - \bar{x_2}}{\sqrt{\left(\frac{\sigma_1^2}{n_1} + \frac{\sigma_2^2}{n_2}\right)}} \tag{6.1}$$

where t_i is the t-statistics value of the i^{th} feature in the feature vector, x_1 and x_2 are means of two classes x_1 and x_2, σ_1 and σ_2 are the within-class standard deviations of the two classes, n_1 and n_2 are the number of samples in the two classes.

The t-statistics evaluates the difference between the mean of two classes and a within-class standard deviation is included to standardize the differences. This t-statistic value is converted to a p-value either by software or by looking it up in a t-table. If p-value is below the significance level (α) then the null hypothesis is rejected and thus conclude that there is a significant difference between the two population means. The value of α is usually 0.05 (5%).

In case of multiclass classification, the result of all the feasible two-class combinations of each feature is summed up to get a predictive score and this indicates the overall significance of the feature. Then the feature with a highest predictive score is selected for the feature subset [Saez-Rodriguez *et al.* , 2014].

6.1.2 Bhattacharyya Distance method

In statistics, the Bhattacharyya distance is used to measure the similarity of two continuous or discrete probability distributions. Therefore, this method can be used as a class separability measure to evaluate the statistical dependence between two classes of a feature [Choi & Lee, 2003]. Bhattacharyya distance between two normally distributed classes is computed using Equation 6.2

$$BD_{x1,x2} = \frac{1}{4}ln(\frac{1}{4}(\frac{\sigma^2_{x_1}}{\sigma^2_{x_2}} + \frac{\sigma^2_{x_2}}{\sigma^2_{x_1}} + 2)) + \frac{1}{4}(\frac{(\bar{x_1} - \bar{x_2})^2}{\sigma^2_{x_1} + \sigma^2_{x_2}}) \tag{6.2}$$

where $\bar{x_1}$ and $\bar{x_2}$ are the means of the two classes x_1 and x_2 and $\sigma^2_{x_1}$ and $\sigma^2_{x_2}$ are the variances of the two classes x_1 and x_2 respectively[Reyes-Aldasoro & Bhalerao, 2006; Kailath, 1967].

A high value of Bhattacharya Distance refers to strong class separability [Klette & Zunic, 2004]. In case of multiclass classification, the distance obtained from all feasible two-class combinations of each feature is averaged to get a predictive score and this indicates strong separability of the classes. Finally, features with highest predictive score are selected for the feature subset.

6.1.3 Entropy Ranking Method

Entropy is a measure of information conveyed by the probability distribution function of a particular feature. Here the divergence of two classes is tested by calculating a measure called Relative Entropy. It is also called Kullback–Leibler divergence and it assumes that both the classes are normally distributed. Let the probability function of the first class distribution is p_k and the second class distribution q_k, then the relative entropy of p with respect to q is defined by the Equation 6.3

$$RE_{p,q} = \sum_k p_k log(\frac{p_k}{q_k}) \tag{6.3}$$

The smaller the value of relative entropy, the more similar is the distribution of two classes and conversely [Theodoridis *et al.* , 2008]. In multiclass distribution, the relative entropy value obtained from all the feasible two-class combinations of each

feature are averaged to get a predictive score and this indicates strong separability of the classes. Finally, features with highest predictive score are selected for the feature subset.

6.1.4 Receiver Operating Characteristics (ROC) Method

Receiver Operating Characteristics (ROC) Curve is a commonly used method to evaluate the performance of a classification algorithm. ROC curve is a feature ranking method which measures the individual significance of features in the feature vector [Fawcett, 2006]. The advantage of ROC curve method is that it provides information about the overlapping of classes. In Figure 6.1(a), we can see two overlapping probability density functions (pdf) describing the distribution of a feature in two classes together with a threshold T. Here one pdf is shown inverted for interpretation purpose. Class 1 of the feature is the values coming on left side of

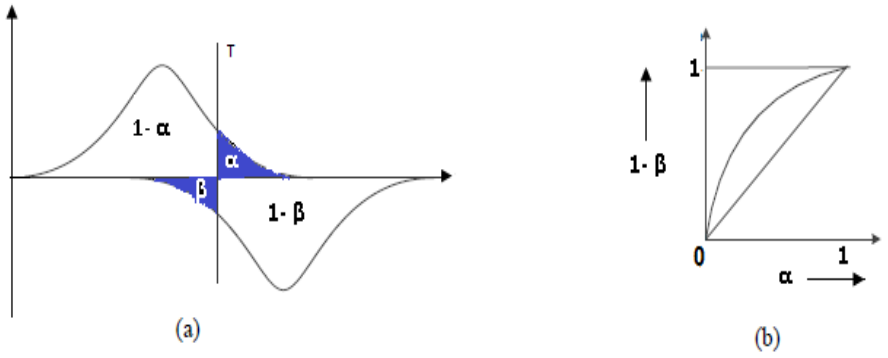

Figure 6.1: (a)Two overlapped class distribution of a feature and (b) ROC curve

threshold line and class 2 is the values at right side of the threshold line. The error probability of class 1 of a feature is indicated as α and the probability of a correct decision of class 1 is $(1-\alpha)$. Similarly, β and $(1-\beta)$ represents the error and correct probabilities of class 2 of the same feature. The ROC curve is a plot of the true positive rate against the false positive rate at different threshold settings. By moving the threshold over all possible positions, we get different values of α and β. If the two classes are completely overlapped, then at any position of the threshold we get $\alpha = 1-\beta$ and the corresponding ROC curve is a straight line shown in Figure

6.1b where the two axes are α and $1-\beta$. As the two-class distributions move apart, the corresponding ROC curve departs from the straight line. Less overlap of the classes contributes larger area between the curve and the straight line in the ROC plot, whereas complete overlapping of the classes contributes zero. Therefore the Area Under the ROC Curve (AUC) can be used as a measure of class discrimination capability of a feature [Theodoridis *et al.* , 2008]. The maximum AUC (=1) represents high separability of the classes and it happens when the two class distributions are not overlapped each other. AUC =0.5 represents a chance of discrimination that the ROC curve is located on the diagonal line in ROC space. The minimum AUC should be considered a chance level i.e. AUC=0.5 while AUC=0 means the incorrect classification of classes [Hajian-Tilaki, 2013].

6.1.5 Wilcoxon rank sum test Method

The Wilcoxon rank sum test is also called Mann-Whitney test, is a statistical test which can be used for ranking the features. It compares two unpaired classes of a feature. It is a non-parametric test in which no assumptions about the distribution of classes are needed [contributors, 2017a].

Let X be a class of a feature with m observations represented as $X = x_1, x_2...., x_m$ and Y be another class with n observations represented as $Y = y_1, y_2...., y_n$ then null hypothesis, H_0 is

- $H_0 : X = Y$; which indicate that two distributions are same and it is to be tested against an alternative hypothesis H_1
- $H_1 : X \neq Y$; or $H_1 : X < Y$; $or H_1 : X > Y$

The test procedure is as follows;

- Step 1: Combine all m + n observations into one group and rank them in ascending order. (If some observations have tied values, then group all the tied observations and assign the average rank to tied values in that group. These ranks are called adjusted ranks)

- Step 2: Find the sum of ranks for all observations in X and Y using the Equations 6.4 and 6.5

$$S_X = \sum_{i=1}^{m} R_{xi} \tag{6.4}$$

$$S_Y = \sum_{j=1}^{n} R_{yj} \tag{6.5}$$

where R_{xi} is the ranks assigned to class X, and R_{yi} be the ranks assigned to Y.

- Step 3: Find the U statistics using the Equations 6.6 and 6.7

$$U_1 = S_X - \frac{m(m+1)}{2} \tag{6.6}$$

$$U_2 = S_Y - \frac{n(n+1)}{2} \tag{6.7}$$

- Step 4: The test statistic, U is the smaller value of U1 and U2 ($min(U1, U2)$) and if the value of U is less than or equal to the critical value in the significance table, then reject H_0 in favor of H_1 and if value of U exceeds the critical value then accept H_0. The critical value is determined from significance table using the number of observations (m and n) and two sided level of significance (α=0.05). For example, if $m = 7$ and $n = 8$ then critical value in the significance table with level of significance (α=0.05) is 10. Here the test condition to accept or reject the hypothesis is U$\leq$ 10. For larger dataset, U is approximately normally distributed therefore the value of U is standardized using the Equation 6.8

$$Z = \frac{U - \mu_U}{\sigma_U} \tag{6.8}$$

where μ_U and σ_U are the mean and standard deviation of U and is given by the equations

$$m_U = \frac{U_1 + U_2}{2} = \frac{mn}{2} \tag{6.9}$$

$$\sigma_U = \sqrt{\frac{mn(m+n+1)}{12}} \tag{6.10}$$

Finally, the significance of Z is checked in the normal distribution table [CONTRIBUTORS, 2017a; NACHAR *et al.* , 2008].

6.2 Kruskal-Wallis(KW) statistical test

Kruskal-Wallis test or One-way ANOVA (Analysis of variance) on ranks is a non-parametric method which checks whether the samples originate from the same distribution or not [Daniel, 1990; Statistics, 2013]. Kruskal-Wallis test will provide the idea of medians of two or more groups and checks whether they are different or not. Similar to other statistical tests, KW test calculates the test statistic and compare it to distribution cut-off point. In KW test, test statistic is called H statistic and the hypotheses are defined as
H_0: Median of two populations is equal. H_1: Median of two populations is different.
Steps for the KW test is as follows

- Step 1: Sort the observations of the features in ascending order.
- Step 2: Rank the sorted data points and if any tied values present then give an average rank.
- Step 3: Add the different ranks of each output class.
- Step 4: Calculate the H statistic using the equation 6.11

$$H = \left[\frac{12}{N(N+1)}\sum_{k=1}^{c}\frac{T_k^2}{n_k}\right] - 3(N+1) \tag{6.11}$$

  where N = Total number of observations across all output class(group)
  c =Number of output class (groups)
  T_k= Sum of ranks of all observations in class k
  n_k = Number of observations in class k

- Step 5: Compute critical chi-square value, $\chi^2_{\alpha:k-1}$ with $k-1$ degrees of freedom and looking under the desired significance of alpha level.
- Step 6: Compare the H value and critical chi-square value. If H statistic is greater than critical chi-square value then reject the null hypothesis (H_0). If H statistic is not greater than chi-square value then there is not enough evidence to suggest that the means are unequal [Chan & Walmsley, 1997; Wikipedia, 2017c].

6.3 Feature classification

In this work, the performance of selected features is assessed by evaluating the class separability nature of features by classifying them as awake, light anaesthesia, moderate anaesthesia and deep anaesthesia. Different classification techniques are popular in EEG based applications. Based on this, present study compares the outcome of different classifiers such as k-Nearest Neighbor (kNN), Support Vector Machine (SVM), Multilayer Perceptron (MLP) and Naive Base Classifier (NBC). The purpose of these classifiers is to select optimum features which classify all the four anaesthetic states for DoA estimation. Finally, classification accuracy is the criterion used to evaluate the performance of classifiers. Classification accuracy is defined as the number of correctly detected anaesthetic states as a fraction of the total number of applied sample sets. It is calculated using the equation 6.12

$$Accuracy(\%) = \frac{N_c}{N_t} * 100 \tag{6.12}$$

where N_c is the number of correctly classified samples and N_t is the total number of samples[Dutta *et al.* , 2010]. Details of different classifiers used are given below

6.3.1 k-Nearest Neighbor (kNN)

kNN classifier is one of the accurate and simplest classifiers used for pattern recognition. It uses a data mining algorithm called kNN algorithm and is widely applied in many fields. Based on this algorithm, an object is classified by a majority vote of its neighbors. That means an object being assigned to the class in which most of it's k nearest neighbors belongs to (k is a positive integer). When $k = 1$, the object is assigned to the class in which its single nearest neighbor belongs to. The neighbors of the object are selected from the training set objects whose class is known to the algorithm. But there is no explicit training required. The training phase of the algorithm performs only the storing of feature vectors and class labels of the training samples. In the classification phase, an unlabeled vector (test vector/query vector) is classified by assigning the label which is nearest to that test (query) instance [Larose, 2005].

Let the test vector $X1_i = X1_1, X1_2, X1_3....., X1_m$ and the training vector $X2_j = X2_1, X2_2, X2_3, ..., X2_n$ then the steps for the kNN classification is as follows

- Step 1: Determine k which is a user-defined constant.
- Step 2: Calculate the Euclidean Distance(ED) between the query instance $X1_i$ and all the training samples of the training vector using the equation 6.13

$$ED_{(X1_i, X2_j)} = \sqrt{\Sigma(X1_i - X2_j)^2} \tag{6.13}$$

- Step 3: Sort the distances and determine k minimum distance (k_{min}) nearest neighbors based on the equation 6.15

$$k_{min} = \left\{MIN(ED_{(X1_i, X2_j)})\right\}_k \tag{6.14}$$

- Step 4: Gather the output class of the k nearest neighbors from the output class of the training vector $Y2_j = Y2_1, Y2_2, Y2_3, ..., Y2_n$
- Step 5: Assign the prediction value of a query instance to majority of output class in which nearest neighbors belongs.

The optimal value of k is selected by inspecting the data. Choosing a small value for k shows higher noise influence on the result. On the other hand, a large value of k is more precise and reduces the overall noise but it is computationally expensive. K-fold cross-validation is one of the methods used retrospectively to determine a good value of k where all observations are used for both training and validation, and each observation is used for validation exactly once. The optimal value of k for most of the datasets used in different fields is between 3-10 [Rashmi *et al.* , 2016]. In the current study, k value selected through k-fold cross validation is 5.

6.3.2 Support Vector Machine (SVM)

Support vector machine (SVM) is a discriminative classifier formally defined by a separating hyperplane. Consider a feature vector consisting of training data set and

corresponding labels, then the SVM classifier can build a model which can predict classes for new data points. That means the classifier assigns class values (label) for the new data points. SVM classifiers are categorized into two: Linear SVM Classifier and Non-Linear SVM Classifier. In linear SVM classifier, training data samples are plotted in space and they are expected to be separated by an apparent gap. This gap is used to predict the hyperplane that divides the two classes. This hyperplane is drawn based on maximum-margin hyperplane which is the maximum distance from the hyperplane to nearest data point of either class. Non-Linear SVM Classifier is implemented using kernel plot to maximum-margin hyperplanes. i.e. If the data points are not linearly separable in a p-dimensional(finite) space then the p-dimensional space is mapped into a much higher dimensional space and the Kernel trick is used to draw the non-linear hyperplanes [Ray *et al.* , 2016; Wikipedia, 2017e]. Kernel trick is a mapping function called kernel functions used to transform the data space to a higher dimensional space and the kernel function holds a non-linear function. In the current research Radial Basis Function (RBF) is used as kernel function. The RBF Kernel function is given by

$$K(X, X') = \exp - \frac{||X - X'||^2}{2\sigma^2} \tag{6.15}$$

where $K(X, X')$ is the kernel on two feature vectors X and X' in the input space, $||X - X'||^2$ is the squared Euclidean distance between the two feature vectors and σ is a free parameter [Wikipedia, 2017d].

Since the SVM classifier is originally designed for binary classification we can effectively extend it to multi-class classification. Several methods have been proposed to construct a multi-class classifier by combining several binary classifiers. Two approaches which are most commonly used for multi-class SVM classification are One-Against-All (OAA) and the One-Against-One (OAO). In One-Against-All approach, a binary SVM is used to distinguish each class from all other classes and the winner-takes-all strategy is used to obtain the final decision. The OAO multi-SVM approach is trained for each of all possible pairs of classes. That means for Q classes, one would need to train $n = C_2^Q$ classifiers and final decision is obtained by majority voting (max-wins voting) [Lajnef *et al.* , 2015]. OAA approach showed less accuracy in many practical situations whereas OAO is computationally more expensive to solve a multi-class problems [Bennani & Benabdeslem, 2006].

In order to achieve high accuracy with limited computation time in multi-class classification problems, present study adopted Dendrogram based Support Vector Machine (DSVM) approach for the classification of anaesthetic stages as awake, light anaesthesia, moderate anaesthesia and deep anaesthesia. DSVM is a decision-tree based SVM classification method and here a dendrogram represents a tree diagram which depicts the hierarchical arrangement of nodes produced as a result of clustering.

Let $X_i = X_1, X_2, ..., X_n$ be a set of samples each one of which is labeled as $Y_i = Y_1, Y_2, ..., Y_n$, $Y_i \in C_1, C_2, ..., C_k$ where $C_1, C_2, ..., C_k$ are k number of classes and $k \leq n$. Then DSVM method of classification has two major steps

- Step 1: Define the tree with its binary branching using known classes which gives the structure of the dendrogram. Practically it is implemented by calculating the centre of gravity of the features for each class and then applying Agglomerative Hierarchical Clustering (AHC) over all the k centers. AHC is a bottom-up approach clustering method in which clusters have sub-clusters, which in turn have sub-clusters [Lajnef *et al.* , 2015]. The dendrogram taxonomy that resulted from an AHC analysis is shown in Figure 6.2

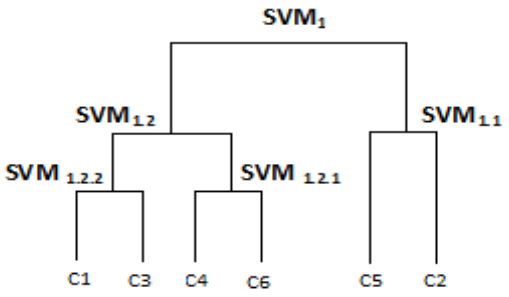

Figure 6.2: Hierarchical grouping of classes using AHC method[Bennani & Benabdeslem, 2006]

- Step 2: Apply SVM algorithm to each node of the tree diagram and train the algorithm using the elements of two subsets of each node. Consider an example shown in Figure 6.2. It represents clustering of 6 classes in which SVM_1 is trained using elements of C5, C2, C1, C3, C6 and C4 where elements of C5 and C2 are considered as positives and elements of C1, C3, C4 and C6

as negatives, $SVM_{12}$is trained using elements of C4, C6, C1 and C3 where elements of C4 and C6 are considered as positives and elements of C1 and C3 as negatives. The concept is repeated for each SVM associated node in the taxonomy [Bennani & Benabdeslem, 2006; Lajnef *et al.* , 2015]

6.3.3 Multilayer Perceptron (MLP) Neural network

Artificial Neural Network (ANN) is a mathematical model which works based on the learning process of neural networks in the human brain. It is normally used as a classifier to discriminate the different signals/data. ANN is widely used in various medical applications because of its adaptive nature. ie. The structure of the model changes based on the external or internal information that flows through the network during the learning phase [Haykin, 1994].

A Multilayer Perceptron (MLP) Neural network is a class of feedforward artificial neural network consisting of minimum three layers: an input layer, hidden layer and an output layer. Each layer consists of a number of highly interconnected processing elements called neurons, which usually operate in parallel. Here each neuron i in the hidden layer add up its input signals X_j after multiplying with its weights W_{ij} which is the strengths of each connection and finally computes its output Y_i using equation 6.16

$$Y_i = f(\Sigma W_{ij} X_j) \tag{6.16}$$

where f is the activation function and is used to transform the weighted sum inputs influencing the neurons. It can be a sigmoidal function, threshold function, hyperbolic tangent or a radial basis function [Übeyli, 2009a]. The input layer of the network supplies input vector (Feature vector in the current study) to the neurons in the hidden layer. There can be multiple numbers of hidden layers and the output of neurons in each hidden layer acts as input to the next layer. Finally, the output of the hidden layer neurons is passed to the output layer. The output of neurons in the output layer of the network constitutes overall response of the network.

Neural network uses an iterative process to learn its environment and applies adjustments to its weights. This type of learning is determined by the manner in which parameter changes take place. Backpropagation algorithm is one of the

methods used for adjusting the weights in a multilayer feed-forward neural network. Backpropagation calculates the error contribution of each neuron after a batch of data is processed and then the weights are adjusted by a gradient descent optimization algorithm. This will adjust the weights of neurons by calculating the gradient of the loss function. This technique is called backward propagation because the error is calculated at the output and distributed back through the network layers [Wikipedia, 2017a].
Basic backpropagation algorithm has three steps.

- Step 1: Input layer of the ANN receives input patterns as input and are propagated within the network to reach output unit. This forward pass results an output called actual or predicted output.
- Step 2: The actual or predicted outputs are subtracted from the desired outputs to produce an error signal, where desired outputs are provided along with input training patterns.
- Step 3: The error signal is passed back through the neural network to compute the contribution of each neuron in the hidden layer and to derive the corresponding adjustment needed to produce the desired output. The connection weights are then adjusted and the neural network has learned from an experience [McCollum, 1998; Blais & Mertz, 2001; Ridella *et al.* , 1997]

6.3.4 Naive Bayes classifiers (NBC)

Naive Bayes classifiers (NBC) are probabilistic classifiers which work based on Bayesian theorem with an assumption of independence between the features. It assumes that value of a particular feature in the class is independent of value of any other feature. Bayes theorem works on conditional probability and it calculates the posterior probability of an event from its prior knowledge.
Let $X = x_1, x_2, \ldots, x_n$ represents n features, then conditional probability of target class C_k given predictor attribute X for each of k possible outcomes of classes C_k is

calculated using Bayes' theorem presented in equation 6.17.

$$P(C_k \mid X) = \frac{P(X|C_k)P(C_k)}{P(X)} \tag{6.17}$$

where $P(C_k|X)$ is the posterior probability of the target class C_k given predictor attribute $X, P(C_k)$ is the prior probability of class C_k, $P(X|C_k)$ is the likelihood probability of predictor given class and P(X) is the prior probability of predictor. Accordingly, NBC predicts the membership probabilities of each class or data point of a particular class. The class with highest probability is recognized as most likely class [Agarwal *et al.* , 2015]. Since the data used in the present study deals with continuous data, it is assumed that each class is distributed according to a Gaussian distribution. Therefore, current work adopted Gaussian Naive Bayes algorithm. Let x_i be a continuous feature of training dataset $X = x_1, x_2...., x_n$. Then the computation of Gaussian Naive Bayes algorithm is as follows

- Step1: Segment the training data based on the target class
- Step2: Compute the mean and variance of x_i in each class
- Step3: Compute the probability distribution of observations(v) of feature x_i given a class C_i (i.e.$p(x_i = v \mid C_i)$) using the equation 6.18

$$P(x_i = v \mid C_i) = \frac{1}{\sqrt{2\pi\sigma_{c_i}^2}} \exp^{-\frac{(v-\mu_{c_i})^2}{2\sigma_{c_i}^2}} \tag{6.18}$$

where μ_{c_i} is the mean of observations in feature x_i associated with class C_i and $\sigma_{c_i}^2$ is corresponding variance of x_i associated with class C_i [Agarwal *et al.* , 2015].

6.4 Experimental Results

Current work takes the advantage of five feature ranking functions to rank the features. Wilcoxon sum-rank test and Student's t-test checks whether each feature is differentially expressed between two classes whereas Entropy and Bhattacharyya distance calculates the distance between the distributions of two classes. Finally, the ROC tests the individual significance of the features. MATLAB Bioinformatics

toolbox is used to compute these scoring functions. EEG extracted features and their corresponding outputs are passed through these scoring functions to get best features according to their class separability measures. Different classifier such as kNN, SVM, MLP, and NBC and their outcomes in terms of accuracy is computed to check the efficiency of features in classifying them as awake, light anaesthesia, moderate anaesthesia and deep anaesthesia.

The datasets for training and validation incorporates extracted features from the EEG signals and hemodynamic signals of all the 25 patients consisting 15302 vectors. 12242 vectors are utilized for constructing the model by training and the remaining vectors 3060 are used for the validation of the classification model. The class separability of features can also be checked using Kruskal-Wallis statistical test. The output class used for feature selection, classification and Kruskal-Wallis test are the anaesthetic depth provided by attending anaesthesiologist as awake, light anaesthesia, moderate anaesthesia and deep anaesthesia for each patient's data. The list of EEG extracted features passed through the feature ranking functions is given in Table 6.1.

Table 6.1: EEG Extracted Features

Feature name	**Domain**	**Abbreviation**
Standard Deviation	Time Domain	SD
Energy		
Entropy		
Mean Absolute Deviation		MAD
Zero Crossing Rate		ZCR
Inter Quartile Range		IQR
Spectral Edge Frequency	Frequency Domain	SEF
Spectral Entropy		SEN
Wavelet Entropy	Time-Frequency Domain	WE
$RelativeWaveEnergy_{\gamma Band}$		RWE_{γ}
$RelativeWaveEnergy_{\beta Band}$		RWE_{β}
$RelativeWaveEnergy_{\alpha Band}$		RWE_{α}
$RelativeWaveEnergy_{\theta Band}$		RWE_{θ}
$RelativeWaveEnergy_{\delta Band}$		RWE_{δ}
Approximate Entropy	NonLinear	ApEn
Permutation Entropy		Pen

The feature ranking helps to select the most relevant features from the available feature vector. The features with higher ranks are selected and features with lower ranks are ignored. This reduces the complexity of classifiers without sacrificing their performance. At first, all the 6-time domain features of the EEG signals are passed through different classifiers like kNN, SVM, MLP and NBC without applying any feature ranking functions. The outcome of different classifiers in classifying different anaesthetic states as awake, light anaesthesia, moderate anaesthesia and deep anaesthesia is depicted in Table 6.2.

TABLE 6.2: Different Classifier outcomes without using any feature ranking methods to the Time domain EEG features

SL No	**Time Domain features**	**Classifier Accuracy**
1	SD	
2	Energy	
3	Entropy	kNN=75%, SVM=74%,
4	MAD	MLP=82.6%, NBC=75%
5	ZOR	
6	IQR	

The outcome of different feature ranking techniques when applied to the time domain EEG features are shown in Table 6.3. The table also presents different classifier outcomes in terms of accuracy when selected ranked features which are highlighted in the table are given as input to the classifiers. The feature name and its corresponding serial number are given in the bracket. The highest classification accuracy obtained are kNN=83%, SVM=76%, MLP=82.8%, NBC=83%. This is obtained when top ranked features of Student's t-test are applied as input to the specified classifiers. Finally, the features selected from the time domain for DoA estimation are ZCR and SD.

The frequency domain features and non-linear features provide good classification accuracy without passing through the feature ranking technique and are depicted in Table 6.4. The classification accuracy obtained when both the frequency domain features as input to the classifiers is kNN=86%, SVM=81%, ANN=86%, NBC=84% which is the highest classification accuracy obtained than if applied

TABLE 6.3: Feature Ranking techniques to Time domain features and different classifier outputs with selected ranked features as input

Ranking Method	Rank	Time Domain Features	Classifier Accuracy
Students t-test	1	ZOR(5)	kNN=83%, SVM=76%, MLP=82.8%,NBC=83%
	2	SD (1)	
	3	Entropy (3)	
	4	MAD (4)	
	5	IQR (6)	
	6	Energy (2)	
Bhattacharya Distance	1	Energy(2)	kNN=75% ,SVM=61%, MLP=63.3%,NBC=63%
	2	IQR (6)	
	3	SD (1)	
	4	MAD (4)	
	5	ZOR (5)	
	6	Entropy (3)	
Entropy	1	ZOR (5)	kNN=75%, SVM=77%, MLP=82.2%, NBC=82%
	2	Energy (2)	
	3	IQR (6)	
	4	Entropy (3)	
	5	MAD (4)	
	6	SD (1)	
Wilcoxon	1	ZOR (5)	kNN=82%, SVM=76%, MLP=82.5%, NBC=82%
	2	Entropy (3)	
	3	IQR (6)	
	4	MAD (4)	
	5	SD (1)	
	6	Energy(2)	
ROC	1	ZOR(5)	kNN=82%, SVM=76%, MLP=82.5%, NBC=82%
	2	Entropy(3)	
	3	MAD (4)	
	4	SD (1)	
	5	Energy (2)	
	6	IQR (6)	

alone. Therefore both features SEF and SEn are selected from the frequency domain analysis. ApEn and PEn are the features selected from non-linear analysis and these two features provide its maximum accuracy when they are applied together to the classifiers. The classifiers output is given by kNN=84%, SVM=74%,

TABLE 6.4: Frequency domain and nonlinear features with their classification accuracy without any feature ranking technique

Feature Domain	EEG Features	Classifier Accuracy
Frequency Domain	SEF SEN	kNN=86%, SVM=81% , ANN=86% , NBC=84%
NonLinear	ApEn PEn	kNN=84%, SVM=74%, ANN=78.2%, NBC=78%

ANN=78.2%, NBC=78%. The classifier outputs of Time-Frequency domain features without applying any feature ranking techniques is kNN=81%, SVM=79%, ANN=82.9%, NBC=80% and this has been represented in Table 6.5.

TABLE 6.5: Different Classifier outcomes without using any feature ranking methods to the Time-Frequency domain EEG features

SL No	**Time-Frequency Domain features**	**Classifier Accuracy**
1	WEn	kNN=81%, SVM=79%, ANN=82.9%, NBC=80%
2	RWE_{γ}	
3	RWE_{β}	
4	RWE_{α}	
5	RWE_{θ}	
6	RWE_{δ}	

From Table 6.6 it is evident that the classifier accuracy is increased when highlighted features from the time-frequency domain are applied to the classifiers. It is high when the features RWE_{γ}, RWE_{β} and WEn are selected as input to the classifiers. These 3 features are selected based on the Bhattacharya Distance feature ranking method which shows highest classification accuracy. When comparing the classification accuracies of features with and without feature ranking techniques, it can be observed that the classification accuracy is increased after applying feature ranking techniques. The EEG features selected after feature ranking technique for the estimation of DoA are shown in Table 6.7. Finally, performance of the classifiers in terms accuracy, sensitivity, specificity and precision are compared in Table 6.8 when all the selected EEG features are given as input to the classifiers. The total

accuracy of the KNN, SVM, MLP, NBC classifiers are 93%, 91%, 93%, 92% respectively. Class wise accuracy also calculated to check the performance of selected features during different stages of anaesthesia.

TABLE 6.6: Feature ranking techniques applied to Time-Frequency domain features and classifier output with selected ranked features

Feature Ranking Method	**Rank**	**Time-Frequency Domain Features**	**Classifier Accuracy**
Students t-test	1	$RWE_{\beta}(3)$	kNN=82%, SVM=76%, ANN=80.2%, NBC=78%
	2	WEn(1)	
	3	$RWE_{\delta}(6)$	
	4	RWE_{γ} (2)	
	5	$RWE_{\alpha}(4)$	
	6	$RWE_{\theta}(5)$	
Bhattacharya Distance	1	RWE_{γ} (2)	kNN=82%, SVM=80%, ANN=84.7%, NBC=82%
	2	$RWE_{\beta}(3)$	
	3	WEn(1)	
	4	$RWE_{\delta}(6)$	
	5	$RWE_{\alpha}(4)$	
	6	$RWE_{\theta}(5)$	
Entropy	1	RWE_{γ} (2)	kNN=81%, SVM=73%, ANN=82.9%, NBC=81%
	2	$RWE_{\beta}(3)$	
	3	$RWE_{\delta}(6)$	
	4	WEn(1)	
	5	$RWE_{\alpha}(4)$	
	6	$RWE_{\theta}(5)$	
Wilcoxon	1	$RWE_{\delta}(6)$	kNN=81%, SVM=76%, ANN=80.9%, NBC=80%
	2	$RWE_{\theta}(5)$	
	3	RWE_{γ} (2)	
	4	$RWE_{\beta}(3)$	
	5	WEn(1)	
	6	$RWE_{\alpha}(4)$	
ROC	1	$RWE_{\gamma}(2)$	kNN=82%, SVM=80%, ANN=84.7%, NBC=82%
	2	WEn(1)	
	3	$RWE_{\beta}(3)$	
	4	$RWE_{\delta}(6)$	
	5	$RWE_{\theta}(5)$	
	6	$RWE_{\alpha}(4)$	

TABLE 6.7: Selected EEG features for DoA Estimation

Feature name	**Domain**	**Abbreviation**
Zero Crossing Rate Standard Deviation	Time Domain	ZCR SD
Spectral Edge Frequency Spectral Entropy	Frequency Domain	SEF SEN
Wavelet Entropy $RelativeWaveEnergy_{\gamma Band}$ $RelativeWaveEnergy_{\beta Band}$	Time-Frequency Domain	WE RWE_{γ} RWE_{β}
Approximate Entropy Permutation Entropy	NonLinear	ApEn Pen

TABLE 6.8: Performance comparison of Classifiers when all the selected EEG features are given as input to the classifiers

Classifier	**Accuracy**	**Sensitivity**	**Specificity**	**Precision**		**Confusion Matrix**			
						Class-1	Class-2	Class-3	Class-4
KNN	93%	84%	94%	82%	Class-1	1427	199	0	0
					Class-2	122	950	27	0
					Class-3	1	47	112	10
					Class-4	0	0	21	143
					Class Accuracy	89%	87%	97%	99%
SVM	91%	79%	93%	76%	Class-1	1397	235	0	0
					Class-2	150	884	24	0
					Class-3	2	76	108	22
					Class-4	1	1	28	131
					Class Accuracy	87%	84%	95%	98%
MLP	93%	84%	94%	84%	Class-1	1436	228	0	0
					Class-2	114	941	29	1
					Class-3	0	27	108	5
					Class-4	0	0	23	147
					Class Accuracy	91%	87%	96%	99%
NBC	92%	84%	94%	80%	Class-1	1377	169	1	0
					Class-2	173	942	27	0
					Class-3	0	85	117	11
					Class-4	0	0	15	143
					Class Accuracy	90%	87%	95%	99%

6.4.1 Kruskal-Wallis test on EEG features

The discrimination ability of selected EEG features extracted from all the 25 patients during the whole surgery can also be tested by applying Kruskal-Wallis statistical test to the features. The output groups for discrimination are awake, light anaesthesia, moderate anaesthesia and deep anaesthesia which is the anaesthetic depth provided by the attending anaesthesiologist for each patient. The p-value obtained after Kruskal-Wallis test are shown in Table 6.9.

TABLE 6.9: p-value of the EEG features as a result of Kruskal-Wallis statistical test

Domain	Features	P-Value
Time Domain	SD	$1.64X10^{-5}$
	Energy	$1.55X10^{-4}$
	Entropy	$7.01X10^{-3}$
	MAD	$3.93X10^{-4}$
	ZCR	$2.01X10^{-6}$
	IQR	0.037
Frequency Domain	SEF	$2.057X10^{-10}$
	SEN	$7.35X10^{-11}$
Time Frequency Domain	Wen	$4.16X10-5$
	RWE_{γ}	$3.27X10-8$
	RWE_{β}	$4.8X10-6$
	RWE_{α}	$1.93X10^{-3}$
	RWE_{θ}	$7.40X10^{-2}$
	RWE_{δ}	$1.46X10^{-4}$
Non Linear	ApEn	$2.15X10^{-6}$
	Pen	$1.28X10^{-6}$

Lowest p-values among time domain features are for the features ZCR and SD which indicates that these features have highest discrimination ability compared to other features. Both the frequency domain features and Non-linear features showed lowest p-value to indicate highest discrimination ability. In case of time-frequency domain features WEn, RWE_{γ} and RWE_{β} features showed highest discrimination ability. The other features with lowest discrimination ability (high p-value) are eliminated from further processing because of its lowest discrimination capability.

The box plots of selected EEG features during different anaesthetic phases obtained as a result of Kruskal-Wallis test is presented in Figure 6.3. Here we can visualize the class separability of the selected EEG features. The features ZCR, SEF, SEn and RWE_{γ} shows good class seperability compared to all other features. The classification classes are overlapped to some extend in the remaining features. The box plots of WEn and RWE_{β} features reveals that the moderate anaesthesia and light anaesthesia classes are overlapped.

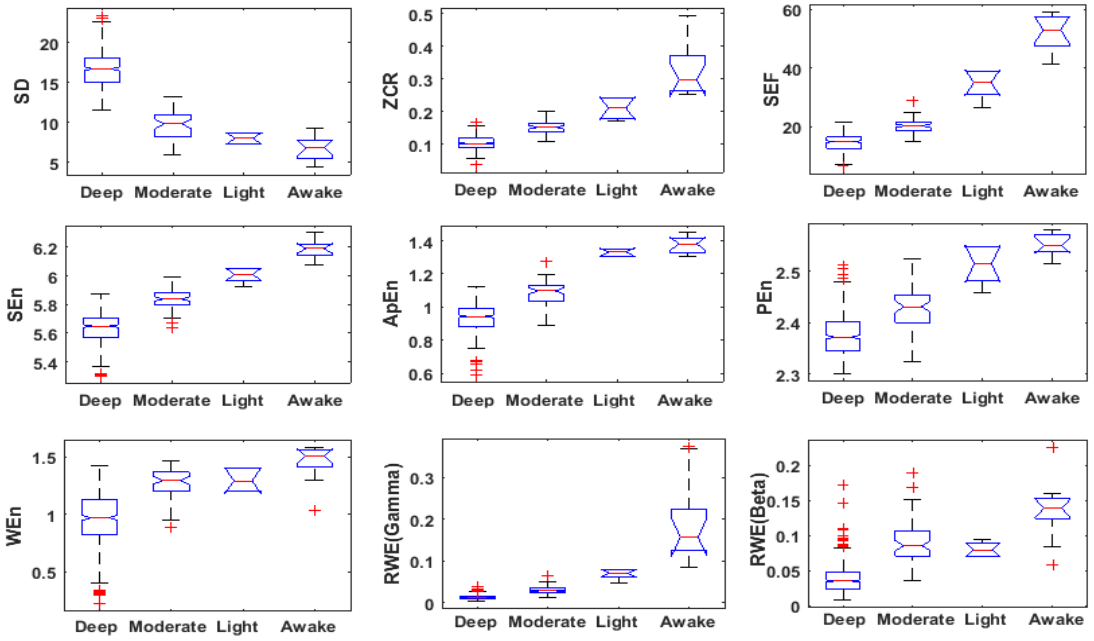

FIGURE 6.3: Box plot of the selected EEG features resulted from Kruskal-Wallis test

6.4.2 Kruskal-Wallis test on hemodynamic parameters

As we have seen in the previous chapter that EEG measures and hemodynamic parameters both change with an anaesthetic drug effect. Therefore, it is important to check the classification capability of hemodynamic parameters according to DoA. Here Kruskal-Wallis test is applied to the extracted hemodynamic parameters such as a change in Heart Rate (ΔHR), change in Mean Arterial Blood Pressure (ΔMBP), Pulse Pressure (PP) and the output class for KW test is the same that we have used

for the classification of EEG features. The p-value obtained after Kruskal-Wallis test are shown in Table 6.10.

TABLE 6.10: p-value of the hemodynamic parameters as a result of Kruskal-Wallis statistical test

Features	P-Value
ΔHR	$3.7X10^{-3}$
ΔMBP	$3.6X10^{-4}$
PP	0.34

The lowest p-value is for the features ΔHR and ΔMBP which indicate that these features have highest discrimination ability compared to the hemodynamic feature Pulse pressure. Therefore, the feature PP is eliminated from further processing because of its lowest discriminating ability. The box plots resulted from the Kruskal-Wallis test is shown in Figure 6.4(a) and (b). When comparing the box plot of selected EEG features and hemodynamic features, hemodynamic parameters have low discrimination ability.

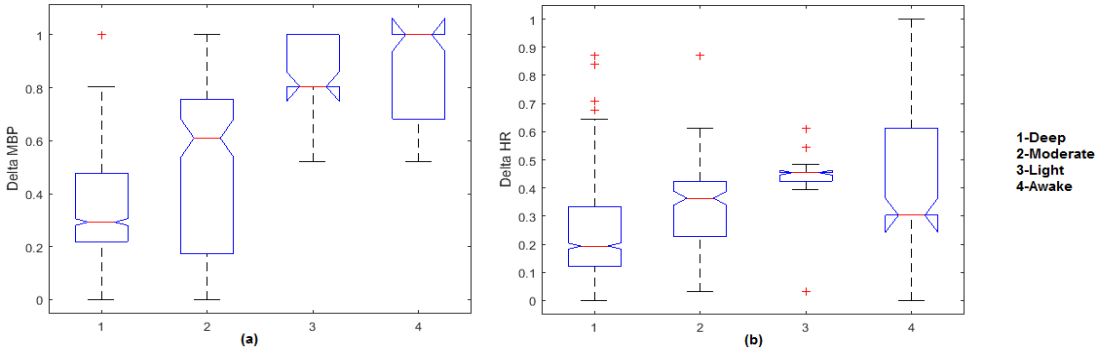

FIGURE 6.4: Box plot of the ΔHR and ΔMBP resulted from Kruskal-Wallis test

6.4.3 Performance comparison with similar work

Performance comparison of selected EEG features and hemodynamic features in classification is done with one recent work by Shalbaf et al. [SHALBAF *et al.* , 2015] and is presented in Table 6.11. Here Shalbaf et al. used the EEG features like Permutation Entropy, Modified Permutation Entropy and the hemodynamic

TABLE 6.11: Comparison of classification accuracy with the results of [SHALBAF *et al.* , 2015]

Author	**Classifier used**	**Features**	**Accuracy**
Shalbaf et al. [SHALBAF *et al.* , 2015]	MLP Classifier	Permutation Entropy	66.90%
		Modified permutation Entropy	85.10%
		Hemodynamic features	53.50%
		Modified Permutation Entropy + Hemodynamic features	89.40%
Proposed method	KNN, SVM, MLP, NBC	All the selected EEG features	86%, 82%, 86%, 84%
		Hemodynamic features	64%, 66%, 47%, 55%
		EEG features + Hemodynamic Features	89%, 84%, 91%, 88%

features like HR and BP for the DoA classification whereas proposed study used all the selected EEG features and selected hemodynamic features. Both the study provides almost similar results.

6.5 Summary

In this chapter different feature ranking methods like 'T-Test', 'Entropy', 'Bhattacharyya', 'ROC' and 'Wilcoxon' are used to select the optimum features from the feature vector. The kNN, SVM, MLP and NBC classifier outputs are compared based on their accuracy to select the best-ranked EEG features in the time domain, frequency domain and non-linear analysis. The feature combination which provided highest classification accuracy in the time domain are Standard Deviation (SD)

and Zero Crossing Rate (ZCR). Both the frequency domain features showed highest classification accuracy and therefore both the features were selected for final model development. Then the time-frequency domain features selected based on their classification accuracy and discrimination ability were WEn, RWE_{γ} and RWE_{β}. The combination of both the non-linear features (ApEn and PEn) were selected because their combination showed comparatively higher classification accuracy than if taken alone. In the case of hemodynamic parameters Kruskal Wallis test is used to select the best features from the extracted hemodynamic parameters. Based on this test, best features selected from the extracted hemodynamic parameters are ΔHR and ΔMBP.

Chapter 7

Adaptive Neuro-Fuzzy Inference System based Estimation of Depth of Anaesthesia

The integration of the expert system with patient monitoring devices improved the quality of medical research. The present chapter is focused to estimate DoA by integrating multiple parameters extracted from EEG signals and hemodynamic variables through Adaptive Neuro-Fuzzy Inference System (ANFIS). These systems works based on fuzzy sets and Artificial Neural Network (ANN) structures and is introduced in the study to develop an integrated Index. The ANFIS structures can successfully model the systems with nonlinear relationships between input and output. The speed and accuracy of parameter learning, the smaller number of adjustable parameters and the performance of model classification are the main motivation for the use of ANFIS models compared to other machine learning methods. EEG extracted features provide the information available on electroencephalogram signals during anaesthesia which help to extract the hypnotic changes due to the anaesthetic drugs. Extracted hemodynamic parameters provide information about changes in autonomic nervous system due to the administration of anaesthetic drugs during surgery. This chapter presents a novel DoA index generated using an Adaptive Neuro-Fuzzy Inference System based on subtractive clustering algorithm. The inputs provided to the ANFIS model are selected EEG features and hemodynamic

features. Finally, the generated index is compared with BIS index.

7.1 Adaptive Neuro-Fuzzy Inference System (ANFIS)

Adaptive Neuro-Fuzzy Inference System is an intelligent system which integrates Artificial Neural Network (ANN) and Takagi-Sugeno fuzzy inference system principles. It captures the advantages of both the systems in a single framework and enhances the overall performance of the system. It takes the advantage of the fuzzy system to present the knowledge which is gained from data in an interpretable manner. On the other hand, it employs neural network to acquire the learning ability to adjust the membership functions parameters and fuzzy rules directly from the data[Abraham, 2005; Wang *et al.* , 2006]. The generated fuzzy rules help to approximate the non-linear functions whereas the membership function parameter describes the system behaviour. At first, ANFIS learns the features from the data set and then it adjusts the system parameters [Jang, 1993].

In the present study, ANFIS model receives selected features (both EEG and hemodynamic) as input and provide a dimensionless index as output which varies in accordance with Depth of Anaesthesia (DoA). Therefore, this model can be effectively used for continuous assessment of DoA. Here the ANFIS model is implemented using both Fuzzy C Means (FCM) clustering and subtractive clustering method to learn and adjust their parameters.

7.1.1 Architecture of ANFIS Model

The architecture of Adaptive Neuro-Fuzzy Inference System consists of five layers. A first-order Sugeno fuzzy inference system model with two inputs x and y, one output f and two fuzzy If-Then rules is as follows:

$$Rule1 = If\ x\ is\ A1\ and\ y\ is\ B1\ Then\ f1 = p_1x + q_1x + r_1 \tag{7.1}$$

$$Rule2 = If\ x\ is\ A2\ and\ y\ is\ B2\ Then\ f2 = p_2y + q_2y + r_2 \tag{7.2}$$

where $A1, A2, B1$ and $B2$ are the fuzzy functions of inputs x and y whereas p_1, q_1, r_1, p_2, q_2 and r_2 are the design parameters of the output function which are determined during the training process of the network model.

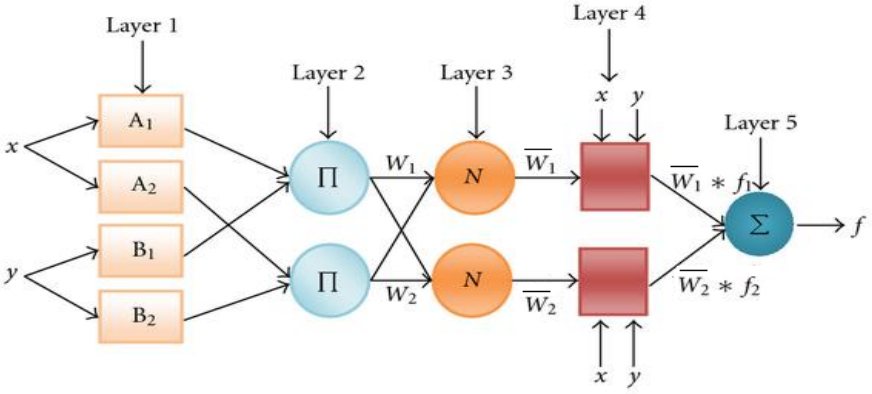

FIGURE 7.1: Architecture of ANFIS model
[MUNIRAJ & CHANDRASEKA, 2011; KESHAVARZI *et al.* , 2017]

In the basic architecture, each layer consists of a set of nodes and they are connected through directed links as in Figure 7.1. Each node is a processing unit that performs a particular function based on the input signals on it. These nodes are of two types: (1) Adaptive node represented by squares (2) Fixed node indicated by circles. An adaptive node contains fuzzy functions with modifiable parameters whereas fixed node contains a fixed function with empty parameter set [CHANG *et al.* , 2014]. The characteristics of each layer in the architecture are described below:

- Layer 1: The main function of this layer is fuzzification of received inputs. All the nodes present in this layer are adaptive nodes and each input is assigned a membership value by the node function. Node output of layer 1 is expressed as

$$O_i^1 = \mu_{Ai}(x); \quad i = 1, 2 \tag{7.3}$$

$$O_i^1 = \mu_{Bi-2}(y); \quad i = 3, 4 \tag{7.4}$$

where μ_{Ai} and μ_{Bi-2} are membership functions of fuzzy sets Ai and Bi respectively. Commonly used membership functions are bell-shaped, Gaussian, sigmoidal and triangular. If Gaussian membership function is selected then Equation 7.5 is used for $\mu_{Ai}(x)$ calculation. For generalized bell membership function Equation 7.6. is employed for the $\mu_{Ai}(x)$ calculation.

$$\mu_{Ai}(x) = \exp\left[- \left(\frac{x - c_i}{2a_i} \right)^2 \right] \tag{7.5}$$

$$\mu_{Ai}(x) = \frac{1}{1 + \left| \frac{x - c_i}{a_i} \right|^2 b_i} \tag{7.6}$$

where a_i, b_i *and* c_i are the parameters of the membership function and that decides the shape of the membership functions. They are called premise parameters.

- Layer 2: Each node in this layer is fixed and is labeled as Π. This layer calculates the firing strength of a rule via multiplication. The output of layer 2 is the multiplication of the signals coming into the nodes and is represented as Equation 7.7.

$$O_i^2 = w_i = \mu_{Ai}(x) * \mu_{Bi}(x); \quad i = 1, 2 \tag{7.7}$$

where w_i is the output that represents the firing strength of each rule.

- Layer 3 : All the nodes in this layer are fixed nodes. They are labeled as N and play an important role of normalization. i.e. The ratio of i^{th} rules firing strength to the sum of all rules firing strengths. The output of this layer is known as normalized firing strength and is represented as

$$O_i^3 = \bar{w_i} = \frac{w_i}{\Sigma_i w_i}; \quad i = 1, 2 \tag{7.8}$$

- Layer 4: In this layer all the nodes are adaptive nodes. Each node computes the contribution of i^{th} rule towards the model output. It is calculated as the product of normalized firing strength and a first order polynomial (which is

the Takagi-Sugeno type linear approximator f_i). It is expressed as Equation 7.9.

$$O_i^4 = \bar{w_i} * f_i = \bar{w_i} * (p_i x + q_i y + r_i); \quad i = 1, 2 \tag{7.9}$$

where $\bar{w_i}$ is the normalized firing strength from the third layer and $p_i x + q_i y + r_i$ is the parameter in the node. These parameters are called consequent parameters.

- Layer 5: The single node present in this layer is a fixed node that computes the overall output of the ANFIS model. The output of this layer is the sum of all incoming signals towards the node. It is represented as Equation 7.10.

$$O_i^5 = \Sigma_i(\bar{w_i} * f_i) = \frac{\Sigma_i w_i * f_i}{\Sigma_i w_i}; \quad i = 1, 2 \tag{7.10}$$

7.1.2 Estimation of parameters for the ANFIS model

The task of estimation of parameters for the ANFIS architecture is required to tune all modifiable parameters namely premise parameters (a_i, b_i, c_i) and the consequent parameters (p_i, q_i, r_i). These parameters are fine-tuned using learning algorithm which can train both the parameters to adapt to its environment. Before applying the learning algorithms the initial membership functions and rules are determined to speed up the learning process.

7.1.2.1 Selection of Initial Fuzzy Functions and Rules for the ANFIS model

In typical fuzzy systems, rules and membership functions are decided by an expert who has a thorough knowledge about the input-output relationship of the system to be modelled. But in ANFIS model no experts are available to determine the number of fuzzy functions and rules. Two commonly used methods for determining the number of membership functions and fuzzy rules for the ANFIS model are Grid partitioning and Scatter partitioning.

Grid partitioning method Grid partitioning is one of the techniques used for initializing the structure of fuzzy inference system. Wang et al. used this fuzzy partition to extract fuzzy rules from numerical data [Wang & Mendel, 1992]. Here fuzzy rules are generated by finding all possible combinations of input membership functions. The numbers of rules are determined based on the number of membership functions of each input variable. The centers of the membership functions are uniformly partitioned in the range of input variables which determines the initial values of premise parameters.

The limitation of Grid partitioning method is that the number of rules grows rapidly as the input dimension increases. If n inputs and N fuzzy subsets for each individual input then the number of rules which is possible for Grid partitioning is n^N. Therefore, the number of rules increases exponentially when the number of inputs increases. For example, if 3 membership functions are used in the fuzzy model with 7 inputs, then the numbers of rules generated are $3^7 = 2187$. This results in poor output and more processing time for a high dimensional input dataset. Scatter partitioning method is the solution to overcome this problem. In MATLAB grid partitioning is implemented using a GENFIS1 function. In the current research 11-dimensional feature vector is selected for ANFIS modelling and this leads to a huge number of rule generations. Therefore, Grid partitioning is not preferred in the current research.

Scatter partitioning method This method eliminates the limitations of grid partitioning and it divides the input space into rule patches. In this method, the if parts of the fuzzy rules are positioned at arbitrary locations in input space. If the rules are represented by n-dimensional Gaussians then the centers of the Gaussians are not confined to corners of a rectangular grid. But are chosen based on clustering algorithm which works on the training data. The two main clustering algorithms available are

(1) Fuzzy C Means clustering

(2) Subtractive clustering

7.1.2.2 Subtractive Clustering

Subtractive clustering method was introduced by Chiu et al, in 1994[Chiu, 1994]. In this method, data points are normalized to [0-1] in each dimension. Subtractive clustering method calculates the density of neighbouring data points to find optimal data point within a cluster. The next cluster and its centre are determined by removing data points within the radial distance of the first cluster. This procedure is continued till all the data points are clustered within a radial distance of a cluster centre. This technique is used for generating fuzzy rules when the input size is large. This method provides optimized rules by considering the radii specified along with the training data set.

Let $X = X_1, X_2, X_3..., X_n$ represent n input data points with M dimension. Then the data points are first normalized within a hypercube as stated by Chiu et al [Chiu, 1994]. X_i is considered as a data point having potential cluster centre under a density measure given by

$$D_i = \sum_{j=1}^{n} \exp\left[-\frac{||X_i - X_j||^2}{(\frac{r_1}{2})^2}\right] \tag{7.11}$$

where r_1 represents a radius that defines a neighbourhood or range of influence. The value of r_1 is a positive constant given by the user along with the data set and ranges from zero to one. Data points outside the radius contribute slightly to the density measure. The data point X_i with the highest density D_i measure is considered as the centre of the first cluster and is denoted as X_{c1} under the density measure D_{c1}.

The density measure then recalculated using the Equation 7.12. Here the first cluster is removed by subtracting an amount that is a function of their distances to the first centre.

$$D_i = D_i - D_{c1} \exp\left[\frac{-||X_i - X_{c1}||^2}{(\frac{r_2}{2})^2}\right] \tag{7.12}$$

where $||X_i - X_{c1}||$ is the distances to the first cluster centre, r_2 represents the radius of the second fuzzy cluster and is given by $r_2 = r_1 * \eta$ and η is the quash factor.

This factor is used to multiply the radii values that determine the neighbourhood of a cluster centre, so as to quash the density measure for outlying points to be considered as part of that cluster. This is used to prevent closely spaced cluster centers.

The process of determining the cluster centers is repeated until the k^{th} cluster centre density measure, D_{ck} satisfies the conditions given in Equation 7.13 and 7.14. That means after the density measure revision, the data point to the next higher density measure is selected as a second cluster centre candidate. Whether this point is accepted as a new cluster centre or not depends on its potential according to the following conditions:

$$D_{ck} < \epsilon D_{c1} \tag{7.13}$$

$$\bar{\epsilon} D_{c1} > D_{ck} > \epsilon D_{c1} \tag{7.14}$$

where ϵ and $\bar{\epsilon}$ are the reject ratio and accept ratio represented as a small fraction. This is because it is difficult to determine the best ϵ since a high ϵ produces too few clusters and a low ϵ produces too many clusters. If the first condition is true then X_{c1} is rejected as a new cluster centre and the clustering is ended. If the second condition is true then X_{c1} is accepted as a new cluster centre and the above procedure is repeated.

The membership function for the cluster center X_{ck} is given as

$$\mu_k = \exp\left[- \frac{||X_i - X_{ck}||^2}{(\frac{r_1}{2})^2} \right] \tag{7.15}$$

where X_i represents an input. Once the cluster centers are established, the number of fuzzy rules and antecedent parameters are found through the membership functions. Optimization of the rule consequent parameters is made through the Least Squares Estimator (LSE).

7.1.2.3 Fuzzy C Means Clustering

Fuzzy C Means clustering method partitions a set of data into several clusters based on the similarity of data points within a cluster. That means the degree of membership functions decides the cluster groups. Fuzzy C-Means clustering was developed by Dunn in 1973 [Dunn, 1973] and was improved by Bezdek in 1981 [Bezdek, 2013]. Here each data point belongs to two or more clusters and the cluster centers are determined by minimizing an objective function. This objective function is defined in Equation 7.16

$$J_m = \sum_{j=1}^{c} \sum_{i=1}^{n} \left[U_{ij} \right]^m \left|\left| x_i - c_j \right|\right|^2 \tag{7.16}$$

Where $\left|\left| x_i - c_j \right|\right|$ is the distance between each data point and the cluster centre, m is the fuzziness coefficient which is a real number greater than 1, x_i is the i^{th} input of d-dimensional data, U_{ij} is the degree of membership function of input x_i in the cluster j and c_j is the center of the cluster. $||x_i - c_j||$ is the Euclidean distance between the j^{th} cluster centers and i^{th} data point. The membership function U_{ij} and the cluster centers c_j are updated during the training process of ANFIS model for the optimization of the objective function using the Equation 7.17 and 7.18

$$U_{ij} = \frac{1}{\sum_{k=1}^{c} \left[\frac{||x_i - c_j||}{||x_i - c_k||} \right]^{\frac{2}{m-1}}} \tag{7.17}$$

$$c_j = \frac{\sum_i [U_{ij}^m] . x_i}{\sum_i [U_{ij}]^m} \tag{7.18}$$

This iteration will stop when $Max[U_{ij}^{k+1} - U_{ij}^k] \leq \epsilon$ where ϵ is a termination criterion and its value is between 0 and 1, whereas k and $k+1$ are the iteration steps. The biggest advantage of the Fuzzy C-Means algorithm is its ability to find clusters of overlapping.

7.1.2.4 Hybrid Learning Algorithm

The first layer of ANFIS architecture contains nonlinear premise parameters and the fourth layer contains linear consequent parameters which are modifiable over time. These parameters are adapted to its input-output dataset using a learning algorithm which trains and update these parameters to adapt to its environment. Present study adopted Hybrid learning algorithm proposed by Jang et al. to train these parameters [Jang, 1993]. It combines the Least Square Estimator (LSE) method and the backpropagation gradient descent method for training.

In ANN, back propagation algorithm is used to learn and adjust the weights between the neurons from input-output training samples. In ANFIS model premise and consequent parameters plays the role of weights. In the parameter estimation process, premise parameters are learnt using backpropagation algorithm and the consequent parameters are determined using LSE method.

The learning process has two steps:

1. In the forward pass, the premise parameters are assumed fixed whereas the output of each node go forward and the consequent parameters are estimated using LSE method. The LSE method is applied to accelerate the convergence rate in the hybrid learning process.

2. In the backward pass, the consequent parameters are assumed fixed and the error signals which is the difference between the actual output and the generated output which is propagated back. This is called backpropagation algorithm and is used to update the premise parameters (a_i, b_i, c_i).

Thus the combination of LSE and backpropagation algorithm is used to train the ANFIS parameters and to develop a model from the input-output dataset. The advantage of this algorithm is overall optimization of the consequent parameters for the given premise parameters [Suparta & Alhasa, 2016].

7.2 Experimental Results

Adaptive Neuro-Fuzzy Inference System is implemented to generate an index that continuously measures the anaesthetic depth based on extracted features. The selected EEG features and hemodynamic parameters are given as inputs to the Adaptive Neuro-Fuzzy System. Present study tried to generate fuzzy membership functions and rules by applying two clustering methods 1. Fuzzy C Means clustering 2. Subtractive clustering. Parameter identification is tackled by hybrid learning algorithm that combines back-propagation gradient descent algorithm and the least squares method. The architecture of ANFIS model for the estimation of DoA is shown in Figure 7.2.

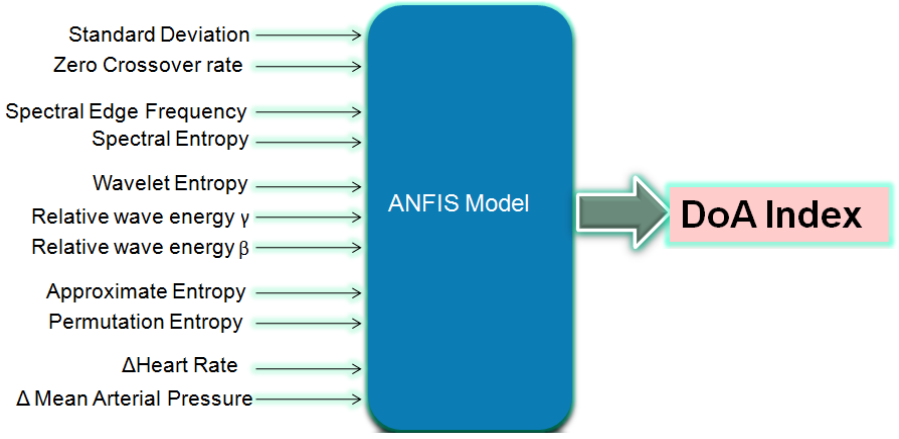

FIGURE 7.2: ANFIS structure for the estimation of DoA

Standard Deviation, Zero Crossing Rate, Spectral Edge Frequency, Spectral Entropy, Wavelet Entropy, Relative Wave Energy of $\gamma Band$, Relative Wave Energy of $\beta Band$, Approximate Entropy, Permutation Entropy, Change in HR and change in MBP are the inputs to the ANFIS model and DoA index is the output which varies in accordance with the depth of anaesthesia. The datasets for training and validation incorporates extracted features from the EEG signals and hemodynamic signals of all the 25 patients consisting 15302 vectors of 11 dimensions. In this work, 80% of the datasets is used as training data and 20% as testing data. Therefore, 12242 vectors of 11 dimensions are utilized for constructing the model by training and the remaining vectors 3060 of 11 dimensions are used for the validation of the developed ANFIS model.

7.2.1 Subtractive clustering

ANFIS model with subtractive clustering method is used in the present DoA estimation study to generate fuzzy membership functions and fuzzy rules. In this method along with the training and validating data, cluster radius is also provided. Present study tried different cluster radius to generate fuzzy membership functions and fuzzy rules. The best fuzzy model that generate fuzzy membership functions and fuzzy rules for the current study is selected through trial and error by specifying the radius which provides four membership functions as awake, light anaesthesia, moderate anaesthesia and deep anaesthesia for each input. Finally, radius value provided along with training and validation data set to generate four membership functions and rules is 0.6. The other parameters selected for subtractive clustering method are quash factor = 1.25, accept ratio = 0.5 and reject ratio = 0.15 [Celikyilmaz & Turksen, 2009]. The MATLAB function GENFIS2 is used to generate an initial Fuzzy Inference System for ANFIS training based on subtractive clustering. GENFIS2 accomplishes this by extracting a set of rules that model the data behavior. The generated input membership function type through GENFIS2 function is 'gaussmf'and output membership function type is 'linear'.
Figure 7.3-7.5 represents the initial membership functions of all the inputs generated through subtractive clustering method.

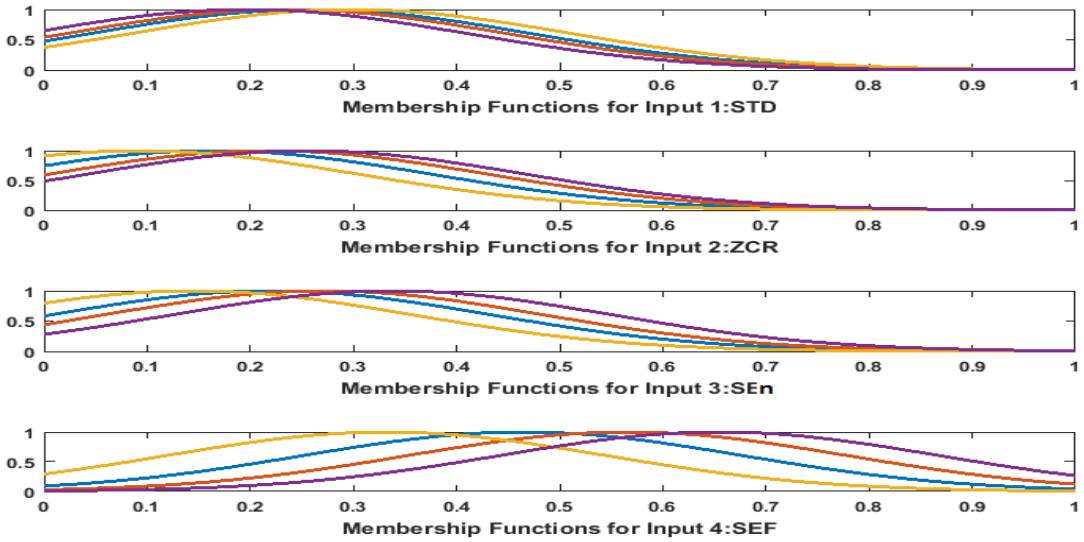

Figure 7.3: Initial Membership functions of ANFIS model based on subtractive clustering of the inputs STD, ZCR, SEF and SEn before training

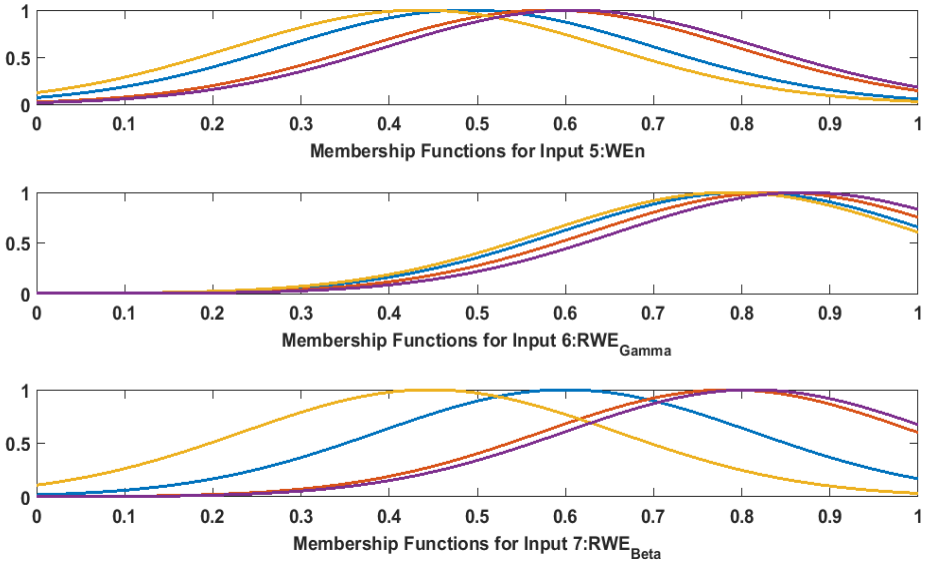

FIGURE 7.4: Initial Membership functions of ANFIS model based on subtractive clustering of the inputs WEn, RWE$_\gamma$ and RWE$_\beta$ before training

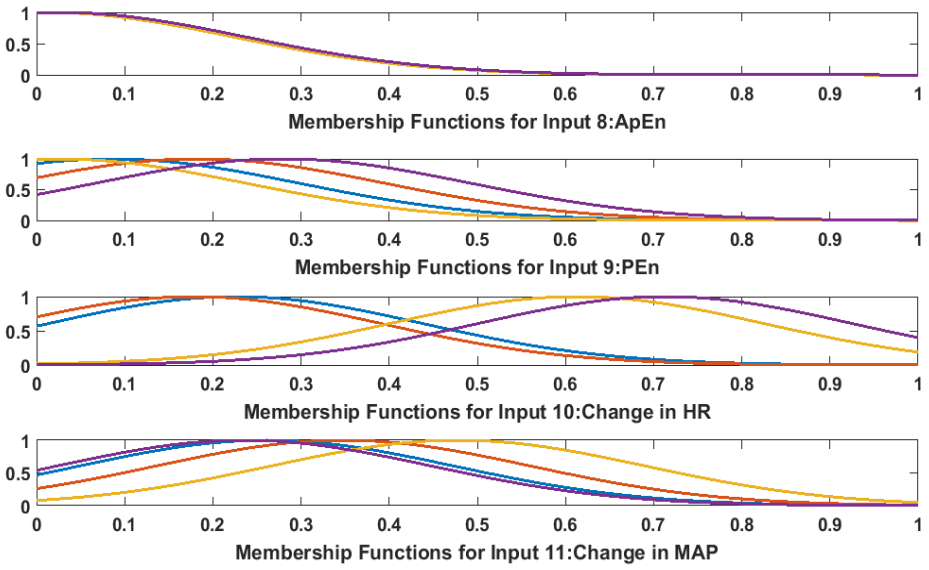

FIGURE 7.5: Initial Membership functions of ANFIS model based on subtractive clustering of ApEn, PEn ΔHR and,ΔMBP before training

Next step is to tune the parameters of ANFIS model for the chosen membership functions and is usually executed by applying learning algorithms. In this study, a most popular hybrid learning algorithm is used to adapt the parameters of the ANFIS model. The initial step size selected for training and validation is

0.01 which is provided to control the learning rate of the network model. The maximum number of training and validation epochs selected is 500. After training, the parameters of the membership functions are adapted to deliver better matching between input data and output data. As a result, the shape of the initial membership functions of all the inputs changes and is shown in Figure 7.6-7.8

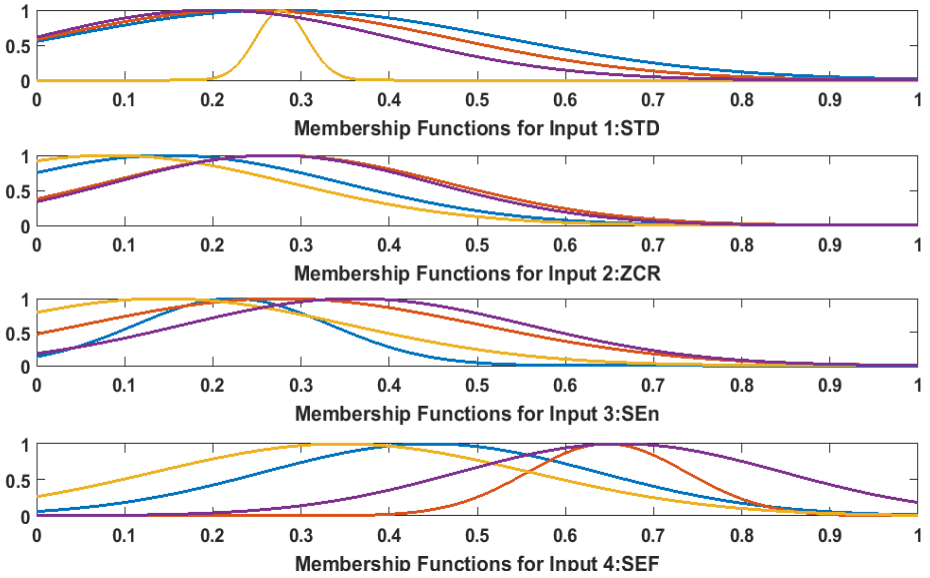

FIGURE 7.6: Membership functions of final ANFIS model based on subtractive clustering of inputs STD, ZCR, SEF and SEn after training

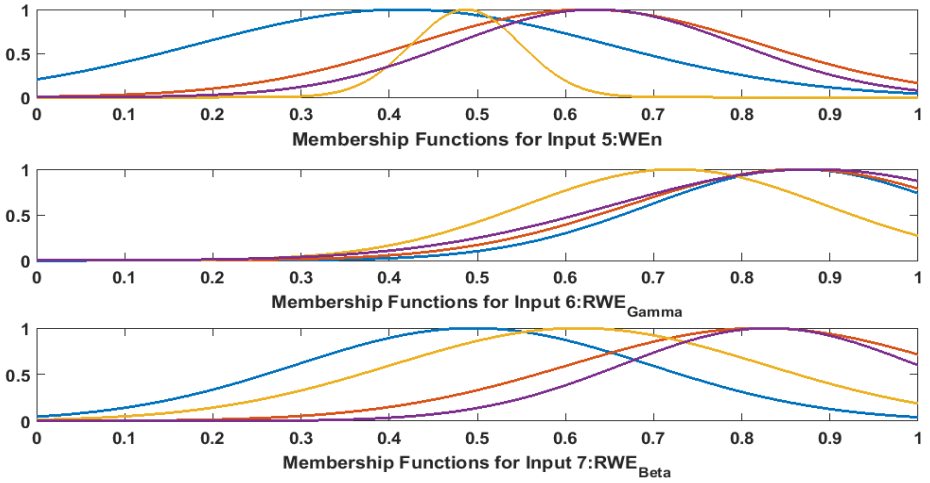

FIGURE 7.7: Membership functions of final ANFIS model based on subtractive clustering of inputs WEn, RWE$_\gamma$ and, RWE$_\beta$ after training

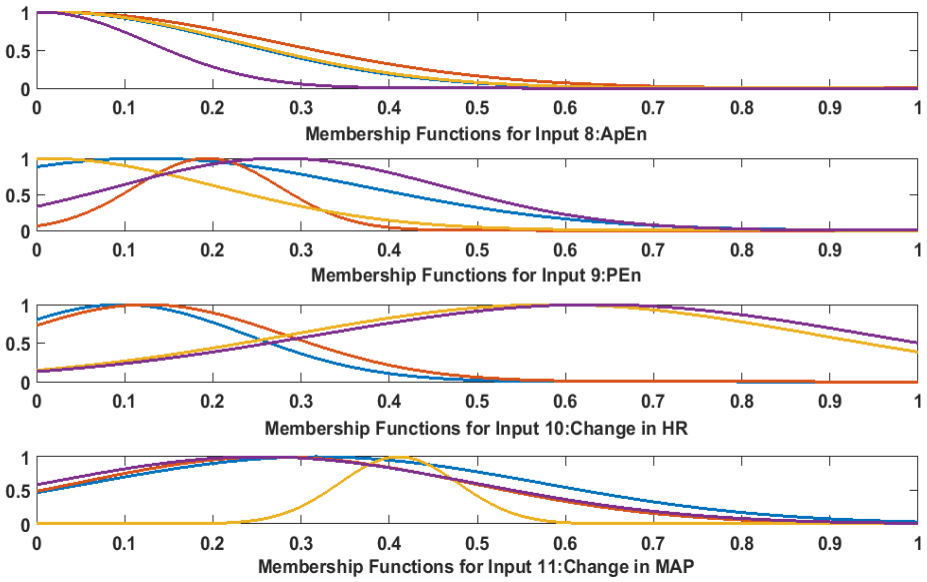

FIGURE 7.8: Membership functions of final ANFIS model based on subtractive clustering of inputs ApEn, PEn ΔHR and,ΔMBP after training

The performance of the ANFIS model with subtractive clustering is evaluated by calculating the statistical measure Root Mean Square Error (RMSE) using Equation 7.19

$$\text{RMSE} = \sqrt{\frac{1}{n}\sum_{i=1}^{n}(\hat{X}_i - X_i)^2} \tag{7.19}$$

where X_i is the actual output and $\hat{X}_i$ is the desired output.

The optimal ANFIS model is selected based on RMSE values of subtractive clustering and Fuzzy C Means clustering algorithms based ANFIS models. The RMSE gives more accurate value of the error between models generated output and desired (target) output. The ANFIS models are trained using the training data sets, while the test datasets are used to evaluate the prediction capability of the trained ANFIS models.

The prediction capability of the developed ANFIS model based on subtractive clustering in the training data set, testing data set and combined dataset are represented in Figure 7.9, 7.10, 7.11 respectively. The comparison between target output and generated output are shown in the figures and it is clear that the generated output follows the same track of target output. The error between the

target output and generated output and the error distribution are also shown in the figures. The RMSE of training data sets, testing datasets and combined data sets are 0.40255, 0.47554 and 0.41793 respectively.

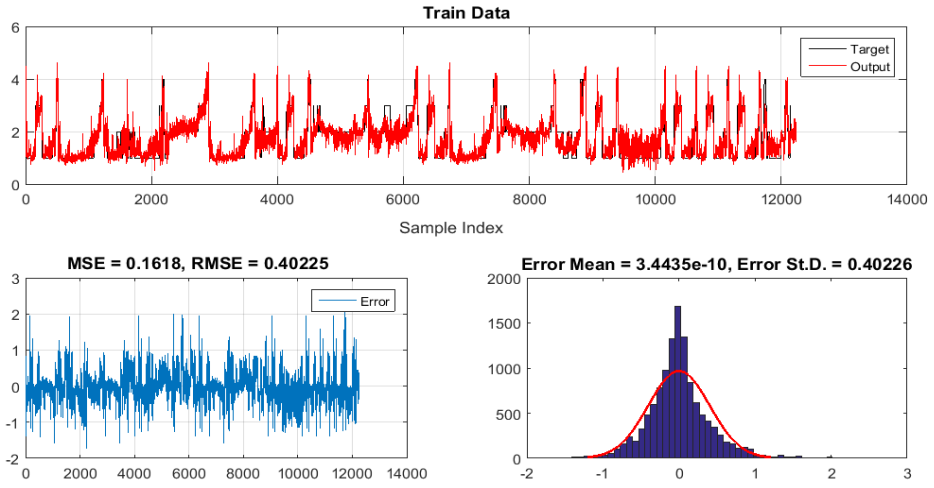

FIGURE 7.9: The performance of subtractive clustering based ANFIS model in the Training data set

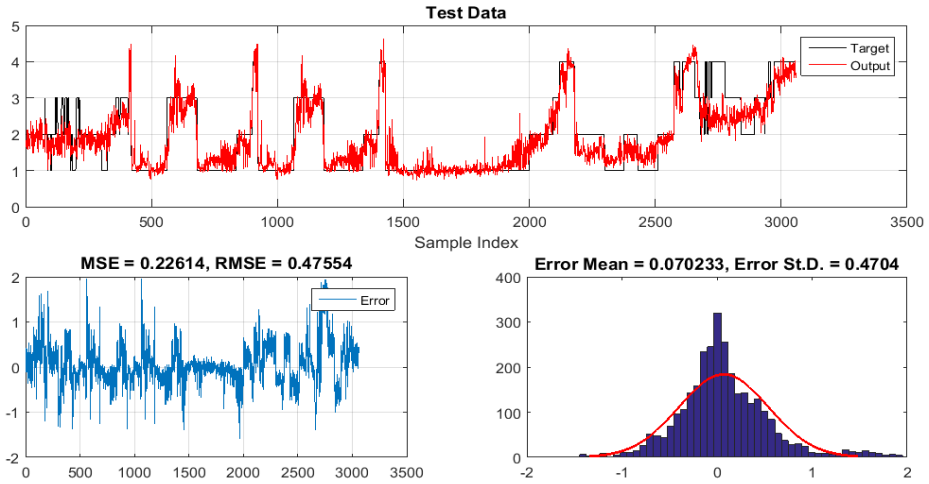

FIGURE 7.10: The performance of subtractive clustering based ANFIS model in the Testing data set

Figure 7.12 depicts RMSE curve during training and validation (testing) of data sets. It can be observed that the model is found to converge in < 500 epochs in both the training and testing datasets and the figure also indicate that no overfitting during training and testing process as both follow approximately the same trends.

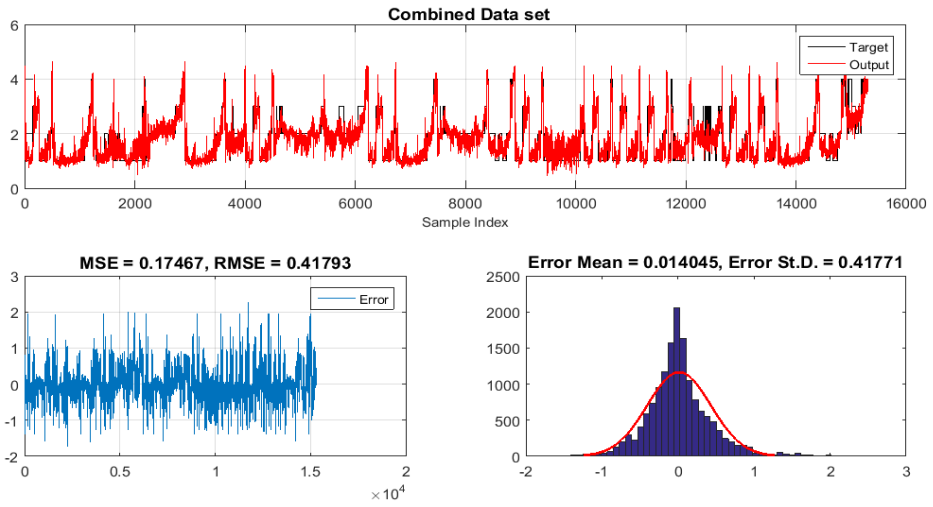

FIGURE 7.11: The performance of subtractive clustering based ANFIS model in the combined data set

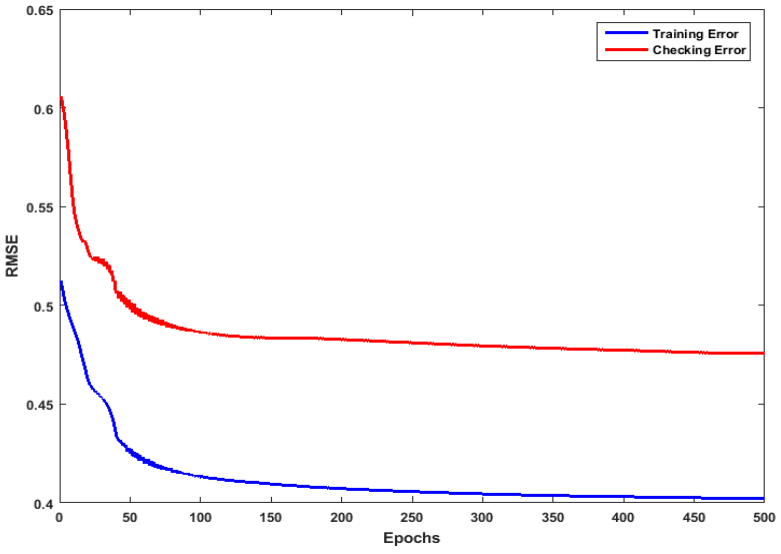

FIGURE 7.12: RMSE for training and validation of ANFIS model with subtractive clustering

7.2.2 Fuzzy C Means Clustering

The Fuzzy C Means algorithm is a clustering algorithm where each item may belong to more than one group and the degree of membership function for each item is given by a probability distribution over the clusters. In this method, the initial condition of cluster centers influences the performance of the algorithm and the rules are

predetermined by fixing the number of centers. The parameters specified in the current study to implement Fuzzy C Means clustering is the fuzziness coefficient as 2 and the number of clusters is 4. The MATLAB function GENFIS3 is used to generate an initial Fuzzy Inference System for ANFIS training based on Fuzzy C Means clustering. The generated input membership function type through GENFIS3 function is 'gaussmf'. Figure 7.13-7.15 represents the initial membership functions of all the inputs generated through Fuzzy C Means clustering method. The hybrid

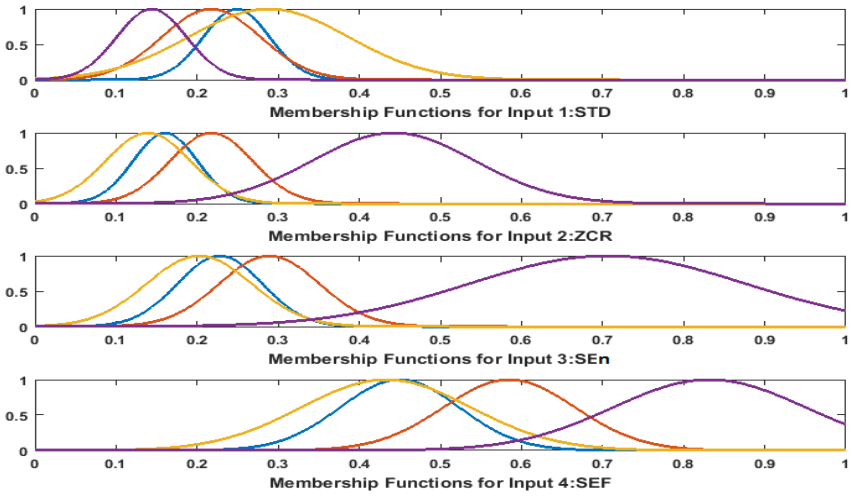

FIGURE 7.13: Initial Membership functions of ANFIS training based on Fuzzy C Means clustering of the inputs STD, ZCR, SEF and SEn before training

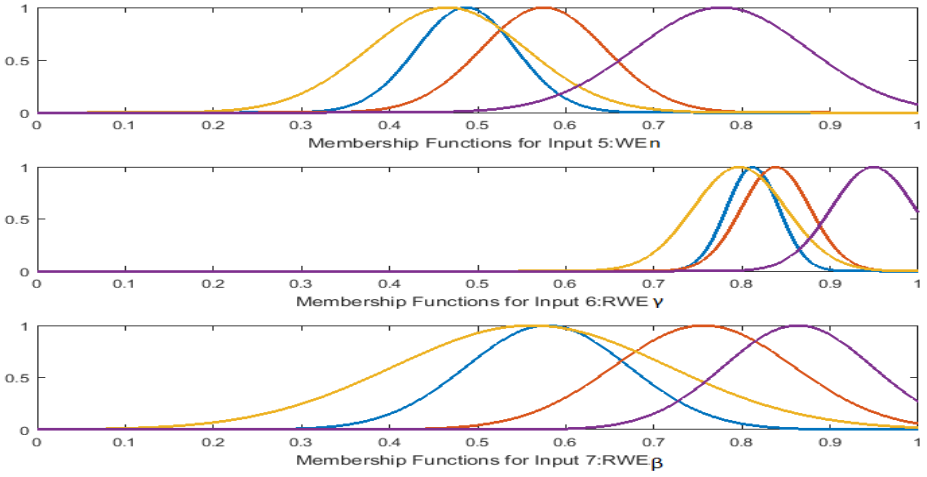

FIGURE 7.14: Initial Membership functions of ANFIS training based on Fuzzy C Means clustering of the inputs WEn, RWE_{γ} and,RWE_{β} before training

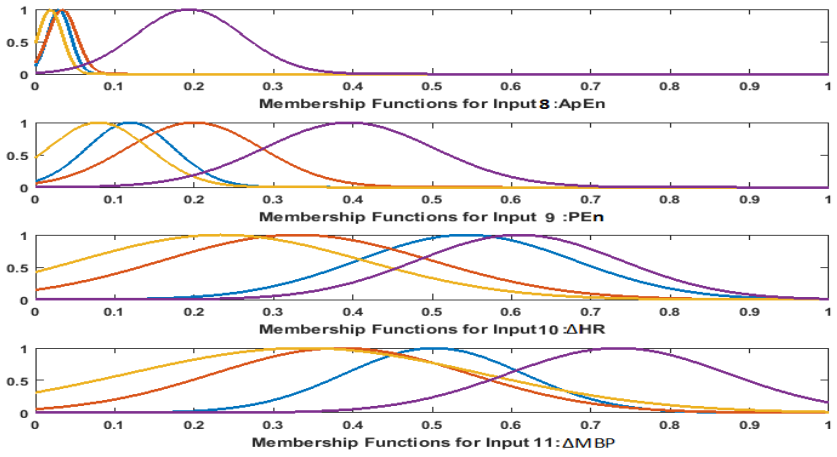

FIGURE 7.15: Initial Membership functions of ANFIS training based on Fuzzy C Means clustering of ApEn, PEn ΔHR and,ΔMBP before training

learning algorithm is used to adapt the parameters of ANFIS model and to get fuzziness functions and rule functions. The initial step size selected for training and validation is 0.1 which is provided to control the learning rate of the network model. The maximum number of training and validation epochs selected is 700. After training, the parameters of the membership functions are adapted to deliver better matching between input data and output data. As a result, the shape of the initial membership functions of all the inputs is changed and are shown in Figure 7.16-7.18

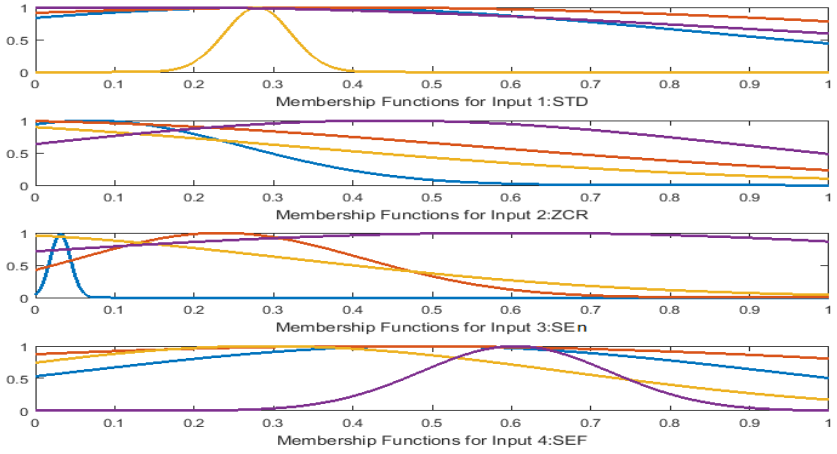

FIGURE 7.16: Membership functions of final ANFIS model based on Fuzzy C Means clustering of inputs STD, ZCR, SEF and SEn after training

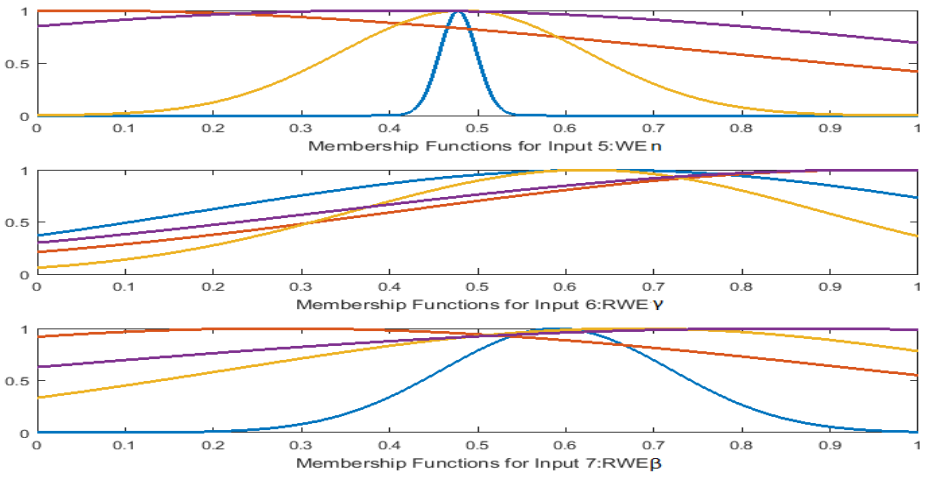

FIGURE 7.17: Membership functions of final ANFIS model based on Fuzzy C Means clustering of inputs WEn, RWE_{γ} and RWE_{β} after training

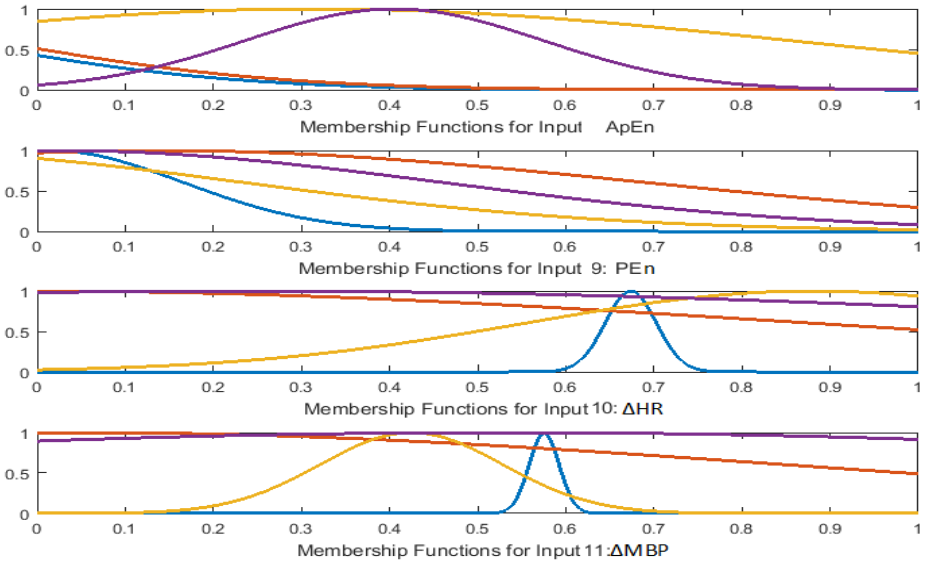

FIGURE 7.18: Membership functions of final ANFIS model based on Fuzzy C Means clustering of inputs ApEn, PEn ΔHR and,ΔMBP after training

The prediction capability of the developed ANFIS model based on Fuzzy C Means clustering in the training dataset, testing data set and combined data set are represented in Figure 7.19, 7.20, 7.21 respectively.

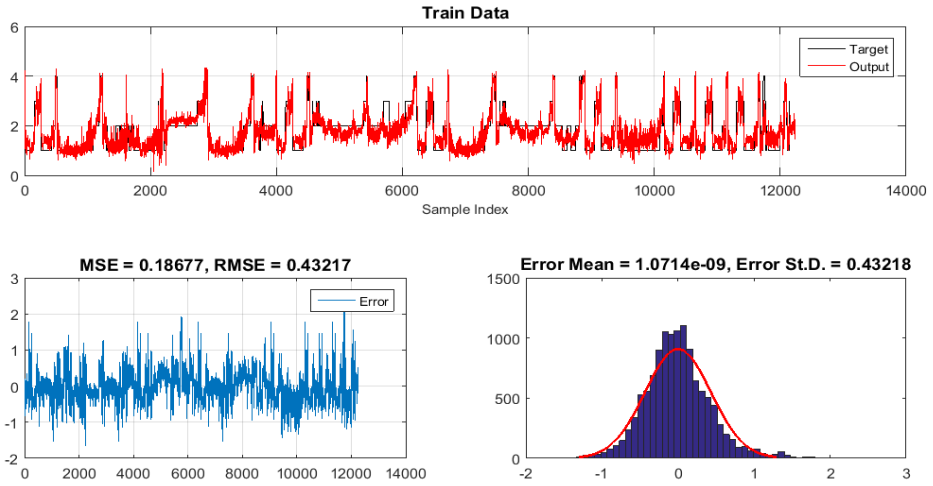

FIGURE 7.19: The performance of Fuzzy C Means clustering based ANFIS model in the Training data set

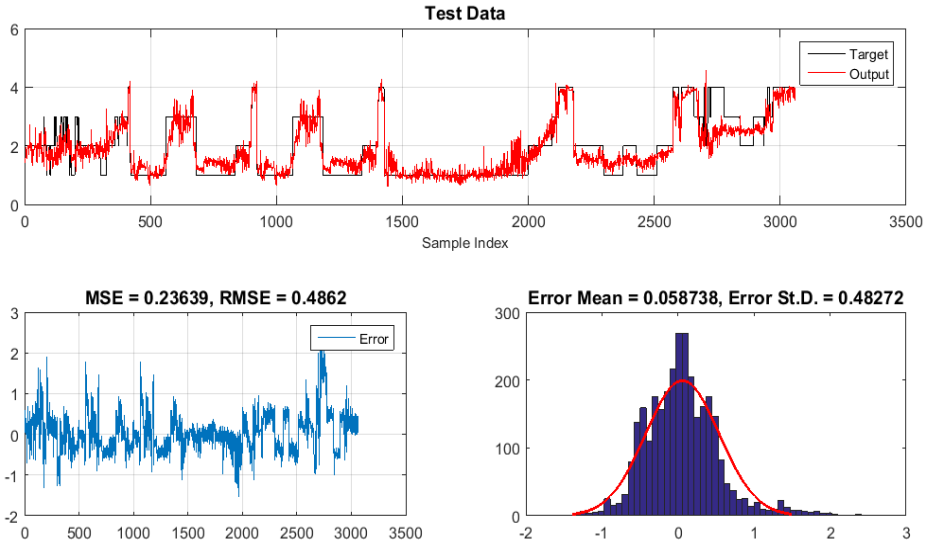

FIGURE 7.20: The performance of Fuzzy C Means clustering based ANFIS model in the Testing data set

The comparison between target output and generated output are shown in the figures and it is clear that the generated output follows the same track of target output. The error between the target output and generated output and the error distribution are also shown in the figures. The RMSE of training data sets, testing datasets and combined data sets are 0.43217, 0.4862 and 0.4435 respectively.

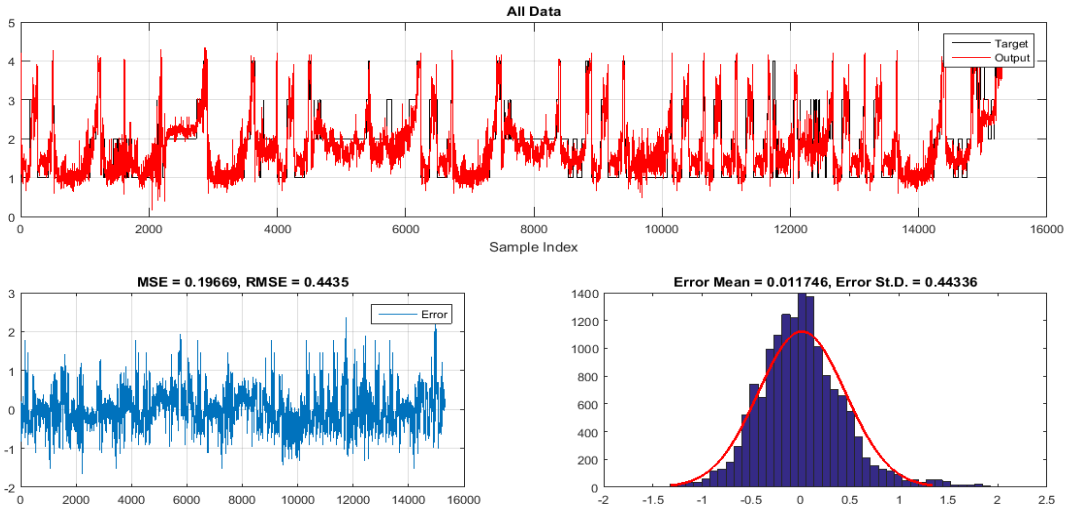

FIGURE 7.21: The performance of Fuzzy C Means clustering based ANFIS model in the combined data set

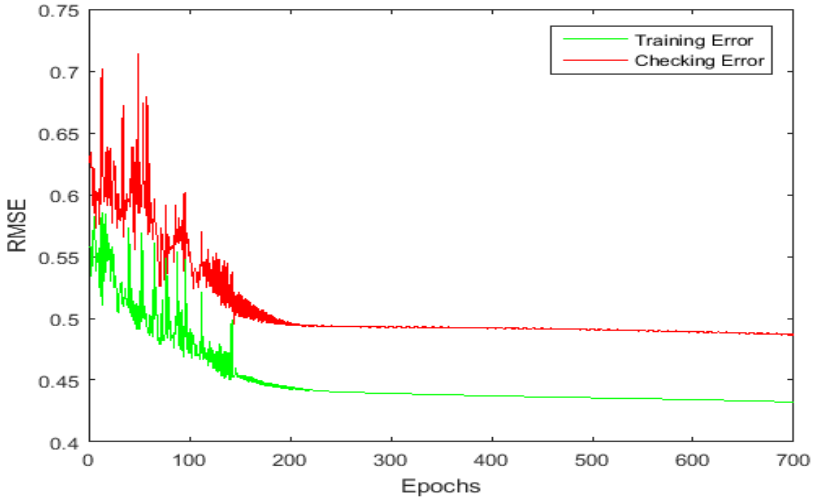

FIGURE 7.22: RMSE for training and validation of ANFIS model with Fuzzy C Means clustering

Figure 7.22 depicts RMSE curve during training and validation (testing) of data sets. It can be observed that the model is found to converge in < 700 epochs in both the training and testing datasets and the figure also indicate that no overfitting during training and testing process as both follows approximately the same trends.

The comparison summary of both the ANFIS models is given in Table 7.1. The subtractive clustering method provides less RMSE for training, testing and

combined data set. Therefore subtractive clustering based ANFIS model is used for DoA index generation.

Table 7.1: Comparison of ANFIS models

ANFIS Model based on	Initial Step Size	Training Iterations	RMSE of Training Dataset	RMSE of Testing Dataset	RMSE of Combined Dataset
Subtractive Clustering	0.01	500	0.40225	0.47554	0.41793
Fuzzy C Means Clustering	0.1	700	0.43217	0.4862	0.4435

7.2.3 Multiparameter DoA Index

Multiparameter DoA Index for the current study is developed using subtractive clustering based ANFIS model. Figure 7.23 represents the DoA index generated for the patient-24 and its comparison with BIS index. Here all the anaesthetic phases and their transitions are well defined and the index values of awake phase are high compared to all other phases. When anaesthetic depth increases the generated DoA index value gets reduced. This shows that the deep anaesthetic state (induction phase) is having the lowest values. The effect of the inhalation agent sevoflurane is also evident in the Figure 7.23 i.e. at time 12:45 and 12:51:43 administration of sevoflurane is increased to increase the DoA which is reflected as a decrease in the index values. When sevoflurane is closed its action is well reflected in the generated index as increased DoA index values. Another important indication that can be observed from the figure that during the maintenance phase HR increases drastically from the time point 12:53:08 PM. This is indicated by an increase in the value of the generated DoA index, but these variations are not seen on the BIS. Here anaesthesiologist administered the analgesic drug Fentanyl-100μg to the patient at 12:57:00 which resulted in reduction of the extracted hemodynamic parameters. This is also clearly visible in the generated DoA index. The effect of hypnotic drugs and the analgesic drugs makes variations on anaesthetic depth and which is visible in the generated DoA index.

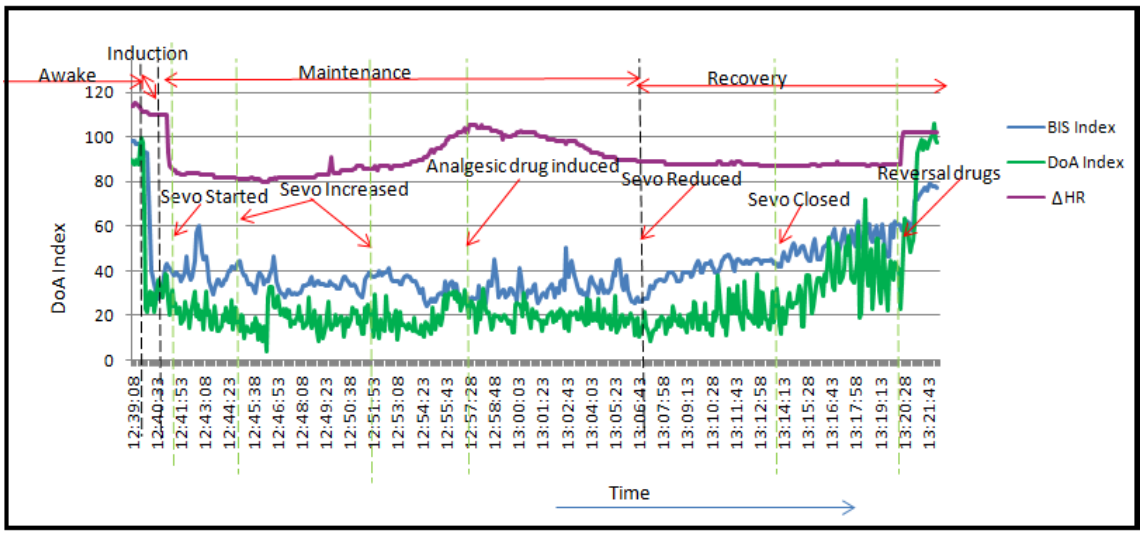

FIGURE 7.23: Comparison of BIS and the generated DoA index

The time delay between the BIS and generated DoA index of patient-24 is shown Figure 7.24. The BIS index shows a delay of 15 sec with DoA index. This indicates that the generated Multiparameter DoA index is much faster than BIS index which helps the anaesthesiologist in quicker decision making.

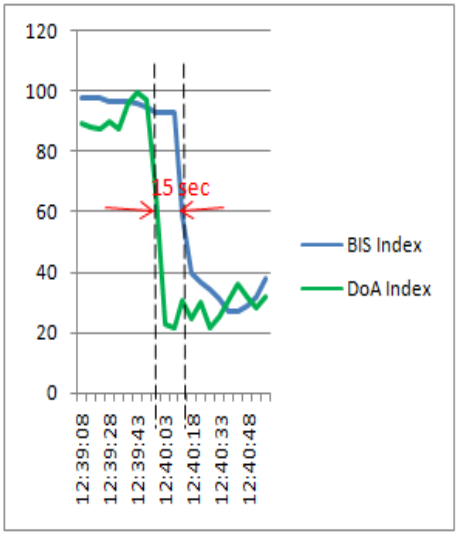

FIGURE 7.24: Time delay between BIS and the generated DoA index

7.3 Summary

The present chapter provides the estimation of Depth of Anaesthesia by combining EEG extracted features and hemodynamic features through Adaptive Neuro-Fuzzy Inference System. EEG extracted features provide the information available on electroencephalogram signals during anaesthesia and which helps to extract the hypnotic changes due to the anaesthetic drugs. The extracted hemodynamic parameters provide information about the changes in the autonomic nervous system due to the administration of anaesthetic drugs during surgery. In the implementation process of ANFIS model, two algorithms subtractive clustering algorithm and Fuzzy C Means clustering algorithm are used to generate fuzzy functions and rules. Hybrid learning algorithm is used to learn and adjust the ANFIS parameters. RMSE is calculated to check the performance of the two ANFIS models. ANFIS model based on subtractive clustering algorithm showed lowest RMSE for the training, testing and combined data set. Therefore, the final Multiparameter DoA index is generated by implementing an ANFIS based subtractive clustering algorithm which uses both the selected EEG and hemodynamic features as inputs.

Chapter 8

Conclusions and Future Options

Estimation of patients DoA is helpful to tailor the dose of anaesthetic drugs administered to a patient during surgery and it is not only for keeping the patient under adequate anaesthesia but also for preventing the patient from overdosing of anaesthetic drugs. Anaesthetic drugs cause effects on Central Nervous System (CNS) and autonomic nervous system. Therefore, the analysis of EEG signals helps to quantify the degree to which the Central Nervous System is depressed by anaesthetic drugs whereas the hemodynamic parameters are the indicators of autonomic nervous system. Main focus of the current study was reliable estimation of DoA by integrating neurophysiological signal and hemodynamic parameters. Understanding of the anaesthetic drug effects and patient's response to the drugs are essential for the quantification of DoA from the information available on neurophysiological signal and hemodynamic signals. The adopted algorithms and modelling techniques in the study helped to characterize these effects in an effective manner.

8.1 Summary of Major Contributions

The significant achievements of the study were presented in Chapters 3 to 7 and the detailed contributions are summarized below:

The data used in the study was obtained from 25 female patients who underwent breast cancer surgery at RCC, Trivandrum. The study protocol was approved by the institutional review board and the medical ethical committee of RCC. A written consent was obtained from all the patients who had participated in the study. The collected dataset includes waveform data such as EEG signal and numerical data such as Heart Rate (HR), Systolic Blood Pressure (SBP) and Diastolic Blood Pressure (DBP). These signals were collected from the patient throughout the surgical procedure which includes all the anaesthetic phases awake, induction, maintenance and recovery for the continuous estimation. The sampling frequency of the EEG signals collected using BIS sensor was 128Hz and the sampling frequency of HR and BP collected from standard monitoring devices was 0.2 Hz.

To improve the accuracy of DoA estimation current study adopted preprocessing steps including segmentation and filtering methods. Both uniform segmentation and non-uniform segmentation was tried on EEG signals for the effective filtration of the signals. Uniform segmentation was implemented on collected EEG signals by splitting the signals into equal time interval of 5 sec duration. Non-uniform segmentation of EEG signals was done by extracting the feature kurtosis and then splitting the signal at the time point at which change occurs. As a result, the EEG signals were segmented when a change from low-frequency high amplitude to high-frequency low amplitude and vice versa occurs. In order to remove the artifacts from the EEG signals, a wavelet-based threshold filtering method was adopted. The threshold level was calculated using SURE Shrink thresholding and Universal thresholding method by applying soft and hard thresholding. The performance of the filter with different thresholding techniques were compared by calculating the measures SNR, MSE and correlation coefficient. The results of these measures revealed that Wavelet denoising using SURE Shrink Threshold and soft Thresholding technique showed high Signal to Noise Ratio, high correlation coefficient values and low MSE compared to other thresholding techniques.

Different feature extraction methods were adopted to extract features from the collected signals. The time domain features extracted from EEG signals includes Standard Deviation, Entropy, Energy, Mean Absolute Deviation, Zero Crossing Rate and Inter-Quartile Range. The feature values of Standard deviation, Energy, Mean Absolute Deviation and Inter-Quartile Range were high for induction phase (deep

anaesthetic phase) EEG signals and low for awake EEG signals. Moderate and recovery phase showed intermediate values. The feature values of recovery phase (light anaesthesia) obtained were higher than the awake phase and lesser than moderate phase. This proved that these feature values increases with increase in DoA. On the other hand, ZCR and Entropy feature values decrease with increase in DoA. The frequency domain features extracted from EEG signals are SEF and SEn and their feature values decrease with increase in DoA. The extracted time-frequency domain features were Wavelet Entropy (WEn) and Relative Wave Energy (RWE) of each EEG frequency band. All these extracted features showed variations in accordance with DoA. Nonlinear features such as ApEn and PEn were extracted from the collected EEG signals to study the complexity and nonlinear behaviour of EEG signals and they showed an inverse relation with DoA. All these features were analysed during the whole duration of surgery involving 25 patients. When comparing with BIS index of each patient these features showed an earlier response than BIS. That means BIS showed a delay of 15 sec with the features Standard Deviation, Energy and SEF, 20 sec delay with Zero Crossing Rate and Wavelet Entropy whereas all the other features showed a delay of 10 sec. In order to study the hemodynamic variability due to the anaesthetic drugs features such as ΔHR, ΔMBP and pulse pressure were extracted from the HR and BP data. Normally, these feature values decreased with increase in DoA. The special cases in which HR or BP increased due to the inadequate dose of analgesic drugs and its effect variations were clearly evident in the extracted hemodynamic features.

Dimensionality of the extracted feature vector was reduced by selecting optimum features by applying different feature ranking methods such as 'T-Test', 'Entropy', 'Bhattacharyya', 'ROC'and 'Wilcoxon'. Outputs of different classifiers such as kNN, SVM, MLP and NBC in terms of accuracy was used to find the discriminating ability of the features as awake, light anaesthesia, moderate anaesthesia and deep anaesthesia. Based on this discrimination capability, the feature combination with highest classification accuracy was selected for the final DoA estimation model. The feature combination which provided highest classification accuracy from the time domain representation was Standard Deviation and Zero Crossing Rate. Both the frequency domain features showed highest classification accuracy and therefore both the features were selected for final model development. Then the

time-frequency domain features selected based on their classification accuracy and discrimination ability are WEn, RWE_{γ} and RWE_{β}. The combination of both the non-linear features ApEn and PEn were selected because their combination showed comparatively higher classification accuracy than if taken alone. Kruskal Wallis test was used to show the discriminating ability of hemodynamic features and the best features selected from the extracted hemodynamic parameters are ΔHR and ΔMBP.

Final Adaptive Neuro-Fuzzy Inference System (ANFIS) model to estimate DoA index was implemented by using selected EEG features and hemodynamic features as inputs. Two algorithms such as Subtractive clustering and Fuzzy C Means clustering were tried to generate fuzzy functions and fuzzy rules. The learning algorithm opted to learn and adjust the ANFIS parameter was hybrid learning algorithm. The performance of the two clustering algorithms and their corresponding ANFIS models were tested by calculating the measure RMSE. ANFIS model based on subtractive clustering algorithm showed lowest RMSE for the training dataset, testing dataset and the combination of two datasets. Finally, multiparameter DoA index was estimated by implementing an Adaptive Neuro-Fuzzy Inference System based on subtractive clustering algorithm which integrates both the selected EEG and hemodynamic features. The estimated index showed the effect of anaesthetic drugs as decreased values when the dose increased and it showed increased values if depth decreases. That means the estimated multiparameter DoA index values decreased with increase in DoA. In addition, the generated index showed 15 sec faster response than BIS index.

8.2 Advantages of the study

Advantages of the present multiparameter DoA estimation method is that

1. The derived features and parameters exposed direct/inverse correlation with DoA

2. The discrimination of different anaesthetic states such as awake, light anaesthesia, moderate anaesthesia and deep anaesthesia was clearly visible in the extracted features

3. Continuous assessment of DoA was performed during the whole surgery
4. A novel DoA index was estimated that clearly respond to the changes due to various anaesthetic drugs
5. The estimated multiparameter DoA Index showed an earlier time response than Bispectral Index (BIS) during the transitions of anaesthetic states
6. The estimated multiparameter DoA index would improve the patient safety by delivering adequate dose of anaesthetic drugs to the patient if they used in real-time
7. It also helps to assist the anaesthesiologist in faster decision making and management during anaesthesia

8.3 Limitations and Future options of the research

Although the study has reached the objectives that specified in the study, there are some limitations which inhibit the efficiency of DoA estimation. The current research did not analyze very deep anaesthetic state signals (BIS value range 0-20) as it may cause hemodynamic instability to the patient and also against the ethical considerations of the study. It would be useful in DoA index calculation of surgeries which last for long time duration.

In this study, single-channel EEG signals were considered for the estimation of DoA. Multi-channel EEG signals can be considered in future which would help in the localisation of the brain activity in the specified regions in which anaesthetic drugs affect.

This study is limited to breast cancer patients only not including pediatric, geriatric, trauma, neurosurgical, cardiothoracic, renal and pregnant patients. In future studies above mentioned cases may be considered for the effective analysis of deeper planes of anaesthesia.

As future option more parameters like $etCO_2$, end-tidal inhalation anaesthetic agent parameters can be considered for more effective analysis.

Appendix A

Institutional Review Board Approval letter

SANCTION FOR CARRYING OUT A RESEARCH STUDY / CLINICAL TRIAL

SANCTION No. IRB / 05 - 2014 /02 May 06, 2014

Institutional Review Board - Scientific Review Committee at its meeting on May 06, 2014 approved the below mentioned project after hearing the presentation by the investigator and adequately discussing the topic, taking into consideration its scientific relevance, methodology, relevance to the institute's policies and study feasibility. Special conditions and comments that the investigator has to comply with (if any) are listed below. All sanctioned studies and projects must submit a first progress report 12 months after the date of sanction.

Name of Project / Study: Monitoring Depth of Anaesthesia

Investigators with affiliations : Dr. Rachel Cherian Koshy, Benzy VK[1],Jasmin EA[1]. Regional Cancer Centre ,TVM, [1] Govt. Engineering College,Thrissur .

Special Conditions & Comments : Ethical Committee clearance must be obtained before study can begin.

First progress report due on : May 2015

The quorum of IRB members present/absent at the meeting and who approved the study/project are:

NAME	ATTENDANCE	APPROVAL SIGNATURE
Dr. PAUL SEBASTIAN	PRESENT / ABSENT	
Dr. P.G. JAYAPRAKASH	PRESENT / ABSENT	
Dr. K. RAMACHANDRAN	PRESENT / ABSENT	
Dr. P. KUSUMAKUMARY	PRESENT / ABSENT	
Dr. K. RAMADAS	PRESENT / ABSENT	
Dr. V. M. PRADEEP	PRESENT / ABSENT	—
Dr. JAYASREE K	PRESENT / ABSENT	
Dr. N. GEETHA	PRESENT / ABSENT	
Dr. ALEYAMMA MATHEW	PRESENT / ABSENT	—
Dr. KANNAN S	PRESENT / ABSENT	—
Dr. FRANCIS V JAMES	PRESENT / ABSENT	

Scientific Review Committee of IRB
Regional Cancer Centre
Trivandrum

Appendix B

Ethical Committee Approval letter

HUMAN ETHICS COMMITTEE

REGIONAL CANCER CENTRE, THIRUVANANTHAPURAM

Ethics Committee Office, Ist Floor, Regional Cancer Centre, P.O. Box No.2417, Medical College Campus, Thiruvananthapuram - 695011
Tel: Office: 0471 252472/ Member Secretary: 9447072333, Chairman: 9388441667. email: ethicsrcc@gmail.com

SANCTION FOR CARRYING OUT A RESEARCH STUDY / CLINICAL TRIAL

HEC No. 20/2014

Place: Conference Hall, RCC
Date : 5th Sep 2014
Time : 2.00 Pm

To

Dr. Rachel Cheriyan Koshy
Professor & Head of Anesthesiology
Regional Cancer Centre, Trivandrum

Project Title: Monitoring depth of Anesthesia.

Dear Dr. Rachel,

The Institute Review Board- Ethics Committee, Regional Cancer Centre reviewed and discussed your request to conduct the above study.

The following documents were reviewed:

1. Protocol
2. Patient Information Sheet and Informed Consent Form in English & Malayalam.

At the Ethics Committee meeting held on 5th Sep 2014 the above mentioned documents were examined, discussed and approved subject to modifications as suggested by the Ethics Committee.

The quorum of members present/absent at the meeting and who approved the project are

NAME	ATTENDANCE	SIGNATURE
Dr M.NARENDRANATHAN, MD, DM,MPH SENOR CONSULTANT IN GASTROENTEROLOGY CHAIRMAN, HUMAN ETHICS COMMITTEE REGIONAL CANCER CENTRE, TRIVANDRUM	PRESENT/ ~~ABSENT~~	
Dr. M. RADHAKRISHNA PILLAI, FRCPath,PhD,FASc DIRECTOR RAJIV GANDHI CENTRE FOR BIOTECHNOLOGY THIRUVANANTHAPURAM	~~PRESENT~~/ ABSENT	ABSENT
Dr. C.C. KARTHA, MD PROFESSOR OF EMINENCE DEPT. OF MOLECULAR MEDICINE RAJIV GANDHI CENTRE FOR BIOTECHNOLOGY THIRUVANANTHAPURAM	~~PRESENT/~~ ABSENT	ABSENT
Dr K.G. RETNAVALLY, MD PROFESSOR & HEAD OF PHARMACOLOGY (Retd), MEDICAL COLLEGE, THIRUVANANTHAPURAM	PRESENT/ ~~ABSENT~~	
Dr SANJEEV.V.THOMAS, MD,DM PRFESSOR OF NEUROLOGY SCTIMST, THIRUVANANTHAPURAM	~~PRESENT~~/ ABSENT	ABSENT
Dr. M. IQBAL AHAMED, MS PROFESSOR & HEAD, DIVISION OF SURGICAL ONCOLOGY REGIONAL CANCER CENTRE, THIRUVANANTHAPURAM	PRESENT/ ~~ABSENT~~	
Fr. SHOJI VECHOORKAROTTU SPIRITUAL DIRECTOR St.ALOYSIUS MINOR SEMINARY CHESHIRE HOME LANE, KURAVANKONAM, KOWDIAR.P.O,THIRUVANANTHAPURAM	PRESENT/ ~~ABSENT~~	
Adv. P. KRISHNANKUTTY NAIR, BA, LLB 'ARATHY', TC 17/28 JERA 21, JAGATHY, THIRUVANANTHAPURAM	PRESENT/ ~~ABSENT~~	
Mrs .DARLY FRANCIS BETHELEHEM, D7D, MOOLAYIL LANE SASTHAMANGALAM, THRIUVANNATHAPURAM	PRESENT/ ~~ABSENT~~	
Mrs. THANKAM GOPALAKRISHNAN A51, 'LEKSHMI', TC 9/2638 (1) ELAMKOM GARDENS, VELLAYAMBALAM	PRESENT/ ~~ABSENT~~	

Dr. N. GEETHA, MD, DNB, DM
PROFESSOR OF MEDICAL ONCOLOGY
REGIONAL CANCER CENTRE
THIRUVANANTHAPURAM

PRESENT/ ~~ABSENT~~ ABSENT

Dr.R. REJNISH KUMAR, MD
ADDITIONAL PROFESSOR OF
RADIATION ONCOLOGY
REGIONAL CANCER CENTRE,
THIRUVANANTHAPURAM

PRESENT/ ~~ABSENT~~

It is hereby confirmed that neither you nor any of the study team members have participated in the voting/decision making procedures of the committee.

Special Conditions:

1. To include Name & Designation of the consenting Investigator.

General Conditions:

1. Any change in protocol/study procedure/ informed consent forms / Investigator must be immediately intimated to the Ethics Committee.
2. First progress / status report to be submitted by 1 year.
3. The Ethics committee approval is effective for a period of one year from the date of issue.
4. Application for renewal should be submitted 2 months prior to expiry along with the progress / status report.
5. Submit the corrected documents to EC before starting the study.

Dr. M.Narendranathan
Chairman

REGIONAL CANCER CENTRE
THIRUVANANTHAPURAM
KERALA STATE, INDIA
HUMAN ETHICS
COMMITTEE

Appendix C

Consent Form

SUBJECT INFORMATION AND INFORMRD CONSENT

"MONITORING DEPTH OF ANAESTHESIA"

We are requesting you to take part in our study on "Monitoring Depth of Anaesthesia" and you are free to take part in the study after understanding the procedure of the study. We request you to take part in this study because you have all the features mentioned in our inclusion criteria of our study protocol. We are requesting you to allow us to monitor your Heart rate, BP, SPO2 (Oxygen saturation), etCO2(Endtidal Carbondioxide), MAC(Minimum Alveolar Concentration), Electroencephalogram(EEG), Bispectral Index(BIS) and Electromyogram(EMG) before , during and after surgery. If you decide to take part, we would monitor your above mentioned parameters after giving Anaesthetic drugs.

In the standard care of monitoring before ,during and after anasthesia Heart rate, BP, SPO2(Oxygen saturation),etCO2 and MAC(Minimum Alveolar Concentration) would be monitored and would ensure adequate level anaethesia .As part of this study further additional parameters such as Electroencephalogram(EEG), Bispectral Index(BIS) and Electromyogram(EMG) are monitored before , during and after surgery. It is not madatory to measure these additional parameters during the standard care of monitoring. The benefit of being part of the study is that we would know the Depth of Anaethesia, but we do not guarantee that you will benefit from taking part in this study. You will not be withheld from standard care of monitoring if you are not willing to take part in the study. You will not be injured or will not have any side effects by monitoring these vital parameters.

The additional expenses involved for the purchase of electrodes for monitoring Electroencephalogram(EEG), Bispectral Index(BIS) and Electromyogram(EMG) before,during and after surgery would be borne by Benzy VK, Research Scholar, Govt. Engineering College, Thrissur.

Everything we learn from you in the study will be confidential. If we publish the result of the study in a scientific magazine or book, we will not identify you in anyway. The monitoring equipment used for this study will be provided from the Department of Anaesthesia, Regional Cancer centre, Trivandrum.

not affect your future medical care at Regional Cancer Centre, Thiruvananthapuram.

This study is conducted as research collaboration between Regional cancer centre and Govt. Engineering College, Thrissur. The data collected would be analysed at Department of Electrical Engineering, Govt. Engineering College, Thrissur by Benzy VK, Research Scholar, Govt. Engineering College, Thrissur under the guidance of Dr.Rachel Cherian Koshy, Professor and Head of the Department, Department of Anaesthesiology, Regional Cancer Centre, Thiruvananthapuram and Dr. Jasmin EA, Associate Professor, Department of Electrical Engineering, Govt. Engineering College, Thrissur.

If you have any queries regarding this, feel free to ask us.Benzy VK,Research scholar ,Govt. Engineering College, Thrissur can be reached at 09447586659 or email-benzyvk@yahoo.com. If she is not available, Dr.Rachel Cherian Koshy, Professor and Head of the Department, Department of Anaesthesiology, Regional Cancer Centre, Thiruvananthapuram can be reached at 09495927019 and/or Dr.Jasmin EA, Associate Professor, Department of Electrical Engineering, Govt. Engineering College, Thrissur can be reached at 09495465409.The Regional Cancer Centre ethics committee that reviews research on human subjects(Ethics)will answer any questions about your rights as a research subject(Dr.M. Narendrenathan-chairman, Dr.Rejnish Kumar, Convenor at 0471 2522472)

We will give you a signed copy of this form to keep.

INFORMED CONSENT

I Mr/Smt .....Saraswathy Mohan..... (Name of the patient), CR NO.....14F516..... have been explained the details of the above study by my doctor. I understand the purpose ,the potential benefits of taking part in the study. By signing this form I give my free and informed consent to participate in this study .I understand that I can withdraw from the study at any time before surgery.

.....

Signature of the Patient (Name) Date Saraswathy (Saraswathy) 31/1/15

.....

Signature of the Witness (Name) Date

Jayaram P 31/1/15

Signature of the Investigator (Name) Date (Benzy V.K)

Bibliography

Abraham, Ajith. 2005. Adaptation of fuzzy inference system using neural learning. *Fuzzy systems engineering*, 914–914.

Acharya, U Rajendra, Molinari, Filippo, Sree, S Vinitha, Chattopadhyay, Subhagata, Ng, Kwan-Hoong, & Suri, Jasjit S. 2012. Automated diagnosis of epileptic EEG using entropies. *Biomedical Signal Processing and Control*, **7**(4), 401–408.

Agarwal, Rajeev, Gotman, Jean, Flanagan, Danny, & Rosenblatt, Bernard. 1998. Automatic EEG analysis during long-term monitoring in the ICU. *Electroencephalography and clinical Neurophysiology*, **107**(1), 44–58.

Agarwal, Sanjana, Jain, Nirav, & Dholay, Surekha. 2015. Adaptive Testing and Performance Analysis Using Naive Bayes Classifier. *Procedia Computer Science*, **45**, 70–75.

Al-Kadi, Mahmoud I, Reaz, Mamun Bin Ibne, & Ali, Mohd Alauddin Mohd. 2013. Evolution of electroencephalogram signal analysis techniques during anesthesia. *Sensors*, **13**(5), 6605–6635.

Antoniadis, Anestis, Bigot, Jeremie, & Sapatinas, Theofanis. 2001. Wavelet estimators in nonparametric regression: a comparative simulation study. *Journal of Statistical Software*, **6**, pp–1.

Astolfi, Laura, Cincotti, Febo, Mattia, Donatella, Babiloni, Fabio, Marciani, Maria Grazia, Fallani, Fabrizio De Vico, Mattiocco, Marco, Miwakeichi, Fumikazu, Yamaguchi, Yoko, Martinez, Pablo, *et al.* . 2006. Removal of ocular artifacts for high resolution EEG studies: a simulation study. *Pages 976–979 of: Engineering in Medicine and Biology Society, 2006. EMBS'06. 28th Annual International Conference of the IEEE*. IEEE.

Atkinson, Richard Stuart, & GB Lee, JL. 1984. A synopsis of anaesthesia.

Azami, Hamed, Mohammadi, Karim, & Bozorgtabar, Behzad. 2012a. An improved signal segmentation using moving average and Savitzky-Golay filter. *Journal of Signal and Information Processing*, **3**(01), 39.

Azami, Hamed, Khosravi, Alireza, Malekzadeh, Milad, & Sanei, Saeid. 2012b. A new adaptive signal segmentation approach based on Hiaguchi's fractal dimension. *Pages 152–159 of: International Conference on Intelligent Computing*. Springer.

Azami, Hamed, Hassanpour, Hamid, Escudero, Javier, & Sanei, Saeid. 2015. An intelligent approach for variable size segmentation of non-stationary signals. *Journal of advanced research*, **6**(5), 687–698.

Bachu, RG, Kopparthi, S, Adapa, B, & Barkana, BD. 2008. Separation of voiced and unvoiced using zero crossing rate and energy of the speech signal. *Pages 1–7 of: American Society for Engineering Education (ASEE) Zone Conference Proceedings*.

Baharav, A, Kotagal, S, Gibbons, V, Rubin, BK, Pratt, G, Karin, J, & Akselrod, S. 1995. Fluctuations in autonomic nervous activity during sleep displayed by power spectrum analysis of heart rate variability. *Neurology*, **45**(6), 1183–1187.

Bai, Yang, Liang, Zhenhu, Li, Xiaoli, Voss, Logan J, & Sleigh, Jamie W. 2015. Permutation Lempel–Ziv complexity measure of electroencephalogram in GABAergic anaesthetics. *Physiological measurement*, **36**(12), 2483.

Baig, Mirza Mansoor, GholamHosseini, Hamid, Kouzani, Abbas, & Harrison, Michael J. 2011. Anaesthesia monitoring using fuzzy logic. *Journal of clinical monitoring and computing*, **25**(5), 339.

Balick Weber, CC, Brillouet Banchereau, AC, Blanchet, AD, Blanchet, P, Safar, ME, *et al.* . 2011. General Anesthesia in Hypertensive Patients: Impact of Pulse Pressure but not Cardiac Diastolic Dysfunction on Intraoperative Hemodynamic Instability. *Journal of anaesthesia and clinical research*, **2**, 114.

Bandt, Christoph, & Pompe, Bernd. 2002. Permutation entropy: a natural complexity measure for time series. *Physical review letters*, **88**(17), 174102.

Bauerle, K, Greim, C-A, Schroth, M, Geisselbrecht, M, Köbler, A, & Roewer, N. 2004. Prediction of depth of sedation and anaesthesia by the NarcotrendTM EEG monitor. *British journal of anaesthesia*, **92**(6), 841–845.

Bedeeuzzaman, M, Fathima, Thasneem, Khan, Yusuf U, & Farooq, Omar. 2014. Seizure prediction using statistical dispersion measures of intracranial EEG. *Biomedical Signal Processing and Control*, **10**, 338–341.

Bennani, Younes, & Benabdeslem, Khalid. 2006. Dendogram-based SVM for multi-class classification. *CIT. Journal of computing and information technology*, **14**(4), 283–289.

Benzy, VK, & Jasmin, EA. 2015. A combined wavelet and neural network based model for classifying depth of anaesthesia. *Procedia Computer Science*, **46**, 1610–1617.

Bezdek, James C. 2013. *Pattern recognition with fuzzy objective function algorithms*. Springer Science & Business Media.

Blais, Andrew, & Mertz, David. 2001. An Introduction to Neural Networks–Pattern Learning with Back Propagation Algorithm. *Gnosis Software, Inc.*

Bowdle, T Andrew. 2006. Depth of anesthesia monitoring. *Anesthesiology Clinics of North America*, **24**(4), 793–822.

Bruhn, J, Myles, PS, Sneyd, R, & Struys, MMRF. 2006. Depth of anaesthesia monitoring: what's available, what's validated and what's next? *BJA: British Journal of Anaesthesia*, **97**(1), 85–94.

Bruhn, Joergen, Bouillon, Thomas W, & Shafer, Steven L. 2000a. Electromyographic activity falsely elevates the bispectral index. *Anesthesiology: The Journal of the American Society of Anesthesiologists*, **92**(5), 1485–1485.

Bruhn, Jörgen, Bouillon, Thomas W, & Shafer, Steven L. 2000b. Bispectral index (BIS) and burst suppression: revealing a part of the BIS algorithm. *Journal of clinical monitoring and computing*, **16**(8), 593–596.

Celikyilmaz, Asli, & Turksen, I Burhan. 2009. Modeling uncertainty with fuzzy logic. *Studies in fuzziness and soft computing*, **240**, 149–215.

Cha, Kab-Mun, Choi, Byung-Moon, Noh, Gyu-Jeong, & Shin, Hyun-Chool. 2017. Novel Methods for Measuring Depth of Anesthesia by Quantifying Dominant Information Flow in Multichannel EEGs. *Computational intelligence and neuroscience*, **2017**.

Chan, Yvonne, & Walmsley, Roy P. 1997. Learning and understanding the Kruskal-Wallis one-way analysis-of-variance-by-ranks test for differences among three or more independent groups. *Physical therapy*, **77**(12), 1755–1761.

Chang, Jing Jing, Syafiie, S, Ahmad, Raja Kamil Raja, & Lim, Thiam Aun. 2014. ANFIS Based Model for Bispectral Index Prediction. *Pages 133–142 of: Recent Advances on Soft Computing and Data Mining*. Springer.

Charan, Jaykaran, & Biswas, Tamoghna. 2013. How to calculate sample size for different study designs in medical research? *Indian journal of psychological medicine*, **35**(2), 121.

Cheng, HD, Shi, XJ, Min, Rui, Hu, LM, Cai, XP, & Du, HN. 2006. Approaches for automated detection and classification of masses in mammograms. *Pattern recognition*, **39**(4), 646–668.

Chiu, Stephen L. 1994. Fuzzy model identification based on cluster estimation. *Journal of Intelligent & fuzzy systems*, **2**(3), 267–278.

Choi, Euisun, & Lee, Chulhee. 2003. Feature extraction based on the Bhattacharyya distance. *Pattern Recognition*, **36**(8), 1703–1709.

Chun-Lin, Liu. 2010. A tutorial of the wavelet transform. *NTUEE, Taiwan*.

contributors, Wikipedia. 2017a. *Mann–Whitney U test — Wikipedia, The Free Encyclopedia*. [Online; accessed 30-December-2017].

contributors, Wikipedia. 2017b. *Naive Bayes classifier — Wikipedia, The Free Encyclopedia*. [Online; accessed 31-December-2017].

Croft, Rodney J, & Barry, Robert J. 2000. Removal of ocular artifact from the EEG: a review. *Neurophysiologie Clinique/Clinical Neurophysiology*, **30**(1), 5–19.

Daniel, Wayne W. 1990. Kruskal-Wallis One-Way Analysis of Variance by Ranks. *Applied Nonparametric Statistics,*, 226–230.

Daniel, Wayne W, & Cross, Chad Lee. 1995. Biostatistics: a foundation for analysis in the health sciences.

De Deyne, C, Struys, Michel, Decruyenaere, Johan, Creupelandt, J, Hoste, E, & Colardyn, Francis. 1998. Use of continuous bispectral EEG monitoring to assess depth of sedation in ICU patients. *Intensive Care Medicine*, **24**(12), 1294–1298.

Deller Jr, John R, Proakis, John G, & Hansen, John H. 1993. *Discrete time processing of speech signals*. Prentice Hall PTR.

DeSmet, Tom. 2000. *RugloopII© MO+Waves*.

Doi, M, Gajraj, RJ, Mantzaridis, H, & Kenny, GN. 1997. Relationship between calculated blood concentration of propofol and electrophysiological variables during emergence from anaesthesia: comparison of bispectral index, spectral edge frequency, median frequency and auditory evoked potential index. *British Journal of Anaesthesia*, **78**(2), 180–184.

Donoho, David L. 1995. De-noising by soft-thresholding. *IEEE transactions on information theory*, **41**(3), 613–627.

Donoho, David L, & Johnstone, Iain M. 1995. Adapting to unknown smoothness via wavelet shrinkage. *Journal of the american statistical association*, **90**(432), 1200–1224.

Donoho, David L, & Johnstone, Jain M. 1994. Ideal spatial adaptation by wavelet shrinkage. *biometrika*, **81**(3), 425–455.

Drover, David, & Ortega, HR Rick. 2006. Patient state index. *Best Practice & Research Clinical Anaesthesiology*, **20**(1), 121–128.

Duarte, Leonardo Teixeira Domingues, & Saraiva, Renato Ângelo. 2009. When the bispectral index (bis) can give false results. *Brazilian Journal of Anesthesiology*, **59**(1), 99–109.

Dunn, Joseph C. 1973. A fuzzy relative of the ISODATA process and its use in detecting compact well-separated clusters.

Dutta, Saibal, Chatterjee, Amitava, & Munshi, Sugata. 2010. Correlation technique and least square support vector machine combine for frequency domain based ECG beat classification. *Medical engineering & physics*, **32**(10), 1161–1169.

Efstathiou, J, Kariuki, S, Huatuco, L Huaccho, Sivadasan, S, & Calinescu, A. 2001. The relationship between information-theoretic and chaos-theoretic measures of the complexity of manufacturing systems. *Pages 421–426 of: ADVANCES IN MANUFACTURING TECHNOLOGY-CONFERENCE-*, vol. 15. TAYLOR & FRANCIS LTD.

Esmaeili, V, Assareh, Amin, Shamsollahi, Mohammad Bagher, Moradi, Mohammad Hassan, & Arefian, NM. 2008. Estimating the depth of anesthesia using fuzzy soft computation applied to EEG features. *Intelligent Data Analysis*, **12**(4), 393–407.

Evans, JM, & Davies, WL. 1984. Monitoring anaesthesia. *Clin Anesth*, **2**, 243–262.

Fan, Shou-Zen, Yeh, Jia-Rong, Chen, Bo-Cun, Shieh, Jiann-Shing, *et al.* . 2011. Comparison of EEG approximate entropy and complexity measures of depth of anaesthesia during inhalational general anaesthesia. *J. Med. Biol. Eng*, **31**, 359–366.

Fawcett, Tom. 2006. An introduction to ROC analysis. *Pattern recognition letters*, **27**(8), 861–874.

Fell, Jürgen, Röschke, Joachim, Mann, Klaus, & Schäffner, Cornelius. 1996. Discrimination of sleep stages: a comparison between spectral and nonlinear EEG measures. *Electroencephalography and Clinical Neurophysiology*, **98**(5), 401–410.

Ferenets, Rain. 2007. *EEG Patterns and Regularity Properties during Propofol Induced Anesthesia/Sedation*.

Ferenets, Rain, Lipping, Tarmo, Anier, Andres, Jäntti, Ville, Melto, Sari, & Hovilehto, Seppo. 2006. Comparison of entropy and complexity measures for the assessment of depth of sedation. *IEEE Transactions on Biomedical Engineering*, **53**(6), 1067–1077.

Ferenets, Rain, Vanluchene, Ann, Lipping, Tarmo, Heyse, Björn, & Struys, Michel MRF. 2007. Behavior of entropy/complexity measures of the electroencephalogram during propofol-induced sedationdose-dependent effects of remifentanil. *The Journal of the American Society of Anesthesiologists*, **106**(4), 696–706.

Geetha, G, & Geethalakshmi, SN. 2011. EEG De-noising using SURE thresholding based on Wavelet Transforms. *International Journal of Computer Applications*, **24**(6).

Ghaffari, A, Homaeinezhad, MR, Khazraee, M, & Daevaeiha, MM. 2010. Segmentation of holter ECG waves via analysis of a discrete wavelet-derived multiple skewness–kurtosis based metric. *Annals of biomedical engineering*, **38**(4), 1497–1510.

Ghoneim, MM. 2001. *Awareness during anesthesia, Awareness during Anesthesia. Edited by Ghoneim MM.*

Ghoneim, MM, & Block, Robert. 1997. Learning and memory during general anesthesia an update. *Anesthesiology: The Journal of the American Society of Anesthesiologists*, **87**(2), 387–410.

Ghoneim, MM, & Block, Robert I. 1992. Learning and consciousness during general anesthesia.

Ghoneim, Mohamed M, Block, Robert I, Haffarnan, Mary, & Mathews, Maya J. 2009. Awareness during anesthesia: risk factors, causes and sequelae: a review of reported cases in the literature. *Anesthesia & Analgesia*, **108**(2), 527–535.

Ghouri, Ahmed F, Monk, Terri G, & White, Paul F. 1993. Electroencephalogram spectral edge frequency, lower esophageal contractility, and autonomic responsiveness during general anesthesia. *Journal of Clinical Monitoring and Computing*, **9**(3), 176–185.

Gifani, P, Rabiee, HR, Hashemi, MR, & Ghanbari, M. 2005. Extraction of anesthesia depth using self similarity and fluctuation analysis on the wavelet coefficients of EEG. *Pages 7–12 of: Medical Applications of Signal Processing, 2005. The 3rd IEE International Seminar on (Ref. No. 2005-1119)*. IET.

Gugino, LD, Chabot, RJ, Prichep, LS, John, ER, Formanek, V, & Aglio, LS. 2001. Quantitative EEG changes associated with loss and return of consciousness in healthy adult volunteers anaesthetized with propofol or sevoflurane. *British Journal of Anaesthesia*, **87**(3), 421–428.

Guo, Ling, Rivero, Daniel, & Pazos, Alejandro. 2010. Epileptic seizure detection using multiwavelet transform based approximate entropy and artificial neural networks. *Journal of neuroscience methods*, **193**(1), 156–163.

Gurman, G, Porath, A, Fajer, S, & Pearlman, A. 1993. Correlation of EEG spectral edge frequency with hemodynamic stability during maintenance of general anesthesia.

Guyon, Isabelle, & Elisseeff, André. 2003. An introduction to variable and feature selection. *Journal of machine learning research*, **3**(Mar), 1157–1182.

Hajian-Tilaki, Karimollah. 2013. Receiver operating characteristic (ROC) curve analysis for medical diagnostic test evaluation. *Caspian journal of internal medicine*, **4**(2), 627.

Hall, JD, & Lockwood, GG. 1998. Bispectral index: comparison of two montages. *British journal of anaesthesia*, **80**(3), 342–344.

Hammarqvist, Ulf. 2011. *Audio editing in the time-frequency domain using the Gabor Wavelet Transform.*

Haykin, Simon. 1994. *Neural networks: a comprehensive foundation*. Prentice Hall PTR.

He, Hong, Tan, Yonghong, & Wang, Yuexia. 2015. Optimal base wavelet selection for ECG noise reduction using a comprehensive entropy criterion. *Entropy*, **17**(9), 6093–6109.

Hjorth, Bo. 1970. EEG analysis based on time domain properties. *Electroencephalography and clinical neurophysiology*, **29**(3), 306–310.

Ho, Tin Kam, & Basu, Mitra. 2002. Complexity measures of supervised classification problems. *IEEE transactions on pattern analysis and machine intelligence*, **24**(3), 289–300.

Horn, Bettina, Pilge, Stefanie, Kochs, Eberhard F, Stockmanns, Gudrun, Hock, Andreas, & Schneider, Gerhard. 2009. A combination of electroencephalogram and auditory evoked potentials separates different levels of anesthesia in volunteers. *Anesthesia & Analgesia*, **108**(5), 1512–1521.

Hosseinzadeh, Hamzeh, Eidy, Mahmood, Golzari, Samad EJ, & Vasebi, Mahmood. 2013. Hemodynamic stability during induction of anesthesia in elderlyPatients: propofol+ ketamine versus propofol+ etomidate. *Journal of cardiovascular and thoracic research*, **5**(2), 51.

Huang, Hui-Hsun, Lee, Yi-Hui, Chan, Hsiao-Lung, Wang, Yong-Ping, Huang, Chi-Hsiang, & Fan, Shou-Zen. 2008. Using a short-term parameter of heart rate variability to distinguish awake from isoflurane anesthetic states. *Medical & biological engineering & computing*, **46**(10), 977–984.

Huiku, M, Uutela, K, Van Gils, M, Korhonen, I, Kymäläinen, M, Meriläinen, P, Paloheimo, M, Rantanen, M, Takala, P, Viertiö-Oja, H, *et al.* . 2007. Assessment of surgical stress during general anaesthesia. *British journal of anaesthesia*, **98**(4), 447–455.

Hussain, MS, Reaz, Mamun Bin Ibne, Mohd-Yasin, Faisal, & Ibrahimy, Muhammad I. 2009. Electromyography signal analysis using wavelet transform and higher order statistics to determine muscle contraction. *Expert Systems*, **26**(1), 35–48.

Ibáñez-Molina, Antonio J, Iglesias-Parro, Sergio, Soriano, María F, & Aznarte, José I. 2015. Multiscale Lempel–Ziv complexity for EEG measures. *Clinical Neurophysiology*, **126**(3), 541–548.

IntelliVue, Monitor. 2006. *IntelliVue Patient Monitor MP20/30, MP40/50, MP60/70/80/90*.

Iser, Bernd, Schmidt, Gerhard, & Minker, Wolfgang. 2008. *Bandwidth extension of speech signals*. Vol. 13. Springer Science & Business Media.

Jang, J-SR. 1993. ANFIS: adaptive-network-based fuzzy inference system. *IEEE transactions on systems, man, and cybernetics*, **23**(3), 665–685.

Jeleazcov, Christian, Schneider, Gerhard, Daunderer, Michael, Scheller, Bertram, Schüttler, Jürgen, & Schwilden, Helmut. 2006. The discriminant power of simultaneous monitoring of spontaneous electroencephalogram and evoked potentials as a predictor of different clinical states of general anesthesia. *Anesthesia & Analgesia*, **103**(4), 894–901.

Jensen, Erik W, Jospin, Mathieu, Gambus, Pedro L, Vallverdu, Montserrat, & Caminal, Pere. 2008. Validation of the Index of Consciousness (IoC) during sedation/analgesia for ultrasonographic endoscopy. *Pages 5552–5555 of: Engineering in Medicine and Biology Society, 2008. EMBS 2008. 30th Annual International Conference of the IEEE*. IEEE.

Jensen, EW. 2005. Cerebral State Monitoring and Pharmacodynamic, Modelling by Advanced Fuzzy Inference—State of the Art. *Präsentation vorgestellt auf: AMCA*.

Jianhui, Wang, Qian, Xiao, Yan, Jiang, Shouping, Guan, & Shusheng, Gu. 2009. An Adaptive Filter Model Based on Wavelet Transform. *Pages 136–139 of: Intelligent Systems, 2009. GCIS'09. WRI Global Congress on*, vol. 3. IEEE.

Johansen, Jay W. 2006. Update on bispectral index monitoring. *Best Practice & Research Clinical Anaesthesiology*, **20**(1), 81–99.

Johansen, Jay W, Sebel, Peter S, & Sigl, Jeff C. 2000. Clinical impact of hypnotic-titration guidelines based on EEG bispectral index (BIS) monitoring during routine anesthetic care. *Journal of clinical anesthesia*, **12**(6), 433–443.

Jospin, Mathieu, Caminal, Pere, Jensen, Erik W, Litvan, Hector, Vallverdú, Montserrat, Struys, Michel MRF, Vereecke, Hugo EM, & Kaplan, Daniel T. 2007. Detrended fluctuation analysis of EEG as a measure of depth of anesthesia. *IEEE Transactions on Biomedical Engineering*, **54**(5), 840–846.

Kailath, Thomas. 1967. The divergence and Bhattacharyya distance measures in signal selection. *IEEE transactions on communication technology*, **15**(1), 52–60.

Kaplan, Daniel. 2006. Detrended Fluctuation Analysis of EEG as a Measure of Depth of Anesthesia. *IEEE Transactions on Biomedical Engineering*, **53**(11).

Kaul, HL, Bharti, Neerja, *et al.* . 2002. Monitoring depth of anaesthesia. *Indian J Anaesth*, **46**(4), 323–332.

Kaushik, Saurav. 2016. Introduction to Feature Selection methods with an example (or how to select the right variables?). *Analytics Vidhya*.

Kavitha, PT, Lau, CT, & Premkumar, AB. 2007. Modified ocular artifact removal technique from EEG by adaptive filtering. *Pages 1–5 of: Information, Communications & Signal Processing, 2007 6th International Conference on*. IEEE.

Kelley, SD. 2003. Monitoring level of consciousness during anesthesia and sedation. *A Clinician's Guide to the Bispectral Index*.

Keshavarzi, Ali, Sarmadian, Fereydoon, Shiri, Jalal, Iqbal, Munawar, Tirado-Corbalá, Rebecca, & Omran, El-Sayed Ewis. 2017. Application of ANFIS-based subtractive clustering algorithm in soil Cation Exchange Capacity estimation using soil and remotely sensed data. *Measurement*, **95**, 173–180.

Kessler, BM, Payne, GL, & Polyzou, WN. 2003. Wavelet notes. *arXiv preprint nucl-th/0305025*.

Klette, Reinhard, & Zunic, Jovisa. 2004. *Combinatorial Image Analysis: 10th International Workshop, IWCIA 2004, Auckland, New Zealand, December 1-3, 2004, Proceedings*. Vol. 3322. Springer.

Koht, Antoun, Sloan, Tod B, & Toleikis, J Richard. 2012. *Monitoring the nervous system for anesthesiologists and other health care professionals*. Springer.

Kortelainen, Jukka, Väyrynen, Eero, & Seppänen, Tapio. 2011. Depth of anesthesia during multidrug infusion: separating the effects of propofol and remifentanil using the spectral features of EEG. *IEEE Transactions on Biomedical Engineering*, **58**(5), 1216–1223.

Krajča, Vladimir, Petránek, Svojmil, Patáková, Ivana, & Värri, Alpo. 1991. Automatic identification of significant graphoelements in multichannel EEG recordings by adaptive segmentation and fuzzy clustering. *International journal of biomedical computing*, **28**(1-2), 71–89.

Kreuer, S, & Wilhelm, W. 2006. The narcotrend monitor. *Best Practice & Research Clinical Anaesthesiology*, **20**(1), 111–119.

Kreuer, Sascha, Biedler, Andreas, Larsen, Reinhard, Altmann, Simone, & Wilhelm, Wolfram. 2003. Narcotrend monitoring allows faster emergence and a reduction of drug consumption in propofol–remifentanil anesthesia. *Anesthesiology: The Journal of the American Society of Anesthesiologists*, **99**(1), 34–41.

Lajnef, Tarek, Chaibi, Sahbi, Ruby, Perrine, Aguera, Pierre-Emmanuel, Eichenlaub, Jean-Baptiste, Samet, Mounir, Kachouri, Abdennaceur, & Jerbi, Karim. 2015. Learning machines and sleeping brains: automatic sleep stage classification using decision-tree multi-class support vector machines. *Journal of neuroscience methods*, **250**, 94–105.

Lan, Jheng-Yan, Abbod, Maysam F, Yeh, Rong-Guan, Fan, Shou-Zen, & Shieh, Jiann-Shing. 2012. Review: intelligent modeling and control in anesthesia. *Journal of Medical and Biological Engineering*, **32**(5), 293–307.

Larose, Daniel T. 2005. K-nearest neighbor algorithm. *Discovering Knowledge in Data: An Introduction to Data Mining*, 90–106.

Lee, Sang-Hong, Lim, Joon S, Kim, Jae-Kwon, Yang, Junggi, & Lee, Youngho. 2014. Classification of normal and epileptic seizure EEG signals using wavelet transform, phase-space reconstruction, and Euclidean distance. *Computer methods and programs in biomedicine*, **116**(1), 10–25.

Lempel, Abraham, & Ziv, Jacob. 1976. On the complexity of finite sequences. *IEEE Transactions on information theory*, **22**(1), 75–81.

Li, Duan, Liang, Zhenhu, Wang, Yinghua, Hagihira, Satoshi, Sleigh, Jamie W, & Li, Xiaoli. 2013. Parameter selection in permutation entropy for an electroencephalographic measure of isoflurane anesthetic drug effect. *Journal of clinical monitoring and computing*, **27**(2), 113–123.

Li, Hongxing, Chen, CL Philip, & Huang, Han-Pang. 2000. *Fuzzy neural intelligent systems: Mathematical foundation and the applications in engineering*. CRC Press.

Li, Jing, Yan, Jiaqing, Liu, Xianzeng, & Ouyang, Gaoxiang. 2014. Using permutation entropy to measure the changes in EEG signals during absence seizures. *Entropy*, **16**(6), 3049–3061.

Liang, Zhenhu, Wang, Yinghua, Ren, Yongshao, Li, Duan, Voss, Logan, Sleigh, Jamie, & Li, Xiaoli. 2014. Detection of burst suppression patterns in EEG using recurrence rate. *The Scientific World Journal*, **2014**.

Liu, David, Görges, Matthias, & Jenkins, Simon A. 2012. University of Queensland vital signs dataset: Development of an accessible repository of anesthesia patient monitoring data for research. *Anesthesia & Analgesia*, **114**(3), 584–589.

Long, Charles W, Shah, Nitin K, Loughlin, Christopher, Spydell, John, & Bedford, Robert F. 1989. A Comparison of EEG Determinants of Near-Awakening from Isoflurane and Fentanyl Anesthesia: Spectral Edge, Median Power Frequency, and [delta] Ratio. *Anesthesia & Analgesia*, **69**(2), 169–173.

Loomis, Alfred L, Harvey, E Newton, & Hobart, GA. 1937. Cerebral states during sleep, as studied by human brain potentials. *Journal of experimental psychology*, **21**(2), 127.

Lui, WHD, Thorp, TAS, Graham, SG, & Aitkenhead, AR. 1991. Incidence of awareness with recall during general anesthesia. *Anaesthesia*, **46**(6), 435–437.

Luo, Guomin, & Zhang, Daming. 2012. Wavelet denoising. *In: Advances in wavelet theory and their applications in engineering, physics and technology*. InTech.

Mallat, Stephane. 2008. *A wavelet tour of signal processing: the sparse way*. Academic press.

Marple, S Lawrence, & Marple, S Lawrence. 1987. *Digital spectral analysis: with applications*. Vol. 5. Prentice-Hall Englewood Cliffs, NJ.

Mateo, J, Sánchez-Morla, Eva M, & Santos, JL. 2015. A new method for removal of powerline interference in ECG and EEG recordings. *Computers & Electrical Engineering*, **45**, 235–248.

McCollum, Pete. 1998. An Introduction to Back Propagation Neural Networks. *The Newsletter of the Seattle Robotics Society*.

Messner, M, Beese, U, Romstöck, J, Dinkel, M, & Tschaikowsky, K. 2003. The bispectral index declines during neuromuscular block in fully awake persons. *Anesthesia & Analgesia*, **97**(2), 488–491.

Miller, Ronald D, Eriksson, Lars I, Fleisher, Lee A, Wiener-Kronish, Jeanine P, Cohen, Neal H, & Young, William L. 2014. *Miller's Anesthesia E-Book*. Elsevier Health Sciences.

Mirsadeghi, M, Behnam, Hamid, Shalbaf, Reza, & Moghadam, H Jelveh. 2016. Characterizing awake and anesthetized states using a dimensionality reduction method. *Journal of medical systems*, **40**(1), 13.

Moerman, N, Bonke, B, Oosting, J, *et al.* . 1993. Awareness and recall during general anesthesia: facts and feelings. *ANESTHESIOLOGY-PHILADELPHIA THEN HAGERSTOWN-*, **79**, 454–454.

Monitor, IntelliVue Patient. 2008. *MP20/30, MP40/50*. Tech. rept. MP60/70/80/90, Release G. 0 with Software Revision G. 0x. xx (PHILIPS) Sep.

Motamedi-Fakhr, Shayan, Moshrefi-Torbati, Mohamed, Hill, Martyn, Hill, Catherine M, & White, Paul R. 2014. Signal processing techniques applied to human sleep EEG signals—A review. *Biomedical Signal Processing and Control*, **10**, 21–33.

MSP430, Murugavel Raju. 2005. Heart-Rate and EKG Monitor Using the MSP430FG439.

Mukhopadhyay, Somnath, & Mandal, JK. 2013. Wavelet based denoising of medical images using sub-band adaptive thresholding through genetic algorithm. *Procedia Technology*, **10**, 680–689.

Muniraj, Chinnusamy, & Chandraseka, S. 2011. Adaptive neurofuzzy inference system-based pollution severity prediction of polymeric insulators in power transmission lines. *Advances in Artificial Neural Systems*, **2011**, 9.

Musizza, Bojan, & Ribaric, Samo. 2010. Monitoring the depth of anaesthesia. *Sensors*, **10**(12), 10896–10935.

Nachar, Nadim, *et al.* . 2008. The Mann-Whitney U: A test for assessing whether two independent samples come from the same distribution. *Tutorials in Quantitative Methods for Psychology*, **4**(1), 13–20.

Nguyen, Thanh, Khosravi, Abbas, Creighton, Douglas, & Nahavandi, Saeid. 2015. EEG signal classification for BCI applications by wavelets and interval type-2 fuzzy logic systems. *Expert Systems with Applications*, **42**(9), 4370–4380.

Nguyen-Ky, Tai, Wen, Peng, & Li, Yan. 2009. Theoretical basis for identification of different anesthetic states based on routinely recorded EEG during operation. *Computers in Biology and Medicine*, **39**(1), 40–45.

Nguyen-Ky, Tai, Wen, Peng, & Li, Yan. 2010. An improved detrended moving-average method for monitoring the depth of anesthesia. *IEEE Transactions on Biomedical Engineering*, **57**(10), 2369–2378.

Nguyen-Ky, Tai, Wen, Peng, Li, Yan, & Malan, Mel. 2012. Measuring the hypnotic depth of anaesthesia based on the EEG signal using combined wavelet transform, eigenvector and normalisation techniques. *Computers in Biology and Medicine*, **42**(6), 680–691.

Nguyen-Ky, Tai, Wen, Peng Paul, & Li, Yan. 2013. Consciousness and depth of anesthesia assessment based on bayesian analysis of EEG signals. *IEEE Transactions on Biomedical Engineering*, **60**(6), 1488–1498.

Nora, Fernando Squeff, Klipel, Rodrigo, Ayala, Gustavo, & Oliveira Filho, Getúlio Rodrigues de. 2007. Remifentanil: does the infusion regimen make a difference in the prevention of hemodynamic responses to tracheal intubation? *Revista brasileira de anestesiologia*, **57**(3), 247–260.

Nunes, Rogean Rodrigues, Chaves, Itagyba Martins Miranda, de Alencar, Júlio César Garcia, Franco, Suyane Benevides, de Oliveira, Yohana Gurgel Barbosa Reis, & de Menezes, David Guabiraba Abitbol. 2012. Bispectral index and other processed parameters of electroencephalogram: an update. *Brazilian Journal of Anesthesiology*, **62**(1), 105–117.

Osei-Bryson, Kweku-Muata, & Barclay, Corlane. 2015. *Knowledge Discovery Process and Methods to Enhance Organizational Performance*. CRC Press.

Otto, Klaus A, Cebotari, Serghei, Höffler, Hans-Klaus, & Tudorache, Igor. 2012. Electroencephalographic Narcotrend index, spectral edge frequency and median power frequency as guide to anaesthetic depth for cardiac surgery in laboratory sheep. *The Veterinary Journal*, **191**(3), 354–359.

Palendeng, Mario Elvis, Wen, Peng, & Li, Yan. 2014. Real-time depth of anaesthesia assessment using strong analytical signal transform technique. *Australasian Physical & Engineering Sciences in Medicine*, **37**(4), 723–730.

Park, Kyung Soo, Hur, Eun Jin, Han, Kyung Woo, Kil, Ho Yeong, & Han, Tae Hyung. 2006. Bispectral index does not correlate with observer assessment of alertness and sedation scores during 0.5% bupivacaine epidural anesthesia with nitrous oxide sedation. *Anesthesia & Analgesia*, **103**(2), 385–389.

Paton, WD. 1976. *An experiment of Claude Bernard on curare: the origins of the Physiological Society [proceedings].*

Phillips, Charles L, Parr, John M, & Riskin, Eve A. 1995. *Signals, systems, and transforms*. Prentice Hall.

Pilge, Stefanie, Zanner, Robert, Schneider, Gerhard, Blum, Jasmin, Kreuzer, Matthias, & Kochs, Eberhard F. 2006. Time Delay of Index CalculationAnalysis of Cerebral State, Bispectral, and Narcotrend Indices. *The Journal of the American Society of Anesthesiologists*, **104**(3), 488–494.

Pincus, Steven M. 1991. Approximate entropy as a measure of system complexity. *Proceedings of the National Academy of Sciences*, **88**(6), 2297–2301.

Pincus, STEVEN M, & Keefe, DAVID L. 1992. Quantification of hormone pulsatility via an approximate entropy algorithm. *American Journal of Physiology-Endocrinology And Metabolism*, **262**(5), E741–E754.

Plourde, G. 2006. Auditory evoked potentials. *Best Practice & Research Clinical Anaesthesiology*, **20**(1), 129–139.

POLIKAR, ROBI. *The Wavelet Tutorial Second Edition Part I.*

Polikar, Robi. 1996. The wavelet tutorial.

Pourhoseingholi, Mohamad Amin, Vahedi, Mohsen, & Rahimzadeh, Mitra. 2013. Sample size calculation in medical studies. *Gastroenterology and Hepatology from bed to bench*, **6**(1), 14.

Prichep, LS, Gugino, LD, John, ER, Chabot, RJ, Howard, B, Merkin, H, Tom, ML, Wolter, S, Rausch, L, & Kox, WJ. 2004. The Patient State Index as an indicator of the level of hypnosis under general anaesthesia. *British journal of anaesthesia*, **92**(3), 393–399.

Prys-Roberts, Cedric. 1987. *Anaesthesia: a practical or impractical construct?*

Rampil, Ira J. 1998. A primer for EEG signal processing in anesthesia. *Anesthesiology: The Journal of the American Society of Anesthesiologists*, **89**(4), 980–1002.

Rantala, Börje. 2006 (Apr. 18). *Measuring blood pressure*. US Patent 7,029,447.

Rashmi, GD, Lekha, A, & Bawane, Neelam. 2016. Analysis of Efficiency of Classification and Prediction Algorithms (kNN) for Breast Cancer Dataset. *Pages 187–197 of: Information Systems Design and Intelligent Applications*. Springer.

Ray, S, Jain, K, Blog, G, & Saraswat, M. 2016. Understanding support vector machine algorithm from examples (along with code). *Analytics Vidhya*.

Revuelta, M, Paniagua, P, Campos, JM, Fernández, JA, Martinez, A, Jospin, M, & Litvan, H. 2008. Validation of the index of consciousness during sevoflurane and remifentanil anaesthesia: a comparison with the bispectral index and the cerebral state index. *British journal of anaesthesia*, **101**(5), 653–658.

Reyes-Aldasoro, Constantino Carlos, & Bhalerao, Abhir. 2006. The Bhattacharyya space for feature selection and its application to texture segmentation. *Pattern Recognition*, **39**(5), 812–826.

Ribeiro, LM, Ferreira, DA, Brás, S, Castro, A, Nunes, CA, Amorim, P, & Antunes, LM. 2009. Correlation between clinical signs of depth of anaesthesia and cerebral state index responses in dogs during induction of anaesthesia with propofol. *Research in veterinary science*, **87**(2), 287–291.

Ridella, Sandro, Rovetta, Stefano, & Zunino, Rodolfo. 1997. Circular backpropagation networks for classification. *IEEE Transactions on Neural Networks*, **8**(1), 84–97.

Rosso, Osvaldo A, Blanco, Susana, Yordanova, Juliana, Kolev, Vasil, Figliola, Alejandra, Schürmann, Martin, & Başar, Erol. 2001. Wavelet entropy: a new tool for analysis of short duration brain electrical signals. *Journal of neuroscience methods*, **105**(1), 65–75.

Russell, IF. 1993. Midazolam–alfentanil: an anaesthetic? An investigation using the isolated forearm technique. *BJA: British Journal of Anaesthesia*, **70**(1), 42–46.

Sadrawi, Muammar, Fan, Shou-Zen, Abbod, Maysam F, Jen, Kuo-Kuang, & Shieh, Jiann-Shing. 2015. Computational depth of anesthesia via multiple vital signs based on artificial neural networks. *BioMed research international*, **2015**.

Saez-Rodriguez, Julio, Rocha, Miguel P, Fdez-Riverola, Florentino, & Santana, Juan F De Paz. 2014. *8th International Conference on Practical Applications of Computational Biology & Bioinformatics (PACBB 2014)*. Vol. 294. Springer.

Sandin, Rolf H, Enlund, Gunnar, Samuelsson, Peter, & Lennmarken, Claes. 2000. Awareness during anaesthesia: a prospective case study. *The Lancet*, **355**(9205), 707–711.

Sanei, Saeid. 2013. *Adaptive processing of brain signals*. John Wiley & Sons.

Sanei, Saeid, & Chambers, Jonathon A. 2013. *EEG signal processing*. John Wiley & Sons.

Schneider, G, & Pilge, S. 2015. *Restrict relaxants, be aware, and know the limitations of your depth of anaesthesia monitor*.

Schneider, Gerhard, Kochs, Eberhard F, Horn, Bettina, Kreuzer, Matthias, & Ningler, Michael. 2004. Narcotrend® does not adequately detect the transition between awareness and unconsciousness in surgical patients. *The Journal of the American Society of Anesthesiologists*, **101**(5), 1105–1111.

Schneider, Gerhard, Jordan, Denis, Schwarz, Gerhard, Bischoff, Petra, Kalkman, Cornelis J, Kuppe, Hermann, Rundshagen, Ingrid, Omerovic, Adem, Kreuzer, Matthias, Stockmanns, Gudrun, *et al.* . 2014. Monitoring depth of anesthesia utilizing a combination of electroencephalographic and standard measures. *The Journal of the American Society of Anesthesiologists*, **120**(4), 819–828.

Schubert, Agnes U, Janda, Matthias, Simanski, Olaf, Bajorat, Jorn, Pohl, Birgit, Hofmockel, Rainer, & Lampe, Bernhard. 2008. A fuzzy system for regulation of the analgesic remifentanil during general anaesthesia. *Pages 1634–1639 of: Control and Automation, 2008 16th Mediterranean Conference on.* IEEE.

Schubert, AU, Simanski, O, Janda, M, Hofmockel, R, & Lampe, B. 2007. Monitoring the stress response during general anaesthesia. *Pages 1–5 of: Control & Automation, 2007. MED'07. Mediterranean Conference on.* IEEE.

Sebel, Peter S, Bowdle, T Andrew, Ghoneim, Mohamed M, Rampil, Ira J, Padilla, Roger E, Gan, Tong Joo, & Domino, Karen B. 2004. The incidence of awareness during anesthesia: a multicenter United States study. *Anesthesia & Analgesia*, **99**(3), 833–839.

Shalbaf, R, Behnam, H, & Moghadam, H Jelveh. 2014. Monitoring depth of anesthesia using combination of EEG measure and hemodynamic variables. *Cognitive Neurodynamics*, **9**(1), 41–51.

Shalbaf, R, Behnam, H, & Moghadam, H Jelveh. 2015. Monitoring depth of anesthesia using combination of EEG measure and hemodynamic variables. *Cognitive neurodynamics*, **9**(1), 41–51.

Shalbaf, Reza, Behnam, Hamid, Sleigh, Jamie W, Steyn-Ross, Alistair, & Voss, Logan J. 2013. Monitoring the depth of anesthesia using entropy features and an artificial neural network. *Journal of Neuroscience Methods*, **218**(1), 17–24.

Sharma, Rajeev, Pachori, Ram Bilas, & Acharya, U Rajendra. 2015. Application of entropy measures on intrinsic mode functions for the automated identification of focal electroencephalogram signals. *Entropy*, **17**(2), 669–691.

Shi, Zongli, Song, Wanqing, & Taheri, Saied. 2016. Improved LMD, permutation entropy and optimized k-means to fault diagnosis for roller bearings. *Entropy*, **18**(3), 70.

Shieh, JS, Linkens, Derek A, & Asbury, AJ. 2005. A hierarchical system of online advisory for monitoring and controlling the depth of anaesthesia using self-organizing fuzzy logic. *Engineering Applications of Artificial Intelligence*, **18**(3), 307–316.

Sinha, Prabhat Kumar, Koshy, Thomas, *et al.* . 2007. Monitoring devices for measuring the depth of anaesthesia-an overview. *Indian Journal of Anaesthesia*, **51**(5), 365.

Snow, John. 1953. On the inhalation of the vapour of ether in surgical operations. *British journal of anaesthesia*, **25**(1), 53–54.

Statistics, Laerd. 2013. Kruskal-Wallis H test using SPSS statistics. *Lund Research Ltd.*

Stoica, Petre, & Moses, Randolph L. 1997. *Introduction to spectral analysis*. Vol. 1. Prentice hall Upper Saddle River, NJ.

Struys, MMRF, Vanpeteghem, CAROLINE, Huiku, M, Uutela, K, Blyaert, NBK, & Mortier, EP. 2007. Changes in a surgical stress index in response to standardized pain stimuli during propofol–remifentanil infusion. *British journal of anaesthesia*, **99**(3), 359–367.

Subha, D Puthankattil, Joseph, Paul K, Acharya U, Rajendra, & Lim, Choo Min. 2010. EEG signal analysis: A survey. *Journal of medical systems*, **34**(2), 195–212.

Suparta, Wayan, & Alhasa, Kemal Maulana. 2016. Adaptive neuro-fuzzy interference system. *Pages 5–18 of: Modeling of Tropospheric Delays Using ANFIS*. Springer.

Theodoridis, Sergios, Koutroumbas, Konstantinos, *et al.* . 2008. Pattern recognition. *IEEE Transactions on Neural Networks*, **19**(2), 376.

Tibdewal, Manish N, Mahadevappa, M, Ray, Ajoy Kumar, Malokar, Monika, & Dey, Himanshu R. 2016. Power line and ocular artifact denoising from EEG using notch filter and wavelet transform. *Pages 1654–1659 of: Computing for Sustainable Global Development (INDIACom), 2016 3rd International Conference on*. IEEE.

Tunstall, ME. 1977. Detecting wakefulness during general anaesthesia for caesarean section. *British Medical Journal*, **1**(6072), 1321.

Übeyli, Elif Derya. 2009a. Analysis of EEG signals by implementing eigenvector methods/recurrent neural networks. *Digital Signal Processing*, **19**(1), 134–143.

Übeyli, Elif Derya. 2009b. Combined neural network model employing wavelet coefficients for EEG signals classification. *Digital Signal Processing*, **19**(2), 297–308.

Unser, Michael. 1999. Splines: A perfect fit for signal and image processing. *IEEE Signal processing magazine*, **16**(6), 22–38.

Vakkuri, A. 2006. EEG monitoring in anaesthesia. *Proceedings of Euroanesthesia*, 41–44.

Van de Velde, M, & Cluitmans, Petrus Johannes Maria. 1991. EEG analysis for monitoring of anesthetic depth.

Vereecke, Hugo EM, Vasquez, Pablo Martinez, Jensen, Erik Weber, Thas, Olivier, Vandenbroecke, Rudy, Mortier, Eric P, & Struys, Michel MRF. 2005. New Composite Index Based on Midlatency Auditory Evoked Potential and Electroencephalographic Parameters to Optimize Correlation with Propofol Effect Site ConcentrationComparison with Bispectral Index and Solitary Used Fast Extracting Auditory Evoked Potential Index. *The Journal of the American Society of Anesthesiologists*, **103**(3), 500–507.

Viertiö-Oja, H, Maja, V, Särkelä, M, Talja, P, Tenkanen, N, Tolvanen-Laakso, H, Paloheimo, M, Vakkuri, A, Yli-Hankala, A, & Meriläinen, P. 2004. Description of the Entropy™ algorithm as applied in the Datex-Ohmeda S/5™ Entropy Module. *Acta Anaesthesiologica Scandinavica*, **48**(2), 154–161.

VISTA, BIS. 2008. *Monitoring System Operating Manual. Aspect Medical Systems, Inc. Norwood, USA*.

Voss, Logan, & Sleigh, Jamie. 2007. Monitoring consciousness: the current status of EEG-based depth of anaesthesia monitors. *Best practice & research Clinical anaesthesiology*, **21**(3), 313–325.

Wang, L-X, & Mendel, Jerry M. 1992. Fuzzy basis functions, universal approximation, and orthogonal least-squares learning. *IEEE transactions on Neural Networks*, **3**(5), 807–814.

Wang, Zhenyu, Palade, Vasile, & Xu, Yong. 2006. Neuro-fuzzy ensemble approach for microarray cancer gene expression data analysis. *Pages 241–246 of: Evolving Fuzzy Systems, 2006 International Symposium on*. IEEE.

Watt, Richard C, Springfield, Christina L, Maslana, Eugene S, Kanemoto, Ansel, & Mylrea, Kenneth. 1994. Human EEG dimensionality and depth of anesthesia. *Pages 223–224 of: Engineering in Medicine and Biology Society, 1994. Engineering Advances: New Opportunities for Biomedical Engineers. Proceedings of the 16th Annual International Conference of the IEEE*, vol. 1. IEEE.

Weiss, BM, Spahn, DR, Keller, E, Seifert, B, & Pasch, T. 1995. Continuous non-invasive blood pressure monitoring by brachial artery displacement method in high-risk surgical patients. *European journal of anaesthesiology*, **12**(6), 555–563.

Wikipedia. 2017a. *Backpropagation — Wikipedia, The Free Encyclopedia*. [Online; accessed 9-November-2017].

Wikipedia. 2017b. *Confusion matrix — Wikipedia, The Free Encyclopedia*. [Online; accessed 12-November-2017].

Wikipedia. 2017c. *Kruskal–Wallis one-way analysis of variance — Wikipedia, The Free Encyclopedia*. [Online; accessed 11-November-2017].

Wikipedia. 2017d. *Radial basis function kernel — Wikipedia, The Free Encyclopedia*. [Online; accessed 8-November-2017].

Wikipedia. 2017e. *Support vector machine — Wikipedia, The Free Encyclopedia*. [Online; accessed 8-November-2017].

Woestenburg, JC, Verbaten, MN, & Slangen, JL. 1983. The removal of the eye-movement artifact from the EEG by regression analysis in the frequency domain. *Biological psychology*, **16**(1), 127–147.

Xiao, Fei, & Zhang, Yungang. 2011. A comparative study on thresholding methods in wavelet-based image denoising. *Procedia Engineering*, **15**, 3998–4003.

Xiao-Feng, Liu, & Yue, Wang. 2009. Fine-grained permutation entropy as a measure of natural complexity for time series. *Chinese Physics B*, **18**(7), 2690.

Xizhi, Zhu. 2008. The application of wavelet transform in digital image processing. *Pages 326–329 of: MultiMedia and Information Technology, 2008. MMIT'08. International Conference on.* IEEE.

Yong, YPA, Hurley, NJ, & Silvestre, GCM. 2005. Single-trial EEG classification for brain-computer interface using wavelet decomposition. *Pages 1–4 of: Signal Processing Conference, 2005 13th European*. IEEE.

Yu, Lanlan. 2009. EEG de-noising based on wavelet transformation. *Pages 1–4 of: Bioinformatics and Biomedical Engineering, 2009. ICBBE 2009. 3rd International Conference on*. IEEE.

Yu, Lei, & Liu, Huan. 2004. Efficient feature selection via analysis of relevance and redundancy. *Journal of machine learning research*, **5**(Oct), 1205–1224.

Yuvaraj, Rajamanickam, Murugappan, Murugappan, Ibrahim, Norlinah Mohamed, Omar, Mohd Iqbal, Sundaraj, Kenneth, Mohamad, Khairiyah, Palaniappan, Ramaswamy, & Satiyan, Marimuthu. 2014. Emotion classification in Parkinson's disease by higher-order spectra and power spectrum features using EEG signals: A comparative study. *Journal of Integrative Neuroscience*, **13**(01), 89–120.

Zanner, R, Pilge, S, Kochs, EF, Kreuzer, M, & Schneider, G. 2009. Time delay of electroencephalogram index calculation: analysis of cerebral state, bispectral, and Narcotrend indices using perioperatively recorded electroencephalographic signals. *British journal of anaesthesia*, **103**(3), 394–399.

Zeng, Hong, Song, Aiguo, Yan, Ruqiang, & Qin, Hongyun. 2013. EOG artifact correction from EEG recording using stationary subspace analysis and empirical mode decomposition. *Sensors*, **13**(11), 14839–14859.

Zhang, Xu-Sheng, Roy, Rob J, & Jensen, Erik Weber. 2001. EEG complexity as a measure of depth of anesthesia for patients. *IEEE Transactions on Biomedical Engineering*, **48**(12), 1424–1433.

Zheng, Cunsheng, Sackellares, J Chris, Williams, WJ, Tornow, A, & Kushwaha, Ramesh. 1990. Reducing EMG Artifact In EEG Recording With Standard Median Filter And FIR-median Hybrid Filter. *Pages 847–848 of: Engineering in Medicine and Biology Society, 1990., Proceedings of the Twelfth Annual International Conference of the IEEE*. IEEE.

Zoughi, Toktam, Boostani, Reza, & Deypir, Mahmood. 2012. A wavelet-based estimating depth of anesthesia. *Engineering Applications of Artificial Intelligence*, **25**(8), 1710–1722.

List of Publications

Journal Publications

- Benzy V. K, E. A Jasmin, Rachel Cherian Koshy, Frank Amal, and K. P Indiradevi. "Relative Wave Energy based Adaptive Neuro-Fuzzy Inference System model for the estimation of depth of anaesthesia." Journal of Integrative Neuroscience Preprint: 1-14(2017), DOI: 10.3233/JIN-170039, Publisher: IOS Press.

- Benzy V. K, E. A Jasmin, K. P Indiradevi, Rachel Cherian Koshy, and Frank Amal. "Monitoring Depth of Anaesthesia Based on Electroencephalogram Extracted Features and Artificial Neural Network." Journal of Medical Imaging and Health Informatics 7, no. 4 (2017): 909-917, DOI:10.1166/jmihi.2017.2091, Publisher: American Scientific Publishers.

Conference Publications

- Benzy V. K, and E. A Jasmin. "A combined wavelet and neural network based model for classifying depth of anaesthesia." Procedia Computer Science 46 (2015): 1610-1617, DOI:10.1016/j.procs.2015.02.093.

- Benzy V. K, E. A Jasmin, and Rachel Cheriyan Koshy. "Approximate Entropy and Wavelet Entropy-based Depth of Anesthesia monitoring" International Conference on Control Communication & Computing India (ICCC)(2015), pp. 371-374, DOI: 10.1109/ICCC.2015.7432923, Publisher: IEEE.

- Benzy V. K, E. A Jasmin, Rachel Cherian Koshy, and Frank Amal. "Wavelet Entropy as a measure of Depth of Anaesthesia." 3rd International Conference on Signal Processing and Integrated Networks (SPIN)(2016), pp. 616-619, DOI: 10.1109/SPIN.2016.7566770, Publisher: IEEE.

- Benzy V. K, E. A Jasmin, Rachel Cheriyan Koshy, and Frank Amal. "Wavelet Entropy-based classification of depth of anaesthesia." International Conference on Computational Techniques in Information and Communication Technologies (ICCTICT)(2016), pp. 521-524, DOI: 10.1109/ICCTICT.2016.7514635, Publisher: IEEE.

About the Author

Benzy V.K was born at Poojappura in Trivandrum district in 1979. She had her B.Tech in Applied Electronics and Instrumentation from M.E.S College of Engineering, Kuttipuram, Kerala in the year 2000 and took her M.Tech in Technology Management from Kerala University, Trivandrum in the year 2004. She had a good academic record and was actively involved in various academic activities. She worked as a lecturer in Applied Electronics and Instrumentation at M.E.S College of Engineering, Kuttipuram, Kerala from January 2005 to August 2007. She worked as Assistant Professor in Electronics and Communication at Prime College of Engineering, Palakkad, Kerala from June 2011 to September 2012. She joined as a full-time research scholar under Centre for Engineering Research and Development (CERD) Fellowship in the Dept. of Electrical Engineering, Govt. Engineering College, Thrissur in September 2012. She had presented several papers at National and International conferences. Her major area of interest includes Biomedical Signal Processing such as EEG, ECG and EMG signal processing, Feature Extraction, Pre-processing and Machine Learning Algorithms etc.

Permanent Address
TC 47/846
Kanaka Nivas
MUDRA-114
Mudavanmugal
Poojappura PO
Trivandrum-695012